

Serine hydrolase activity and roles for monoacylglycerol lipase in innate immunity and intestinal inflammation

Timothy James William Ambrose

Green Templeton College

University of Oxford

Supervisors

Professor Alison Simmons & Professor David Greaves

Thesis submitted for the degree of

Doctor of Philosophy in Clinical Medicine

Hilary 2018

© Timothy James William Ambrose, 2018

All rights reserved.

This thesis is the result of my own work and includes nothing that is the outcome of work done in collaboration except where specifically indicated in the text.

It is not substantially the same as any that I have submitted, or is being submitted, for any other degree, diploma or other qualification.

No part of my thesis has already been submitted, or is being submitted, for any other degree, diploma or other qualification.

The thesis does not exceed 50,000 words exclusive of appendices, bibliography, diagrams and tables.

All trademarks used in this thesis are acknowledged to be the property of their respective owners

Abstract

Detection of evolutionarily conserved pathogen motifs by pattern recognition receptors (PRRs), particularly on dendritic cells (DCs), is crucial for adequate immune responses. Defects in DC function are known to be associated with inflammatory bowel disease (IBD). The endocannabinoid system (ECS) is the system through which exocannabinoids such as Δ^9-tetrahydrocannabinol and cannabidiol signal. Regarding inflammation, cannabinoids generally exert anti-inflammatory effects, including on experimental colitis. However, most work has been performed in animal models and less is known about the function of this system in human immune cells, particularly DCs. Monoacylglycerol lipase (MGLL) is the key enzyme for hydrolysis of the endocannabinoid 2-arachidonoylglycerol, and a member of the serine hydrolase enzyme superfamily. This thesis defines the activity of serine hydrolase enzymes for the first time in human DCs upon stimulation by NOD2/TLR2 ligands using activity-based protein profiling (ABPP). MGLL is shown to be ubiquitously upregulated upon stimulation of DCs and in monocyte-derived macrophages. Through pharmacological inhibition studies, MGLL is demonstrated to regulate cellular and secreted lipids, not limited to endocannabinoids. However, overall DC function is independent of this enzyme suggesting that the effects of lipid modulation may be on bystander cells. Challenging the current literature, MGLL inhibition with a novel inhibitor worsens murine *Citrobacter rodentium* colitis. Finally, ABPP demonstrates a rich serine hydrolome in colonic tissue from human IBD with many enzymes previously undefined in this disease. Gene expression of ECS components suggests the enzymes ABHD12 and DAGLα/β may be potential markers of field change in IBD.

Acknowledgements

As with most research programmes this journey has been marked by ecstatic highs and disappointing lows. From a background as a clinical gastroenterologist who had minimal exposure to practical laboratory science since undergraduate studies, this has been an intense learning curve. I count myself fortunate to exit from this period with a better understanding of myself and my limitations; of my research interests; of the relationship between academia, clinical medicine, and industry; and of the challenges facing the pursuit of rigorous scientific study. For my future career this can only be a positive outcome.

None of this would have been possible were it not for my supervisor, Professor Alison Simmons who not only took the time to understand what I wanted to achieve during my research but who has also been a seemingly never-ending source of ideas, patience and encouragement. Through her continued approach of utilising cutting edge technology in her research the collaboration with Abide Therapeutics developed. Little could I have predicted what tremendous colleagues they have been. Particular thanks must extend to Alan Ezekowitz, Gary O'Neill, Jackie Blankman, Olesya Ulanovskaya, Andreu Viader, Anna Knize, Aundrea Coppola, Dallas Jones, Iain Fraser and Julianne Hunt. Their knowledge and expertise has led to fruitful discussions and I am immensely grateful to the company for funding my DPhil research.

I have been fortunate to have Professor David Greaves as my second supervisor and his expertise in cannabinoid-mediated effects on immune cell migration has

been particularly informative. Similarly I am grateful to Professor Benedikt Kessler for being part of my Thesis Committee and providing essential insights into lipidomic and fluxomic profiling.

I extend gratitude to the members of the Simmons group at the Human Immunology Unit, Weatherall Institute of Molecular Medicine. In particular, Leyuan Bao for providing postdoctoral support especially in the earlier stages of my work. My thanks is also offered to Daniele Corridoni, Lorena Preciado-Llanes, Anna Aulicino, Mei-Yi Sun, Kaushal Parikh, Hannah Chen, Marta Jagielowicz and my fellow DPhil student Tom Chapman.

It would have been impossible to have completed the study of human IBD without the support of both the Endoscopy Unit and the Translational Gastroenterology Unit based at the John Radcliffe Hospital, Oxford. Moreover, the persistence of the Oxford Research Nurses for Immunology and Inflammatory Disease, led by Simona Fourie, who have been instrumental in sample gathering and safe record keeping. None of the *in vivo* modelling would have been possible without the expertise of Claire Pearson, from the Kennedy Institute of Rheumatology, University of Oxford and to her I am especially grateful. Special thanks are given to Professor Simon Travis for encouraging me to study basic science for my higher degree.

Lastly are the people who have dealt with the fallout from failed experiments or the excitement of finding an antibody which worked! Fiona for putting my life in perspective, and my parents for providing continued personal and financial investment in my education.

Table of Contents

Abstract i

Acknowledgements ii

Abbreviations xii

Chapter 1 - Introduction 1

1.1 The innate immune system 1

1.1.1 Dendritic cells and pattern recognition receptors (PRR) 3

1.1.2 Types of PRR 5

1.1.3 MyD88 dependent and independent signalling pathways 9

1.2 Inflammatory bowel disease (IBD) 12

1.2.1 NOD2 and dendritic cell function in IBD 14

1.3 Cannabinoids and the endocannabinoid system (ECS) 15

1.3.1 Cannabinoid receptors 16

1.3.2 Roles for β-arrestin in cannabinoid signalling 18

1.3.3 Downstream signalling pathways from cannabinoid receptors 19

1.3.4 Endogenous cannabinoid ligands and the metabolism of 2AG 20

1.4 Monoacylglycerol lipase (MGLL) 23

1.4.1 Structure and distribution 23

1.4.2 Development of MGLL inhibitors and characterisation of JZL184 26

1.4.3 MGLL inhibition and CB1 desensitisation 27

1.4.4 MGLL inhibition and immune cells 30

1.4.5 MGLL and neuroinflammation 32

1.4.6 MGLL and pain 34

1.4.7 MGLL and fever 36

1.4.8 MGLL in other inflammatory models 36

1.4.9 MGLL and colitis 36

1.5 Other ECS targets in *in vivo* colitis 39
1.5.1 Cannabinoid receptors 39
1.5.2 Endocannabinoid lipid ligands 42
1.5.3 Hydrolytic enzymes 42
1.5.4 Other ECS targets 43
1.6 Exocannabinoids and *in vivo* colitis 44
1.7 Cannabinoids in human IBD 45
1.7.1 *Ex vivo* studies 47
1.7.2 Clinical studies including trials of exocannabinoids 47
1.8 Summary and research objectives 49
Chapter 2 - Materials and Methods 51
2.1 Cell culture techniques 51
2.1.1 Generation of human moDCs, macrophages, and murine bone marrow derived DCs (BMDC) 51
2.1.2 Culture of cell lines 52
2.1.3 Stimulation with PRR ligands 52
2.1.4 Reconstitution of MGLL inhibitors for *in vitro* studies 53
2.2 Protein techniques 53
2.2.1 ABPP (Gel-based and MuDPIT) 53
2.2.2 Immunoblotting 55
2.2.3 Enzyme-linked immunosorbent assay (ELISA) 56
2.3 Cell biology 56
2.3.1 RNA extraction and real time (quantitative) polymerase chain reaction 56
2.3.2 Adenosine Triphosphate (ATP)-luminescence cell viability assay 57
2.3.3 Fluorescence-based migration assay 57
2.3.4 Flow cytometry 58
2.3.5 MelanA assay 59

2.3.6 Pathogen handling experiments....60
2.3.6.1 Human Immunodeficiency Virus (HIV) replication assay....60
2.3.6.2 Salmonella handling in THP-1-derived macrophages....61
2.3.6.3 *E coli*/influenza in PBMCs....62
2.3.7 Microarray sample preparation, running, and analysis....63
2.3.8 Trained immunity in monocytes....64
2.3.9 THP-1 inflammasome assay....65
2.4 Transfection techniques....65
2.4.1 siRNA transfection of moDCs....65
2.4.2 shRNA transfection of THP-1 cells....66
2.5 Lipidomics....68
2.6 *In vivo* murine techniques....68
2.6.1 Animals....68
2.6.2 Administration of MGLL inhibitor (ABD1970)....69
2.6.3 Induction of colitis....69
2.6.4 Macroscopic and histological grading of colitis....70
2.6.5 Colony forming unit (CFU) quantification....70
2.6.6 Tissue cytokine quantification by qPCR....71
2.6.7 Systemic cytokine production by ELISA....71
2.7 *Ex vivo* techniques....72
2.7.1 Obtaining colonic tissue....72
2.7.2 RNA analysis of colonic tissue....72
2.7.3 ABPP analysis of colonic tissue....73
2.8 Statistical analysis....73
2.9 List of materials....74
2.9.1 Antibodies for immunoblotting....74
2.9.2 shRNA clones....74

2.9.3 Inhibitors 75
2.9.4 Human primers for qPCR 75
2.9.5 Murine primers for qPCR 76
Chapter 3 – MGLL is induced upon PRR ligation of moDCs and regulates cellular and secreted lipids 77
3.1 Introduction 77
3.1.1 Activity-based protein profiling 79
3.1.2 Therapeutic potential of covalent drugs 81
3.2 Aims 82
3.3 Results 83
3.3.1 Gel-based ABPP highlights altered serine hydrolase expression on NOD2/TLR2 stimulation of moDCs 83
3.3.2 TLR2 engagement has a greater effect on MGLL activity than NOD2 and synergy between these ligands is not seen by gel-based ABPP 84
3.3.3 ABPP-MuDPIT identifies 64 serine hydrolases in moDCs and demonstrates MGLL activity to be the most increased following combined MDP/PAM stimulation 86
3.3.4 Validation of the top five most significantly altered serine hydrolases 88
3.3.5 The induction of MGLL following MDP/PAM stimulation is concentration dependent, remains elevated beyond 24h, and is not restricted to NOD2/TLR2 ligation 90
3.3.6 MGLL can be knocked down using siRNA in moDCs and inhibited using the small molecules JZL184 and MJN110 92
3.3.7 MGLL is upregulated in other myeloid immune cells 97
3.3.8 Profiling the ECS by qPCR in moDCs demonstrates a dynamic system upon stimulation of NOD2/TLR2 100
3.3.9 Profiling ECS receptors and hydrolytic enzymes in cell lines 103

3.3.10 MGLL inhibition with JZL184 affects cellular abundance of endocannabinoid-related lipids in moDCs 106
3.3.11 MGLL inhibition affects other cellular lipids beyond the endocannabinoid system 110
3.3.12 MGLL inhibition affects secreted 2AG and other MAGs 114
3.3.13 MGLL levels following MDP stimulation are impaired by the RIPK2 inhibitor ponatinib 118
3.3.14 MGLL levels are impaired by small molecule inhibitors of MAPK, TBK1 and Syk following PAM stimulation but not in TBK1, IKKε or MyD88 THP-1 knockdown cell lines 120
3.4 Discussion 128
3.5 Conclusion 132
Chapter 4 – moDCs and other innate immune cells function independently of MGLL activity across a range of assays 133
4.1 Introduction 133
4.2 Aims 136
4.3 Results 137
4.3.1 The small molecules JZL184 and MJN110 do not reduce viability of moDCs as measured by an ATP-luminescence assay 137
4.3.2 MGLL inhibition does not impair production of cytokines in moDCs following NOD2/TLR2 stimulation 139
4.3.3 MGLL inhibition does not impair inflammasome activation in THP-1 cells 146
4.3.4 Gene expression measured by microarray in moDCs shows no significant effect of JZL184 147
4.3.5 Expression of cell surface maturation markers and chemotactic migration of moDCs is not impaired by JZL184 153
4.3.6 Optimisation of a direct antigen presentation assay with MGLL inhibition 156

4.3.7 MGLL inhibition does not affect handling of *Salmonella enterica* serovar Typhimurium, replication of human immunodeficiency virus, or cytokine production by T cell subsets in response to *E coli* or influenza infection of PBMCs 159

4.3.8 Trained immunity in monocytes is not affected by MGLL inhibition 162

4.3.9 MGLL can be stably knocked down in THP-1 cells using shRNA interference 165

4.3.10 MGLL targeting shRNA affects production of TNFα, IL12p40 and IL23 from THP-1 cells 168

4.4 Discussion 170

4.5 Conclusion 173

Chapter 5 – Prophylactic MGLL inhibition worsens *Citrobacter*-induced murine colitis and profiling of human UC by ABPP highlights novel changes in serine hydrolases 174

5.1 Introduction 174

5.2 Aims 178

5.3 Results 180

5.3.1 ABD1970 inhibits MGLL in C57BL/6 mice and does not result in an adverse phenotype 180

5.3.2 Induction of colitis with *Citrobacter rodentium* and confirmation of target engagement by ABD1970 182

5.3.3 ABD1970 worsens histological colitis induced by *Citrobacter rodentium* and this is not due to differences in bacterial colonisation and translocation 185

5.3.4 The histopathological differences in colitis are mirrored by effects on mucosal cytokine production 189

5.3.5 Serine hydrolases can be detected by gel-based ABPP profiling of primary human colonic tissue 193

5.3.6 ABPP-MuDPIT of colonic biopsies from IBD patients reveals a dynamic serine hydrolome but with differences between patients 195
5.3.7 Profiling of the ECS by ABPP and qPCR in human IBD show promising but discordant results 201
5.4 Discussion 205
5.5 Conclusion 209
Chapter 6 - Discussion 210
6.1 Serine hydrolase profiling of dendritic cells confirms increased MGLL activity following PRR ligation which modulates lipid levels 212
6.2 MGLL transcription following NOD2 ligation is RIPK2-dependent but the pathways following TLR2 ligation are less clear 214
6.3 The role of MGLL in dendritic cell biology may involve communication with other cells 215
6.4 MGLL inhibition in intestinal inflammation *in vivo* is not always beneficial 216
6.5 The ECS and wider serine hydrolases are altered in inflamed colonic IBD tissue 217
6.6 Future directions for this research 219
6.6.1 *In vitro* experiments 219
6.6.2 *In vivo* experiments 220
6.6.3 *Ex vivo* experiments 220
6.7 Conclusion 221
References 222
Supplementary Figure 256
Appendix 1 – List of serine hydrolases identified in moDCs by ABPP-MuDPIT 257

Appendix 2 - List of lipids identified by high throughput screening of moDCs.....259

Abbreviations

Abbreviation	Full name
1AG	1-arachidonoylglycerol
2AG	2-arachidonoylglycerol
2OG	2-oleoylglycerol
2PG	2-palmitoylglycerol
5ASA	5-aminosalicylic acid
ABHD	αβ-hydrolase domain containing
ABPP	Activity-based protein profiling
AEA	Anandamide
AIEC	Adherent invasive *E coli*
ANOVA	Analysis of variance
AP-1	Activator protein 1
APC	Antigen presenting cell
ATP	Adenosine triphosphate
BCAP	B cell adaptor for PI3K
BG	β-glucan
BMDC	Bone-marrow derived dendritic cell
cAMP	Cyclic AMP
CB	Cannabinoid
CB1	Cannabinoid receptor 1
CB2	Cannabinoid receptor 2
CBD	Cannabidiol
CCL	Chemokine ligand
CCR	Chemokine receptor
CD	Crohn's disease
CD(14)	Cluster of differentiation (14)
CDAI	Crohn's disease activity index
cDNA	Complementary DNA
CE	Cholesterol ester
CES	Carboxylesterase
CFU	Colony forming units
CLR	C-type lectin receptor
CO_2	Carbon dioxide
COX2	Cyclo-oxygenase 2
CRISPR	Clustered regularly interspaced short palindromic repeats
CTSG	Cathepsin G
DAG	Diacylglycerol
DAGL	Diacylglycerol lipase
DAMP	Damage associated molecular pattern

DAP	γ-D-glutamyl-meso-diaminopimelic acid
DC	Dendritic cell
DMEM	Dulbecco's modified Eagle's medium
DMSO	Dimethyl sulfoxide
DNA	Deoxyribonucleic Acid
DNBS	Dinitrobenzene sulphate
DSS	Dextran sulphate sodium
E coli	*Escherichia coli*
ECS	Endocannabinoid system
ELISA	Enzyme-linked immunosorbent assay
ERK	Extracellular receptor kinase
FAAH	Fatty acid amide hydrolase
FaCN	Fatty acyl carnitine
FaCoA	Fatty acyl coenzyme A
FACS	Fluorescence-activated cell sorting
FCS	Foetal calf serum
FFA	Free fatty acid
FP-Rh	Rhodamine labelled fluorophosphonate
GDP	Guanosine diphosphate
GFP	Green fluorescent protein
GM-CSF	Granulocyte-macrophage colony stimulating factor
GPR	G-protein coupled receptor
GRK	G-protein coupled receptor kinase
GSK3	Glycogen synthase kinase 3
GTP	Guanosine triphosphate
GWAS	Genome wide association study
HIV	Human immunodeficiency virus
HLA	Human leucocyte antigen
IBD	Inflammatory bowel disease
IFN	Interferon
IgA	Immunoglobulin A
IKK	IκB kinase
IL	Interleukin
ILC	Innate lymphoid cell
iNOS	Inducible nitric oxide synthase
IRAK	IL-1R associated kinase
IRF	Interferon-regulatory factor
ISRE	Interferon-stimulated response elements
JNK	c-Jun N-terminal kinase
LOX	Lipoxygenase
LPA	Lysophosphatidic acid
LPC	Lysophosphatidylcholine
LPE	Lysophosphatidylethanolamine

LPS	Lipopolysaccharide
LRR	Leucine rich repeat
LRRK2	Leucine-rich repeat kinase 2
M-CSF	Macrophage colony stimulating factor
M&P	MDP & PAM
MAG	Monoacylglycerol
MAL	MyD88-adaptor-like protein
MAPK	Mitogen-activated protein kinase
MAVS	Mitochondrial antiviral signalling protein
MDP	Muramyl dipeptide
MEK	MAPK kinase
MGLL	Monoacylglycerol lipase
MHC	Major Histocompatibility Complex
MLN	Mesenteric lymph node
moDC	Monocyte-derived dendritic cell
MOI	Multiplicity of infection
mTOR	Mammalian target of rapamycin
MuDPIT	Multidimensional protein identification technology
MyD88	Myeloid differentiation primary response 88
NAE	N-acylethanolamides
NF-κB	Nuclear factor kappa enhancer of B cells
NLR	NOD-like receptor
NSAID	Non-steroidal anti-inflammatory drug
OD	Optical density
OEA	Oleoylethanolamine
PAM	Pam3CSK4
PAMP	Pathogen associated molecular pattern
PBMC	Peripheral blood mononuclear cells
PBS	Phosphate buffered saline
PC(A)	Principal Component (Analysis)
(q)PCR	(Quantitative) Polymerase chain reaction
PEA	Palmitoylethanolamine
PG	Phosphatidylglycerol
PGE2	Prostaglandin E2
PI3K	Phosphoinositide-3-kinase
PKA	Protein kinase A
PLA2G4A	Phospholipase A2 group 4a
PMA	Phorbol 12-myristate-13-acetate
PPAR	Peroxisome proliferator-activated receptor
PRR	Pattern recognition receptor
RCT	Randomised controlled trial
RFP	Red fluorescent protein
RIG-I	Retinoic acid inducible protein 1

RIPK2	Receptor-interacting serine/threonine protein kinase 2
RISC	RNA-induced silencing complexes
RLR	RIG-I-like receptor
RNA	Ribonucleic Acid
ROS	Reactive oxygen species
RPMI	Roswell Park Memorial Institute medium
SARM1	Sterile-α-and-armadillo-motif-containing protein 1
SCBT	Santa Cruz Biotechnology
SD	Standard deviation
SEM	Standard error of the mean
shRNA	Short hairpin RNA
siRNA	Short interfering RNA
(a)TAG	(Alkyl) Triacylglycerol
TAK1	TGFβ-activated kinase 1
TANK	TRAF-associated NF-kB activator
TBK1	TANK-binding kinase
TGFβ	Transforming growth factor beta
THC	Δ^9-tetrahydrocannabinol
TICAM1	TIR-domain containing adaptor molecule 1
TICAM2	TIR-domain containing adaptor molecule 2
TIR	Toll/IL-1R
TIRAP	TIR-domain containing adaptor protein
TLR	Toll-like receptor
TNBS	Trinitrobenzene sulphate
TNF	Tumour necrosis factor
TRAF6	TNFR-associated factor 6
TRAM	TRIF-related adaptor molecule
TRIF	TIR-domain containing adaptor protein inducing interferon beta
TRPV1	Transient receptor potential cation channel subfamily V member 1
TXB2	Thromboxane B2
UC	Ulcerative colitis
UCEIS	Ulcerative colitis endoscopic index of severity
US	Unstimulated

Chapter 1 - Introduction

Human immunity can be divided into the innate and adaptive immune responses. Immunity has evolved to ensure that pathogens can be destroyed whilst commensal microbes (and dietary antigens in the gastrointestinal tract) do not result in an active inflammatory response. Perturbed immune responses, particularly to commensal microbes or other usually innocuous antigens, can result in persistent inflammation with a detrimental effect on the host. This is manifested in diseases such as inflammatory bowel disease, rheumatoid arthritis, psoriasis and other autoimmune conditions. Understanding the biology of immunity in health should enable a better understanding in disease, thus providing opportunity for novel therapeutics to halt or limit disease progression.

1.1 The innate immune system

The innate immune system is the so-called 'first line of defence' and represents a rapid and powerful response. This broadly allows detection and control of pathogens whilst the more specific adaptive response, mediated through T and B cells, develops over a few days to assist with elimination of pathogens and acquisition of immunological memory. Epithelial barriers such as that found in the gastrointestinal tract act as a physical barrier to invasion. Within the gastrointestinal tract the production of mucus by goblet cells traps bacteria and prevents interaction with the epithelial cells[1]. Goblet cell depletion and abnormal mucus is seen in ulcerative colitis[2-4] with genetic variations in MUC2 being associated with colitis in mice[5] and humans[6]. Furthermore, production of antimicrobial peptides such as defensins and lysozyme by Paneth cells in the small intestine contributes

to innate defence and may be abnormal in inflammatory bowel disease (reviewed in [7] and [8]). Finally, secretory IgA enhances innate immunity at the intestinal epithelium through reinforcing barrier function, downregulation of local pro-inflammatory responses, and influencing the composition of the gut microbiota (reviewed in [9]).

More generally, innate immune responses are orchestrated by phagocytic cells such as monocytes and macrophages, dendritic cells which specialise in the presentation of antigen to cells of the adaptive immune system, and granulocytes (neutrophils, eosinophils, and basophils) which destroy pathogens through degranulation of enzymes stored in cytoplasmic vesicles. Innate lymphoid cells (ILCs), whilst deriving from the same precursor cell as T cells and having similar appearances, lack specific antigen receptors[10] and so are grouped with cells of the innate immune system. Group 1 ILCs (including Natural Killer cells) produce IFNγ similar to T_H1 cells; group 2 ILCs produce cytokines similar to T_H2; and group 3 ILCs produce IL-17 and 22 similar to T_H17 cells[11]. Recently a further subgroup was identified, ILC_{reg}, which can be induced in the intestine to protect against inflammation by the secretion of IL-10 and TGFβ[12]. Historically, innate immunity was not felt to develop immunological memory, a feature being reserved for the adaptive response. This concept has been challenged in recent years with the identification of 'trained innate immunity' through epigenetic reprogramming of monocytes and macrophages[13]. Thus the innate immune system, far from being a crude, non-specific means of initial defence, is rapidly being understood to be a refined, targeted and balanced system whose purpose is more than simply activating the adaptive immune response.

1.1.1 Dendritic cells and pattern recognition receptors (PRR)

Unlike many other cells of the innate immune system, a main function of dendritic cells is to ingest pathogens, digest proteins and communicate with other cell types, particularly those of the adaptive immune system, by presenting antigens. Broadly, dendritic cells *in vivo* can by subdivided into plasmacytoid DCs (pDCs) and myeloid dendritic cells (mDCs, also referred to as conventional/classical dendritic cells, cDCs)[14]. Plasmacytoid dendritic cells respond to viral infection by secreting large amount of interferon and can present antigen to $CD4^+$ T cells[15] although this latter feature is predominantly a feature of mDCs. *In vitro* assays often use the monocyte-derived dendritic cell (moDC), derived from $CD14^+$ monocytes by culture with GM-CSF and IL-4[16] to yield sufficient numbers for cell-based assays. Through their antigen-presentation ability, dendritic cells are a crucial bridge between innate and adaptive immune responses.

Dendritic cells recognise pathogens through PRRs, germline encoded receptors which sense motifs known as pathogen-associated molecular patterns (PAMPs)[17]. PAMPs are unique to pathogens and are not a feature of healthy vertebrate cells and are essential for the survival of the organism[18] so are not subject to significant change. PRRs, in particular members of the Toll-like receptor (TLR) family, can also sense danger-associated molecular patterns (DAMPs)[19,20]. These endogenous ligands, also referred to as alarmins, are released from damaged tissue and necrotic cells. They can include heat shock proteins, S100 proteins, high mobility group box 1, and components of the extracellular matrix such as hyaluronate[21].

Prior to PRR engagement, DCs exist in an immature state, adept at surveillance of their environment and endocytosis of antigens but with low levels of surface major histocompatibility complex (MHC) and co-stimulatory molecule expression so are unable to interact with T cells of the adaptive immune system. Upon activation, DCs mature, largely losing their endocytic capacity, and this results in a number of effects. Processed antigen from the endocytic pathway is presented on the cell surface in association with MHC class 2 molecules to naïve $CD4^+$ T cells or through cross-presentation on MHC class 1 to naïve $CD8^+$ T cells[22]. Antigen from the cytosol is presented on MHC class 1 molecules to naïve $CD8^+$ T cells[22]. Simultaneously to the trafficking of MHC-peptide complexes to the cell surface, DCs upregulate cell surface expression of co-stimulatory molecules such as CD80 and CD86[23] which can interact with CD28 on the T cell. Although the MHC-peptide complex alone is sufficient to activate, co-stimulation is essential for survival of T cells.

Circulating pathogens are largely sensed in the spleen but activated (mature) DCs residing in peripheral tissues migrate to the regional lymph nodes through the upregulation of cell surface CCR7 which interacts with CCL21 in lymphoid tissue[24]. Furthermore, DCs secrete cytokines such as IL-1β, IL-6, components of the IL-12 system, TNFα and the chemokine IL-8. These have pro-inflammatory effects such as increasing vascular permeability, attracting and differentiating lymphocytes, and the induction of acute-phase proteins.

The ability of DCs to prime naïve T cells may, in part, be related to the presence or absence of prostaglandin E2 (PGE2). moDCs produce PGE2 following lipopoly-

saccharide (LPS) stimulation via the induction of cyclo-oxygenase 2 (COX2)[25]. PGE2 has been shown to disrupt early stages of DC development[26], can affect differentiation and maturation[27], and inhibits the production of IL-12p70[28]. It is required for effective migration to CCL19 and 21[29] perhaps by affecting CCR7 signal transduction and intracellular calcium mobilisation[30]. Furthermore it has been shown that PGE2 inhibits CCL19 production by DCs[31] and that moDCs matured in the presence of PGE2 acquire migratory capacity but those that are not become cytokine secreting, non-migratory[32]. Effects have also been demonstrated on T_H polarisation shifting from a T_H1 to T_H2 response[33]. However, another study has shown that PGE2 acting through EP4, one of its four receptors, amplifies $T_H1/17$ responses *in vitro* whereas *in vivo* blockade of EP4 resulted in reduced $T_H1/17$ responses[34].

1.1.2 Types of PRR

The TLR family comprises the largest number of PRRs and has been extensively studied. The Toll protein was originally described in Drosophila with relevance for the development of the fruit fly (history discussed in[35]) but was subsequently shown to have roles in antifungal immunity[36]. The cytoplasmic domain of Toll exhibits similarity to the human IL-1 receptor[37] with both being important for signalling through nuclear factor kappa enhancer of B cells (NF-κB). To date, eleven human TLRs have been identified, responding to different components of pathogens (summarised in Table 1.1), although TLR11 is encoded by a pseudogene and is non-functional possibly because its ligand, profilin, has human homologs[38].

Group	Receptor	Native ligand	Cellular location	Adaptor protein	Pathogens sensed
TLR	TLR1/2	Triacyl lipopeptides	Cell membrane	MyD88 MAL	Bacteria, mycobacteria
	TLR2	Phospholipomannan Peptidoglycan Porins Lipoarabinomannan	Cell membrane	MyD88 MAL BCAP	Gram positive bacteria, Neisseria, mycobacteria, Candida
	TLR3	dsRNA	Endosome	TRIF SARM	Viruses
	TLR4	Lipopolysaccharide Mannan Envelope proteins	Cell membrane	MyD88 MAL TRIF SARM TRAM BCAP	Gram negative bacteria, Candida, viruses
	TLR5	Flagellin	Cell membrane	MyD88	Bacteria
	TLR6/2	Diacyl lipopeptides Lipoteichoic acid Zymosan	Cell membrane	MyD88 MAL	Mycobacteria, Group B streptococci, saccharomyces cerevisiae
	TLR7	ssRNA	Endosome	MyD88	RNA viruses
	TLR8	ssRNA	Endosome	MyD88	RNA viruses
	TLR9	CpG DNA	Endosome	MyD88	Viruses
	TLR10	Unknown	Cell membrane	Unknown	Unknown
	TLR11	Profilin	NA	NA	NA
NLR	NOD1	DAP	Cytoplasm	RIPK2	Bacteria
	NOD2	MDP	Cytoplasm	RIPK2	Bacteria

Table 1.1 Summary of types of human Toll- (TLR) and NOD-like receptors (NLR) including cellular location, key adaptor molecules and ligands
Abbreviations referenced in text unless otherwise stated. NA = not applicable.

TLRs are integral membrane glycoproteins comprising a leucine rich repeat (LRR) extracellular domain and a cytoplasmic Toll/IL-1R (TIR) homology domain[39]. They may be found on the cell surface (TLR1, 2, 4, 5, 6, 10) or in endosomes (TLR3, 7, 8, 9)[17] and in addition to DCs, may be found in macrophages, eosinophils, B cells, and even intestinal epithelial cells[40]. Following TLR activation, adaptor proteins are recruited to the receptor which mediates downstream signalling to induce genes required for host defence. To date, six adaptor proteins have been identified[41]:

1. Myeloid differentiation primary response 88 (MyD88)
2. MyD88-adaptor-like protein (MAL) / TIR-domain containing adaptor protein (TIRAP)
3. TIR-domain containing adaptor protein inducing interferon beta (TRIF) / TIR-domain containing adaptor molecule 1 (TICAM1)
4. TRIF-related adaptor molecule (TRAM) / TIR-domain containing adaptor molecule 2 (TICAM2)
5. Sterile-α-and-armadillo-motif-containing protein 1 (SARM1) – acts to inhibit the role of TRIF
6. B cell adaptor for phosphoinositide-3-kinase (PI3K) (BCAP) – produced by B cells to modulate activation by TLRs

Less is known about the fifth and sixth adaptor proteins but SARM1 has been shown to inhibit the function of TRIF[42]. BCAP is produced by B cells to alter TLR signalling through PI3K[43] and has recently been shown to associate with TLR2/4 and MAL/TIRAP[44]. The downstream pathways induced in a MyD88-dependent and independent manner are discussed in the subsequent section.

Part of the nucleotide-binding oligomerisation domain (NOD)-like receptor family (NLR), NOD1 and 2 are intracytoplasmic PRRs which recognise the bacterial peptidoglycan motifs γ-D-glutamyl-meso-diaminopimelic acid (DAP)[45] and muramyl dipeptide (MDP) respectively[39]. Once bound to ligand the receptors oligomerise and interact with receptor-interacting serine/threonine protein kinase 2 (RIPK2). This activates downstream TGFβ-activated kinase 1 (TAK1) which is required for NF-κB nuclear translocation and subsequent gene transcription. The signalling pathways engaged by these receptors on sensing peptidoglycan have recently been reviewed in detail[46]. Ligands for NOD1/2 extend beyond peptidoglycan with evidence for sensing of GEF-H1 (involved in Rho GTPase sensing), ssRNA, and endoplasmic reticulum stress[47]. In addition to NOD1 and 2, the NLR family comprises a number of other receptors including NLRP1/3/6/7/12 which act via engaging the inflammasome[48]. Inflammasome activation results in the production of the pro-inflammatory cytokines IL-1α, IL-1β and IL-18, activation of caspase-1 and pyroptosis[49].

RIG-I-like receptors (RLRs) are important cytoplasmic PRRs for the innate antiviral response, detecting viral dsRNA. Retinoic acid inducible protein 1 (RIG-I), which detects the 5'-phosphorylated blunt ends of viral genomic RNA, and melanoma-differentiation-associated gene 5, which has no end specificity, are the key members of this family[50]. As an overview of the signalling cascade, the adaptor molecule mitochondrial antiviral signalling protein (MAVS) is recruited upon ligand binding which acts through TANK-binding kinase (TBK1) and IκB kinase epsilon (IKKε) to activate interferon regulatory factor 3 (IRF3) and NF-κB. Upon

translocation to the nucleus these induce the transcription of type 1 interferons and other anti-viral genes.

The final group of PRRs are the C-type lectin receptors (CLRs), including dectin-1, dectin-2 and mincle, which detect mannose, fucose and glucan carbohydrate moieties on pathogens[51].

Whole pathogen stimulation of dendritic cells will inevitably result in activation of more than one PRR simultaneously. Indeed it is well established that there is cross-talk within[35] and between families of PRR to modulate the inflammatory response. Combined stimulation of NOD1 and TLR5 results in increased NF-κB dependent cytokine production and enhanced resistance to murine *Salmonella typhimurium*[52]. Similarly, NOD1 and 2 are important for cytokine production in *Listeria monocytogenes* infection of macrophages stimulated with TLR2 or 4 ligands[53] and NOD2 acts synergistically to elevate cytokine production in response to TLR9 stimulation[54]. The interplay between TLR2 and NOD2, which are both activated by bacterial peptidoglycan, has been shown to be synergistic in both mice and humans[55-57], as has the interplay between NOD1 and TLR stimulation[58].

1.1.3 MyD88 dependent and independent signalling pathways

With the exception of TLR3, TLR stimulation results in the association of MyD88 with the cytoplasmic tail of the TLR (Figure 1.1). IL-1R associated kinase (IRAK) 1, 2 and 4 are recruited; the former two are phosphorylated by the latter. IRAK 1 and 2 associate with TNFR-associated factor 6 (TRAF6) which both polyubiquitinates itself and IKKγ, and also recruits the TAK1 complex. This phosphorylates

IκB resulting in proteosomal degradation and translocation of NF-κB to the nucleus to result in transcription of pro-inflammatory genes. The TAK1 complex also results in the activation of c-Jun N-terminal kinase (JNK) and p38, components of the MAPK pathway. This activates the transcription factor activator protein 1 (AP-1)[17,39]. In addition, in pDCs following TLR7 & 9 stimulation, the MyD88 pathway can result in the production of type 1 interferons via IRF7[59].

TLR3 & 4 may also induce a type 1 interferon response but not via MyD88-IRF7 interactions (Figure 1.1). Upon ligand binding, TRIF (in addition to TRAM in the case of TLR4) is recruited to the PRR and associates with receptor-interacting protein 1 (RIP1/RIPK1). RIP1 may be polyubiquitinated and associate with TRAF6[60] to activate TAK1, NF-κB and AP-1 as described above. TRIF also activates TBK1 and IKKε which directly phosphorylate IRF3 and 7 which translocate to the nucleus to bind to interferon-stimulated response elements (ISRE) for the transcription of type 1 interferons[17,39]. The action of TRIF may be inhibited by SARM1, with SARM1 knockdown leading to enhanced IFNβ transcription but not the MyD88-dependent IL-8[42].

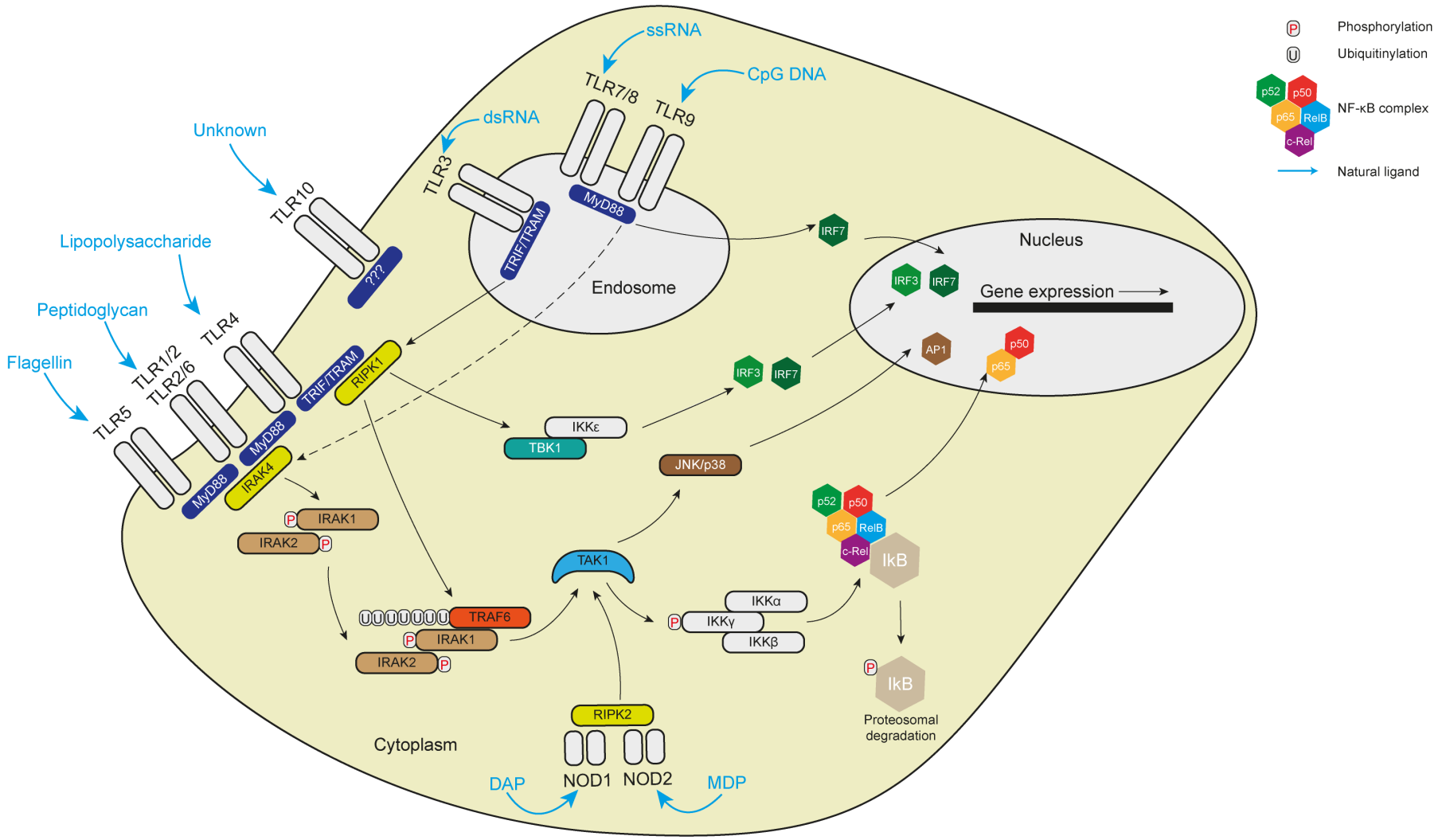

Figure 1.1 Key signalling pathways downstream of pattern-recognition receptors

Toll- and NOD-like receptors bind ligands and signal through key adaptor proteins and signalling cascades to mediate effects on gene expression through MAPK, IRF, or NF-κB. All abbreviations are referenced in the text.

1.2 Inflammatory bowel disease (IBD)

IBD can be classified into Crohn's disease (CD) and Ulcerative Colitis (UC) based on characteristic clinical, radiological, endoscopic, and histological features. Although incompletely understood, the aetiology is thought to represent a complex interaction between genetic background, intestinal microbiota, environmental factors and host immune response resulting in persistent and dysregulated inflammation (Figure 1.2).

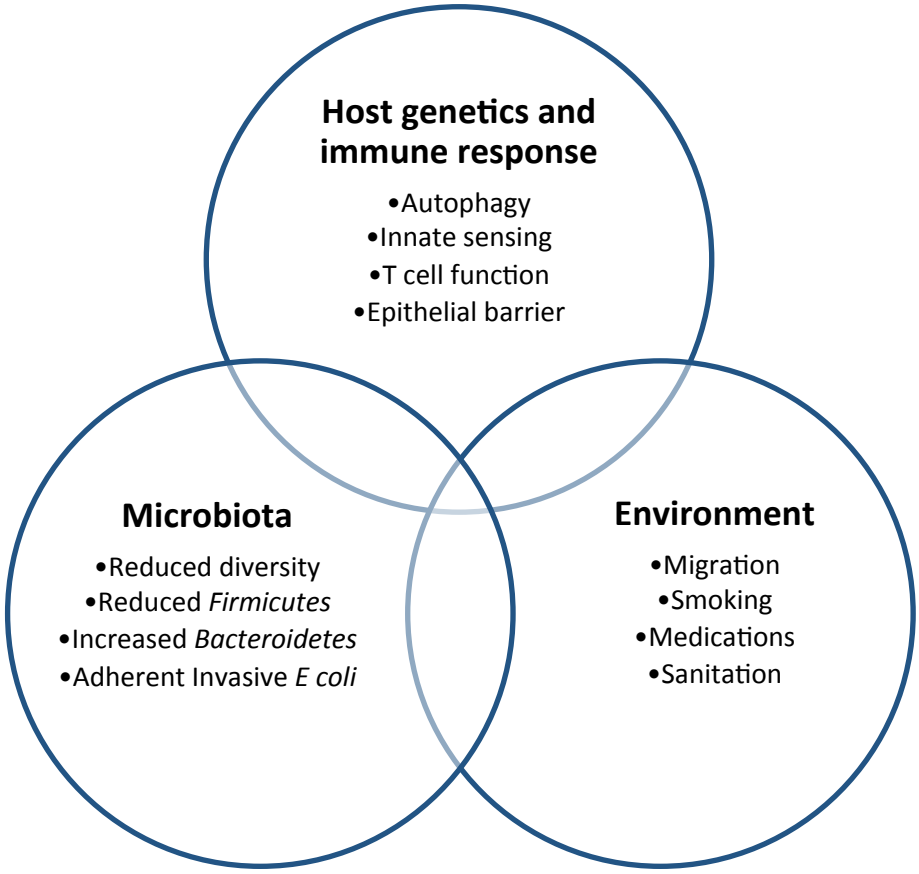

Figure 1.2 Factors involved in the development of IBD
The aetiology of human inflammatory bowel disease is a complicated interplay between genetic risk factors particularly immune-related, microbial and environmental influences.

The incidence of IBD has increased in Western populations[61,62] although may be plateauing[63]. However, this is not the case in the Asia-Pacific region where both incidence and prevalence are increasing[64]. The increased incidence cannot be ac-

counted for by substantial changes in host genetics, with environmental factors likely to be of critical importance (reviewed in [65] and briefly summarised in Table 1.2). Although there has been an explosion in therapies for IBD there remains an unmet clinical need for novel therapies and improved understanding of disease biology.

Factor	General effect on rates of IBD
South to North migration	Increase
East to West migration	Increase
Smoking	Reduction (UC); Increase (CD)
Appendectomy	Reduction (UC); Increase (CD)
Antibiotics in childhood	Increase (Western populations); Reduction (Asia)
Improved hygiene/sanitation	Increase
COX inhibition	Increase (NSAIDs, aspirin); Reduction (COX2-inhibitors)
Reduced dietary fibre	Increase (CD)
High ω-6:ω-3 PUFA	Increase
Vitamin D deficiency	Increase
Stress	Increase
Increased physical activity	Reduction

Table 1.2 Effect of environmental factors on rates of IBD
All abbreviations referenced in text apart from PUFA = polyunsaturated fatty acids.

Genetic association studies have identified approximately 200 loci associated with IBD with many shared between CD and UC[66,67]. Differences in susceptibility alleles exist between ethnic backgrounds with, for instance, NOD2 and IL23R variants over-represented in European populations compared to East Asian[64,67]. More recently, using high density genotyping, 45 variants have been fine-mapped as potentially causal for IBD[68] and this approach may aid better understanding of disease mechanisms. Grouping of susceptibility loci using ontogeny has highlighted broad mechanisms of relevance in the immunological response in IBD and this has informed subsequent study. This includes autophagy (ATG16L1, IRGM, LRRK2), endoplasmic reticulum stress (XBP1), innate immune cell sensing (NOD2), T cell tolerance (IL10, IL10R), IL23-pathways (IL23R, IL12B), lympho-

cyte trafficking (CCL7, IL8), and epithelial barrier function (MUC1, MUC3)[69-72]. Another exciting development in the field of IBD genetics is evidence that genetic associations may be related to disease prognosis in addition to, or instead of, disease susceptibility[73]. This might provide a novel avenue to stratify patients and target therapies accordingly.

1.2.1 NOD2 and dendritic cell function in IBD

Innate immune sensing is of particular interest given the strong association between NOD2 polymorphisms (R702W, G908R, and 1007fs (3020insC))[74,75] and CD. Patients with a NOD2 variant are more likely to have disease affecting the terminal ileum, exhibit a fibrostenosing phenotype, and to require surgical intervention[76]. Interestingly there are no differences in phenotype between homozygotes or compound heterozygotes for the three polymorphisms listed. Approximately half of patients with CD have at least one mutation in NOD2[76] and importantly not everyone in the wider population with NOD2 variants develop intestinal inflammation[77,78] highlighting the complexities of this disease and the non-essential role of NOD2 in disease pathogenesis. Unlike NOD1, NOD2 is expressed predominantly in myeloid cells[79]. However, a role for recognition of intracellular bacteria in intestinal epithelial cells, which is lost in 3020insC mutants, has been demonstrated[80].

Whilst NOD2 polymorphisms are generally felt to lead to a loss-of-function phenotype some groups have argued for a gain-of-function[81,82]. Assuming the former to be accurate it is intriguing to reconcile the loss-of-function of a pathway with an increased risk of intestinal inflammation. One explanation may lie in the func-

tion of antigen presenting cells (APC). Dendritic cells taken from patients with CD and NOD2 variants exhibit defects in bacterial handling through processes including autophagy induction, trafficking, and antigen presentation[83] leading to bacterial persistence. Induction of micro-RNA-29 on NOD2 activation leads to downregulation of IL-23 and this effect is lost in dendritic cells with NOD2 polymorphisms leading to enhanced levels of IL-12p40 on bacterial challenge[84] with potential effects on T_H17 polarisation. These cells also fail to upregulate key co-stimulatory molecules for T cell activation[85] and lack the usual synergistic relationship between NOD2 and TLR signalling[86] resulting in altered levels of pro/anti-inflammatory cytokines[85]. A reduction in TLR2-induced, anti-inflammatory cytokine production, particularly IL-10, is seen in mononuclear cells with NOD2 mutations leading to a relative increase in pro-inflammatory cytokine production in CD[87]. So a loss of function of the NOD2 pathway may lead to an inability to adequately regulate TLR signalling with some evidence this leads to a T_H1 polarised response to commensal organisms[88]. Certainly treatment of mice with MDP, to activate the NOD2 signalling cascade, prior to induction of chemical colitis resulted in complete protection from disease with suppression of TLR pathways, a result which was recapitulated in human dendritic cells[89].

1.3 Cannabinoids and the endocannabinoid system (ECS)

Although used for centuries both medicinally and recreationally, one of the earliest published observational case series of the medicinal effects of the plant *Cannabis sativa* came midway through the nineteenth century by Dr John Clendinning. The author observes that an alternative was needed to opium which, alt-

hough effective in many instances, came with drawbacks particular with relation to the GI tract:

"It's tendency is to produce torpor in the stomach and bowels, and to stop the digestive process and the peristaltic actions; and thus to cause anorexia, constipation and active indigestion; it deranges the hepatic and renal secretions as well as those of the mucous linings of the whole alimentary canal."[90]

He concluded that *Cannabis sativa* had medicinal properties, should be added to the pharmacopoeia, and might have advantages over opium except in the "diarrhoea of phthisis…, of old ulcerations of the bowels, …and in dysenteric affections"[90]. Despite these observations work continues to understand the role of cannabinoids in gastrointestinal disease.

1.3.1 Cannabinoid receptors

The major active ingredient of *Cannabis sativa*, and that which causes the psychotropic effects, is Δ^9-tetrahydrocannabinol (THC) and was only isolated from the plant in 1964[91] when technology advanced to allow isolation and characterisation of individual components of mixtures. However, the plant contains up to 100 cannabinoid constituents including cannabidiol (CBD)[92]. For some years after the identification of THC, the potential target(s) of action of cannabinoids remained elusive. Cannabinoid receptor 1 (CB1) was first defined as a 7-transmembrane domain G-protein coupled receptor (GPR) in rat brain and related cell lines[93,94]. It is an abundant GPR in the human brain[95] and, although expressed in immune cells[96-101], levels are greatest in the central nervous system[97].

Recently a positron emission tomography tracer ligand has been used to map the distribution of CB1 in the rat[102], and a fluorescent probe used to investigate CB1 expression in human blood[103]. Together these may enable *in vivo*, rather than *ex vivo*, mapping of this receptor in health and disease.

Following the identification of CB1, a 'peripheral' receptor was identified from the human HL60 promyelocytic leukaemia cell line, termed cannabinoid receptor 2 (CB2) with 44% homology to CB1[104]. This was not found in brain but instead located in the rat splenic marginal zone and in macrophage/monocyte populations. Subsequently this receptor has been described in human immune cell subsets[97,100,101] particularly those of a myeloid lineage[105]. The cellular location of the receptor varies between cell subtypes. In B cells, CB2 is predominantly on the cell surface whereas in monocytes and T cells it is mainly intracellular[106] but this may alter upon cell stimulation[107,108]. Receptor expression in humans may also vary by gender and ethnicity and this is also the case with CB1[109].

Recently the crystal structure of CB1 has been resolved. Hua et al[110] utilised the antagonist AM6538 to promote CB1-ligand crystal formation. They demonstrated the antagonist to have three arms which interact with a binding pocket network to ensure high affinity binding and to induce conformational change in the receptor which may have effects on downstream signalling. At a similar time a second group bound the inverse agonist taranabant to CB1 and demonstrated similar findings[111]. The first group went on to resolve agonist-bound CB1 using the full agonists AM11542 and AM841 and clearly demonstrated conformational differences to the antagonist-bound receptor[112]. This included alterations in the

ligand binding site and intracellular G-protein binding site. This may provide novel avenues to develop reagents to interrogate CB1 signalling. As yet, the crystal structure of CB2 remains unresolved.

1.3.2 Roles for β-arrestin in cannabinoid signalling

The cannabinoid receptors are coupled to $G_{i/o}$ proteins. In the resting state, the G-protein bound to the receptors exists as α-GDP subunit linked to a βγ subunit. Upon ligand binding the GDP is exchanged for GTP and the subunits dissociate allowing either (α-GTP or βγ) to interact with downstream effectors. The GTP-ase activity of the α subunit converts GTP to GDP and the inactive G protein is re-constituted to terminate signalling. In addition, the activated receptor can be phosphorylated by G-protein coupled receptor kinase (GRK) which recruits β-arrestins[113]. This inhibits further G protein activations, initiates receptor internalisation by coupling to endocytic mechanisms and clathrin-coated pits, and thus acts to desensitise the receptor to ongoing stimulation. The internalised GPR-β-arrestin complex may also result in sustained signalling through mechanisms which are only now beginning to be appreciated[114]. Recently, constitutive CB1 internalisation was shown to be negatively regulated by cannabinoid receptor interacting protein 1a (CRIP1a) and that this required five amino acids in the C-terminus of CB1[115].

In addition to effects on GPR internalisation, β-arrestins may interact themselves with other signalling molecules including Src and components of the MAPK pathway[116,117]. Therefore downstream effects from GPRs may be mediated through G-proteins or β-arrestins and so there is the potential to develop biased

GPR ligands to exploit one or both of these pathways[118]. Protocols have been developed to study β-arrestin recruitment to cannabinoid receptors[119] and biased signalling has been shown with CB1[120]. Similarly, CB2 demonstrates biased signalling depending on the ligand and this has cast doubt on the exact function of many commercially available agonists/antagonists for this receptor[121].

Since the identification of CB1/2, other putative cannabinoid receptors have been identified, including GPR18[122], GPR55[123], GPR119[124], transient receptor potential channels[125,126], and peroxisome proliferator-activated receptors[126].

1.3.3 Downstream signalling pathways from cannabinoid receptors

Whilst the β-arrestin mediated downstream signalling cascades remain poorly defined, more is known about G-protein signalling particularly for CB1 but less so for CB2:

1) Cyclic AMP (cAMP) - As $G_{i/o}$ receptors, activation of CB1 and CB2 results in inhibition of adenylyl cyclase and a reduction in cAMP[127]. The consequent reduction in protein kinase A (PKA) levels reduces phosphorylation of serine and threonine residues on downstream proteins. Interestingly, the effects on cAMP levels may be dependent on duration of incubation with ligand. Short term incubation of Jurkat cells with cannabinoid agonists reduces cAMP levels but longer timepoints resulted in a sustained increase[128].
2) Ion channels – A-type potassium channels are activated by CB1 receptors and this is mediated through effects on reduced PKA levels[127]. CB1 also

activates inwardly rectifying potassium channels and inhibits L-, N-and Q-type voltage-gated Ca channels[127]. CB2 does not seem to affect potassium channels[129].

3) Intracellular calcium – CB1 agonists have been shown to induce a rapid, transient elevation in intracellular calcium levels and that may be caused by βγ stimulation of phospholipase Cβ and subsequent IP_3 release[130]. This binds to cation receptors on the endoplasmic reticulum which releases calcium into the cytoplasm. Similar effects on intracellular calcium are seen with CB2[129].
4) MAP kinases – CB1 results in MAP kinase activation (p38, JNK, ERK1/2 depending on the cell type[131]) most probably in a Raf1-PI3K manner[127]. CB2 activation results in similar MAPK phosphorylation[132-134] but not through PI3K but rather through protein kinase C[127,129].
5) Ceramide synthesis – Both CB1 and CB2 have been linked with ceramide synthesis[127,135] which may have implications for cannabinoid-induced apoptosis.
6) Small GTPase – CB1 activation reduces RhoA activity in a prostate cancer cell line with effects on cell migration[136].

1.3.4 Endogenous cannabinoid ligands and the metabolism of 2AG

In parallel with the identification of the two key cannabinoid receptors through which THC exerts its effects, endogenous ligands were identified: the arachidonate derivatives arachidonoyl ethanolamine (anandamide, AEA) derived from porcine brain[137] and the monoacylglycerol 2-arachidonoylglycerol (2AG) isolated from canine gut[138] and rat brain[139]. AEA is a partial agonist of CB1 and CB2, with

2AG acting as a full agonist at both these receptors although with greater potency for CB1 than CB2[126,140]. Other bioactive lipids related to these classical endocannabinoids have been described including N-acyl-ethanolamines (palmitoylethanolamine (PEA), oleoylethanolamine (OEA)) and other monoacylglycerols (2-oleoylglycerol (2OG), 2-palmitoylglycerol (2PG)). These related monoacylglycerols have been shown to potentiate 2AG signalling, termed the 'entourage effect'[141], but have also been shown to be antagonists of 2AG action[142] depending on the experimental models used. They may also bind to other cannabinoid-related receptors[143] to exert actions independent of CB1/2. Gut microbes have been shown to produce lipid ligands with similarities to the wider endocannabinoids to signal through GPRs including GPR119 to modulate host physiology particularly with glucose handling[144].

AEA and 2AG are made and released, often referred to as synthesised 'on demand' in the literature, from membrane phospholipids rather than stored in vesicles. In the central nervous system, 2AG is synthesised in the post-synaptic neuron, where its synthetic enzymes are located, following depolarisation. It then acts trans-synaptically through CB1 on the pre-synaptic terminal to limit further neurotransmission. 2AG is rapidly degraded to prevent ongoing receptor stimulation[145]. The exact mechanism by which 2AG is transported across the synapse, and taken up in order to be degraded, is not understood. Some work has been performed with AEA suggesting that this may be more than simple diffusion and be mediated by specific proteins[146].

The complex metabolic pathway for 2AG is increasingly understood (Figure 1.3). Phosphoinositol-bis-phosphate and phosphatidic acid are metabolised to diacylglycerols (DAGs) containing the arachidonate moiety. Through the action of DAG lipases (DAGL) α and β to hydrolyse DAGs, 2AG results. Metabolism of 2AG may proceed through hydrolysis, oxidation by COX2 or LOX enzymes, or epoxidation by components of the cytochrome P450 system[147,148]. Hydrolysis of 2AG produces arachidonic acid and glycerol which feeds into the eicosanoid system. Arachidonic acid and eicosanoids may also be formed direct from membrane phospholipids through the actions of phospholipase A2 group 4a (PLA2G4A). Thus, 2AG provides a link between the endocannabinoid and eicosanoid systems.

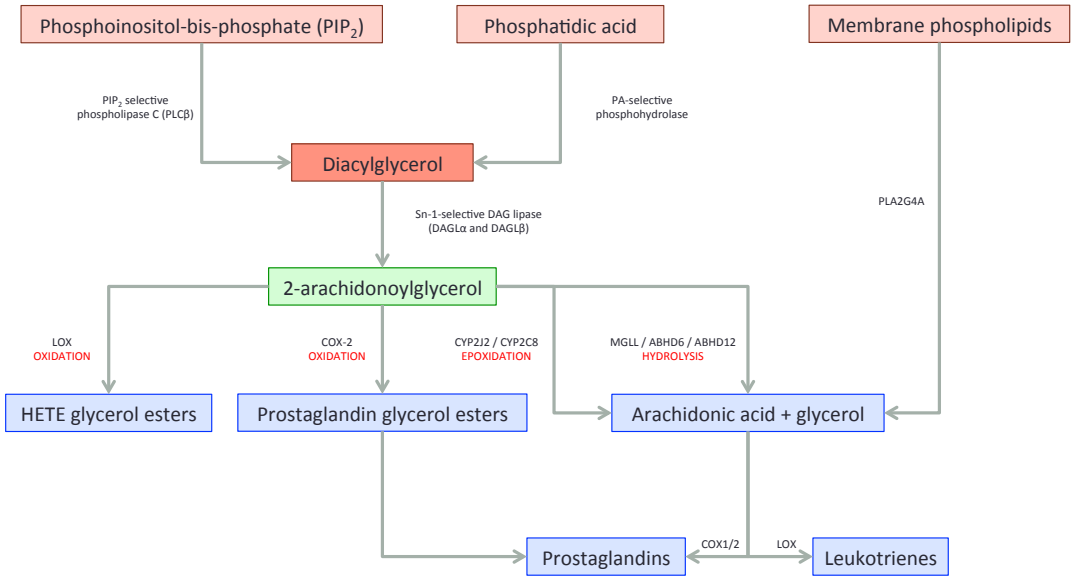

Figure 1.3 Synthesis and metabolism of 2AG is complex and regulated by multiple enzymes
Several metabolic pathways exist downstream of 2AG with conversion into prostaglandins and leukotrienes thus linking the endocannabinoid and eicosanoid systems.

Of the 2AG degradative pathways, the best studied to date has been that of hydrolysis. Monoacylglycerol lipase (MGLL, MGL, MAGL) has been shown to hydrolyse 1- and 2-monoacylglycerols[149] and specifically 2AG[150]. In the murine brain,

MGLL accounts for 85% of 2AG hydrolytic activity with further contributions by αβ-hydrolase domain 6 (ABHD6) and ABHD12[151]. Fatty acid amide hydrolase (FAAH), the chief hydrolytic enzyme for AEA[152], also contributes slightly to 2AG hydrolysis. The contribution of MGLL to 2AG hydrolysis may vary between cell/tissue type and between species. In the human monocytic cell line THP1, carboxylesterase-1 (CES1) and palmitoyl protein thioesterase-1 (PPT1), but not MGLL, have key roles in 2AG hydrolysis[153]. Furthermore, the contribution of MGLL to prostaglandin production downstream of 2AG appears to vary by tissue type – MGLL regulates prostaglandin production in murine liver and lung, PLA2G4A in gut and spleen, with contributions from both enzymes in brain tissue[154]. MGLL has also been demonstrated to hydrolyse prostaglandin glycerol esters (produced from 2AG by COX2 oxidation) and so may have more substrates than just monoacylglycerols[155]. Therefore, in exploring the function of MGLL in humans it may not be straightforward to simply extrapolate data from animal studies.

The cannabinoid receptors together with their endogenous ligands and synthetic/degradative enzymes form the endocannabinoid system.

1.4 Monoacylglycerol lipase (MGLL)

1.4.1 Structure and distribution

MGLL, a member of the serine hydrolase enzyme family, is a 33kDa protein, with 303 amino acids, located on chromosome 3q21.3. It was purified from rat adipose tissue in the 1960s[156] and the cDNA cloned from a mouse adipocyte library in 1997[157]. MGLL is conserved across eukaryotes with orthologs in dog, cow,

mouse, and zebrafish[158]. Human MGLL has been characterised by mass spectrometry using an *Escherichia coli* overexpression system. This has demonstrated that the protein does not contain disulphide bridges and that it is subject to the removal of an N-terminal methionine residue as a post-translational modification[159]. The crystal structure demonstrates that it exists as a dimer with the active site comprising a serine, aspartic acid and histidine residue[160]. The serine residue is of particular importance for catalysis[161]. A cap domain covers the active site within which, and near the active site, is the α4 helix which is hydrophobic and so facilitates the interaction of MGLL with membranes[160]. In the presence of a ligand to the active site of MGLL, the cap domain folds over to ensure they remain in proximity. These authors identify a change in electrostatic potential in the closed state which they hypothesise may lead to loss of interaction with membranes[162]. A recent study using surface plasmon resonance has illustrated that MGLL can remove phospholipids from membranes resulting in membrane disintegration through interactions with the cap domain[163]. Thus the cap domain appears critical to the function of MGLL.

MGLL is able to effectively hydrolyse not only 2AG but also 1AG, related MAGs (e.g. 2OG)[164], and even prostaglandin glycerol esters[155]. Similarly, the number of unsaturated bonds in the fatty acid side chain makes only minor impact on hydrolysis by MGLL although the preference appears to be for unsaturated substrates[158,165]. In addition to detection in rodent adipose tissue, MGLL mRNA has been detected elsewhere including kidney, testis and adrenal gland in the rat[157]. It is also expressed in the rat brain, particularly in presynaptic regions and in proximity to CB1 receptors[150,166]. MGLL has been demonstrated both in cytosolic

and membrane cellular compartments of rodent brain, HeLa and COS7 cells, and in lipid aggregates in adipocytes (summarised in [158]). Notably, the technique of activity-based protein profiling (ABPP) has demonstrated MGLL in both soluble (cytoplasmic) and membrane (particulate) fractions of murine brain[151].

The distribution of MGLL in human cells and tissues is less well studied. However, MGLL is detected in cancer cells of various tissue origins including prostate[167], melanoma[168], ovarian[169], and hepatocellular[170]. Interestingly, gene expression of MGLL in colorectal cancer cell lines was reduced compared to healthy colon[171]. Contrary to these findings another study profiled MGLL by immunohistochemistry in colorectal cancer tissue and found higher levels than in adjacent normal tissue[172]. This may represent differences in gene/protein expression or highlight issues with antibody specificity. MGLL mRNA has been demonstrated at greater levels in heart, smooth muscle, brain and spleen than testis, ovary and prostate[171]. The Human Protein Atlas suggests highest expression of MGLL in brain, gastrointestinal tract and adipose tissue in keeping with findings from animal studies[i]. A better understanding of tissue distribution of MGLL may be possible through radiological positron emission tomography (PET) tracers. This would not only allow dynamic *in vivo* imaging of MGLL expression but also efficacy of drug inhibition. Recently such a tracer has been evaluated successfully in rodents and non-human primates[173], and a second is in the evaluation stages (Abide Therapeutics, personal communication and [ii]).

[i] The Human Protein Atlas. https://www.proteinatlas.org/ENSG00000074416-MGLL/tissue Accessed 1st February 2018
[ii] Abide Therapeutics. http://abidetx.com/news/abide-therapeutics-announces-first-subject-dosed-in-pet-occupancy-study-with-18fabx-1488-a-proprietary-human-monoacylglycerol-lipase-mgll-specific-pet-ligand/ Accessed 1st February 2018

1.4.2 Development of MGLL inhibitors and characterisation of JZL184

As discussed above, the cannabinoid receptors are subject to biased signalling depending on the ligand. Furthermore, GPR drug targets may show variation in response due to genetic polymorphisms[174]. Due to expression across a number of body systems, cannabinoid receptor agonists/antagonists may yield unacceptable side effects limiting their utility. An example is the CB1 antagonist rimonabant which although successful as an anti-obesity agent was withdrawn from the market due to adverse psychiatric side effects. Therefore, modulation of the endogenous tone of the ECS in cells/tissues where it is already active is arguably preferable. To this end, and to better understand the roles of 2AG in health and disease, a number of pharmacological inhibitors of MGLL have been developed (summarised in [175]).

Early inhibitors such as URB602[176] were non selective for MGLL over FAAH and were thus not suitable to dissect the respective roles of these enzymes. Shortly after the discovery that MGLL was the key enzyme responsible for 2AG hydrolysis in the mouse brain, the covalent inhibitor JZL184 was synthesised and described[177]. Inhibition is dependent on the presence of the Cys242 residue which, if mutated, reduces the effect of JZL184 and skews substrate preference to 2-MAGs[178]. Near complete blockade of MGLL activity, assessed by ABPP techniques, is achieved after incubation with 50nM JZL184 for 30 minutes with no effects on FAAH or ABHD6 at this dose. *In vivo* studies demonstrated a dose-dependent effect on MGLL inhibition. At 16mg/kg, MGLL was almost completely inhibited with minimal off-target effects on FAAH. Timecourse studies demonstrated that MGLL inhibition was rapid (within 30 minutes) and this correlated with eleva-

tions in 2AG levels. At least 80% inhibition was maintained for over 24h but, despite this, 2AG levels were seen to gradually normalise by 24h suggestive of alternative pathways for 2AG metabolism or negative feedback mechanisms. Given that 2AG is known to signal through CB1 in the central nervous system, JZL184 was assayed for behavioural effects in mice – known as the tetrad test for cannabinoid activity. Similar to CB1 agonists, JZL184 was demonstrated to have an analgesic effect, and result in hypothermia and hypomotility. It did not result in catalepsy.

A more in-depth study of the effects of JZL184 in mice revealed that the role of MGLL in 2AG hydrolysis varies between tissues, and the substrate preference varies peripherally to centrally[179]. The effects of MGLL inhibition on C16:0 and C18:1 MAGs was greater peripherally with little effect on 2AG levels. In the peripheral tissues, arachidonic acid levels were also not modulated with MGLL inhibition. However, this study did confirm that JZL184 had equivalent inhibitory activity in mice and human tissues. Several years later, MJN110 was characterised, was demonstrated to have greater selectivity for MGLL over FAAH but with off-target effects on LYPLA1/2, and was effective *in vivo* for analgesia[180].

1.4.3 MGLL inhibition and CB1 desensitisation

The advent of selective MGLL inhibitors has resulted in major advances in understanding the function of MGLL, cannabinoid signalling more widely, and the identification of potential therapeutic avenues. A critical discovery was that chronic MGLL inhibition results in desensitisation of the CB1 receptor. Schlosburg et al administered high-dose JZL184 (40mg/kg) to mice daily for 6 days (chronic inhi-

bition) and noted not only was there an effect on AEA levels in these mice confirming some off-target FAAH effects of the inhibitor, but also that these mice did not display the analgesic effects seen with acute JZL184[181]. This was mediated through desensitisation of CB1 signalling and disruption of synaptic plasticity. Similar effects to chronic pharmacological blockade were seen with a $MGLL^{-/-}$ mouse where chronically elevated 2AG were seen along with poor analgesic responses[181]. Using an alternative $MGLL^{-/-}$ mouse, chronically elevated 2AG resulted in CB1 desensitisation and reduced cannabimimetic effects of exogenous 2AG or CB1 agonists[182].

The effects of repeated high dose JZL184 on CB1 desensitisation have also been demonstrated for gastric haemorrhage induced by non-steroidal anti-inflammatory drugs (NSAIDs). Prophylactic administration of JZL184 prior to diclofenac, a NSAID, attenuates gastric haemorrhages in a dose-dependent manner when given acutely[183]. However, when administered chronically, the gastroprotective effect of JZL184 is lost at doses greater than 8mg/kg but maintained at lower doses[184]. Repeated low-dose JZL184 is also effective at reducing neuropathic[184] and inflammatory pain[185]. The effects of chronic MGLL inhibition on CB1 desensitisation is not unique to JZL184 and is also seen with KML29[186]. It is also not dependent on FAAH genotype with similar tolerance seen in $FAAH^{+/+}$ mice to $FAAH^{-/-}$ mice[187]. Although it has not been directly studied it is probable that CB2 is subject to similar desensitisation as CB1 in response to chronic MGLL inhibition. Paw oedema in an inflammatory pain model was reduced by JZL184[185]. This response was shown to be CB2-dependent by co-administration of SR144528, a CB2 antagonist. With chronic JZL184 treatment the effects were

lost at doses greater than 8mg/kg suggestive of CB2 desensitisation. However, this view has been challenged recently by the observation in $MGLL^{-/-}$ murine macrophages that there was no effect on CB2 expression or of cytosolic Ca^{2+} responses to 2AG, suggesting that perhaps CB2 is not subject to the same desensitisation as CB1[188]. It is probable that endogenous MGLL functions to finely balance 2AG levels to prevent receptor desensitisation and cannabimimetic effects.

FAAH inhibition is effective for antinociception[189] and chronic FAAH inhibition alone does not result in CB1 desensitisation[181]. To this end, complete FAAH inhibition combined with partial MGLL inhibition results in improved analgesia but without the loss of CB1 sensitisation[190], and the combined FAAH/MGLL inhibitor JZL195 is more effective than inhibition of individual enzymes at relieving pain[191]. Thus careful modulation of multiple ECS ligands may represent an optimal therapeutic strategy without affecting cannabinoid signalling.

Similar to pharmacological inhibitor studies, MGLL knockout techniques have unravelled critical pieces of information about the ECS in neuronal signalling. By selectively knocking out MGLL in murine neurons, astrocytes or microglia, Viader *et al.* demonstrated neuronal and astrocytic MGLL to be key in terminating CB1 signalling by 2AG and that expression in either cell type is sufficient to prevent CB1 desensitisation[192]. Furthermore, the capacity of the two cell types to produce eicosanoids were different. Neurons were able to produce and secrete 2AG but had little capacity to convert this to eicosanoids. Conversely, astrocytes had less capacity to increase 2AG levels but were able to effectively shuttle 2AG into eicosanoids. These findings were corroborated by a second group[193]. Global

MGLL knockout has been shown to reduce neuroinflammation by reducing prostaglandins rather than by increasing 2AG[154]. Deletion of MGLL specifically in murine astrocytes resulted not only in modestly elevated 2AG but also impaired production of arachidonic acid and prostaglandins in response to LPS[194]. Deletion in astrocytes was sufficient to mimic the effects seen with global MGLL deletion without receptor desensitisation or cannabimimetic side effects.

Therefore the traditional view that 2AG is released from post-synaptic neurons to act on pre-synaptic neurons to terminate neurotransmission is only part of the story. It is plausible that a similar situation exists in the immune system whereby 2AG is released from one cell type to act on another. Furthermore, these studies highlight the complexity and cell-specific functions of MGLL and 2AG.

1.4.4 MGLL inhibition and immune cells

Human and murine innate and adaptive immune cells express ECS components including receptors, ligands, and degradative enzymes[96,97,105,195,196]. 2AG is produced by a range of immune cells including bone marrow derived dendritic cells (BMDCs) and murine macrophages[197,198], human lung macrophages[199], activated T and B cells[200], and human moDCs[201]. Where studied, 2AG is generally, although not exclusively[202], found to be increased upon stimulation with LPS. 2AG has roles as a chemoattractant[203,204] and induces migration of macrophage-like cell lines[205] but suppresses neutrophil migration[206]. Probably through effects on IL-2 production[207-209], 2AG acts to inhibit T cell proliferation[200]. However there is some evidence that the effects of 2AG on proliferation are dependent on cell density, with an inhibitory effect at low cell density and enhanced proliferative effect

at high cell density[210]. Effects have also been demonstrated for 2AG on optimisation of zymosan phagocytosis[211,212] and reduction of pro-inflammatory cytokine release by Müller glia[100], murine macrophages[213], BMDCs[214] and splenocytes[215].

Therefore, 2AG is generally considered to have anti-inflammatory effects. However there are some controversies in the literature. Whilst 2AG may impair proliferation of T cells, it increases proliferation of rat microglial cells[216]. There are also studies demonstrating 2AG to increase IL-8 production in LPS-stimulated Müller glia[100] and HL60 cells[217]. Similarly, 2AG does not affect release of angiogenic factors from LPS-stimulated human lung macrophages[199]. Whilst some of the effects of 2AG will be mediated by CB2, some effects may be mediated by CB1 as it is a full agonist at both receptors. Signalling through this receptor appears to be pro- rather than anti-inflammatory. CB1 signalling promotes a pro-inflammatory M1 macrophage phenotype with increased ROS production[218] and CB1 blockade reduces pro-inflammatory cytokine release[99]. In a murine model of diabetes, CB1 signalling through M1 macrophages induces the NLRP3 inflammasome to cause pancreatic beta cell failure[219]. There are also conflicting accounts of the effects of 2AG on nitric oxide production by innate immune cells demonstrating a reduction in J774 macrophages[220], no change in murine macrophages[213], and an increase in human monocytes[221]. Some of these differences may be inter-species but may also reflect an increasingly complex system with effects at multiple receptors and across multiple cell types. Therefore, studies of 2AG modulation and MGLL inhibition in *in vivo* models are an essential adjunct to *in vitro* studies and have previously been demonstrated to yield different results[222].

1.4.5 MGLL and neuroinflammation

Having established the roles of MGLL inhibition on prostaglandin production in LPS-induced neuroinflammation[154], and the role of astrocytes in this[194], other groups have investigated roles for MGLL in neuroinflammatory models. In a rat model of LPS-induced neuroinflammation, JZL184 was demonstrated to reduce IL1β, IL6, and TNFα gene expression in the frontal cortex[223]. MGLL inhibition, or 2AG administration, also reduced oligodendrocyte cytotoxicity acting via CB1 and mediated by effects on mitochondrial dysfunction and ROS generation[224]. However, in murine microglia in isolation, treatment with JZL184 or lentiviral knockdown of MGLL did not affect cytokine production in response to LPS[225]. This was despite MGLL being demonstrated to be upregulated following 24h LPS stimulation by immunoblot. Similarly, MGLL inhibition using MJN110 did not affect production of cytokines in the rat hypothalamus or spleen following TLR3 stimulation with poly(I:C)[226].

A number of groups have identified beneficial effects of MGLL inhibition on brain injury of various aetiologies, but all characterised by neuroinflammation. The MGLL inhibitor URB602 reduces ischaemic brain injury following hypoxia through effects on necrosis and apoptosis[227], and 2AG has been shown to protect astrocytes against ischaemic injury through effects on STAT3 and NDRG2[228]. However, exogenous 2AG results in worsened ischaemic injury in a rodent stroke model through enhancing platelet aggregation[229]. MGLL inhibition also reduces pro-inflammatory cytokine production in rodent models of traumatic brain injury[230,231] and HIV-associated neurocognitive disorder[232]. 2AG is protective in a single study of sulphur dioxide-induced neuroinflammation[233]. However, MGLL

does not provide neuroinflammatory arachidonic acid in a rodent model of alcohol binge drinking[234].

In rodent models of Alzheimer's disease, using transgenic mice, 2AG and JZL184 have been shown to reduce β-amyloid induced apoptosis and neurodegeneration *in vitro*[235] and *in vivo*[236] through reducing expression of beta-site amyloid precursor protein cleaving enzyme 1 (BACE1)[237] which is required to form β-amyloid. This mechanism has been demonstrated to be through restoration of the anti-inflammatory micro-RNA-188-3p which is required for 2AG to reduce BACE1 expression with subsequent beneficial effects on neuroinflammation and disease progression[238]. The mechanism is not dependent on CB2 with similar effects seen in a $CB2^{-/-}$ mouse[239].

In vivo models of the neurodegeneration seen with Parkinson's disease have shown JZL184 to reduce dopaminergic neuronal loss and associated proinflammatory cytokines in a cannabinoid-receptor independent manner, likely through effects on prostaglandin production[154]. A mechanism through increasing nigrostriatal TGF-β and glial cell line-derived neurotrophic factor has also been proposed[240], the latter possibly mediated by microglial cells[241]. Similar effects are seen with exogenous 2AG[242]. *In vitro*, JZL184 is also neuroprotective in SH-SY5Y human neuroblastoma cells but unlike *in vivo*, may act, at least in part, through CB2[243].

Modulation of 2AG either by exogenous application or inhibition of MGLL has shown beneficial effects in models of the cognitive decline seen in Down's syn-

drome[244] and neuroinflammation of Motor Neuron Disease[245]. Conversely, MGLL inhibition exacerbates neuronal death in a model of Huntington's disease hypothesised to be due to an increase in prostaglandin glycerol esters[246].

1.4.6 MGLL and pain

Cannabis has been used for centuries to manage pain of various aetiologies. Currently a combination therapy of THC + CBD (Nabiximols, Sativex®) is licensed in the UK for spasticity and spasms in multiple sclerosis. However, exocannabinoids may have an unfavourable neuropsychiatric side effect profile. Although many *in vivo* studies of FAAH inhibition showed benefit on pain modulation, a clinical trial of the FAAH inhibitor PF-04457845 was ineffective in osteoarthritic pain although well tolerated[247,248]. Recently a trial of BIA 10-2474, an alternative FAAH inhibitor, was terminated due to unexpected and severe neurological outcomes subsequently identified to be caused by off-target effects[249].

MGLL inhibition has been evaluated across a number of animal models of pain including neuropathic[250,251], osteoarthritic[252], migrainous[253], and inflammatory. MGLL inhibition has shown efficacy in models of this latter pain (including formalin, complete Freud's adjuvant, and carrageenan) across a range of routes of administration – localised subcutaneous[254], spinal[255], intraperitoneal[185] and intracerebroventricularly[256]. However there is disagreement between studies on the involvement of cannabinoid receptors in this effect. Two studies have shown that the effect is lost by blocking CB1 or CB2[185,254], whereas another showed that only CB1 was required for this effect[255]. The authors of this last study also hypothesised that very localised alterations in 2AG levels may be sufficient to exert

meaningful physiological outcomes. The effects of MGLL inhibition may also act via TRPV1 as the knockout mouse is resistant to the antinociceptive effects of JZL184[256]. In the carrageenan model of inflammatory pain, MGLL inhibition with KML29 is effective at reducing oedema via CB2 and pain via CB1 and CB2[186]. Inflammatory pain induced by complete Freud's adjuvant results in activation of the NLRP3 inflammasome and is improved by acupuncture, acting in a CB2-dependent manner[257]. This adds yet further confusion to the exact mode of action of MGLL inhibition in analgesia. Similar to other models, $MGLL^{-/-}$ or chronic pharmacological inhibition results in CB1 receptor desensitisation and augmentation of inflammatory pain responses[258]. However, combined FAAH and MGLL inhibition results in improved analgesic responses than inhibition of either enzyme alone[190,259,260].

The beneficial effects of MGLL inhibition on pain may also be through modulating sensitivity to other analgesic agents. JZL184 has been shown to augment the antinociceptive effects of peltatoside in the carrageenan model of inflammatory pain[261], and of gabapentin[262] and COX inhibitors[263] in neuropathic pain. Furthermore, and of particular interest for clinical medicine, MJN110 and morphine act synergistically via μ-opioid and cannabinoid receptors to relieve neuropathic pain but without the unwanted side effects of reduced gastrointestinal motility and cannabimimetic side effects[264]. This may be due to increased sensitivity to opioids caused by MGLL inhibition. Certainly CB2 agonists have been shown to induce μ-opioid receptor transcription in Jurkat cells[265], and $MGLL^{-/-}$ mice are hypersensitive to the μ-opioid agonist, loperamide[266].

1.4.7 MGLL and fever

Two studies published almost simultaneously and in the same journal demonstrated important roles for MGLL in mediation of murine fever[267,268]. An attenuated febrile response to low dose LPS administration was seen in MGLL$^{-/-}$ mice but not PLA2G4A$^{-/-}$. This was CB1- and DAGLβ-independent, and also seen with acute pharmacological MGLL inhibition with JZL184. Lipidomic profiling of murine hypothalami demonstrated reductions in PGE2 and increased 2AG. Notably, the febrile response could be recapitulated in MGLL$^{-/-}$ by exogenous administration of PGE2. Conversely to these predominantly genetic studies of MGLL and fever, another demonstrated that JZL184 potentiated hypothermia induced both by high dose LPS or environmental cold in a CB1-dependent manner[269]. Therefore, in mice, MGLL regulates fever response to low dose LPS by producing hypothalamic proinflammatory prostaglandins, but in high dose LPS challenge may exacerbate hypothermia via CB1.

1.4.8 MGLL in other inflammatory models

JZL184 reduces inflammation in LPS-induced acute lung injury[270], in hepatic reperfusion injury[271], and may improve stability of atherosclerotic plaques[272]. Diclofenac induces gastritis and gastric haemorrhage in mice and this can be inhibited by either THC, JZL184, or KML29 acutely[183,186]. Chronic low-dose JZL184 retains the gastroprotective effects without desensitisation of CB1[184].

1.4.9 MGLL and colitis

To date, only one study has assessed the role of MGLL inhibition in colitis[273]. Rectal administration of trinitrobenzene sulphate (TNBS) was used to induce colitis.

Intraperitoneal injection of 16mg/kg JZL184 twice daily both before and during the 3-day study increased 2AG levels and prevented both macroscopic and microscopic colitis. This was associated with a reduction in mucosal and systemic pro-inflammatory cytokines such as IL-6, TNFα, and IL-12. MGLL inhibition also reduced LPS-induced endotoxaemia which may suggest effects on mucosal barrier function. Certainly THC and CBD have beneficial effects on intestinal permeability induced by EDTA in unstimulated Caco-2 (colonic carcinoma) cells[274]. The effects of 2AG and AEA in this model were dependent on apical (worsened permeability) versus basolateral (improved permeability) administration. The same is true for JZL184 administration in unstimulated Caco-2 cells[275]. When cytokines were administered to Caco-2 cells to mimic inflammation, JZL184 worsened permeability when applied apically either at the same time as the cytokines[276] or after inflammation has been induced[275]. The benefits of MGLL inhibition on TNBS-colitis involved both CB1 and CB2 as inhibition of either abrogated the effects of JZL184[273]. However, the CB2 antagonist used, AM630, has recently been shown to have numerous off-target effects[121] and so it would be useful to have data using alternative CB2 antagonists to confirm the role of this receptor in mediating the effects seen. It is also worth noting that the dose of JZL184 used here is high (32mg/kg daily in divided doses) and is within the dose to desensitise CB1[184] although it is not clear whether this happens within the 3-day timeframe used in this model.

This chemical model of colitis utilises ethanol to disrupt the mucosal barrier, with TNBS haptenising colonic proteins[277] to render them immunogenic. It is used as a model of Crohn's disease (CD) as it is straightforward to administer and

consistently induces colitis in wildtype mice. It results in a predominant $T_H1/17$ response with $IL17^{-/-}$ mice resistant to TNBS colitis[278]. Certainly there are histological similarities as well with transmural inflammation, mucosal oedema, crypt distortion, crypt abscesses, and granulomas[278]. However, human IBD is not caused by chemical disruption of the epithelial barrier and haptenisation of otherwise innocuous antigens. Furthermore, whilst human CD can be colonic in distribution, it predominantly affects the terminal ileum, and TNBS does not reproduce ileal disease. In addition to TNBS, chemical colitis can be induced by intrarectal administration of dinitrobenzene sulphate (DNBS) or oral administration of dextran sulphate sodium (DSS). DSS induces colitis in a similar manner to TNBS and DNBS by destroying the epithelial barrier and allowing secondary translocation of intestinal contents. However, it produces a phenotype more similar to UC than CD[279]. Furthermore, the DSS model does not require an adaptive immune response unlike human IBD[279].

Therefore it is important to be circumspect about the translational potential of *in vivo* models of IBD especially where the evidence comes from a single model. More generally, it is increasingly recognised that the microbial makeup of laboratory animals can alter experimental results not to mention fundamental immunological differences between species[280]. Use of MGLL inhibitors in other models of IBD and intestinal inflammation would therefore reinforce this study. The development of a first-in-class MGLL inhibitor for human clinical trials, ABX-1431

(Abide Therapeutics[iii]), provides opportunity to investigate this in human IBD if further pre-clinical study is supportive.

An exciting development in support of the potential effects of MGLL inhibition in chemical colitis was recently published[281]. Here the authors used carbon nanotubes linked to 2AG with the aim of reducing rapid hydrolysis and improving the overall pharmacological profile. A single dose administered rectally two days before the instillation of TNBS in rats and then a second dose 8 days after resulted in improvement of colitis. No effect was seen of free 2AG or of the carbon nanotubes alone.

1.5 Other ECS targets in *in vivo* colitis

Although only two studies have assessed the role of 2AG or MGLL inhibition in colitis, several studies have assessed the impact of modulating ECS signalling in other ways.

1.5.1 Cannabinoid receptors

One of the earliest studies of the effect of cannabinoid receptor modulation identified that $CB1^{-/-}$ mice exhibited more severe colitis following either DNBS or DSS administration[282]. Subsequently this finding was confirmed in TNBS colitis and extended to demonstrate that $CB2^{-/-}$ and $CB1^{-/-}/CB2^{-/-}$ double knockout mice also display worsened colitis[283]. Although not reaching statistical significance there was an additive effect of double knockout on macroscopic colonic inflammation but not histological inflammation. The effects of $CB2^{-/-}$ have also been confirmed

[iii] Abide Therapeutics. http://abidetx.com/news/abide-therapeutics-announces-first-subject-dosed-in-first-in-human-clinical-study-of-abx-1431-an-investigational-endocannabinoid-system-modulator/ Accessed 1st February 2018

in DSS colitis. The authors also demonstrated that murine peritoneal macrophages stimulated *ex vivo* with LPS/DSS upregulated components of the NLRP3 inflammasome, that this was exacerbated in $CB2^{-/-}$ cells, and improved by the CB2 agonist HU308[284].

The findings of genetic knockout studies have largely been confirmed by CB agonists/antagonists. DNBS colitis is worsened by prophylactic administration of the CB1 antagonist SR141716A[282] with DSS and oil-of-mustard colitis improved by prophylactic ACEA, a CB1 agonist[285]. Similarly the CB2 agonists JWH133[285], HU308[284], or ALICB459[286] are beneficial at ameliorating chemical colitis models when administered prophylactically. ALICB459 is particularly appealing from a translational medicine perspective as it was effective with oral rather than intraperitoneal administration. CB2 agonists improve, and CB2 antagonists worsen, chemical colitis when administered therapeutically and that this is CB2-dependent[287-289].

Although most studies have utilised a chemical colitis model, JWH133 ameliorates colitis in the $IL10^{-/-}$ model where mice develop spontaneous colitis by 12 weeks of age[288]. GP-1a, purported to be a CB2 agonist, improves ileitis when administered retro-orbitally in the $TNF^{\Delta ARE}$ model of Crohn's-like ileitis. However, recent evidence would suggest this compound may in fact be an inverse agonist of both CB1 and CB2 *in vitro*[121] and so it remains to be confirmed whether CB2 agonism or inverse agonism is effective in this model.

Complementing the results from double knockout studies, use of less selective agonists also display benefits on colitis. WIN55,212 is an agonist of both CB1 and CB2 and ameliorates colitis whether used prophylactically or therapeutically in TNBS and DSS models[290-292]. AM841 (CB1 agonist) improves colitis in a cannabinoid receptor dependent manner, with the effect lost in $CB1^{-/-}$ and $CB2^{-/-}$ mice[293]. The same is true for the CB1 agonist, HU210[282], which also has effects on sustaining intestinal barrier function in a TLR4 independent manner[294]. Interestingly the effect of non-selective cannabinoid receptor activation may be through central rather than peripheral mechanisms. CB13 is an agonist of both CB1 and CB2 with poor penetration of the central nervous system[295]. However, this compound was not effective in murine TNBS or DSS colitis when administered intraperitoneally but was when injected intracerebroventricularly[293]. Equally ineffective was the peripherally-restricted, non-selective agonist, SAB378[290].

Two studies have suggested interplay between cannabinoid signalling and p38 MAPK in the modulation of colitis severity. In the first[291], $Mk2^{-/-}$ mice, who lack a downstream substrate of p38, exhibit a less severe colitis in response to DSS. This study also demonstrated that WIN55,212 impairs phosphorylation of p38 in response to DSS in both wildtype and $Mk2^{-/-}$ mice. Subsequently a similar result has been obtained by using the p38 inhibitor SB203580[292]. One mechanism therefore by which colitis is ameliorated by cannabinoids may be through effects on MAPK pathways.

1.5.2 Endocannabinoid lipid ligands

In addition to the effect of 2AG on colitis detailed above, intraperitoneal AEA improves TNBS colitis[296]. No other studies have been performed using 2AG or AEA. More evidence exists for the role of PEA in colitis. Intraperitoneal injection of PEA is beneficial in both established chemical colitis and when administered prophylactically[297]. The effects are dose-dependent and require PPARα but not PPARγ[298]. This study demonstrated a reduction in TLR4 and S100B expression on enteric glial cells and a reduction in MAPK signalling as potential mechanisms of action. The effect of PEA is also dependent upon CB2 and GPR55[299]. Adelmidrol is a PEA analogue which is effective orally in established colitis in a PPARγ but not PPARα dependent manner, contrary to the earlier study[300].

1.5.3 Hydrolytic enzymes

Although only one *in vivo* study has been performed using MGLL inhibition, several studies have investigated FAAH inhibition. Firstly, $FAAH^{-/-}$ mice exhibit less severe chemical colitis[282]. Use of pharmacological FAAH inhibitors corroborates the findings from the genetic study with amelioration of disease[301-304] in a CB1- and CB2-dependent manner[303]. A combined FAAH/COX inhibitor, ARN2508 was effective in a CB1 and PPARα-dependent manner[305]. Inhibition using FAAH-II not only improved colitis and reduced pro-inflammatory cytokine production, but also impaired infiltration by immune cells and affected expression of micro-RNAs in mesenteric lymph nodes and Peyer's patches of colitic mice[306] as a potential mechanism of action. One study has suggested that therapeutic FAAH inhibition may have additional benefits over prophylactic administration although this remains to be replicated[307]. Despite several studies demonstrating a benefit of

FAAH inhibition, findings are not unanimous. One study demonstrated that PF3845 is effective at ameliorating colitis in the TNBS model but not the DSS model[308]. The beneficial effects on TNBS were not replicated by a second group[297].

Inhibition of N-acylethanolamine-hydrolysing acid amidase (NAAA), results in increased levels of PEA, and not AEA, and improvement in colitis[297]. This corroborates the studies performed using PEA.

1.5.4 Other ECS targets

It is not well understood to what extent the non-CB1, non-CB2 cannabinoid receptors have roles in colitis. The atypical cannabinoid, O-1602, is a derivative of CBD and is known to bind to GPR55. Although it exerts anti-inflammatory effects on both DSS and TNBS colitis, this is independent of GPR55 as genetic knockout of this receptor, and indeed of both CB1/2, does not alter the effect of O-1602[309]. It is not known therefore which pathways this compound acts on in colitis. The GPR55 antagonist CID16020046 and GPR55$^{-/-}$ mice exhibit less severe colitis in response to DSS or TNBS, contrary to genetic knockout or pharmacological inhibition of CB1/2[310]. Therefore whilst CB1/2 are likely to have anti-inflammatory effects, GPR55 triggers a pro-inflammatory cascade.

Inhibition of AEA reuptake using the endocannabinoid membrane transport inhibitor VDM11 has also been shown to improve experimental colitis[302,303].

1.6 Exocannabinoids and *in vivo* colitis

Further to the studies modulating endocannabinoid levels, administration of exocannabinoids in experimental colitis has largely demonstrated similar benefit. B-caryophyllene is available orally and acts via CB2 and PPARγ to limit colitis[311]. The phytocannabinoid, CBD, has been most extensively studied. It reduces intestinal inflammation induced by LPS as measured by TNFα[312]. A reduction in inducible nitric oxide synthase (iNOS) expression has been demonstrated by CBD which also reduces IL-1β and increases IL-10 levels[313]. The effect of CBD is maintained when administered intraperitoneally or rectally but not orally[314]. It has also been shown to potentiate the anti-inflammatory effects of THC in chemical colitis[315]. Synthetic derivatives such as abnormal CBD ameliorates colitis independently of CB1/2 and possibly through GPR18[316] whilst the highly concentrated CBD known as CBD botanical drug substance (a major ingredient of nabiximols) was effective orally and intraperitoneally unlike pure CBD[317]. Reference has been made to benefit of CBD in the $IL10^{-/-}$ mouse in a related publication[318] but this study has not been published independently. Despite these promising findings, CBD has been shown to worsen LPS-induced pulmonary inflammation in mice[319] and so some caution should be maintained.

Other exocannabinoids which have been beneficial at ameliorating colitis include MFF (an extract of medicinal cannabis)[320], cannabigerol[321], and cannabichromene[322].

1.7 Cannabinoids in human IBD

Although studies of cannabinoids in experimental colitis generally appear positive it is important to consider if and how this information might be translated to improved outcomes for patients with IBD. Single nucleotide polymorphisms in some ECS genes have been investigated in human IBD (Table 1.3). The Q63R mutation in the CNR2 gene impairs endocannabinoid-induced inhibition of T cell proliferation[323]. In an Italian paediatric IBD cohort this mutation was associated with a more severe disease phenotype[324] but this was not replicated in a Turkish cohort of adult patients[325]. This may be due to either age or ethnic differences between patients. The G1359A mutation in CNR1 has been shown to have a lower prevalence in patients with UC than controls, and be associated with lower BMI and later age of onset in CD[326]. The C385A substitution in FAAH results in reduced FAAH expression but there are no differences in genotype prevalence in IBD[303,327]. However, there is a possible association of the AA genotype with a penetrating phenotype and increased extra-intestinal manifestations in CD, and earlier age of onset in UC[327]. Interestingly, the FAAH mutation is more prevalent in patients with diarrhoea-predominant or mixed picture irritable bowel syndrome[328].

		Genotype			
FAAH C385A		**CC**	**CA**	**AA**	**Associations**
Storr 2008	CD (n=202)	67.3%	31.2%	1.5%	No differences in prevalence between groups. Phenotype not assessed in this study
	Controls (n=206)	63.6%	35.0%	1.5%	
Storr 2009	CD (n=435)	65.8%	30.1%	4.1%	No differences in prevalence between groups. AA associated with more EIMs and penetrating phenotype in CD; earlier age of onset in UC.
	UC (n=167)	65.3%	32.9%	1.8%	
	Controls (n=406)	61.6%	34.5%	3.9%	
CNR1 G1359A		**GG**	**GA**	**AA**	
Storr 2010	CD (n=216)	53.3%	39.8%	6.9%	Lower prevalence of AA in UC versus controls. AA associated with lower body mass index and later age of onset of CD.
	UC (n=166)	58.4%	38.0%	3.6%	
	Controls (n=197)	52.3%	37.0%	10.7%	
CNR2 Q63R		**QQ**	**QR**	**RR**	
Yonal 2014	CD (n=101)	10.9%	38.6%	50.5%	No differences in prevalence or phenotype in this study.
	UC (n=101)	6.9%	43.6%	49.5%	
	Controls (n=101)	11.9%	37.6%	50.5%	
Striscuglui 2016	CD (n=112)	2.7%	48.2%	49.1%	Paediatric cohort. RR genotype more prevalent in IBD than controls and associated with more severe disease activity at diagnosis. In UC, associated with higher risk of relapse.
	UC (n=105)	18.1%	38.1%	43.8%	
	Controls (n=600)	16.0%	51.7%	32.3%	

Table 1.3 Single nucleotide polymorphisms of components of the ECS studied in human IBD
Prevalence of genotypes are displayed alongside associations with disease phenotype. All abbreviations are referenced in the text.

1.7.1 *Ex vivo* studies

CBD reduces iNOS and S100B expression in cultured biopsies from patients with UC indicating effects on enteric glial cell activation. These effects were dependent on PPARγ, being abrogated by a PPARγ antagonist[312]. Furthermore, fractions of THC have recently been extracted and assayed for effects on colonic IL-6/8 in *ex vivo* biopsies with the greatest benefit seen with Δ^9-tetrahydrocannabinolic acid (THCA) which does not have psychoactive effects[329]. THCA has not yet been used in clinical trials.

1.7.2 Clinical studies including trials of exocannabinoids

Several questionnaire-based studies have confirmed current use of cannabis in 10-15.9% of patients with IBD, with lifetime use in 48.1-67.3% of patients[330-333]. A Canadian study found that 17.6% of IBD patients were current or previous users of cannabis specifically for IBD[334]. The commonest reasons given for cannabis use were to alleviate abdominal pain, diarrhoea or anorexia[331,332,334,335] and use is higher in patients with previous surgery or chronic analgesic requirements[331,332]. Improvements in quality of life have also been demonstrated[332] along with a reduction in estimated clinical disease severity score (Harvey-Bradshaw Index)[335]. A large population based survey confirmed a younger age of onset of cannabis use in patients with IBD and with overall heavier consumption[333]. Another group has identified an association between cannabis use in CD and a higher incidence of surgery[334].

An open label, single arm study of inhaled THC used 'as required' for pain in IBD patients (n=13) demonstrated effects on analgesia, improved quality of life and

increased body mass index[336]. A reduction in Harvey-Bradshaw Index from 11.36 to 5.72 was seen in patients with CD (11/13) and a slight decrease in partial Mayo score for patients with UC (2/13). Subsequently a prospective, placebo-controlled trial of inhaled THC (23% THC, <0.5% CBD) in CD failed to meet its primary endpoint of increased clinical remission[337]. However, effects were seen on clinical response as assessed by the CD Activity Index (CDAI) – a scoring system based on largely clinical parameters with no objective assessment of inflammation[338]. Patients reported improved quality of life and reduced pain which likely accounts for the reduction in CDAI without there necessarily being an effect on inflammation. Alternatively the choice of patients with medically refractory disease in this trial may mask subtle benefits.

The same group performed a double-blind randomised controlled trial (RCT) of oral CBD in CD[339]. There were no safety issues identified but they failed to meet the primary endpoint of a reduction in CDAI after 8 weeks. Whilst this may represent a failure of CBD to exert anti-inflammatory effects in human IBD the randomisation procedure results in 6/10 (60%) of those treated with CBD versus 0/9 (0%) of placebo being current smokers. Smoking is well known to associated with a more difficult-to-treat disease and this may mask an effect of CBD.

A double-blind RCT of GW42003 (96% CBD, 4% THC) in active UC has been published in abstract form only[340-342]. The trial failed to meet the primary endpoint of clinical remission but a reduction in Mayo score and improvement in quality of life was favoured by GW42003. However, only 59% of those treated complied with protocol due to adverse effects likely due to the THC component.

It is interesting to hypothesise why the experimental data is not yet translating into meaningful improvements for patients. This may simply represent immunological differences between species; that chemical experimental colitis models are poor representations of human disease; that the route of drug administration is wrong; or that the inclusion criteria for patients in these trials selected for patients with more advanced, and therefore inherently more difficult to treat, disease. In addition, a recent study has shown that the Jurkat cell line (T cells) is more resistant to the effects of CBD when cultured at physiological normoxia (12%) than at 21%[343]. Given that the intestine is relatively hypoxic[344], especially in the context of active inflammation, this may also explain why exocannabinoids have so far failed to live up to expectations.

1.8 Summary and research objectives

The ECS, although a young field, is highly complex and probably tightly regulated through a combination of synthetic and degradative enzymes, receptor desensitisation, and 'on demand' ligand production. There is accumulating evidence for an anti-inflammatory role for endo and exocannabinoids both *in vitro* and *in vivo* although there are areas of controversy. Much research to date has focussed on animal, particularly murine, cells or models of disease and it is not know to what extent this is translatable to human cells and disease. The innate immune system is of critical importance in the initial response to pathogen challenge. Defects in innate immunology, particularly in dendritic cell function, are associated with the development of IBD. Observational and *in vivo* studies point to a potential benefit of cannabinoids in reducing intestinal inflammation although the results of clini-

cal trials of CBD and THC in human IBD have been disappointing. 2AG, as a full agonist at CB1 and CB2 has been poorly explored in human dendritic cells and the effects of MGLL inhibition are not known. Furthermore, it is not known whether MGLL and other serine hydrolases are expressed in human dendritic cells, including in response to PRR ligation, and in primary human inflamed colonic tissue.

Through a collaboration between Abide Therapeutics (San Diego, USA), who have expertise in serine hydrolase profiling and have recently developed a selective MGLL inhibitor for clinical use, and The University of Oxford the broad aims of this research were:

1) To profile serine hydrolases in moDCs including differential expression on PRR ligation focussing on NOD2/TLR2.
2) To identify whether MGLL is present in moDCs, altered upon PRR ligation and explore its function.
3) To explore the role of *in vivo* MGLL inhibition in a non-chemical murine model of colitis.
4) To profile serine hydrolases including components of the ECS in human colonic tissue from patients with IBD.

Chapter 2 - Materials and Methods

2.1 Cell culture techniques

2.1.1 Generation of human moDCs, macrophages, and murine bone marrow derived DCs (BMDC)

Anonymised leucocyte cones were obtained from the United Kingdom National Health Service Blood and Transplant service using local ethical guidelines (Milton Keynes Research Ethics Committee Ref. 07/H063/43). The cones were centrifuged on a gradient using Lymphoprep™ (StemCell Technologies) to isolate peripheral blood mononuclear cells (PBMCs). CD14 magnetic beads (Miltenyi Biotech) were used to positively select monocytes which were then cultured in RPMI 1640 (Sigma) supplemented with 1% glutamine, 1% penicillin/streptomycin, and 10% foetal calf serum (FCS) in the presence of GM-CSF and IL-4 (Peprotech) in an incubator (37°C, 21% O_2, 5% CO_2) to differentiate into moDCs. Differentiated moDCs were used between days 4-6 unless otherwise stated.

For serum-free studies the cells were washed twice in sterile, room temperature, PBS, centrifuging at 1500rpm for 5 minutes at room temperature between washes. The cells were then resuspended in XVivo-15 media (Lonza) supplemented with 1% glutamine and 1% penicillin/streptomycin for the individual experiment.

To generate primary macrophages, human $CD14^+$ monocytes were differentiated to macrophages over 5-7 days with either 100ng/ml M-CSF or 100ng/ml GM-CSF,

and then polarised for 48h with media alone (M0), LPS 100ng/ml + IFNγ 25ng/ml (M1), or IL-4 20ng/ml (M2) (protocol adapted from [345]).

Murine BMDCs were generated from femurs (a kind gift from Tamara Davenne, University of Oxford) with the assistance of Daniele Corridoni (University of Oxford). The bones were provided stripped of fur and muscle. The femurs were flushed with sterile PBS to isolate bone marrow. The sample was centrifuged at 1500rpm, 3 minutes, 4°C, and resuspended in ice cold PBS. Cells were counted and resuspended at $0.5x10^6$/ml in R10. 20ng/ml IL-4 and 20ng/ml GM-CSF were added to differentiate the cells into BMDCs over 5 days.

2.1.2 Culture of cell lines

THP-1, U937 and Jurkat cell lines, from laboratory stocks, were cultured in RPMI 1640 (Sigma), Hct116 and HeLa in Dulbecco's Modified Eagle Medium (DMEM) (Sigma), and HT29 in McCoy's 5A (Modified) Medium (ThermoFisher Scientific). All media was supplemented with 1% glutamine, 1% penicillin/streptomycin, and 10% FCS and maintained in an incubator (37°C, 21% O_2, 5% CO_2) unless specified otherwise. For subsequent descriptions, R10 refers to RPMI 1640 supplemented with 10% FCS, and D10 to DMEM supplemented with 10% FCS, and usually 1% glutamine + 1% pencillin/streptomycin. Knockdown THP-1 cell lines for TBK1, IKK**ε**, and MyD88 were a kind gift from Daniel Gaughan.

2.1.3 Stimulation with PRR ligands

Cells were plated to a concentration of $1x10^6$/ml and stimulated with PRR ligands. MDP & PAM were used at 10µg/ml and 1µg/ml respectively unless stated

otherwise. Concentrations of other ligands for individual experiments are specified in the text.

Receptor	Ligand	Company	Concentration
NOD2	MDP	Invivogen	0.01-10µg/ml
NOD2	L18-MDP	Invivogen	10µg/ml
TLR1/2	PAM	Invivogen	0.001-1µg/ml
TLR3	Poly(I:C)	Invivogen	1µg/ml
TLR4	LPS	Sigma	100ng-1µg/ml
TLR5	Flagellin	Invivogen	100ng/ml
TLR7/8	R848	Invivogen	1µg/ml

2.1.4 Reconstitution of MGLL inhibitors for *in vitro* studies

The MGLL inhibitors JZL184 and MJN110 were obtained from Abide Therapeutics (San Diego, USA) as dry powder and reconstituted in dimethyl sulfoxide (DMSO) to achieve 10mM stock concentrations which were stored at -20°C. Serial dilution with DMSO was performed to achieve further concentrations. Inhibitors were brought to room temperature before use and incubated with samples for at least 30 minutes prior to stimulation – a time period which has been demonstrated to inhibit MGLL activity in human cells (Abide Therapeutics, personal communication).

2.2 Protein techniques

2.2.1 ABPP (Gel-based and MuDPIT)

Cells were harvested from culture dishes with gentle scraping to remove adherent cells, washed twice with ice cold PBS, centrifuged for 5 minutes at 1500rpm at 4°C, and the supernatant aspirated to dryness with a vacuum aspirator. Cell

pellets were immediately frozen at -80°C and shipped to Abide Therapeutics (San Diego, USA) using a commercial liquid nitrogen dry vapour shipper (Cryoport).

ABPP experiments were performed by the scientists of Abide Therapeutics using methods as previously described[346]. Briefly, the cells were resuspended in ice-cold PBS before lysis by sonication and centrifugation to remove unbroken cells and nuclei. For experiments separating soluble and particulate fractions (to maximise resolution of serine hydrolases) a further centrifugation at 100,000G for 45' was performed. The pellet was resuspended in PBS, protein quantified using the Bradford protein assay and adjusted to a protein concentration of 1mg/ml.

For gel-based ABPP the proteomes were incubated with either a rhodamine-labelled fluorophosphonate probe (FP-Rh) or HT01 and incubated for 30 minutes at room temperature. The reaction was quenched with 4x loading buffer and 30µl added to a 10% sodium dodecyl sulphate (SDS) gel. The mixture was then run for 850VHr by gel electrophoresis and fluorescently labelled proteins visualised in-gel using a flatbed scanner (BioRad). Where control inhibition studies were performed in-house at Abide Therapeutics to confirm band position on gels, small molecule inhibitors were added to the samples for 30 minutes at room temperature before the addition of the fluorescently-labelled probe.

For ABPP-MudPIT the proteomes were adjusted to a concentration of 1-2mg/ml before the addition of a biotin-labelled fluorophosphonate probe to bind all active serine hydrolases. The protein was precipitated using methanol and chloroform before denaturation, reduction and alkylation. Streptavidin beads were

added to each sample and incubated for 1.5h at room temperature to enrich for biotin-bound enzymes. The proteins were digested to individual peptides using trypsin to cut the protein at the carboxyl end of the peptide bond of arginine or lysine residues. Cells were then labelled with either 4% light or 4% heavy formaldehyde to allow isotopic distinction between groups. Samples were stored in formic acid at -80°C until analysed by liquid chromatography-mass spectrometry. The individual proteins were identified by peptide fragment identification with at least two unique peptide fragments required to confirm an individual serine hydrolase. The ratio of heavy to light chain formaldehyde was used to measure relative activity of proteins between samples.

2.2.2 Immunoblotting

Cells were harvested and washed in ice-cold PBS and lysed in lysis buffer. The samples were centrifuged and the supernatant harvested. Protein concentration was measured using the BCA assay (Pierce) and a Fluostar Optima plate reader (BMG Labtech). Dithiothreitol (DTT) and NuPage LDS Sample Buffer (Life Technologies) were added before heating to 70°C for 5 minutes. Equal amounts of protein were loaded into each lane of a 4-12% Bis-Tris NuPage gel (Life Technologies) and a control ladder (RPN800E, GE Life Sciences). Gels were placed in a NuPage tank with NuPage MOPS running buffer (Life Technologies) and run at 120V for 2 hours. Gels were transferred to polyvinylidene fluoride (PVDF) membranes (Amersham, GE Life Sciences) in a NuPage tank contained NuPage transfer buffer (Life Technologies) at 30V for 90 minutes. Membranes were blocked with 5% Bovine Serum Albumin (BSA) (Sigma) in Tris-buffered saline with Tween (TBST) for 1 hour prior to incubation with primary antibody overnight at

4°C. Membranes were then washed in TBST and incubated with the secondary HRP-linked antibody (Cell Signalling) in 5% skimmed milk with TBST for 1 hour at room temperature at a concentration of 1:3000. Membranes were washed in TBST before the addition of ECL detection reagents (Amersham, GE Life Sciences) and development of films. Antibodies used are in Table 2.9.1.

2.2.3 Enzyme-linked immunosorbent assay (ELISA)

Human cells were treated as detailed for individual experiments. Supernatants were aspirated, centrifuged to remove residual cellular debris, and transferred to sterile, flat-bottomed, 96-well plates (Corning). Plates were either used immediately or sealed with Parafilm before being frozen at -20°C.

Sandwich-ELISA kits (R&D systems) were used as per the manufacturer's instructions. Briefly, 96-well plates were coated with capture antibody overnight before washing and adding samples/standards. After the addition of a detection antibody, streptavidin-HRP and substrate solution, the reaction was stopped. Plates were analysed immediately on a Fluostar Optima plate reader (BMG Labtech). A 7-point serial dilution standard curve was calculated on each plate, and samples were processed in technical triplicate, diluted if necessary.

2.3 Cell biology

2.3.1 RNA extraction and real time (quantitative) polymerase chain reaction

RNA was extracted from cells using the RNeasy Mini Kit (Qiagen) following manufacturer's instructions and incorporating a 20-minute DNase (Qiagen) incuba-

tion step. In order to maximise RNA quality, a third RPE wash step was incorporated to the extraction technique which resulted in improved 260/230 values. RNA quality and quantity was measured on a Nanodrop 1000 spectrophotometer (Thermo Scientific). Equal amounts of RNA were converted to cDNA using the High Capacity RNA to cDNA kit (Applied Biosystems) and then real time PCR performed on a BioRad C1000 Thermal Cycler CFX Realtime system using Taqman primers (Life Technologies). Each reaction was performed in triplicate with the mean subsequently calculated. Fold change was measured using the ΔΔCT method normalised to a housekeeping gene (RPLP0 for human studies and β-actin for murine).

2.3.2 Adenosine Triphosphate (ATP)-luminescence cell viability assay

moDCs were suspended in R10 to a concentration of $0.5x10^6$ cells/ml. Cells were incubated with JZL184, MJN110 or DMSO control for 30 minutes and then PRR ligands added. 100µl was aliquoted into wells of a white, tissue-culture treated 96-well plate (Greiner Bio One) before leaving for 30 minutes at room temperature to equilibrate. 100µl CellTiter-Glo® reagent (Promega) was added as per manufacturer's recommendations and the plate mixed on an orbital shaker for 2 minutes before incubation for 10 minutes at room temperature. Luminescence was recorded using the Fluostar Optima plate reader (BMG Labtech).

2.3.3 Fluorescence-based migration assay

moDCs were obtained as detailed above and either left unstimulated or stimulated with MDP/PAM for 16 hours with or without JZL184. CellTracker™ Green (ThermoFisher Scientific) was warmed to 37°C before incubating with cells at a

final concentration of 2.5μM for 40 minutes in an incubator (37°C, 21% O_2, 5% CO_2). Cells were then washed once in R10 media before resting for 30 minutes in fresh media. 500,000 cells (or media for the 'standards' wells) were then added to the top insert of a FluoroBlok® plate (Corning) according to plate design. To the lower chamber either a known number of cells were added ('standards' wells) or media with 25ng/ml CCL21 (R&D Systems). The plate was sealed with Parafilm and immediately placed in a fluorescent plate reader at 37°C (Synergy HT, Biotek) with readings taken every 15 minutes over an 8 hour period.

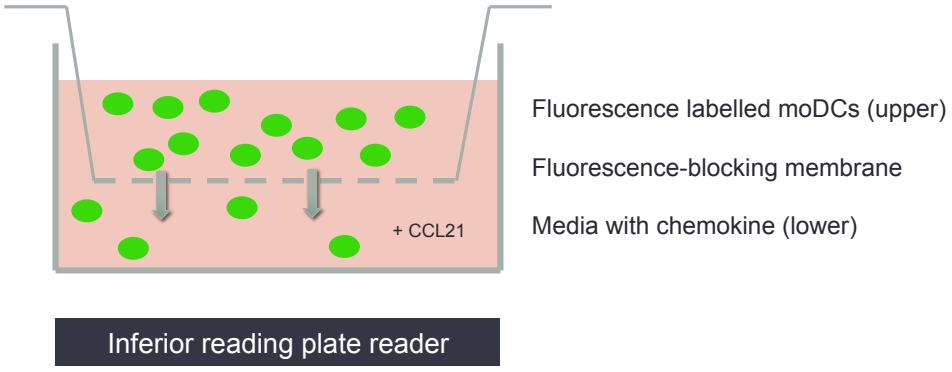

2.3.4 Flow cytometry

Cells were exposed to small molecule inhibitors and stimulation conditions as described in individual experiments. Cells were harvested and transferred on ice before being washed twice in ice cold PBS, centrifuging at 1500rpm, 5 minutes, 4°C between washes. Cells were then resuspended in FACS buffer (either 1% FCS in PBS, or Cell Staining Solution (Biolegend)) and aliquoted either into individual polystyrene round-bottomed flow cytometry tubes (Falcon, Fisher Scientific) or cluster tubes. Antibody or isotype control was added to each tube at a concentration of 1:100, covered with foil, and incubated on ice for 30-60 minutes. Cells

were washed twice with FACS buffer and then resuspended in buffer. Samples were immediately processed either on an LSRII or LSRFortessa (BD Biosciences) but if there was any delay the samples were kept covered with foil and on ice. Data were analysed using FlowJo software version 10.2 (FlowJo LLC, Oregon).

2.3.5 MelanA assay

$CD14^+$ monocytes were isolated from buffy coats as described above. HLA-A2 status (positive/negative) was determined by flow cytometry. $15x10^6$ monocytes were differentiated into moDCs in R10 supplemented with 50μM β-mercaptoethanol, non-essential amino acids, sodium pyruvate, and 12.5mM HEPES. The autologous $CD14^-$ fraction was frozen in 10% DMSO in FCS at a concentration of $20x10^6$ cells/ml per cryovial at -80°C. On day 3, the moDCs were matured with 50ng/ml LPS for 36h, with preincubation with JZL184 for 30 minutes where indicated. Mature dendritic cells were then pulsed with 100ng/ml MART-1 peptide (Proimmune) for 2h at 37°C at a concentration of $3x10^6$ cells/ml in media without serum (RPMI 1640 supplemented with 50μM β-mercaptoethanol, non-essential amino acids, sodium pyruvate, and 12.5mM HEPES) with or without JZL184/DMSO as indicated. The dose of MART1 had previously shown to be effective at expanding melanA specific $CD8^+$ T cells[347]. Negative control cells were not pulsed with peptide.

moDCs were then washed with serum-free media and resuspended to 200,000 cells/ml in fresh serum-free media and plated in a clear 24-well plate (Corning). Autologous thawed $CD14^-$ PBMCs were added to the moDCs at a concentration of 1:5 in media containing 5% human AB serum, 1% glutamine, 1% penicil-

lin/streptomycin. This represents day 0 for the remainder of the experiment. On day 4, recombinant human IL-2 (10U/ml) and IL-7 (5ng/ml) were added (both from Peprotech). On day 10, further IL-2 (500U/ml) was added. Cells were harvested on day 14 and processed by flow cytometry. Where media became yellow over the period of incubation indicating metabolically active cells, 500µl media was removed from all wells and replaced with 500µl fresh media containing 5% human serum with or without JZL184/DMSO as indicated. JZL184 or DMSO was incorporated into the media throughout the experiment.

For flow cytometry, the samples were first incubated with matched MART-1 pentamer (Proimmune) at room temperature for 10 minutes before being washed and incubated with the remaining antibodies as described in the 'Flow Cytometry' section.

2.3.6 Pathogen handling experiments

2.3.6.1 Human Immunodeficiency Virus (HIV) replication assay

moDCs were generated as described and autologous $CD4^+$ T cells isolated from the $CD14^-$ fraction by incubation with biotin-conjugated antibodies to $CD4^-$ cells (Miltenyi) prior to the addition of avidin magnetic beads and isolation of highly pure $CD4^+$ cells by depletion of magnetically labelled cells. Isolation of $CD4^+$ cells and subsequent HIV replication assay performed by Mei-Yi Sun.

On day 5 following isolation of moDCs, cells were harvested and washed to remove IL-4 and GM-CSF and 100µl plated in a 96-well plate (Corning) at a concentration of $1x10^6$ cells/ml. JZL184 was added as indicated at a concentration of

100nM. As a positive control to inhibit HIV replication, the antiretroviral agent nevirapine was used at a concentration of 5μM.

moDCs were exposed to 10,000ng p24 virus (from laboratory stocks) in 10μl R10, mixed and cultured for 90 minutes prior to washing twice (addition of 200μl R10, centrifuge at 1700rpm, 5 minutes, room temperature, discard supernatant). Cells were then resuspended in R10 alone or R10 with autologous CD4 cells, previously treated with phytohaemagglutinin 40μg/ml (Merck), at a ratio of 1:3. After 7 days co-culture, supernatant was harvested and assayed for p24 by ELISA in triplicate.

2.3.6.2 Salmonella handling in THP-1-derived macrophages

To differentiate THP-1 cells into macrophages, the cells were seeded in a 24-well plate (Corning) at a density of $1x10^6$ cells/well in 1ml media and incubated with 25 ng/ml of phorbol 12-myristate 13-acetate (PMA, Sigma) for 24 hours.

Before the infection, the medium was replaced with fresh R10 with glutamine but without antibiotics. Cells were rested for 2h before the addition of JZL184 100nM. 30 minutes later, the cells were infected with *Salmonella enterica* Serovar Typhimurium (LT2 strain) to achieve a multiplicity of infection (MOI) of 20:1 (bacteria:cells). This MOI had been determined on the basis of previous experiments performed by Anna Aulicino and Lorena Preciado-Llanes. Non-infected control macrophages received culture media only. Both non-infected and infected macrophages were prepared in duplicate and incubated at 37°C. The time zero of the experiment was set at the beginning of this incubation.

At 30 minutes post-infection cells were washed twice with PBS to remove extracellular bacteria and fresh media supplemented with 100µg/ml gentamicin was added. After a further 30 minutes incubation (1h post infection) cells were washed once with PBS and fresh medium supplemented with 30 µg/ml gentamicin was added. Gentamicin is necessary to avoid overgrowth of bacteria in the medium. After each wash, fresh JZL184 100nM was added. At each time point following infection (1h, 8h, 24h), medium was removed and 500µl of Saponin 0.1% in PBS was added. After incubation for 5 minutes at 37°C, 500 µl of PBS was added and a 10-fold dilution of the lysates was plated in quadruplicate on LB Agar (Sigma). Plates were incubated overnight and the number of intracellular bacteria was assessed by counting the number of Colony Forming Units (CFU).

2.3.6.3 *E coli*/influenza in PBMCs

PBMCs were isolated from human whole blood using the method outlined above. Cells were counted and resuspended to $10x10^6$ cells/ml. 85µl was added to each well of a round-bottomed 96-well plate and made up to 250µl with R10 containing NEAA, sodium pyruvate and HEPES. Inhibitors were added for 30 minutes before stimulation with either *Escherichia coli* (MOI 7.5:1, from laboratory stocks), 3µl influenza human split virion vaccine 2014 (from laboratory stocks), or PMA/ionomycin. After 90 minutes incubation, gentamicin 100µg/ml was added for 90 minutes, before the addition of brefeldin. Cells were incubated for 14h and flow cytometry performed for cytokine analysis using markers and gating for

T-cell subtypes. The gating strategy was determined, and data collected, by Lorena Preciado-Llanes based on previous optimisation.

2.3.7 Microarray sample preparation, running, and analysis

moDCs were generated as previously described and incubated with or without MGLL inhibitor for 30 minutes prior to the addition of MDP/PAM for 8, 16 or 24h. Cells from the 8 and 16h timepoints were harvested, washed twice in ice cold PBS, resuspended in RLT (Qiagen) with β-mercaptoethanol and frozen at -80°C. Cells from the 24h timepoint were harvested, washed twice in ice-cold PBS, and frozen at -80°C prior to ABPP analysis.

Samples were defrosted on ice and RNA extracted. RNA quality and quantity was measured on a Nanodrop 1000 spectrophotometer (Thermo Scientific) along with calculation of the RNA integrity number (RIN) and 28S/18S ratio (Agilent 3100 Bioanalyser). RNA concentrations were normalised across all samples to 100ng/μl and randomly plated in a 96-well, white, skirted PCR plate and frozen at -80°C before being taken to the Wellcome Trust Centre for Human Genetics (WTCHG) (Helen Lockstone, Benjamin Wright, Dilair Baban).

There the RNA was prepared and hybridised to Illumina BeadChip microarrays following manufacturers' protocols. Raw data were imported into the R statistical software[348] for further processing and analysis using BioConductor packages[349]. Raw signal intensities were background corrected (using array-specific measures of background intensity based on negative control probes), prior to being transformed and normalised using the 'vsn' package[350]. A range of quality control

checks were made which did not identify concerns in data quality. The dataset was then filtered to remove probes not detected above background levels (detection score <0.95) in any of the samples, resulting in a final dataset of 20,135 probes.

Statistical analysis to identify differential gene expression was performed with the Linear Models for Microarray Analysis (limma) package[351]. Raw p-values were corrected for multiple testing using the false discovery rate (FDR) controlling procedure of Benjamini and Hochberg[352], corrected at 5% FDR. Results were annotated with gene information using the relevant BioConductor annotation package (Mark Dunning, Andy Lynch and Matthew Eldridge (). illuminaHumanv4.db: Illumina HumanHT12v4 annotation data (chip illuminaHumanv4). R package version 1.22.1.). Assistance with data analysis was also provided by Steve Taylor (Computational Biology Research Group, Weatherall Institute of Molecular Medicine, Oxford).

2.3.8 Trained immunity in monocytes

The protocol described here is based on previously published methods[353] and helpful discussions with Dominik Aschenbrenner, University of Oxford. $CD14^+$ monocytes were isolated from peripheral human blood as described above and resuspended to a concentration of $1x10^6$ cells/ml in RPMI1640 supplemented with 1% penicillin/streptomycin, 1% glutamine, NEAA, 1mM sodium pyruvate and 20% pooled human serum. $1x10^5$ cells (100µl) were added to each well of a 96 well and incubated with either DMSO or 100nM JZL184 for 2 hours prior to the addition of the first stimulation (media alone; β-glucan 5µg/ml; LPS

100ng/ml). Cells were incubated for 24h before being washed and resuspended in R10 (pooled human serum) with/without M-CSF and with DMSO or JZL184. Cells were rested for 6 days with the media refreshed at day 3. On day 6, the second stimulation was added (media alone; β-glucan 5μg/ml; LPS 10ng/ml) with DMSO or JZL184. Supernatant was harvested after a further 24h and processed for ELISA.

2.3.9 THP-1 inflammasome assay

500μl THP-1 cells were plated into 24 well plates at a concentration of $1x10^6$/ml. 100nM JZL184 was added for 2h prior to 1μg/ml LPS. After 3h, 5μM nigericin was added for 45 minutes. The supernatant was aspirated and processed by ELISA.

2.4 Transfection techniques

2.4.1 siRNA transfection of moDCs

moDCs were transfected with short interfering RNA (siRNA) by electroporation (Neon Transfection System, ThermoFisher Scientific) with either gene-specific siRNA, obtained as a mix of 4 different siRNA (ON-TARGET*plus* SMARTpool, Dharmacon, UK), or non-targeting siRNA (ON-TARGET*plus*, Dharmacon, UK). siRNA were reconstituted according to the manufacturer's guidelines in RNase-free water to a stock solution of 20μM, aliquotted and frozen at -20°C before use.

moDCs were harvested on day 3 and washed in sterile PBS to remove serum. Cells were resuspended in Buffer R and a variable concentration of gene-specific siRNA added according to the individual experiment. Non-targeting siRNA was

added at a concentration of 1:100. The Neon electroporation machine was set at 1475V, width 20ms, pulse 2 and prepared according to manufacturer's guidelines. R10 with 1% glutamine, but no antibiotics, was prewarmed to 37°C and aliquots placed into wells of a 6-well plate (Corning). The cell suspension-siRNA mix was loaded into the Neon pipette and placed on the machine for electroporation with care taken to avoid the introduction of bubbles. The suspension was carefully observed for signs of arcing during the electroporation and cells discarded if this was observed.

2.4.2 shRNA transfection of THP-1 cells

Plasmid DNA targeting five different sequences of the MGLL gene, a control scrambled plasmid DNA (shc216), or GFP-encoding plasmid DNA (shc203) were obtained (Mission, Sigma, St Louis; Table 2.9.2). 100ng of each plasmid DNA were added to individual 50µl vials of Stbl3 chemically competent *E coli* (Invitrogen) and incubated on ice for 30 minutes. A waterbath was heated to 42°C and the plasmid DNA-Stbl3 mix subjected to heat shock for 45 seconds before being immediately placed back on ice for 2 minutes. 250µl of SOC media was added and the mix then shaken for 1 hour at 225rpm, 37°C. Aliquots of the mix were then spread onto pre-warmed selective plates containing LB agar with 100µg/ml ampicillin. The plates were incubated overnight and then a single colony transferred to a 15ml conical tube (Falcon) containing 3ml LB broth with 100µg/ml ampicillin. The tube was incubated for 4 hours at 37°C. 200µl of this starter culture was then added to 200ml of the LB broth/ampicillin mix and incubated overnight at 37°C shaking at 250rpm. The following day the cultures were harvested and centrifuged at 6000 x g for 15 minutes at 4°C and the resulting pellet frozen at -80°C.

The pellet was thawed and the DNA isolated using an endo-free plasmid maxi-prep kit (Qiagen) and the amount of DNA verified using a Nanodrop 1000 spectrophotometer (Thermo Scientific) before being frozen at -20°C.

$1x10^6$ Hek293TLA cells were seeded at a concentration of $0.5x10^6$ cells/ml into wells of a 6-well plate (Corning) in D10 with 1% glutamine but without antibiotics. The cells were allowed to reach approximately 75% confluence and the media refreshed. The transfection mastermix per well comprised; 8µl Fugene-6 (Promega), 1µg PAX2 packaging vector, 0.4µg pMD2.G VSV-G envelope plasmid. 1.6µg plasmid DNA, made up to 200µl with Optimem (Life Technologies) and added dropwise to the Hek293TLA cells and incubated overnight at 37°C.

The following day the media was refreshed with 3mls D10 without antibiotics for a further 24 hours. The supernatant from each well was then transferred to 15ml conical tubes (Falcon) and centrifuged at 1500rpm for 5 minutes and then filtered through a 0.45µm filter (Sartorius) into new 6-well plates. THP-1 cells were resuspended at $2x10^6$ cells/ml in R10 without antibiotics and 2ml added to wells of a 6 well plate (Corning). 2µl Polybrene was added to give a final concentration of 8µg/µl and the mix left for 2 minutes before the addition of pre-warmed viral supernatant. After incubation at 37°C for 3 hours, the wells were harvested into conical tubes and centrifuged at 1500rpm for 5 minutes. The pellets were resuspended in R10, plated into 6-well plates and incubated for 3 days. After 3 days the media was refreshed and cells were resuspended in R10 containing puromycin 1µg/ml and subsequently passaged every 3-4 days.

2.5 Lipidomics

Similar methods for lipidomic analysis were used by Abide Therapeutics and the Babraham Institute, Cambridge. For cultured cells, lipids were extracted using methanol/chloroform and spiked with internal standards (for example, 1 nmol of 2-AG-d5, 0.1 nmol of AEA-d4, 1 nmol of AA-d8, and 0.1 nmol of PGE2-d9). For media, lipids were extracted from 4ml of media in an analogous manner and then spiked with standards. Lipid metabolites were separated by liquid chromatography and identified/quantified by tandem mass spectrometry using in-house methods. Metabolite species were quantified by measuring the area under the peak in comparison with the appropriate unnatural internal standard and normalizing for protein concentration for cultured cells.

2.6 *In vivo* murine techniques

2.6.1 Animals

Female C57BL/6 mice aged 8 weeks (Charles River Laboratories, UK) were housed in individually ventilated cages (maximum 6 mice per cage) with corn cob bedding, balconies, red tubes and a sizzle nest. The mice were fed ad libitum with Rat & Mouse No. 3 Breeding pellets (Special Diet Service, UK) and had free access to water. Interventions were performed in the light cycle. Experiments were conducted in accordance with local animal care committees (UK Scientific Procedures Act 1986). Animals were culled by carbon dioxide inhalation and subsequent cervical dislocation. Animal handling, administration of drugs, gavage of *Citrobacter*, and culling was performed by Claire Pearson with assistance from Daniele Corridoni (both University of Oxford).

2.6.2 Administration of MGLL inhibitor (ABD1970)

ABD1970 (Abide Therapeutics, San Diego, USA) was received as a dry powder in individual glass vials for each day of administration, and reconstituted in a vehicle of PBS (Sigma), PEG35 castor oil (Kolliphor EL CAS 61791-12-6, Sigma), and 100% ethanol (Sigma) at a ratio of 18:1:1. Reconstitution was performed in a microbiological safety cabinet and reconstituted compound constantly inverted before administration to mice within 1 hour. The PEG35 castor oil was kept protected from light at all times.

To make the higher dose (6mg/kg) a 1:1 mixture of PEG35 castor oil and ethanol was made and then a certain volume added to the compound based on weight (10% final volume). The mixture was vortexed and bath sonicated for 30 minutes to achieve a fine homogeneous suspension. PBS was added to achieve the final volume, the mixture then vortexed and bath sonicated for a further 30 minutes. An aliquot of the higher dose was then mixed with complete vehicle to dilute to 2mg/kg.

Mice were weighed and 10ml/kg of high dose, low dose, or vehicle administered by intraperitoneal injection. The first dose was given 4 hours prior to the administration of *Citrobacter rodentium* and then once daily thereafter.

2.6.3 Induction of colitis

Citrobacter rodentium was prepared by Claire Pearson. The bacteria was defrosted from laboratory glycerol stocks and spread across an LB agar plate (Sigma) supplemented with nalidixic acid (Sigma) overnight at 37°C. The following morn-

ing a single colony was inoculated into LB broth supplemented with nalidixic acid and incubated on a shaker at 37°C overnight. The optical density was assessed until bacteria reached the log phase (OD 1-1.5). Inoculation of mice was with $5x10^9$ CFU by oral gavage. Weight loss was monitored throughout the experiment.

2.6.4 Macroscopic and histological grading of colitis

After sacrifice, colonic length was measured and samples of distal colon and caecum were placed in buffered 10% formalin (3.7% w/v formaldehyde). 4-5µm paraffin-embedded sections were cut and stained with haematoxylin and eosin. Inflammation was assessed using a structured pathological assessment of epithelial hyperplasia and goblet cell depletion (score 0-3), lamina propria inflammation (score 0-3), area affected (score 0-3), and markers of severe infection such as crypt abscesses and crypt branching (score 0-3)[354]. Scores were added to give an overall score between 0-12 and was scored by two independent, blinded, and experienced assessors.

2.6.5 Colony forming unit (CFU) quantification

CFU quantification performed by Claire Pearson. After sacrifice, samples of colon, caecum, liver and spleen were placed into homogenisation tubes (Percellys) containing 800µl PBS, weighed, and homogenised for 40 seconds at 6.5m/s (Fastprep, MP Biomedicals). Homogenate was then plated onto LB agar plates containing nalidixic acid with serial dilutions for colon/caecum and incubated overnight. CFU were counted manually the following day.

2.6.6 Tissue cytokine quantification by qPCR

Samples of colon and caecum were taken at the time of sacrifice and immediately placed in 500µl RNALater (Ambion). RNA was extracted using the RNeasy mini-kit (Qiagen) as previously described with a preceding homogenisation step. Samples were transferred into homogenisation tubes (Percellys) containing 350µl RLT/β-mercaptoethanol and homogenised at 6.0m/s for 20-30 seconds (Fastprep, MP Biomedicals) before the lysate was transferred to QIAShredder columns. The columns were centrifuged at maximum speed for 15s and the flowthrough mixed with 70% ethanol (in RNase free water) and transferred to RNeasy mini spin columns and RNA extracted as previously described.

2.6.7 Systemic cytokine production by ELISA

Prior to murine sacrifice, 24-well plates (Corning) were coated with 200µl 0.5µg/ml murine anti-CD3e (BD Biosciences) for 24h at 4°C, washed with sterile PBS, and then coated with 500µl 1µg/ml murine anti-CD28 (BD Biosciences). Mesenteric lymph nodes (MLN) were harvested at the time of sacrifice and stored on ice in 15ml polypropylene tubes (Falcon) containing 5ml sterile PBS. On the same day as sacrifice the MLN was passed through a 0.2µm cell strainer using the end of a 1ml syringe, into a 50ml polypropylene tube (Falcon). The strainer was then washed with 10ml sterile PBS. The 50ml tubes were centrifuged at 1500rpm for 10 minutes at 4°C. The supernatant was discarded and the cells resuspended in 3ml sterile PBS and counted. After a further centrifugation step the cells were resuspended in R10 to a concentration of $2x10^6$/ml. 500µl was then aliquoted into wells of the 24-well plates (Corning) prepared with anti-CD3e and anti-CD28. The plates were incubated for 72h (37°C, 21% O_2, 5% CO_2,

humidified). After 72h the supernatants were harvested into sterile 1.5ml Eppendorfs, centrifuged at 1500rpm for 10 minutes at 4°C. The supernatant was transferred into fresh Eppendorfs and immediately frozen at -80°C. The supernatants were then defrosted as required for ELISA analysis of cytokines.

2.7 *Ex vivo* techniques

2.7.1 Obtaining colonic tissue

Colonic biopsies were obtained endoscopically from healthy controls and patients with IBD. A maximum of 12 biopsies per patient were obtained. Ethical permission was granted through the Oxford GI Biobank (Research Ethics Committee ref. 11/YH/0020) and IBD Cohort (Research Ethics Committee ref. 09/H1204/30).

2.7.2 RNA analysis of colonic tissue

Biopsies for RNA analysis were immediately placed in 500µl RNAlater (Ambion) and frozen at -80°C. Samples were transferred into 1.5ml homogenisation tubes containing autoclaved glass beads, together with 350µl RLT/β-mercaptoethanol. Samples were homogenised at 6.0m/s for 20-30 seconds (Fastprep, MP Biomedicals) before the lysate was transferred to QIAShredder columns. The columns were centrifuged at maximum speed for 15s and the flowthrough mixed with 70% ethanol (in RNase free water) and transferred to RNeasy mini spin columns and RNA extracted as previously described.

2.7.3 ABPP analysis of colonic tissue

Immediately after endoscopic collection, biopsies were placed in cryovials (Fisher Scientific), snap frozen in liquid nitrogen, and stored in liquid nitrogen before shipment to Abide Therapeutics (San Diego, USA) using a liquid nitrogen dry vapour system (Cryoport).

The biopsies were thawed and resuspended in PBS and homogenized in a Bullet Blender homogenizer (Next Advance, Inc.) using the tissue-specific protocols recommended by Next Advance. The tissue homogenates were dispersed by probe sonication (performed in a biosafety cabinet) and centrifuged at 1000G for 10 min at 4°C to remove debris. The supernatant was centrifuged at high speed (100,000G for 45 min at 4°C) and the supernatant of the high-speed spin was collected and saved as the soluble homogenate. The pellet was washed and resuspended in PBS, dispersed by probe sonication, and saved as the membrane (particulate) homogenate. The total protein concentration of each homogenate was determined using a DC Protein Assay kit (Bio-Rad). The proteomes were diluted to 0.5 mg/mL and aliquots were stored at -80°C until processing by gel-based methods and mass spectrometry as previously described.

2.8 Statistical analysis

Statistical analysis and graphical representation was performed using GraphPad Prism 7.0a software (GraphPad, La Jolla, CA) and Adobe Illustrator (Adobe, USA) Image intensity quantification was performed using ImageJ version 2.0.0 (National Institutes of Health, USA). Generally the Student's t-test (paired, two-tailed) was used to compare two samples, and ANOVA with Bonferroni's multiple

comparison test to compare multiple samples. Bar charts are displayed as mean +/- standard error of the mean (SEM) unless stated otherwise. Technical replicates are from the same sample, analysed on the same day. Biological replicates are from independent experiments.

2.9 List of materials

2.9.1 Antibodies for immunoblotting

Antibody	Company	Catalogue number
β-actin HRP linked	CST	5125S
CB2	Sigma	SAB1306696
CB2	Santa Cruz	sc-293188
IKKε	CST	2905S
MGLL	Santa Cruz	sc-398942
MyD88	CST	4283
pDRP1 (S616)	CST	3455
PLA2G4A	Sigma	SAB2501599
PLA2G15	Sigma	HPA041702
LIPA	Sigma	SAB1406085
LPL	Sigma	SAB2700761

2.9.2 shRNA clones

MGLL plasmid DNA clone (Sigma)	Sequence
TRCN0000048709	CCGGGCATGTGGATTCCATGCAGAACTCGAGTTCTGCATGGAATCCACATGCTTTTTG
TRCN0000048711	CCGGCAACTCCGTCTTCCATGAAATCTCGAGATTTCATGGAAGACGGAGTTGTTTTTG
TRCN0000048712	CCGGCCAATCCTGAATCTGCAACAACTCGAGTTGTTGCAGATTCAGGATTGGTTTTTG
TRCN0000301052	CCGGCCAGGACAAGACTCTCAAGATCTCGAGATCTTGAGAGTCTTGTCCTGGTTTTTG
TRCN0000331408	CCGGCAACTCCGTCTTCCATGAAATCTCGAGATTTCATGGAAGACGGAGTTGTTTTTG

2.9.3 Inhibitors

Inhibitor	Company	Catalogue number
ABD101970	Abide Therapeutics	N/A
Apigenin	Enzo	BML-EI345
Bay613606	Alexis Biochemicals	270-479-M001
BIO	Not known	
BX795	Invivogen	Tlrl-bx7
GSK2578215A	Tocris	4629
H89	CST 98445	9844
JZL184	Abide Therapeutics	N/A
MJN110	Abide Therapeutics	N/A
PD0325901	Axon Medchem	1408
Ponatinib	Cayman Chemicals	11494
PP2	Enzo	BML-EI297
Raf 1 kinase inhibitor	Calbiochem	553008
SB203580	CST	5633
SP600125	Not known	
VX745	Santa Cruz	sc361401
Wortmannin	Calbiochem	681675

2.9.4 Human primers for qPCR

Gene	Company	Catalogue number
ABHD6	Life Technologies	Hs00977889_m1
ABHD12	Life Technologies	Hs00385102_m1
CNR1	Life Technologies	Hs01038522_s1
CNR2	Life Technologies	Hs00275635_m1
CYSLTR1	Life Technologies	Hs00929113_m1
CXCR5	Life Technologies	Hs00540548_s1
DAGLA	Life Technologies	Hs00391374_m1
DAGLB	Life Technologies	Hs00373700_m1
FAAH	Life Technologies	Hs01038660_m1
FCHO1	Life Technologies	Hs00322606_m1
GPR34	Life Technologies	Hs00758331_m1
HHEX	Life Technologies	Hs00242160_m1
IFNβ	Life Technologies	Hs01077958_s1
IL1α	Life Technologies	Hs00174092_m1
IL1β	Life Technologies	Hs01555410_m1
IL6	Life Technologies	Hs00985639_m1
IL8	Life Technologies	Hs00174103_m1
IL10	Life Technologies	Hs00961622_m1
IL12B	Life Technologies	Hs01011518_m1
IL18	Life Technologies	Hs01038788_m1

IL23A	Life Technologies	Hs00900828_g1
KLF4	Life Technologies	Hs00358836_m1
MGLL	Life Technologies	Hs00200752_m1
NDRG2	Life Technologies	Hs01045114_g1
PLA2G4A	Life Technologies	Hs00233352_m1
RPLP0	Life Technologies	Hs99999902_m1
SCN1B	Life Technologies	Hs03987893_m1
SSBP4	Life Technologies	Hs04184691_g1
TNFα	Life Technologies	Hs01113624_g1
TOP1MT	Life Technologies	Hs01080056_m1

2.9.5 Murine primers for qPCR

Gene	Company	Catalogue number
18s rRNA	Life Technologies	Mm04277571_s1
β-actin	Life Technologies	Mm02619580_g1
CCL2	Life Technologies	Mm00441242_m1
GAPDH	Life Technologies	Mm99999915_g1
IFNγ	Life Technologies	Mm01168134_m1
IL1α	Life Technologies	Mm00439620_m1
IL1β	Life Technologies	Mm00434228_m1
IL4	Life Technologies	Mm00445259_m1
IL6	Life Technologies	Mm0044619_m1
IL10	Life Technologies	Mm00439614_m1
IL12A	Life Technologies	Mm00434169_m1
IL17A	Life Technologies	Mm00439619_m1
IL18	Life Technologies	Mm00434225_m1
IL23A	Life Technologies	Mm01160011_g1
MGLL	Life Technologies	Mm00449274_m1
TNF	Life Technologies	Mm00443258_m1

Chapter 3 – MGLL is induced upon PRR ligation of moDCs and regulates cellular and secreted lipids

3.1 Introduction

The serine hydrolase family comprises about 240 enzymes in humans with a diverse range of functions. They are characterised by an active site serine nucleophile, as part of a catalytic dyad (e.g. Ser-Lys) or triad (e.g. Ser-His-Asp), which binds covalently to substrate[355]. This releases the first reaction product to form an intermediate. A water molecule then binds, hydrolysing the intermediate to release a second reaction product and regenerate the enzyme[356]. Broadly these enzymes can be divided into serine proteases, which exist as zymogens, and metabolic serine hydrolases. The latter group are less well studied but comprise a greater set of functions including lipases, esterases, and peptidases. Inhibitors of enzymes within the serine hydrolase family are in use clinically and include the DPP4 inhibitors for diabetes[357], acetylcholinesterase inhibitors for dementia[358], and some of the novel oral anticoagulants such as dabigatran[359] and rivaroxaban[360]. Deficiencies in many metabolic serine hydrolases are associated with human disease, particularly lysosomal storage disorders and lipid balance, emphasising their essential role in normal physiology and function (Table 3.1, adapted from [355]). The endocannabinoid-hydrolysing enzymes including MGLL, FAAH, ABHD6 and ABHD12 are all members of the metabolic serine hydrolase family. Further understanding of the prevalence and mode of action of serine hydrolase enzymes may not only improve understanding of biology of disease but also yield novel therapeutic approaches.

Serine hydrolase	Abbreviation	Effect
αβ-hydrolase domain containing 11	ABHD11	Deleted in Williams-Beuren syndrome
αβ-hydrolase domain containing 12	ABHD12	PHARC syndrome (polyneuropathy, hearing loss, ataxia, retinitis pigmentosa, and cataract)
Cathepsin A	CTSA	Galactosialidosis
Lecithin-cholesterol acyltransferase	LCAT	HDL deficiency and changes in VLDL/LDL fractions
Lysosomal acid lipase	LIPA	Wolman's disease or cholesterol ester storage disease with widespread fat accumulation
Hepatic lipase	LIPC	Case reports of deficiencies associated with elevations in VLDL and LDL
Lipoprotein lipase	LPL	Loss of function mutations associated with elevations in chylomicrons, triglycerides and VLDL
Ovarian tumour suppressor candidate 2	OVCA2	Deleted in 80% of ovarian cancers
Phospholipase A2 group 7	PLA2G7	4% of the Japanese population have a missense mutation which correlates with respiratory symptoms
Palmitoyl protein thioesterase 1	PPT1	Infantile neuronal ceroid lipofuscinosis
Prolyl endopeptidase	PREP	Hypotonia-cystinuria syndrome
Sialate O-acetylesterase	SIAE	Mutations are associated with autoimmune disorders

Table 3.1 Deficiencies in serine hydrolases associated with human disease

3.1.1 Activity-based protein profiling

ABPP is a technique designed to assess the activity of enzymes within biological samples. Conventional protein detection methods, such as immunoblotting, provide information on abundance of protein but do not necessarily provide information on the functional relevance of protein abundance. For instance, function of an enzyme may be affected by post-translational modifications (such as phosphorylation or ubiquitinylation) or conformational adjustment which renders the active site inaccessible to substrate but may still be detectable by immunoblot. Furthermore, immunoblotting requires the investigator to know which protein they are interested in and for there to be a selective and specific antibody. This technique is not conducive to screening a family of enzymes in a biological sample.

ABPP utilises an activity probe, which binds covalently to the active site of a family of enzymes which share similar structural features, linked to a reporter tag to measure enzyme activity[356]. Activity may be reported either by a fluorophore such as rhodamine or, for instance, biotin to allow for enrichment and downstream identification of proteins. Serine hydrolases, such as MGLL, avidly bind fluorophosphonate (FP) derivatives resulting in irreversible inhibition, and this binding requires the enzyme to be catalytically active[361]. Therefore, inactive enzymes (such as serine protease zymogens) or those to which an inhibitor has bound to the active site, will not bind the FP-probe and will not be measured as active. Although the FP probes cover about 80% of metabolic serine hydrolases[362], further coverage can be achieved using other activity probes such as HT-01 which is of benefit in detecting activity of DAGL[363].

The active proteome using a rhodamine-tagged probe may be read using standard gel electrophoresis techniques to separate individual proteins by molecular weight[346]. The intensity of the resulting band correlates with active enzyme rather than, necessarily, total protein abundance. Inhibitor specificity can be assayed using competitive gel-based ABPP whereby the proteome is first incubated with a small molecule inhibitor before adding the activity-probe. The resulting band intensity can be compared with a control, uninhibited, proteome with off targets visualised[356].

Using a biotinylated activity probe, samples can be analysed using MultiDimensional Protein Identification Technology (MuDPIT). This technique was first described in 2001 to profile the proteome of *Saccharomyces cerevisiae*[364]. This technique does not require gel electrophoresis prior to mass spectrometric analysis nor does it require operator intervention once the sample is loaded. Instead the sample is loaded onto a microcapillary tube before being separated by liquid chromatography and tandem mass spectrometry, so-called shotgun proteomics[365]. The resulting peptides are automatically mapped to databases within the system i.e. both resolution of peptides and generation of mass spectrometry profiles occurs within the same system. The technique has been described as both representative and unbiased[364]. The resulting peptide spectra can be counted (spectral counting) and this has been shown to correlate with relative abundance between samples with higher abundance proteins being sampled more frequently[365]. Coupling MuDPIT to ABPP enables the formal identification of active/functional serine hydrolase enzymes within samples[346]. Comparative protein abundance between samples can be assessed by labelling peptides with

heavy or light formaldehyde to enable isotopic distinction of the resulting spectra[366]. A particular limitation of ABPP-MuDPIT is the large amount of sample material required (approximately 1mg)[346].

ABPP is not limited to the serine hydrolase family with probes designed for cysteine proteases, tyrosine phosphatases, and kinases[367] in humans, and the development of probes for microbes[368] which may have beneficial implications for anti-microbial therapy[369].

3.1.2 Therapeutic potential of covalent drugs

Covalent-binding drugs offer potential benefits including higher potency, lower dose and extended duration of action over their non-covalent counterparts[370]. However, there has been historical concern over off-target effects of such drugs largely because of indiscriminate modification of biological processes[371]. The covalent mechanism of action of many historical drugs was often discovered after the drug was introduced clinically rather than as part of the drug design process. The process of design of targeted covalent inhibitors requires an in depth pipeline including bioinformatics, *in vitro* biology, chemistry and proteomics, and extensive pharmacological studies to minimise the risk of off-target effects[371]. The potential for catastrophe should drug design go wrong is, however, substantial. A recent phase 1 clinical trial of a novel FAAH inhibitor, BIA 10-2474, resulted in adverse neurological sequelae in 5 of 6 participants including one brain death and two with persistent symptoms[372]. Subsequent profiling, by competitive ABPP, of the actions of the therapeutic compound demonstrated multiple off-target effects on other serine hydrolases with remodelling of lipid networks in

human cortical neuron cultures[249]. This study also highlighted differences in off-target activities between mouse and human emphasising the difficulties in extrapolating animal work directly to humans.

ABPP has been used extensively in cancer tissues[373] and cancer cell lines to identify novel pathways underlying cancer pathogenesis but has not previously been applied to primary human immune cells. It is not known to what extent serine hydrolase activity, and MGLL in particular, is modulated upon engagement of PRRs, what influence this may have upon dendritic cell function, and whether this could lead to novel drug design for inflammation.

3.2 Aims

1. To profile and validate serine hydrolase activity including MGLL in primary human moDCs and effects of PRR stimulation.
2. To explore expression of ECS genes in moDCs and cell lines relevant for myeloid immune cells and colonic epithelial cells.
3. To identify a role for MGLL on regulating lipid levels in moDCs.
4. To screen key signalling molecules which might govern MGLL transcription in moDCs.

3.3 Results

3.3.1 Gel-based ABPP highlights altered serine hydrolase expression on NOD2/TLR2 stimulation of moDCs

In order to interrogate the serine hydrolase family and how this might alter upon engagement of PRRs, moDCs were stimulated with either MDP, a NOD2 ligand, or PAM, a TLR2 ligand, over a timecourse up to 24 hours. Gel-based ABPP was performed on the samples and demonstrated dynamic changes in activity of some serine hydrolases (Figure 3.1A). Of particular note was a band appearing at 33kDa after 24 hours stimulation with either ligand. By incubating the 24h proteome with a specific inhibitor (ABD1970) for 30 minutes prior to performing ABPP, this was demonstrated to be MGLL (Figure 3.1B/C).

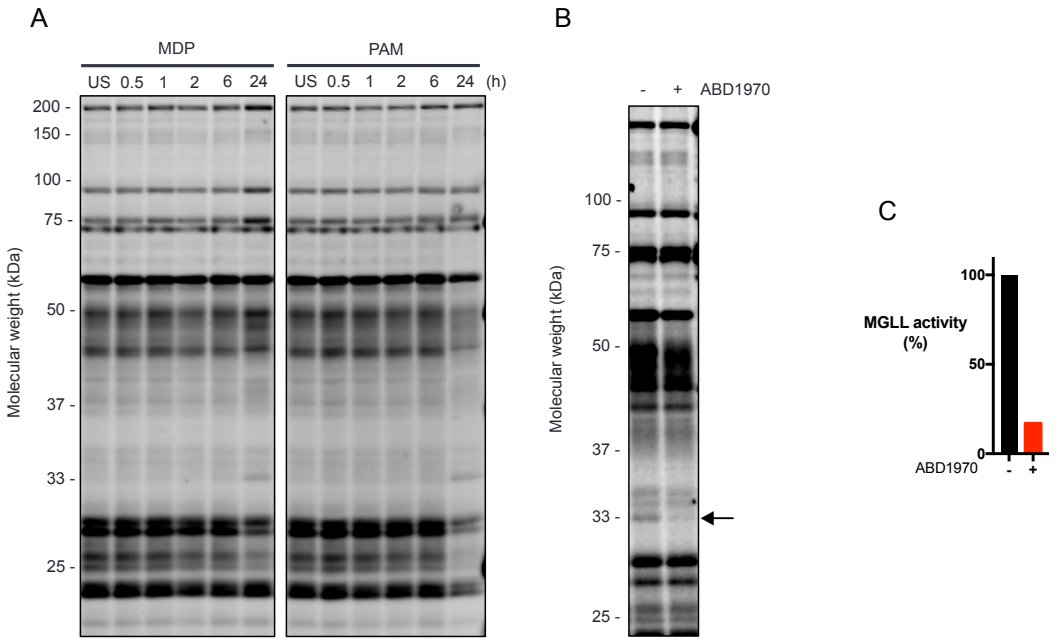

Figure 3.1 MGLL is upregulated following MDP or PAM stimulation in moDCs
(A) moDCs were stimulated with 10μg/ml MDP or 1μg/ml PAM and profiled by gel-based ABPP for changes in serine hydrolase activity over time. **(B)** The proteome at 24h was incubated with the MGLL inhibitor ABD1970 for 30 minutes prior to performing gel-based ABPP which confirmed the band at 33kDa to be MGLL (black arrow). **(C)** Densitometry of the gel in (B) confirmed a reduction in MGLL activity with ABD1970. Results are representative of two biological replicates.

3.3.2 TLR2 engagement has a greater effect on MGLL activity than NOD2 and synergy between these ligands is not seen by gel-based ABPP

Given the known interaction between NOD2 and TLR2 in innate immune sensing, moDCs from a further three donors were generated and exposed to each ligand individually or with combined MDP/PAM. Three timepoints were chosen based on the earlier results: unstimulated, 8h, and 24h. The results highlighted striking similarity in serine hydrolase activity between donors, across timepoints, and stimulation conditions (Figure 3.2A). MGLL activity was increased initially at 8h and further at 24h, corroborating the results of the previous experiment. This was predominantly by TLR2 stimulation with no additive or synergistic effect of combined NOD2/TLR2 stimulation (Figure 3.2B). The moDCs from each donor were confirmed to be functioning by immunoblotting for phosphorylated dynamin related protein 1 (pDRP1; Figure 3.2C), a protein our group have recently shown to be induced on PRR ligation in moDCs (unpublished data).

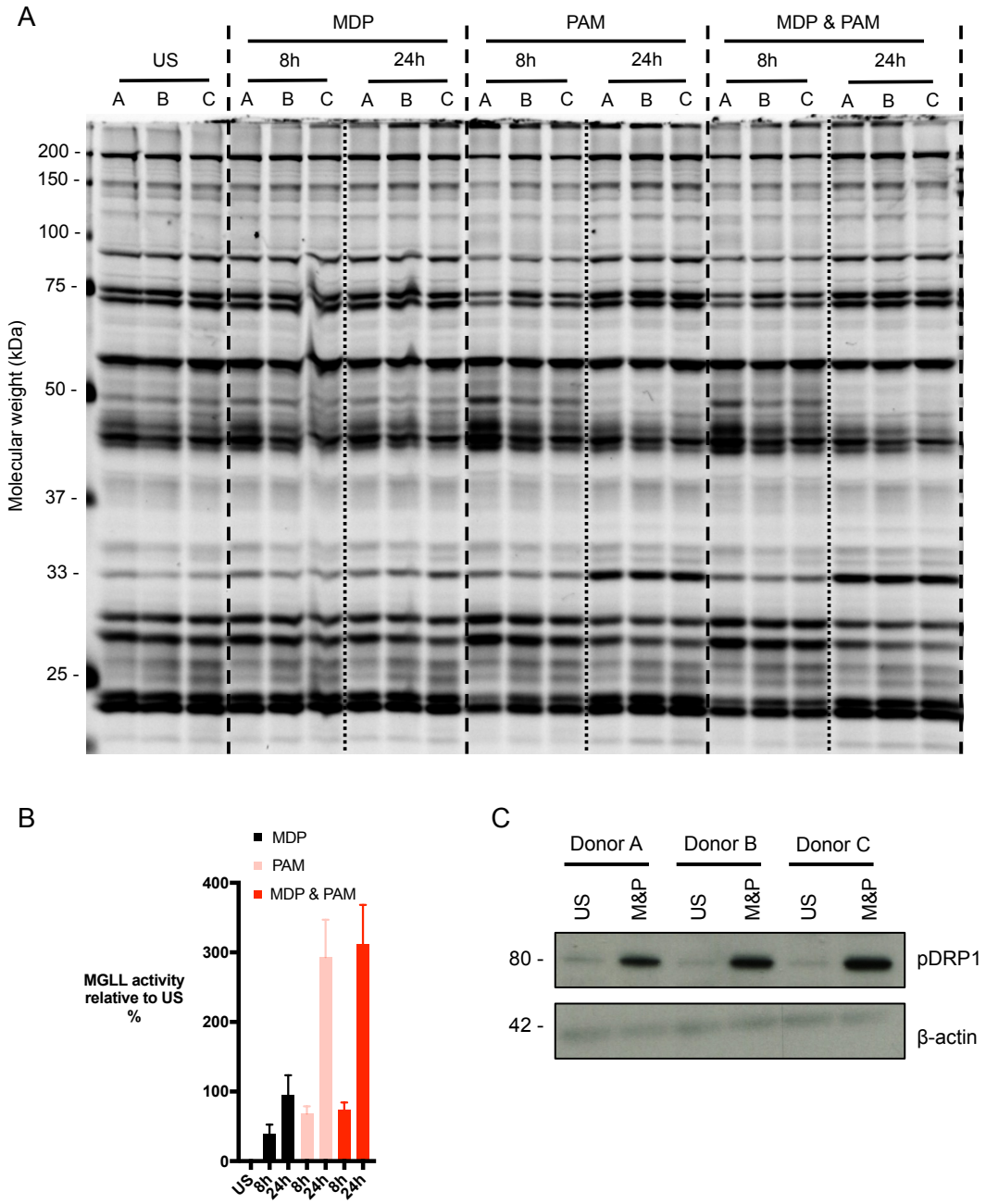

Figure 3.2 Serine hydrolase expression is similar between donors and the increase in MGLL activity is predominantly TLR2-driven

(A) moDCs from three donors A-C were stimulated with 10μg/ml MDP, 1μg/ml PAM, or both for 8h or 24h. Similar changes in serine hydrolase activity were seen between donors at each timepoint and stimulation condition including for MGLL. **(B)** Densitometry of the gel in (A) quantified the relative MGLL activity with each stimulation condition and confirmed a greater effect of TLR2 than NOD2 but with no additivity or synergy between ligands. Mean +/- SEM of 3 biological replicates. **(C)** moDCs from each donor were confirmed to be functioning by immunoblotting for phospho-DRP1 (pDRP1) after 45 minutes stimulation with 10μg/ml MDP & 1μg/ml PAM. US = Unstimulated; M&P = MDP & PAM.

3.3.3 ABPP-MuDPIT identifies 64 serine hydrolases in moDCs and demonstrates MGLL activity to be the most increased following combined MDP/PAM stimulation

So that the serine hydrolases altered on stimulation of moDCs could be mapped to individual enzymes using ABPP-MuDPIT, sufficient material was required. In order to achieve this the proteomes from all three donors were combined for the following timepoints: unstimulated, 8h, and 24h MDP/PAM. This is an acceptable strategy in this instance given how similar the gel based ABPP results were.

ABPP-MuDPIT identified 64 serine hydrolases in moDCs (Appendix 1) with a protein only being confidently mapped if 2 or more unique peptides were detected. Of these, many did not show significant differences between the stimulated and the unstimulated conditions at the timepoints used in this experiments (Figure 3.3A). It is likely that some of these would exhibit stimulation effects at earlier, or perhaps later timepoints. Of the 64 identified in this experiment, 8 altered significantly upon stimulation (Figure 3.3B). The greatest increase was seen with MGLL and PLA2G4A both of which feed into the production of arachidonic acid from phospholipids - the former via 2AG (see Figure 1.3). The fold change for the remaining enzymes was reduced upon stimulation. The function of these enzymes in moDCs is poorly annotated. No significant difference in FAAH activity was seen upon stimulation indicating that 2AG, as opposed to AEA, may be the predominant endocannabinoid in moDCs at these timepoints.

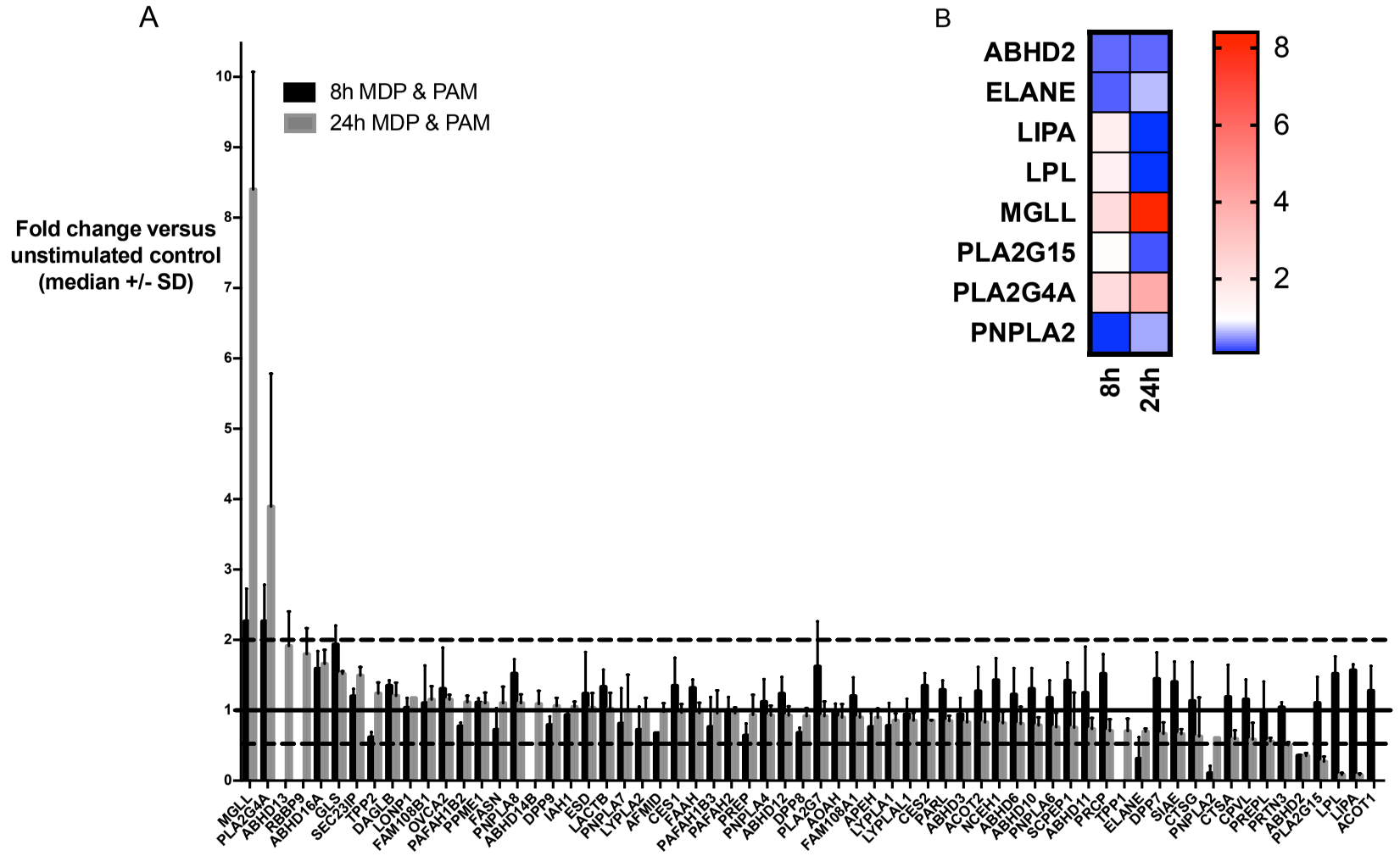

Figure 3.3 ABPP-MuDPIT identifies 64 serine hydrolases in moDCs with MGLL the most upregulated following stimulation with MDP & PAM for 24h

The unstimulated and 8h/24h MDP & PAM stimulated proteomes from donors A-C (Figure 3.2A) were combined for ABPP-MuDPIT analysis. **(A)** Activity levels of the identified serine hydrolases were ranked by activity at 24h compared to unstimulated (high to low). The solid black line represents no difference in activity between stimulated and unstimulated samples. The dashed black lines represent significant differences in activity either greater than 2 (increased activity) or less than 0.5 (decreased activity) between stimulated and unstimulated samples. A fold change of zero implies the protein was not identified. Median +/- SD of all peptides identified for that protein. **(B)** MGLL was the most upregulated enzyme upon 24h stimulation with MDP & PAM followed by PLA2G4A. Several other enzymes were significantly downregulated upon stimulation.

3.3.4 Validation of the top five most significantly altered serine hydrolases

As with any screening experiment, but particularly given the necessity to pool the samples from three donors in this experiment, it was necessary to validate the results. Antibodies for each of the top five most altered enzymes were obtained and immunoblotting of moDC lysate from 2-4 further donors was performed. In the case of MGLL, qPCR was also performed to ascertain the timecourse for gene transcription following MDP/PAM stimulation and the effects of individual MDP or PAM stimulation (Figure 3.4B). As a positive control IL6 mRNA was measured at 6h (Figure 3.4C).

In the cases of MGLL (Figure 3.4A), LIPA (Figure 3.4F), LPL (Figure 3.4G) and PLA2G15 (Figure 3.4H) these were successfully validated with immunoblotting confirming the changes seen on ABPP-MuDPIT. Immunoblotting for MGLL also confirmed that MGLL is present at lower levels in unstimulated moDCs. This information could not have been ascertained from the mass spectrometry data which identifies relative, rather than absolute, activity between two samples. It was not possible to validate PLA2G4A with the antibody used in this experiment (Figure 3.4D). However, PLA2G4A mRNA was induced at 6h (Figure 3.4E). Further attempts to validate this enzyme with other antibodies was not performed as part of this work.

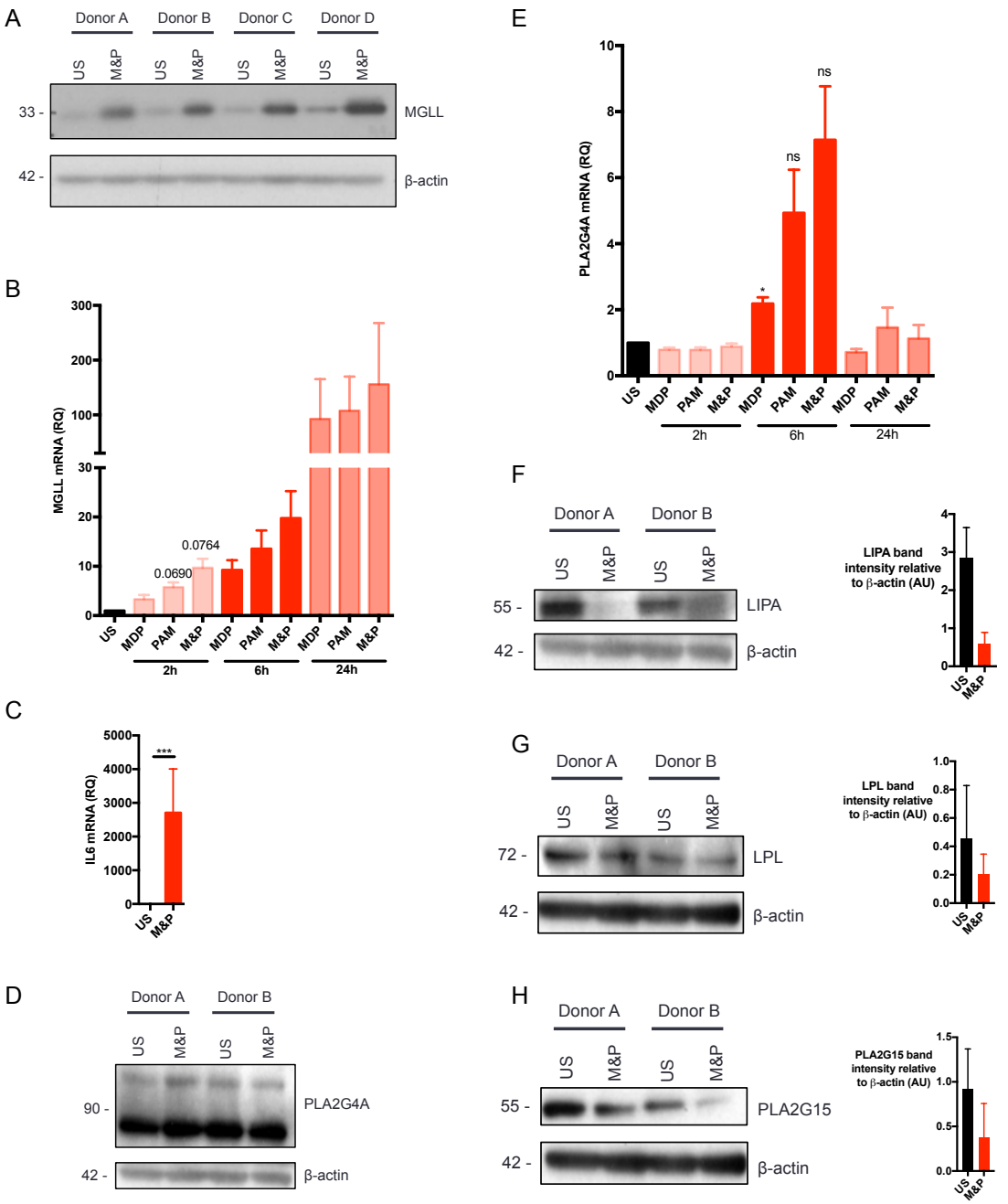

Figure 3.4 Validation of the ABPP-MuDPIT findings for the top five altered serine hydrolases from ABPP-MuDPIT by a combination of immunoblot and/or qPCR

(A, F-H) Validation of MGLL, LIPA, LPL, and PLA2G15 was successful by immunoblot of US and 24h M&P samples. Densitometry shown for LIPA, LPL and PLA2G15. Results show 2 (LIPA, LPL, PLA2G15) or 4 (MGLL) biological replicates. **(B)** MGLL mRNA, assessed by qPCR, was non-significantly increased following stimulation with MDP, PAM or both ligands. Mean +/- SEM of 5 biological replicates. ANOVA with Bonferroni's correction for selected pairs comparing each stimulated condition with US. **(C)** The moDCs used in (B) were confirmed to be functioning by analysis of IL-6 mRNA by qPCR following MDP & PAM stimulation for 6h. 5 biological replicates. Paired t-test. ***p<0.0002. **(D)** Validation of PLA2G4A (n=2) was unsuccessful by immunoblot of US and 24h M&P samples. **(E)** PLA2G4A mRNA, assessed by qPCR, was increased at 6h in all conditions but only met statistical significance with MDP. Mean +/- SEM of 5 biological replicates. ANOVA with Bonferroni's correction for selected pairs comparing each stimulated condition with US. *p<0.0332.

3.3.5 The induction of MGLL following MDP/PAM stimulation is concentration dependent, remains elevated beyond 24h, and is not restricted to NOD2/TLR2 ligation

To understand how the concentration of ligand affects the induction of MGLL, gel-based ABPP was performed on moDCs stimulated with different concentrations of MDP (0.01-10μg/ml) or PAM (1-1000ng/ml)(Figure 3.5A). As seen previously, PAM was a more potent inducer of MGLL than MDP with effects particularly at concentrations greater than 10ng/ml. MDP also exhibited concentration-dependent effects with minimal induction of MGLL at concentrations less than 1μg/ml and optimal effects at 1-10μg/ml. Therefore the chosen ligand concentrations for subsequent *in vitro* experiments were reasonable and would be expected to induce MGLL.

MGLL is not induced early following PRR ligation with MDP or PAM unlike proteins such as IL-6, TNFα and DRP1. In order to understand how enzyme activity changes after 24h, prolonged stimulation was performed up to 48h (Figure 3.5B). This demonstrated persistent elevation in MGLL activity and even suggests that activity increases further at this timepoint. Strikingly there was little alteration in activity when the cells were washed at 24h to remove MDP/PAM and resuspended in fresh, ligand-free, media.

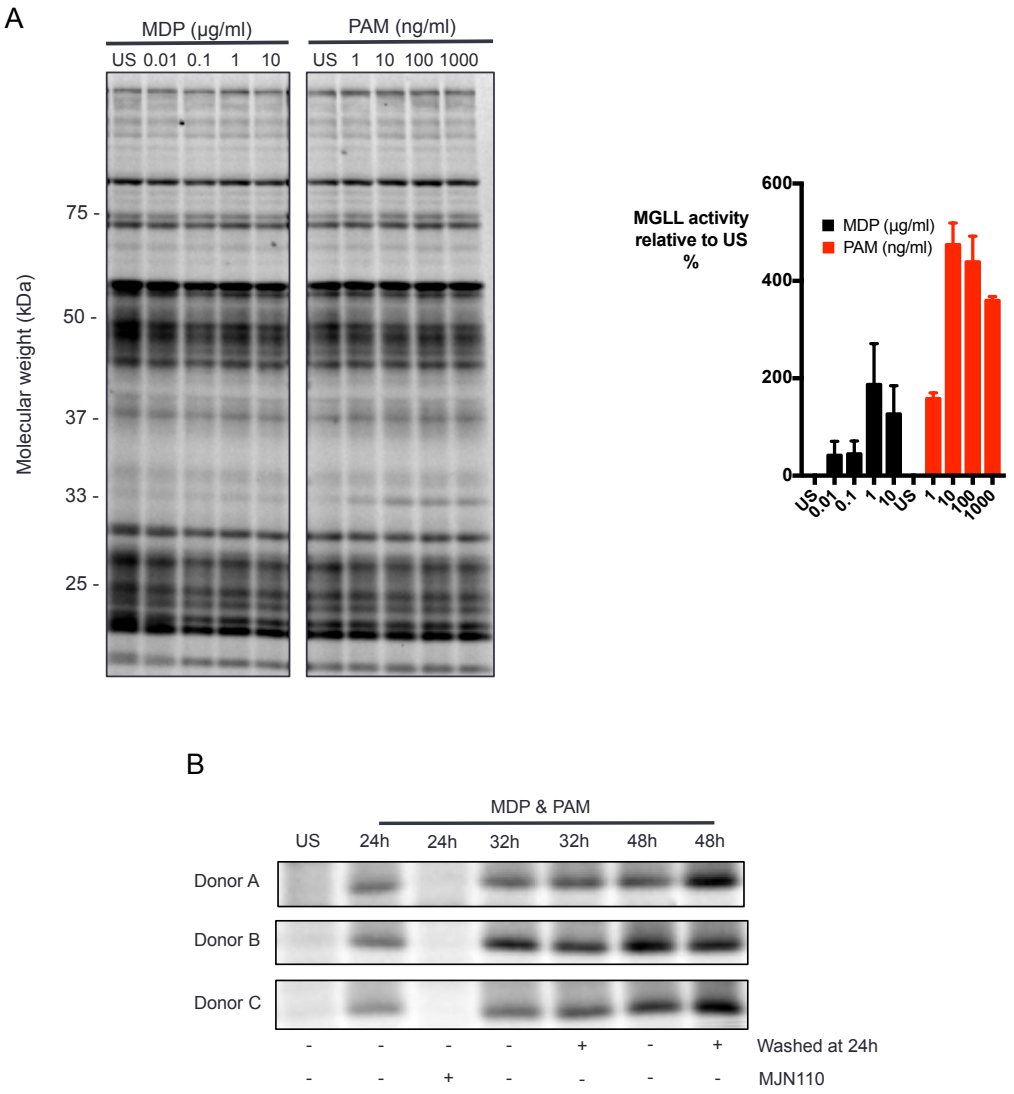

Figure 3.5 The increase in MGLL activity following stimulation of moDCs is concentration dependent and remains elevated to 48h despite removal of the initial stimulus
(A) Gel-based ABPP and densitometry of moDCs stimulated with increasing concentrations of MDP or PAM for 24h. Gel is representative of 3 biological replicates. Densitometry is displayed as mean +/- SEM of all 3 biological replicates. **(B)** Gel-based ABPP of moDCs stimulated for 32h or 48h demonstrated persistent elevations in MGLL activity even when the initial ligand was washed at 24h. Incubation of the proteome with the MGLL inhibitor MJN110 prior to ABPP confirmed the band to be MGLL. Results are shown for 3 biological replicates.

Exposure of moDCs to other PRR ligands, including LPS, R848, Flagellin and Poly(I:C) as ligands for TLR4, TLR8, TLR5, and TLR3 respectively, demonstrated similar induction of MGLL at 8 and 24h (Figure 3.6A/B). The effect of L18-MDP, a synthetic version of MDP, was reduced in magnitude compared to TLR ligands but was similar to the effects of bacterial-derived MDP.

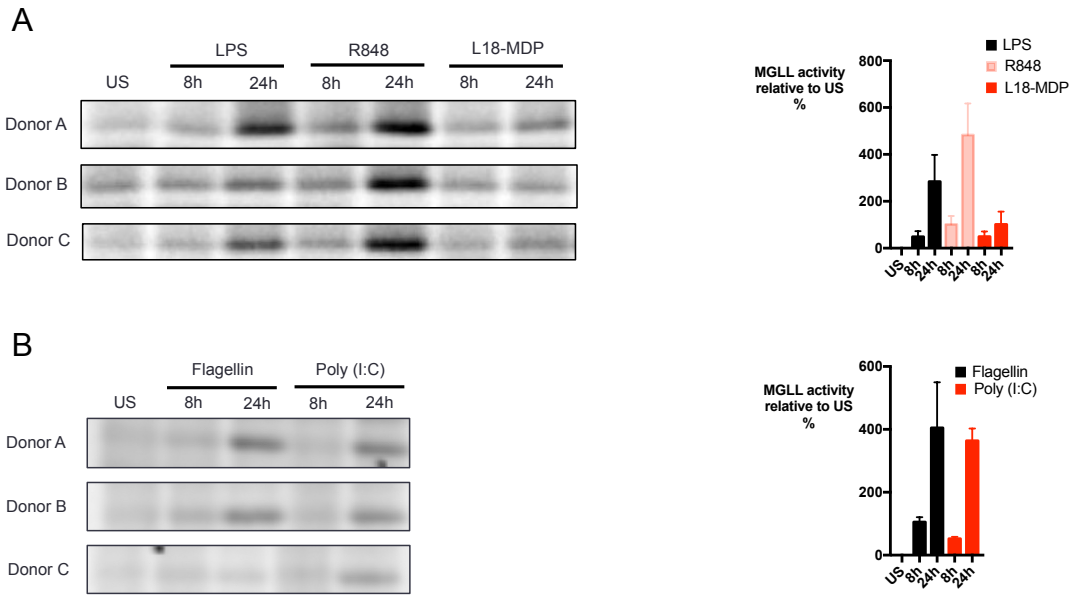

Figure 3.6 MGLL activity increases on stimulation of moDCs with other PRR ligands
Gel-based ABPP and densitometry of moDCs stimulated with **(A)** LPS 100ng/ml (TLR4), R848 1µg/ml (TLR8), or L18-MDP 10µg/ml (synthetic NOD2 ligand), and **(B)** Flagellin 100ng/ml and poly(I:C) 1µg/ml. Results are shown for 3 biological replicates. Mean +/- SEM for densitometry.

3.3.6 MGLL can be knocked down using siRNA in moDCs and inhibited using the small molecules JZL184 and MJN110

In order to explore the function of MGLL in moDCs it was essential to develop methods to inhibit protein production or alternatively inhibit protein function. A pilot experiment of siRNA knockdown by electroporation identified that 200nM efficiently knocked down MGLL at 24h (mean knockdown efficiency 68%; Figure 3.7A). A further experiment confirmed that knockdown persisted to 48h (mean knockdown efficiency 82% (24h) and 70% (48h); Figure 3.7B). This was important because not only did the moDCs need to be transfected and rested for 24h but then subsequently would need to be stimulated for 24h to attempt to induce MGLL for functional assays. The knockdown of MGLL mRNA correlated to a reduction in MGLL protein (Figure 3.7C) which also confirmed that the MGLL antibody being used was specific for MGLL.

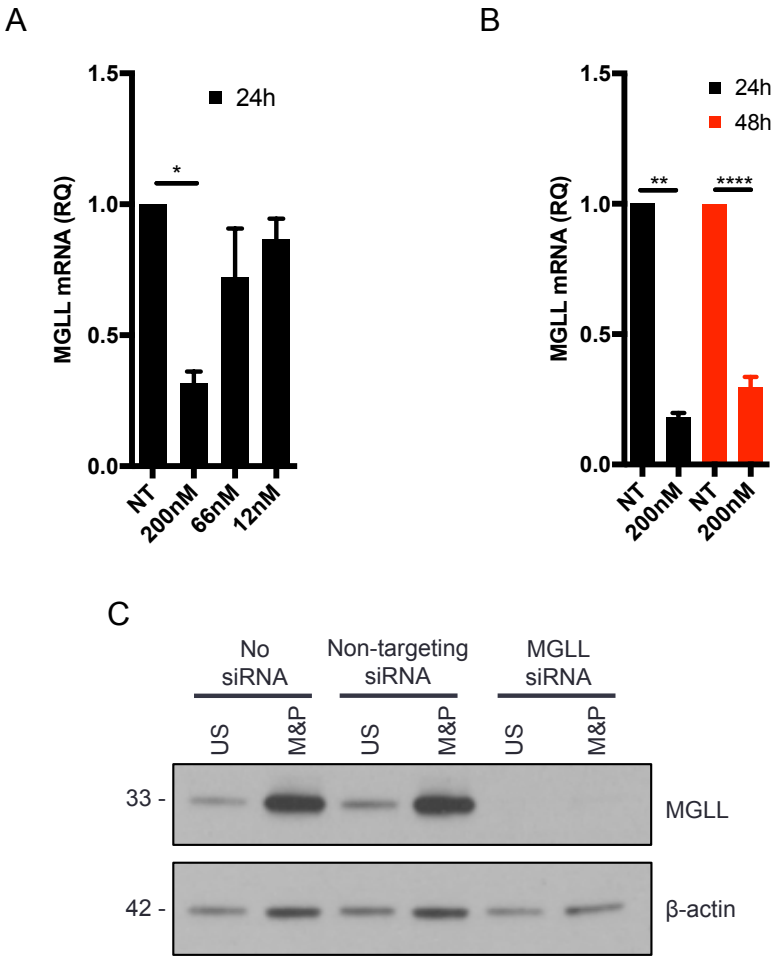

Figure 3.7 MGLL can be successfully knocked down using siRNA interference in moDCs
(A) siRNA was introduced by electroporation to moDCs and concentrations titrated to determine the minimum dose needed to knockdown MGLL at 24h. Mean +/- SEM of 2 biological replicates. ANOVA with Bonferroni correction of selected pairs. *p<0.0332. **(B)** Transfection of siRNA by electroporation reduced MGLL mRNA at 24h and 48h. Mean +/- SEM of 2 (24h) or 4 (48h) biological replicates. Paired t-test. **p<0.0021, ****p<0.0001. **(C)** Immunoblot confirmed the knockdown at gene level corresponded to knockdown at protein level. Representative of 2 biological replicates. NT = non-targeting.

As discussed earlier, several pharmacological inhibitors of MGLL have been developed, many exploiting the ABPP method. At the time of commencing this period of research, the most widely used inhibitor in the literature was JZL184. MJN110 had recently been described but had yet to gain significant traction scientifically. Never before used in primary human immune cells, it was necessary to confirm the minimum concentrations of these agents to inhibit MGLL activity and minimise off target effects. moDCs were left unstimulated or stimulated for

24h with MDP/PAM in the presence of DMSO or a concentration titration of JZL184 or MJN110. Gel-based ABPP was performed on the cellular proteome and demonstrated inhibition of MGLL activity with increasing concentration of JZL184 or MJN110 (Figure 3.8A) which was reproducible between donors (Figure 3.8B). The known off-target effect of JZL184 on Ces1c was clearly demonstrated on the gel and not seen with MJN110 which is known to have different off-target effects. Both inhibitors were effective at 100nM concentration to achieve inhibition of MGLL activity (Figure 3.8C).

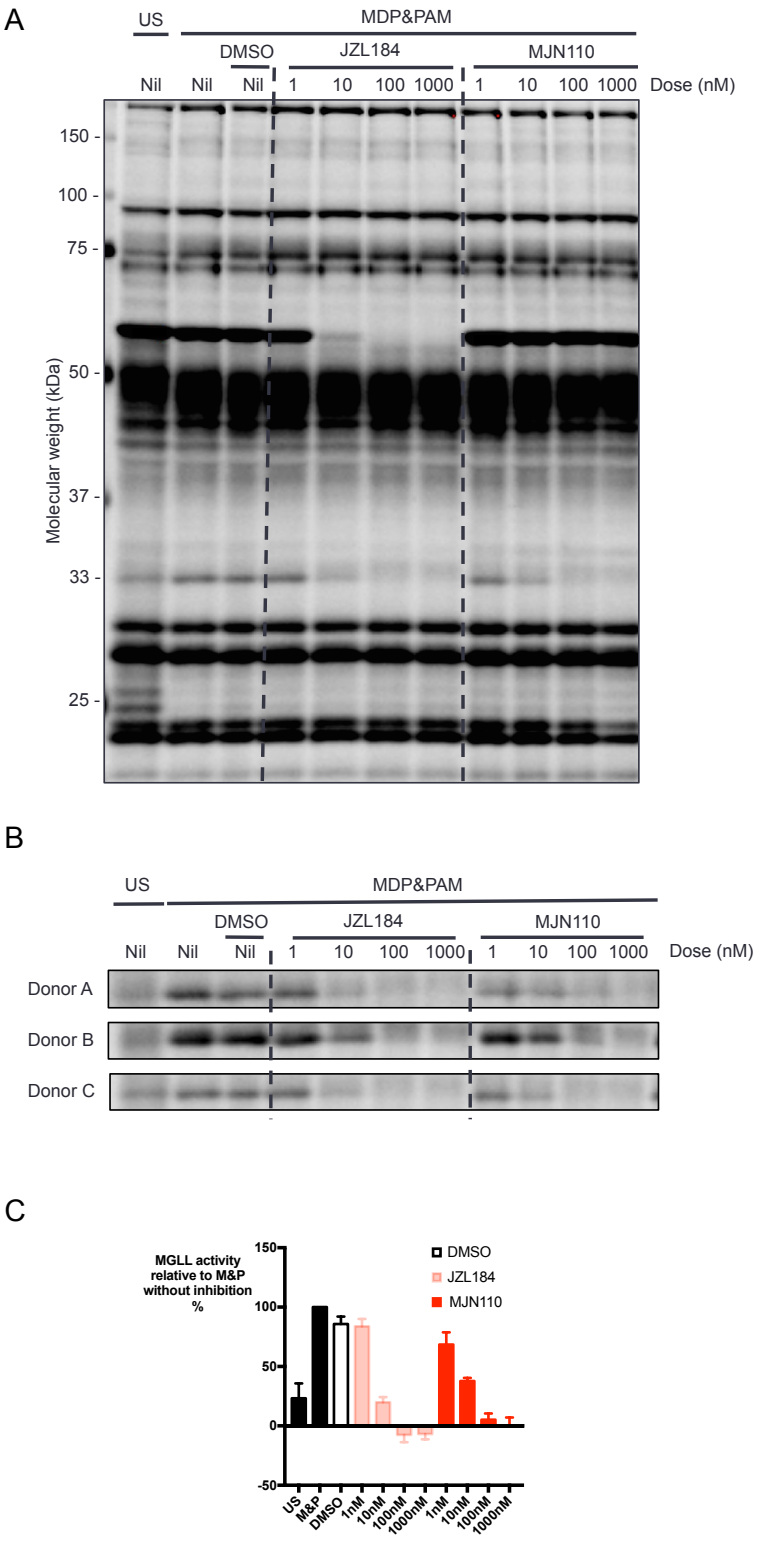

Figure 3.8 JZL184 and MJN100 are small molecule inhibitors of MGLL effective at doses of 100nM

(A) Gel-based ABPP of moDCs incubated with increasing concentration of JZL184 or MJN110 and stimulated with MDP & PAM for 24h highlighted the off-target effect of JZL184 on a carboxylesterase at 60kDa. Representative of 3 biological replicates. **(B)** ABPP gel and **(C)** densitometry of MGLL band confirmed inhibition of enzyme activity at 100nM concentrations of inhibitors. Results are shown for 3 biological replicates. Mean +/- SEM for bar chart.

By binding covalently to Ser122 in the active site of MGLL[179], JZL184 acts to inhibit MGLL activity but is not known to directly affect transcription or translation. No effect of JZL184 was identified on MGLL transcription following stimulation with MDP/PAM (Figure 3.9A). Effects were seen on MGLL detection by immunoblot in the presence of JZL184 (Figure 3.9B). A reduction in band intensity and also molecular weight was reproducibly seen across three donors. It is conceivable that by binding covalently to the active site that the conformation of the MGLL protein is altered such that this affects the binding of the immunoblot antibody – which is raised against full length MGLL.

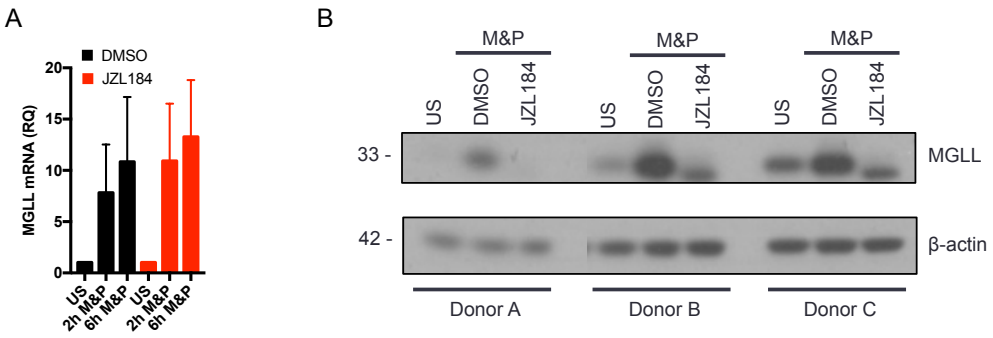

Figure 3.9 Effects of JZL184 on MGLL transcription and translation
(A) qPCR of moDCs showed no effect of JZL184 on MGLL transcription. Mean +/- SEM of 3 biological replicates. **(B)** MGLL detection by immunoblot was affected by JZL184 with reduction in intensity and molecular weight. 3 biological replicates. US = Unstimulated; M&P = MDP & PAM.

For subsequent experiments JZL184 was used as the primary pharmacological tool to interrogate the effects of MGLL inhibition. The different off-target effects of MJN110 would allow this compound to be used to confirm any functional effects of JZL184 are due to MGLL rather than Ces1c for instance.

3.3.7 MGLL is upregulated in other myeloid immune cells

The abundance of MGLL in other human innate immune cells of myeloid lineage has not been described. CD14$^+$ cells were separated from PBMCs and differentiated into moDCs or monocyte-derived macrophages.

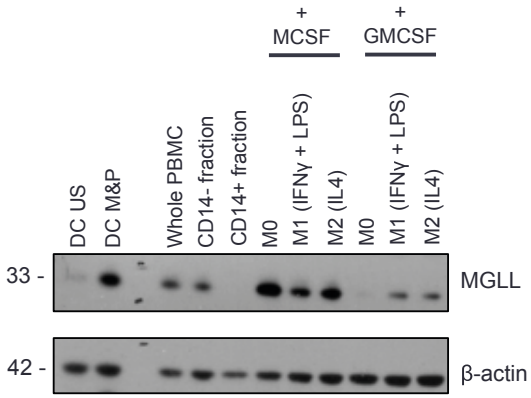

Figure 3.10 MGLL is upregulated in monocyte-derived macrophages
PBMCs were incubated with CD14$^+$ magnetic beads and the CD14$^+$ monocytes differentiated with M-CSF or GM-CSF and then polarised into M0, M1 or M2 macrophages. Immunoblot was then performed for MGLL. Representative of 4 biological replicates.

MGLL is seen to be induced in moDCs upon stimulation as a positive control. MGLL is identified at lower levels in the whole PBMC and CD14$^-$ fractions but not the purified CD14$^+$ fraction (Figure 3.10). This is likely due to contamination from myeloid cells but it is not possible to exclude the possibility that MGLL is abundant in lymphoid cells for example. This has not been explored in the work that constitutes this thesis. A striking effect of M-CSF over GM-CSF is seen on MGLL induction although there is incongruence between macrophage subsets between the two polarisation arms. Whilst insufficient to accurately annotate MGLL levels in these subsets this experiment does demonstrate that MGLL is present in other primary immune cells of myeloid origin.

MGLL has previously been shown to be present in cancer cell lines of prostate[167], ovarian, melanoma, breast[169] and colorectal[171] origin. However, it has not previously been profiled in cancer cell lines of myeloid origin. The THP-1 cell line is a monocytic line derived from acute monocytic leukaemia. These cells can be differentiated into THP-1 derived macrophages and so provide a useful surrogate for primary monocytes and monocyte-derived macrophages. U937 cells, isolated from a histiocytic lymphoma, are similarly useful as surrogates for monocytes.

Gel-based ABPP was performed on THP-1 cells including on stimulation under the same conditions as with moDCs earlier. Serine hydrolase profiling demonstrated induction of MGLL upon stimulation with little detectable in the unstimulated condition by ABPP (Figure 3.11A/B). This suggested THP-1 cells to be an appropriate cell line to use alongside experiments with primary cells. U937 cells demonstrate MGLL activity in the unstimulated condition (Figure 3.11C) although a stimulation experiment was not performed with this cell line.

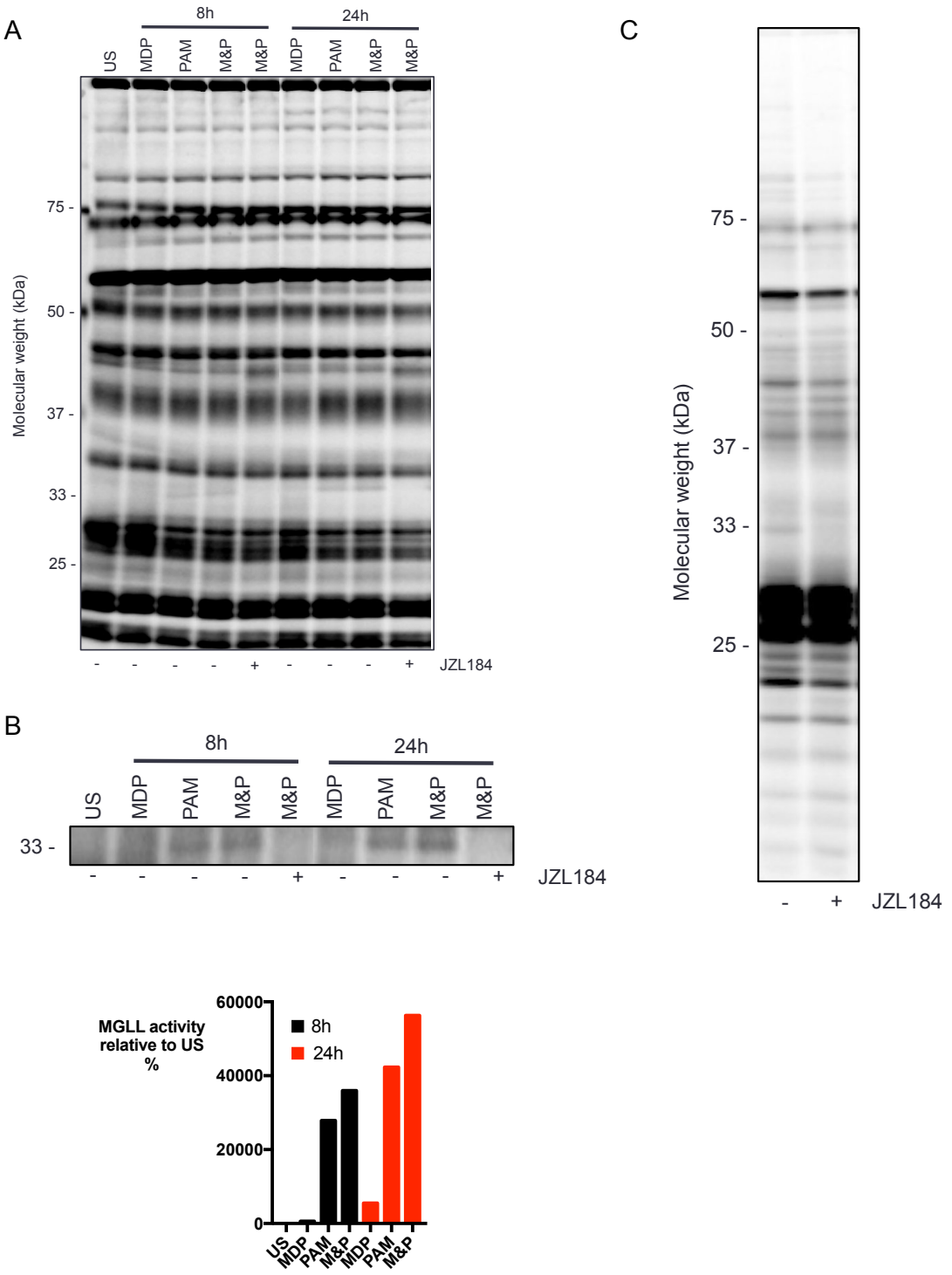

Figure 3.11 MGLL is present in THP-1 and U937 monocytic cell lines and the activity increases upon stimulation of THP-1 cells

(A) Gel-based ABPP of the serine hydrolome in THP-1 cells upon stimulation with MDP & PAM. **(B)** Isolation of the MGLL band from (A) and densitometry analysis confirmed an increase in MGLL activity with 8 and 24h stimulation. **(C)** Gel-based ABPP of unstimulated U937 cells and pre-incubation with JZL184 identified a MGLL band at 33kDa. All results are representative of 3 biological replicates for each cell line.

3.3.8 Profiling the ECS by qPCR in moDCs demonstrates a dynamic system upon stimulation of NOD2/TLR2

Having identified MGLL to be upregulated in moDCs upon PRR ligation this highlighted a need to better understand the profile of the ECS in moDCs upon PRR ligation. The only work to date examining the ECS in moDCs highlighted the presence of CB1 and 2 mRNA and protein with a reduction in CB2 expression in some, but not all samples, following LPS stimulation over 24 hours[201]. FAAH was also identified in this study. A subsequent study confirmed the presence of CB1 and 2 mRNA, and detected intracellular but not cell-surface protein by flow cytometry[374]. However, no study has to date profiled mRNA of the wider synthetic and degradative enzymes for 2AG alongside the receptors nor looked at the effects over time of MDP/PAM stimulation on gene expression.

Expression of CNR1 did not significantly alter upon stimulation with either ligand or at any timepoint (Figure 3.12A). However, there was a numerical reduction in CNR2 expression in almost every condition (Figure 3.12B) although this only met statistical significance in four. Ideally the results of gene expression would be correlated with effects on CB2 protein levels. This is problematic for the cannabinoid receptors as it is acknowledged that many antibodies for these targets are subject to lack of specificity[375,376]. Two anti-CB2 antibodies were obtained (sc293188, Santa Cruz Biotechnology (SCBT); SAB1306696, Sigma). As the T cell line, Jurkat, has previously been shown to express CB2, and corroborated by my own qPCR profiling of cell lines (Figure 3.13B), knockdown of CB2 by siRNA techniques was attempted. This was unsuccessful by qPCR (Supplementary Figure A) and immunoblotting using the two antibodies demonstrated wide-

spread non-specific binding (Supplementary Figure B). Separately, CB2 was successfully knocked down in moDCs using siRNA techniques (Supplementary Figure C) but corresponding protein knockdown could not be confirmed due to poor antibody selectivity. This being the case, further exploration of CB2 in moDCs does not form a further part of this thesis.

Having already profiled MGLL transcription in moDCs upon stimulation (Figure 3.4B), demonstrating a numerical but non-significant increase in gene expression with stimulation and time, further hydrolytic and synthetic enzymes were profiled. ABHD6 showed a significant reduction in mRNA levels early after stimulation (Figure 3.12D) but these returned to normal levels with time. The function of ABHD6 has not been explored in moDCs to date but if these results correlated with changes in protein level this may suggest a more refined mechanism for balancing 2AG tone in moDCs than MGLL alone. Certainly in the central nervous system, ABHD6 regulates 2AG levels even in the absence of MGLL[377]. No differences in ABHD12 or FAAH expression (Figure 3.12C/E) were seen at these timepoints. An early reduction of DAGLβ (Figure 3.12G) and a late reduction of DAGLα expression (Figure 3.12F) is suggestive of some effects of NOD2/TLR2 stimulation on the enzymes responsible for 2AG synthesis. Collectively, these results indicate a dynamic endocannabinoid system in moDCs involving more than changes in receptor expression alone.

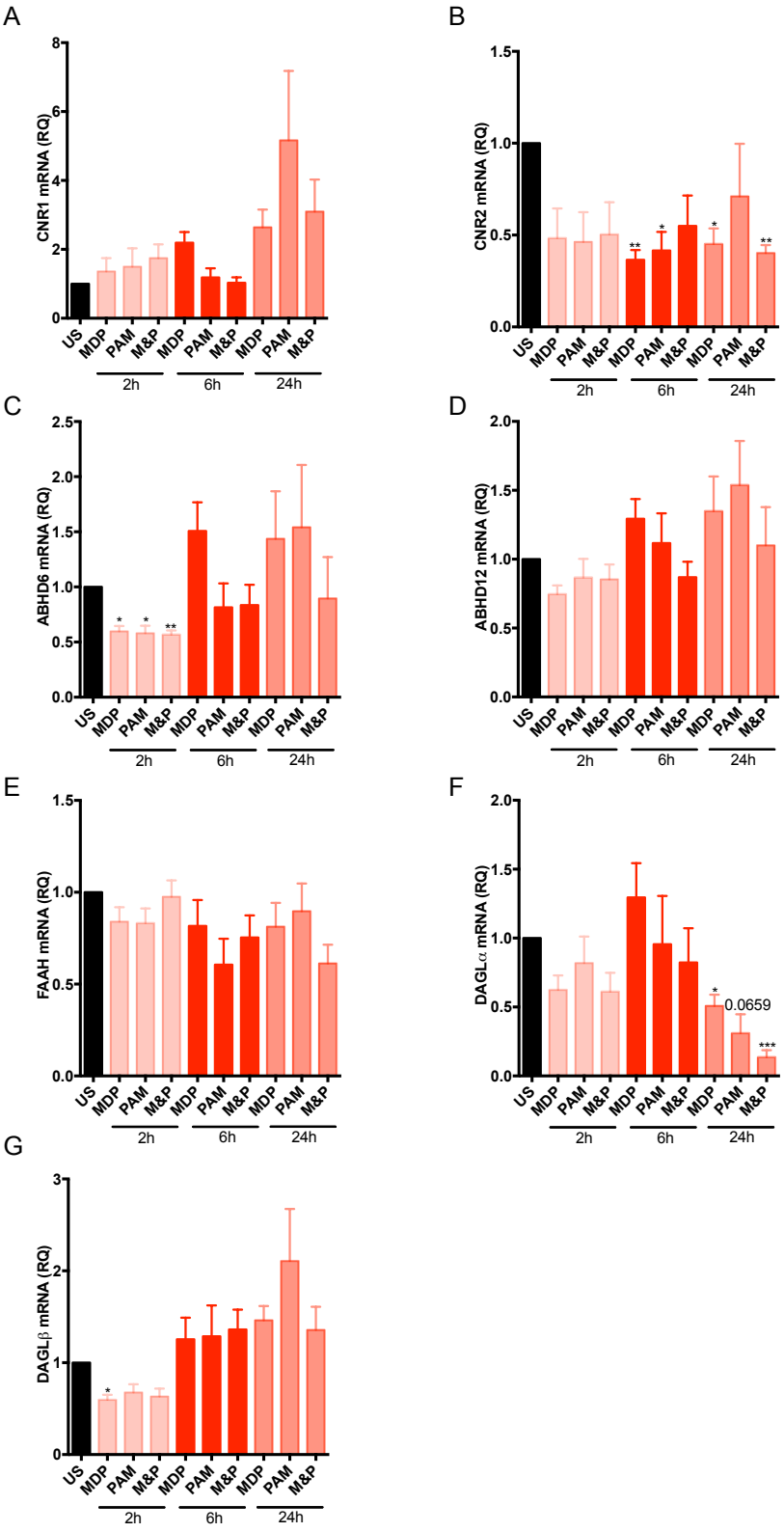

Figure 3.12 Profiling of endocannabinoid system gene expression in moDCs upon PRR stimulation demonstrates transcriptional change in some but not all components

RNA was extracted from moDCs and qPCR performed for **(A)** CNR1, **(B)** CNR2, **(C)** FAAH, **(D)** ABHD6, **(E)** ABHD12, **(F)** DAGLα and **(G)** DAGLβ. Mean +/- SEM of 5 biological replicates. ANOVA with Bonferroni's correction for selected pairs comparing each stimulated condition with US. *p<0.0332, **p<0.0021, ***p<0.0002.

3.3.9 Profiling ECS receptors and hydrolytic enzymes in cell lines

Cell lines are commonly used as surrogates for primary cells including in transfection experiments. MGLL activity is present in unstimulated U937 cells and increases upon stimulation of THP-1 cells (Figure 3.11). However, it was not known to what extent expression of other hydrolytic enzymes or the cannabinoid receptors differed between these cell types. As discussed earlier, Jurkat cells are known to express CB2 and so this cell line was included as a control for CB2 expression. HeLa and HEK293 cells were included as commonly used cell lines for transfection experiments. HCT116 and HT29 cells were chosen as colonic cancer epithelial lines given the planned profiling of primary human colonic tissue (see Chapter 5). Gene expression was measured by qPCR across unstimulated cell lines (Figure 3.13A-F) and plotted alongside the previously generated data from moDCs (unstimulated versus 24 hour stimulation with MDP/PAM).

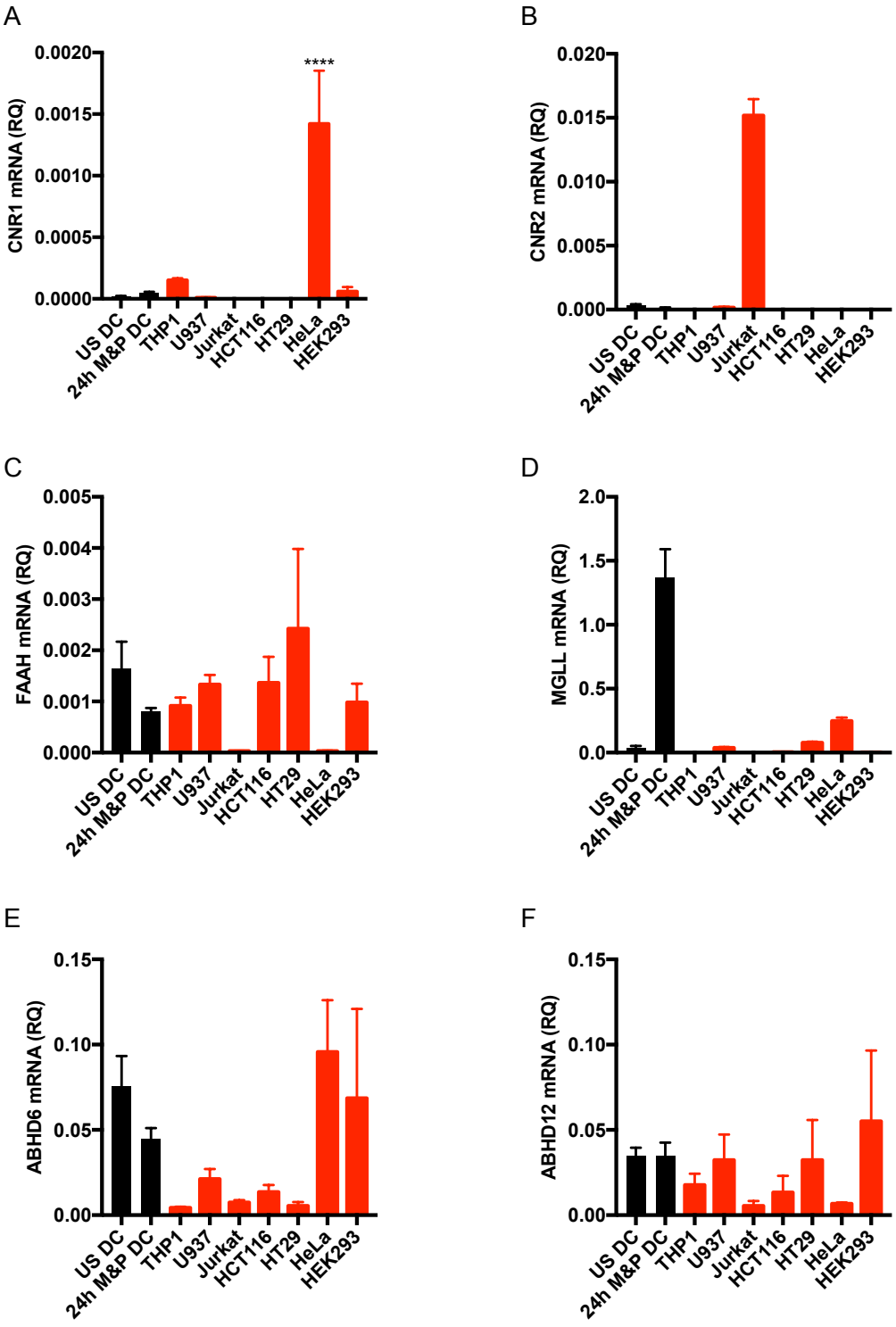

Figure 3.13 Profiling of endocannabinoid system gene expression in cell lines compared to moDCs

RNA was extracted from the monocytic cell lines THP1 and U937, T cell line Jurkat, colonic epithelial cell lines HCT116 and HT29, the cervical cancer cell line HeLa, and the human embryonic kidney cell line HEK293. Results are displayed alongside moDCs (Figure 3.4B). qPCR was performed for **(A)** CNR1, **(B)** CNR2, **(C)** FAAH, **(D)** MGLL, **(E)** ABHD6, and **(F)** ABHD12. Mean +/- SEM of 3 biological replicates (cells for each replicate were harvested on different days). ANOVA with Bonferroni's correction for selected pairs comparing each stimulated condition with US moDCs. ****p<0.0001.

CNR1 expression was identified predominantly in THP-1 and HeLa cells and at greater levels than moDCs. CNR2 expression was predominantly in cell lines of immune origin particularly Jurkat cells in line with published literature. Few differences in FAAH expression were noted although this enzyme was largely absent in Jurkat and HeLa cells. Expression of MGLL was largest in stimulated moDCs and of the other immune cell lines was otherwise only expressed in U937 cells correlating with the ABPP data. HeLa cells express MGLL, although not meeting statistical significance, and so this cell line could be a useful surrogate to investigate MGLL function. Similar to MGLL, HeLa cells express a greater amount of ABHD6 transcript compared to other immune cell lines and colonic epithelial cells although this was non-significant. Few differences were seen between cell lines for ABHD12 expression.

This profiling confirms that the expression pattern of ECS components in moDCs is different to any individual cell line studied here. However, the function of individual components could potentially be explored in cell lines such as HeLa (CB1 and MGLL), and Jurkat (CB2). Importantly this profiling does not include stimulation with PRR ligands which may fundamentally alter expression levels such as that seen with MGLL expression in stimulated THP-1 cells. Furthermore, the effect of transcription on protein levels in these cells is not investigated here.

3.3.10 MGLL inhibition with JZL184 affects cellular abundance of endocannabinoid-related lipids in moDCs

Having demonstrated unequivocally that MGLL is induced by PRR stimulation in moDCs the next hypothesis was that this would affect levels of endocannabinoid-related lipids. With knowledge of the 2AG metabolic pathway it could be surmised that MGLL inhibition would result in increased 2AG and decreased arachidonic acid levels. It does not necessarily follow that an alteration in prostaglandin/leukotriene levels will ensue due to the alternative metabolic pathways for 2AG including oxidation and epoxidation, and the alternative pathway of generating arachidonic acid directly from membrane phospholipids via the action of PLA2G4A.

Endocannabinoid-related lipids have not been investigated in detail in moDCs other than by Matias et al[201] who described an increase in 2AG following stimulation of moDCs with LPS for 24h with no change in anandamide levels. This being the case it was essential to perform a pilot experiment to determine the number of cells needed to extract endocannabinoid-related lipids. moDCs from a single donor were separated into pellets of different cell numbers (12, 20, 40x10^6). Lipids were extracted and quantified for diacylglycerols (DAG), monoacylglycerols (MAG), N-acylethanolamides (NAE), free fatty acids (FFA) and a composite of prostaglandin E2/D2 (PGE2/D2) (Figure 3.14). Given that the leucocyte cones used to extract monocytes typically yield approximately 80-120x10^6 moDCs (data not shown), it was determined that 20x10^6 cells per condition would be sufficient to both confidently identify the lipids of interest whilst also allowing for up to 6 conditions per donor.

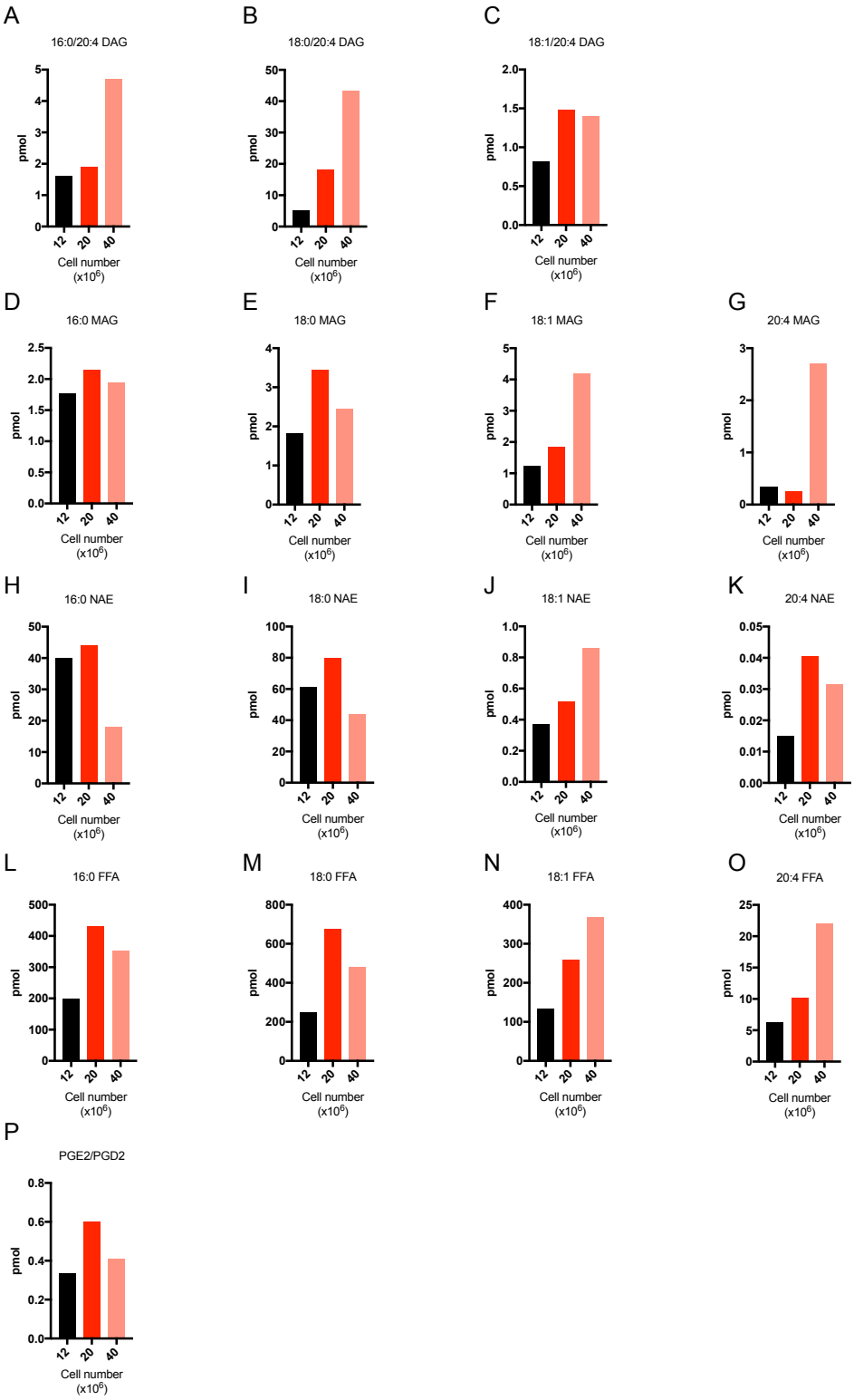

Figure 3.14 Pilot study of endocannabinoid-related cellular lipidomics in unstimulated moDCs

Pellets of unstimulated moDCs containing either 40, 20 or 12x10^6 cells were processed for lipidomic analysis by mass spectrometry. **(A-C)** Diacylglycerol (DAG) precursors for 2AG; **(D-G)** Monoacylglycerols (MAG); **(H-K)** N-acylethanolamides (NAE); **(L-O)** Free fatty acids (FFA); **(P)** Composite of PGE2/D2 quantification. Results are absolute lipid quantification of a single biological replicate.

moDCs from 6 independent donors were incubated with DMSO or 100nM JZL184 prior to the addition of MDP/PAM for 24 hours in the stimulated conditions. The only significant difference between unstimulated moDCs incubated with DMSO or JZL184 was for C18:0 MAG (Figure 3.15B). Upon stimulation there was a significant reduction in all measured MAGs which correspond not only to 2AG (C20:4 MAG) but also the endocannabinoid-related MAGs 2PG (C16:0 MAG), 1SG (C18:0 MAG) and 2OG (C18:1 MAG) (Figure 3.15A-D). Incubation with JZL184 results in partial rescue of 2AG and 2OG levels. However, the incomplete rescue of levels is suggestive that there are other routes for 2AG metabolism in moDCs perhaps through hydrolysis by other enzymes such as ABHD6 or 12, by oxidation or epoxidation.

The results for NAEs mirrors those of MAGs and highlights the off target effect of JZL184 on FAAH (Figure E-H). Notably there is no difference between unstimulated and stimulated moDCs on AEA (C20:4 NAE) levels and this is probably because FAAH activity does not alter at this timepoint (Figure 3.3).

Although there is a reduction in 2AG levels upon stimulation this does not correspond with an increase in arachidonic acid (Figure 3.15L). The hypothesis that JZL184 might reduce arachidonic acid levels was not confirmed. However, the increase in PGE2/D2 and TXB2 (Figure 3.15M/N) would suggest that arachidonic acid may be being converted into prostaglandins. Interestingly, no effect of MGLL inhibition was identified on levels of any FFA or measured prostaglandin. This raises the possibility that MGLL may not be a critical enzyme for the generation of arachidonic acid and prostaglandins in moDCs.

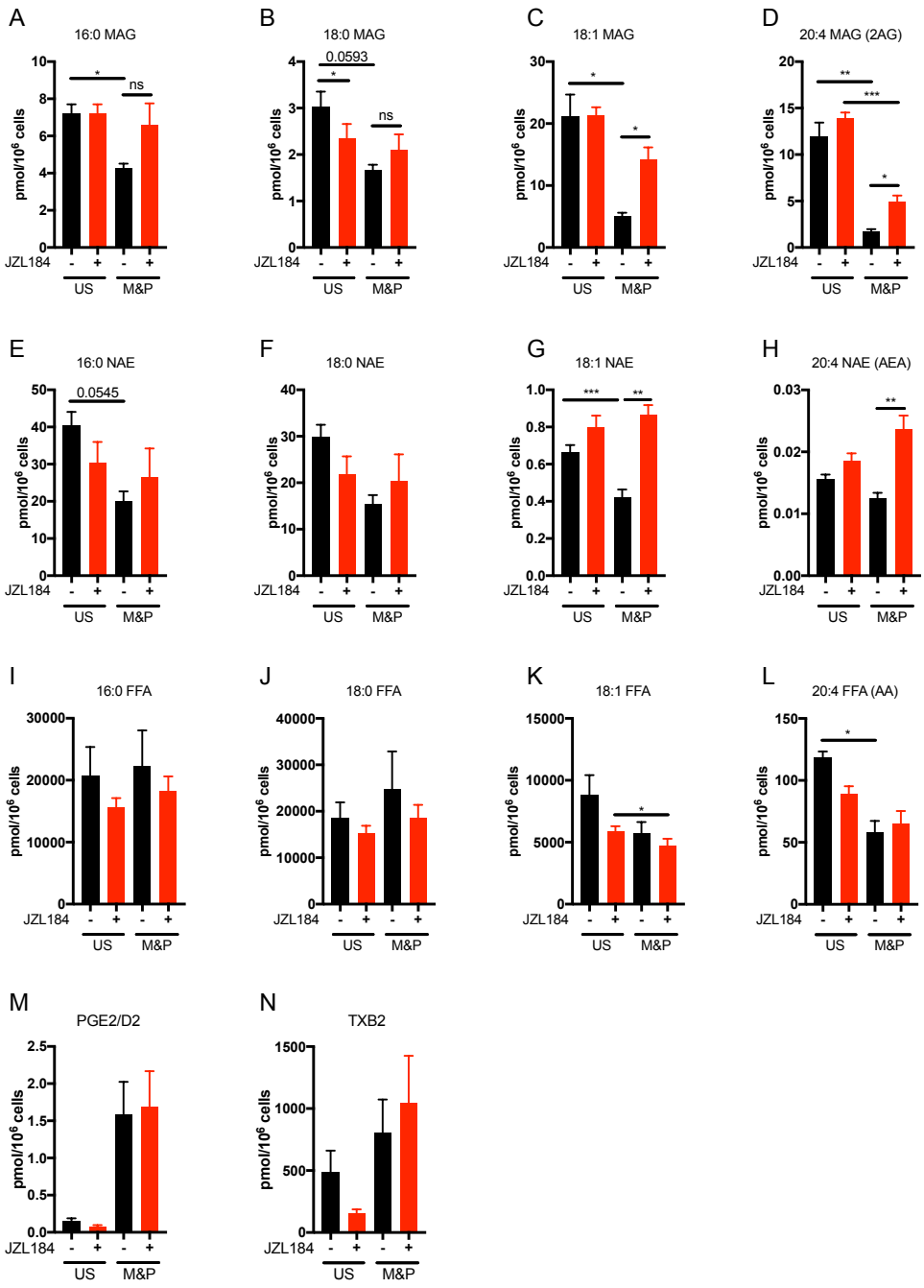

Figure 3.15 Stimulation of moDCs with MDP & PAM results in changes in levels of cellular endocannabinoid and related lipids and MGLL inhibition partially rescues a reduction in 2AG

moDCs were stimulated for 24h with MDP & PAM with or without JZL184 and lipid abundance measured by mass spectrometry. Stimulation resulted in a reduction of **(A-D)** intracellular MAGs and **(E-H)** NAEs, including **(D)** 2AG and **(H)** AEA. MGLL inhibition partially rescued the reduction in 2AG, 18:1 MAG, AEA and 18:1 NAE. A reduction in 20:4 FFA was seen on stimulation but there were no effects on **(I-L)** other FFAs. **(M)** PGE2/D2 and **(N)** TXB2 increased non-significantly upon stimulation. Mean +/- SEM of 6 biological replicates. *p<0.0332, **p<0.0021, ***p<0.0002.

3.3.11 MGLL inhibition affects other cellular lipids beyond the endocannabinoid system

It has been demonstrated in cancer cell lines that MGLL controls an extended lipid network beyond those directly related to the ECS. In prostate cancer cell lines, levels of certain lysophosphatidylcholines (16:0, 18:0, 18:1 LPC) were increased by JZL184, whereas levels of phosphatidic acids (16:0/18:1, 18:0/18:2 PA), lysophosphatidic acids (18:0 LPA) and lysophosphatidylethanolamines (16:0, 18:0, 18:1 LPE) were reduced[167]. In aggressive melanoma and ovarian cell lines, JZL184 also reduced LPA (17:0) and increased LPC (16:0, 18:0, 18:1, 17:0) levels[169]. However, contrary to prostate cancer cell lines, JZL184 increased LPE (16:0, 18:0, 18:1, 17:0) levels suggesting MGLL may act differently on lipid networks depending on the cell type.

To investigate this further, an untargeted lipidomic screen was performed with moDCs from 3 independent donors ($2x10^6$ cells per condition). A total of 500 lipids were identified from twenty nine lipid classes (Appendix 2). Statistically significant differences between conditions for each lipid, rather than just the overall lipid classes, were analysed by ANOVA. For key lipids, graphs were plotted of individual donors alongside the combined results. There were marked differences in lipid quantification between donors. A numerical reduction in abundance of 16:0, 18:0 and 18:1 LPC and LPE was found with MGLL inhibition on stimulation (Figure 3.16 A-C, E-G) but this did not meet statistical significance. An increase in 20:4 LPC and 20:4 LPE was seen with MGLL inhibition of unstimulated moDCs but not stimulated (Figure 3.16 D/H). Therefore effects on these lipids may be seen at earlier timepoints.

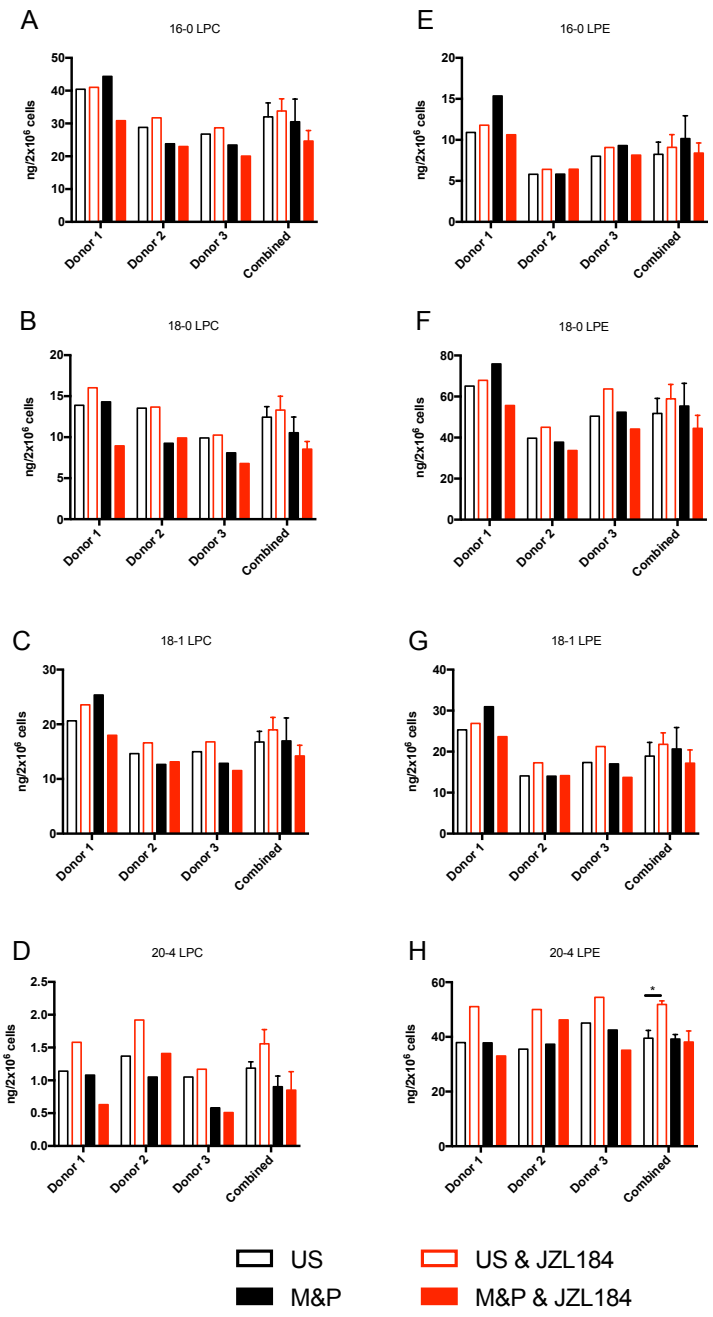

Figure 3.16 Effects of JZL184 on lysophosphatidylcholine (LPC) and lysophosphatidylethanolamine (LPE) using an untargeted lipidomic approach

moDCs were stimulated for 24h with MDP & PAM with or without JZL184 and abundance of LPC and LPE measured by mass spectrometry. Results for individual donors is shown alongside combined data. Combined data is mean +/- SEM of 3 biological replicates. ANOVA with Bonferroni correction for selected pairs (US vs US & JZL184; US vs M&P; M&P vs M&P & JZL184). *p<0.033. US = Unstimulated; M&P = MDP & PAM.

Furthermore, effects of JZL184 reduced levels of 16:0 FaCN on stimulation (Figure 3.17A) with some numeric but non-significant effects on 17:1 FaCoA (Figure 3.17B). The effects of stimulation on levels of ceramides varied by subclass but

no significant effect of MGLL was seen (Figure 3.17C/D). Similarly an effect of stimulation was seen for 34:1 PG but no additional effect of MGLL inhibition (Figure 3.17F). An effect of MGLL on 52:3 TAG in unstimulated moDCs was not replicated in other subclasses or on stimulation (Figure 3.17G-L).

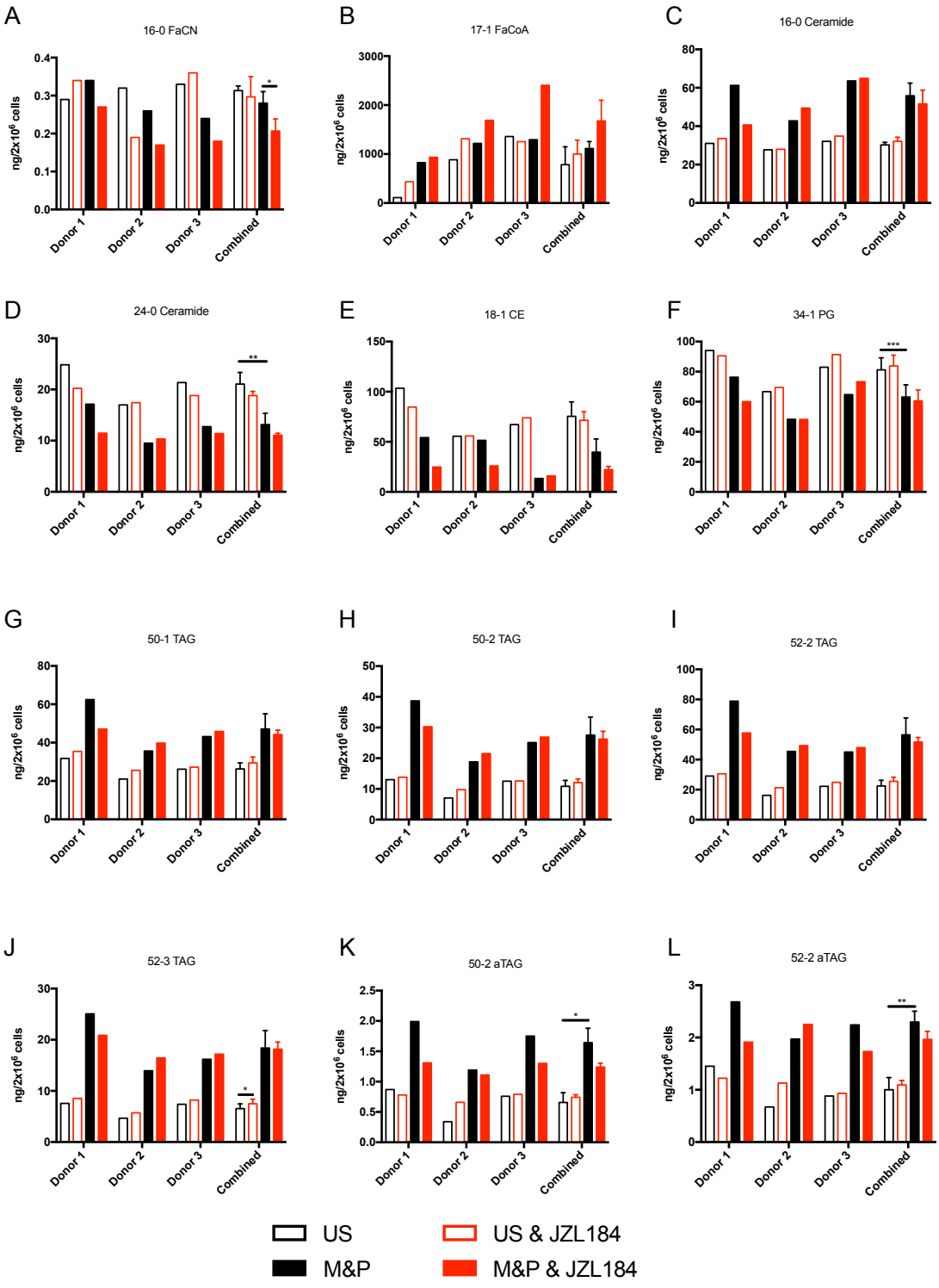

Figure 3.17 Effects of JZL184 on other cellular lipids using an untargeted lipidomic approach
moDCs were stimulated for 24h with MDP & PAM with or without JZL184 and abundance of other cellular lipids measured by mass spectrometry. Results for individual donors is shown alongside combined data. Combined data is mean +/- SEM of 3 biological replicates. ANOVA with Bonferroni correction for selected pairs (US vs US & JZL184; US vs M&P; M&P vs M&P & JZL184). *p<0.0332, **p<0.0021, ***p<0.0002. CE = cholesterol ester; FaCN = Fatty acyl carnitine; FaCoA = Fatty acyl CoA; (a)TAG = (alkyl)triacylglycerol; PG = phosphatidylglycerol; US = Unstimulated; M&P = MDP & PAM

3.3.12 MGLL inhibition affects secreted 2AG and other MAGs

There are a number of hypotheses as to why the effects of MGLL inhibition on cellular lipidomics were not as dramatic as anticipated. Firstly, only one timepoint was used (24h). Given that MGLL is induced at 6-8h following stimulation it is possible that some lipid flux occurs at earlier timepoints. Secondly, there may be unwanted effects of foetal calf serum (FCS) in the culture media on lipidomic profiles. It is known that the inhibitory effects of THC on murine splenocytes is reduced with 10-20% FCS compared to 5% FCS[378]. It may, therefore, be that serum has a direct effect on cannabinoid lipids and cannabinoid signalling in moDCs as has been shown in macrophages[379]. Thirdly, extrapolating from the neurological literature where endocannabinoids act trans-synaptically, it may be that ECS lipids are secreted from moDCs to act in an autocrine or paracrine manner.

To attempt to address these questions secreted lipids were assessed at earlier timepoints and in chemically-defined serum free media (XVivo15, Lonza). It has previously been demonstrated that moDCs generated in serum free media (including XVivo15) still function to efficiently stimulate T cell responses despite slightly reduced maturation and lower cytokine production[380]. A pilot experiment was performed to ascertain the volume of media required to extract and identify lipids. A slight reduction in viability was recorded in the serum free media compared to R10 (58% vs 77%). Similar concentrations of lipid were harvested from each volume (Figure 3.18). However, it was deemed preferable to use larger cell numbers to minimise undetected lipids and so for the main experiment $15x10^6$ cells were used per condition (in 15ml serum free media).

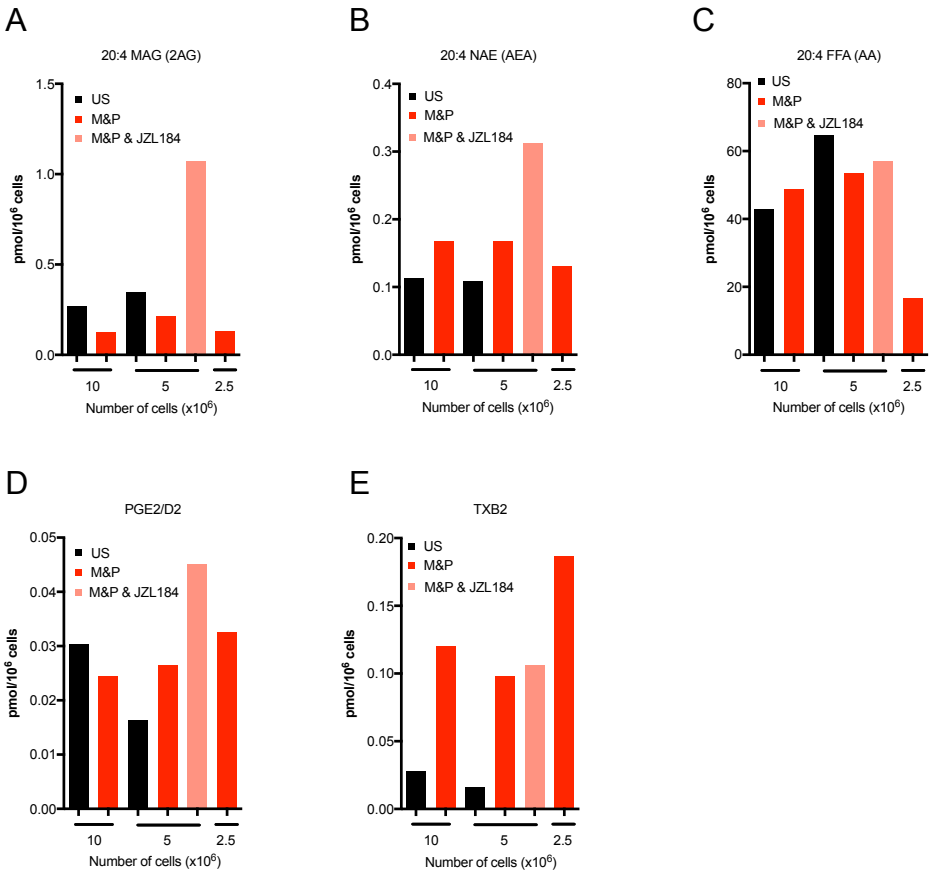

Figure 3.18 Pilot study of endocannabinoid-related secreted lipidomics in moDCs in serum-free media

Pellets of moDCs containing either 2.5, 5 or 10x10^6 cells were left unstimulated or stimulated with MDP & PAM for 24h with/without JZL184 in balanced serum-free media. Supernatant was aspirated and immediately frozen at -80°C prior to analysis for lipidomics by mass spectrometry. **(A)** 2AG; **(B)** AEA; **(C)** AA; **(D)** composite PGE2/D2; **(E)** TXB2. Results are absolute lipid quantification in media relative to number of cells of 1 biological replicate (1 donor provided cells for the 10x10^6 samples, and a second donor for the 5 and 2.5x10^6 samples).

MGLL inhibition dramatically increased both secreted 2AG but also 18:1 MAG upon stimulation (Figure 3.19C/D). Neither of these lipids were altered upon stimulation in the absence of MGLL inhibition. Minimal 2AG was detected in the media alone suggesting this is being generated and released from moDCs earlier than 6h following stimulation. This could be consistent with the timecourse of MGLL induction to normalise 2AG levels and restore homeostasis. Similar to the cellular lipidomic profile, effects of JZL184 were seen on NAEs reflective of off-target FAAH action (Figure 3.19G/H). Similar to 2AG, AEA was not detected in the

media alone and is therefore generated and released by moDCs. No effects of JZL184 were seen on arachidonic acid (Figure 3.19L) or downstream prostaglandins (Figure 3.19M/N). FFAs were detected in abundance in the media alone fraction and this is difficult to explain other than through technical failure of FFA measurement in the 'media alone' sample or because they act as a substrate for moDC function.

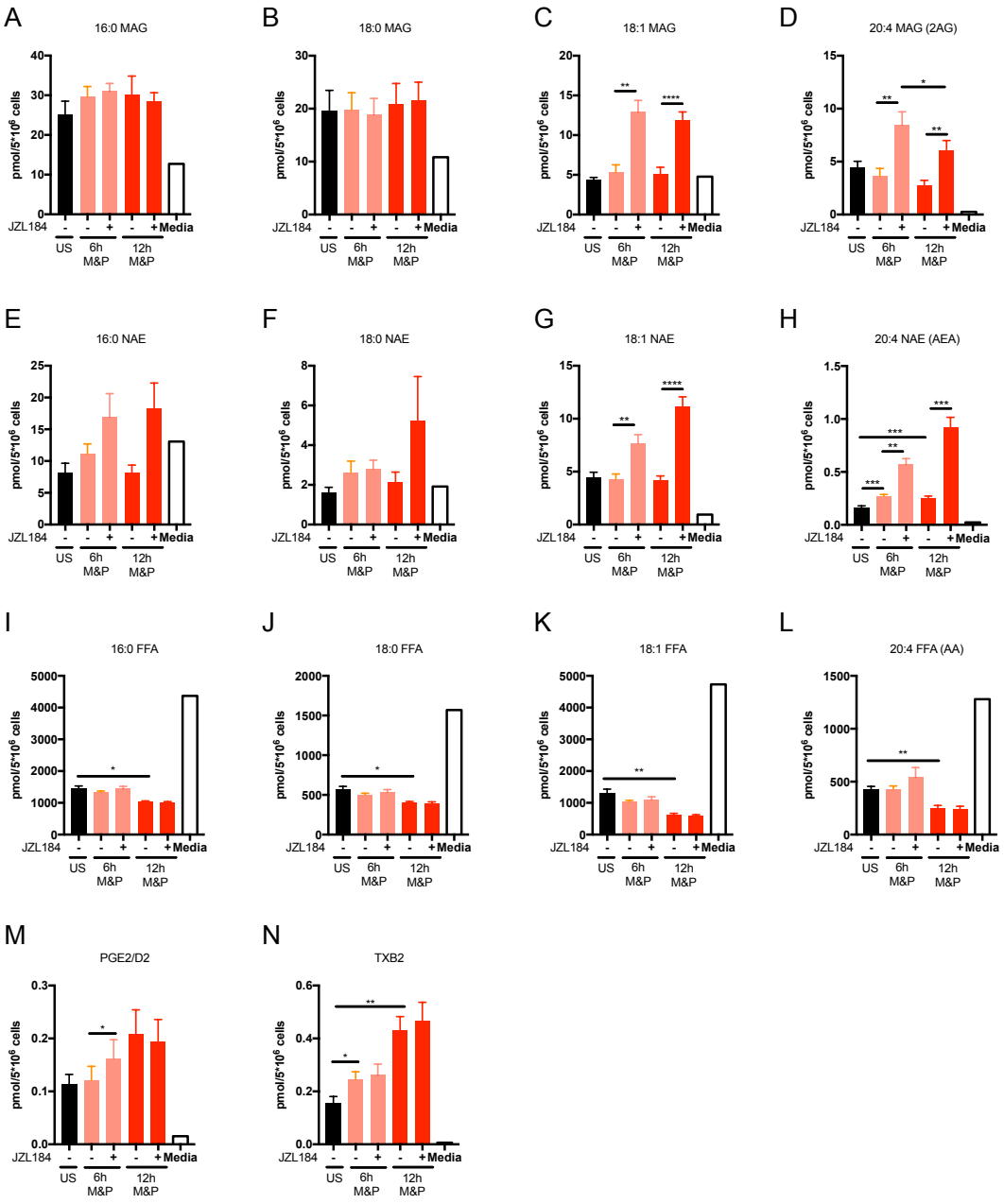

Figure 3.19 MGLL inhibition results in increased levels of 2AG, 18:1 MAG, AEA, and 18:1 NAE secreted into the media following stimulation

moDCs were stimulated with MDP & PAM for 6h or 12h with or without JZL184 in balanced serum-free media. Supernatant was aspirated and immediately frozen at -80°C prior to analysis for lipidomics by mass spectrometry. Secreted **(A-D)** MAGs; **(E-H)** NAEs; **(I-L)** FFAs; **(M)** composite PGE2/D2; **(N)** TXB2. Absolute quantification of each lipid subset in media alone is displayed for reference. Mean +/- SEM of 7 biological replicates. ANOVA with Bonferroni's correction for selected pairs. *p<0.0332, **p<0.0021, ***p<0.0002, ****p<0.0001.

3.3.13 MGLL levels following MDP stimulation are impaired by the RIPK2 inhibitor ponatinib

Although MGLL inhibition results in alterations in cellular and secreted lipids in moDCs upon stimulation it is not well understood how MGLL transcription is triggered following engagement of PRRs. As discussed in Chapter 1, NOD2 oligomerises and interacts with RIPK2 upon ligand binding to trigger downstream gene transcription via NF-κB and MAPK. To investigate the role of RIPK2, moDCs were incubated with a selective RIPK2 inhibitor, ponatinib[381], prior to stimulation with MDP. At a concentration of 50nM, ponatinib abrogated an increase in MGLL transcription (Figure 3.20A) and this was concentration-dependent (Figure 3.20B). TNFα transcription was used as a positive control with inhibition shown at 50nM and 5nM concentrations (Figure 3.20C). The reduction in transcription correlated with reduced MGLL protein as assessed by both ABPP (Figure 3.20D/E) and immunoblotting (Figure 3.20F).

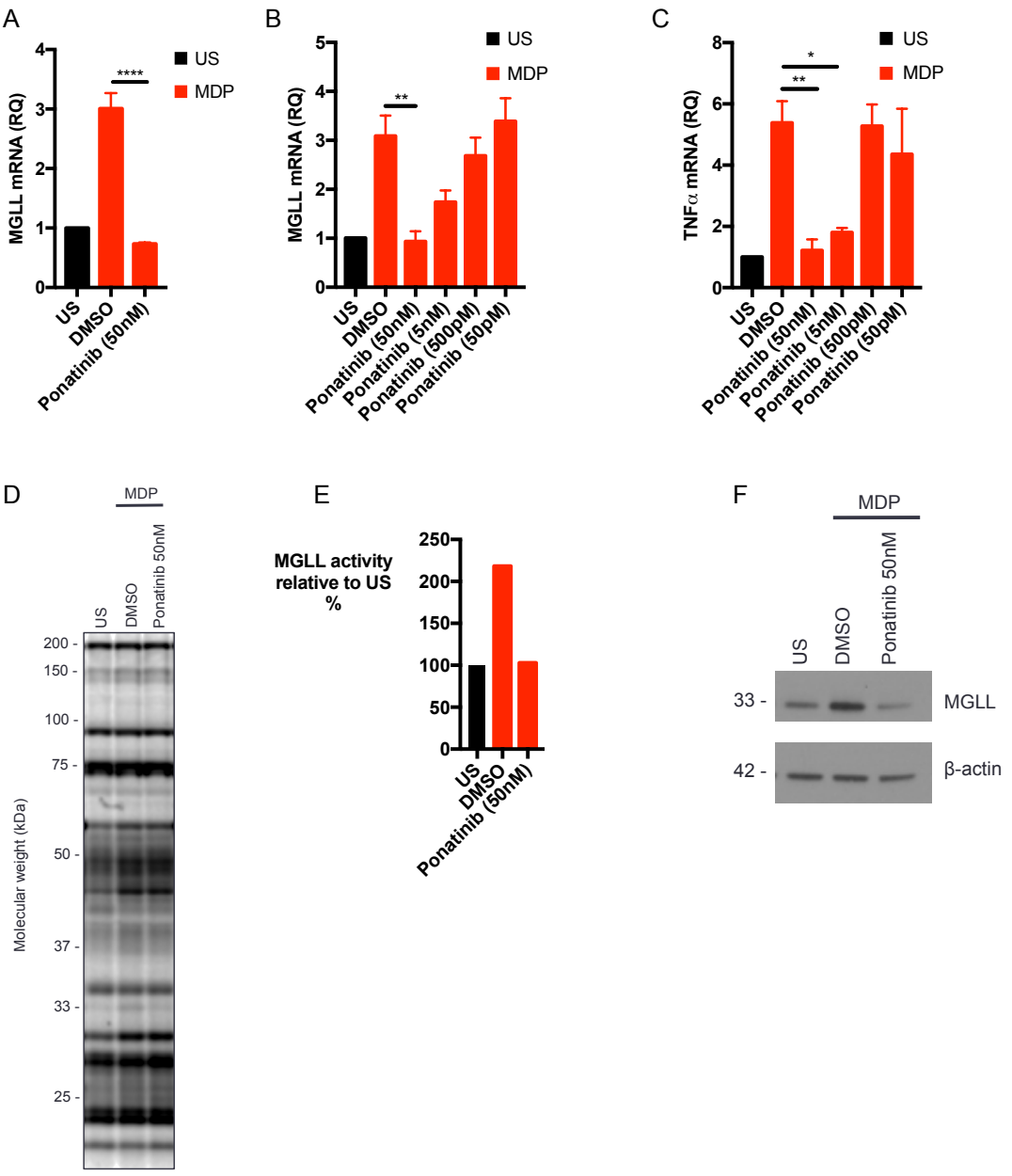

Figure 3.20 MGLL activity following stimulation with MDP is dependent on RIPK2
moDCs were incubated with ponatinib, a selective RIPK2 inhibitor, for 30 minutes prior to stimulation for 6h with MDP and qPCR for MGLL expression. Ponatinib inhibits MGLL transcription following 6h MDP stimulation **(A)** and is concentration dependent **(B)** with effects on TNFα as a positive control **(C)**. This corresponds with effects on MGLL protein as assessed by ABPP following 24h stimulation **(D)**, densitometry analysis of gel **(E)** and immunoblot **(F)**. qPCR data is mean +/- SEM of 4 biological replicates (A) or 3 biological replicates (B, C). ANOVA with Bonferroni's correction for selected pairs. *p<0.0332, **p<0.0021, ****p<0.0001. ABPP gel and immunoblot are representative of 2 biological replicates.

3.3.14 MGLL levels are impaired by small molecule inhibitors of MAPK, TBK1 and Syk following PAM stimulation but not in TBK1, IKKε or MyD88 THP-1 knockdown cell lines

To assess potential contributors to MGLL transcription/translation following TLR2 stimulation, moDCs were incubated with various small molecule inhibitors of key signalling enzymes prior to stimulation with PAM. Knockdown THP-1 cell lines for TBK1, IKK**ε**, and MyD88 were also assessed.

TLR2 activation may result in gene transcription either through TRAF6-TAK1-MAPK or TRAF6-TAK1-NF-κB pathways as discussed in Chapter 1. Similarly, TLR2 can activate the PI3K pathway[382] perhaps by recruiting the adaptor protein BCAP which has been shown to induce signalling through PI3K[43]. Furthermore, in murine BMDCs, TLR2 stimulation has been shown to activate TBK1/IKKε and that this is MyD88 and TANK dependent[383]. PAM activates human platelets via the tyrosine kinases src and syk[384] but the roles of these kinases in moDCs is not well understood. Both src and syk can signal through CARD9 and NF-κB to induce gene expression, and inflammasome responses are muted in dendritic cells deficient in syk[385]. Inhibitors of these and other pathways including Raf-1, LRRK2, protein kinase A, and GSK3 were screened for effects on MGLL transcription.

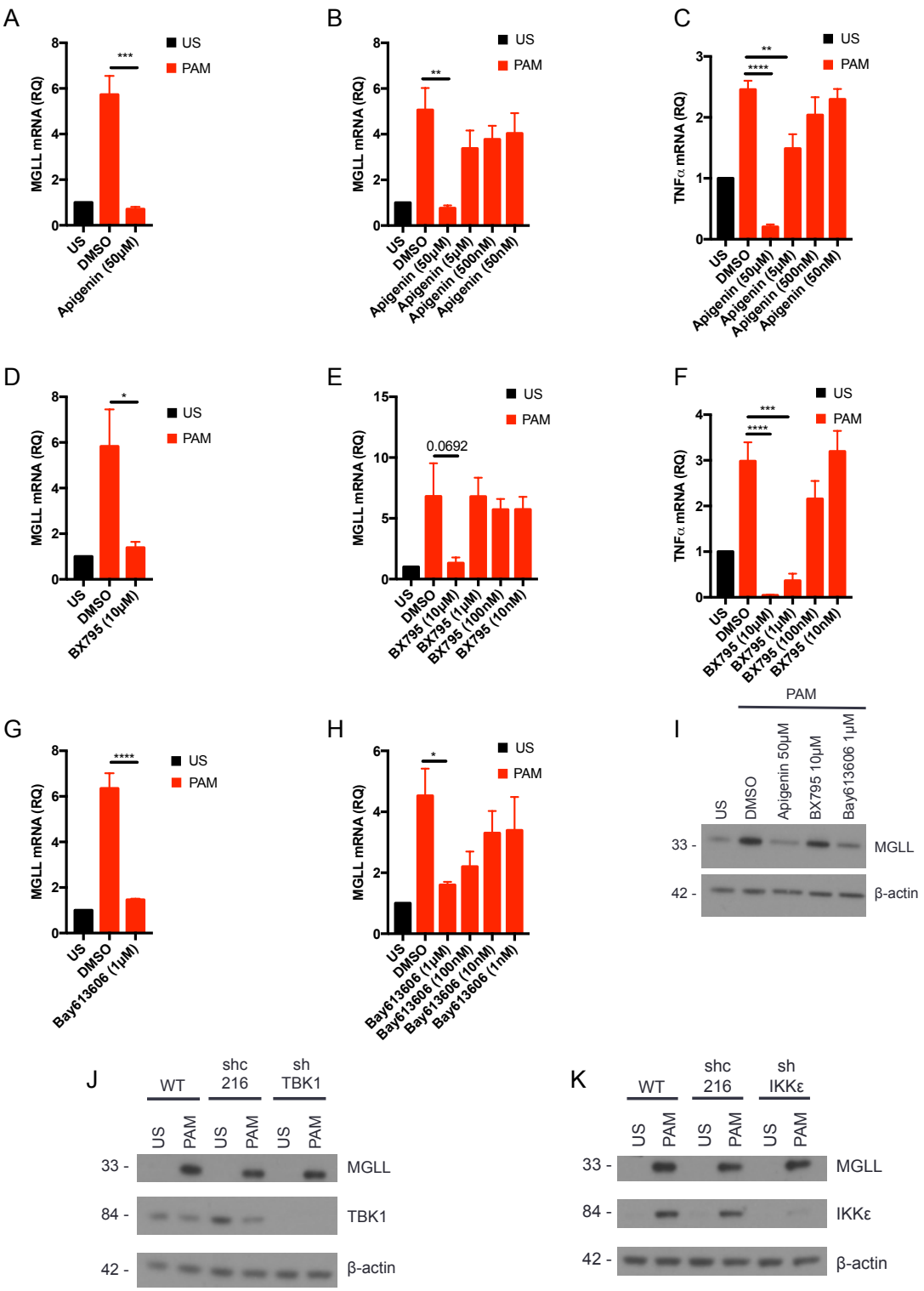
A
MGLL mRNA (RQ)
US
PAM
***
US
DMSO
Apigenin (50μM)
B
MGLL mRNA (RQ)
US
PAM
**
US
DMSO
Apigenin (50μM)
Apigenin (5μM)
Apigenin (500nM)
Apigenin (50nM)
C
TNFα mRNA (RQ)
US
PAM
**
****
US
DMSO
Apigenin (50μM)
Apigenin (5μM)
Apigenin (500nM)
Apigenin (50nM)
D
MGLL mRNA (RQ)
US
PAM
*
US
DMSO
BX795 (10μM)
E
MGLL mRNA (RQ)
US
PAM
0.0692
US
DMSO
BX795 (10μM)
BX795 (1μM)
BX795 (100nM)
BX795 (10nM)
F
TNFα mRNA (RQ)
US
PAM
***
****
US
DMSO
BX795 (10μM)
BX795 (1μM)
BX795 (100nM)
BX795 (10nM)
G
MGLL mRNA (RQ)
US
PAM
****
US
DMSO
Bay613606 (1μM)
H
MGLL mRNA (RQ)
US
PAM
*
US
DMSO
Bay613606 (1μM)
Bay613606 (100nM)
Bay613606 (10nM)
Bay613606 (1nM)
I
PAM
US
DMSO
Apigenin 50μM
BX795 10μM
Bay613606 1μM
33 -
MGLL
42 -
β-actin
J
WT
shc 216
sh TBK1
US
PAM
US
PAM
US
PAM
33 -
MGLL
84 -
TBK1
42 -
β-actin
K
WT
shc 216
sh IKKε
US
PAM
US
PAM
US
PAM
33 -
MGLL
84 -
IKKε
42 -
β-actin

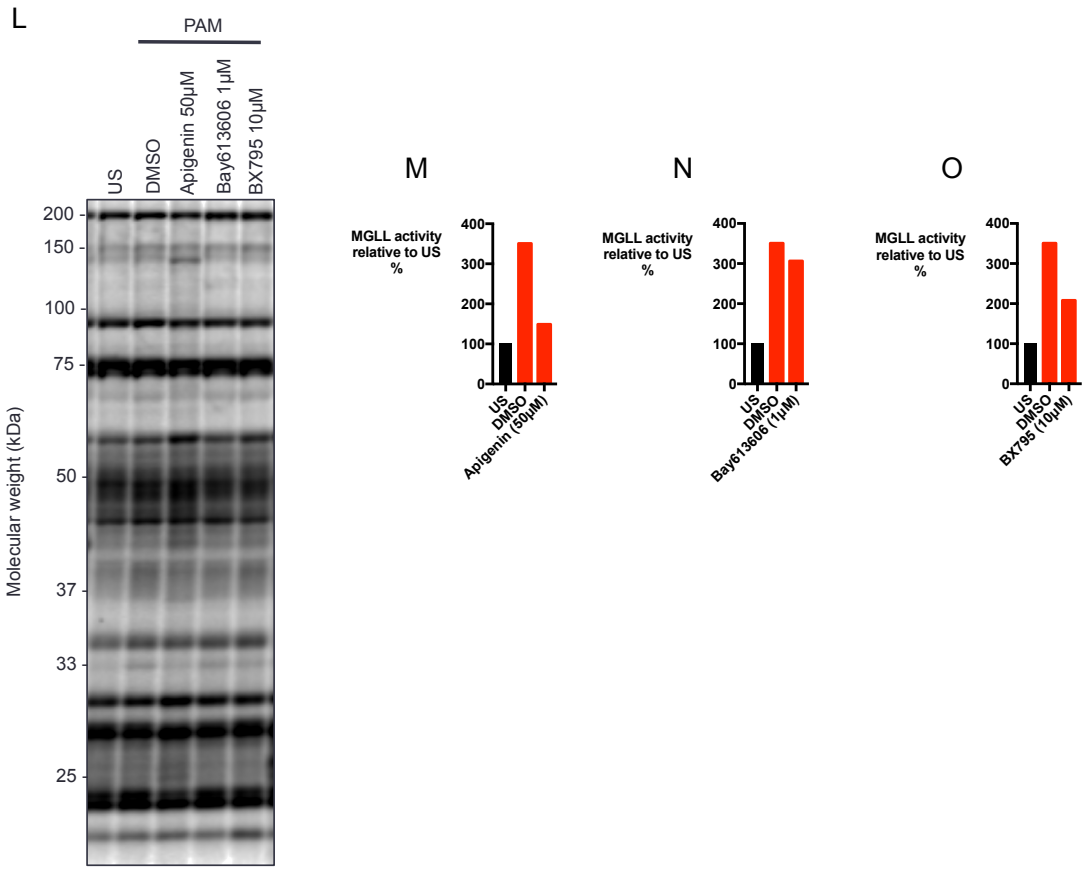

Figure 3.21 Small molecule inhibitors of MAPK/ERK (Apigenin), TBK1 (BX795) and Syk (Bay613606) inhibit MGLL following stimulation of moDCs with PAM

moDCs were incubated with small molecule inhibitors for 30 minutes prior to stimulation for 6h with PAM and qPCR for MGLL expression. **(A-C)** Apigenin and **(D-F)** BX795 inhibit MGLL transcription in a concentration dependent manner with effects on TNFα as a positive control. **(G, H)** Bay613606 inhibits MGLL transcription with some effect of concentration. **(I)** MGLL protein, assessed by immunoblot, is reduced after 24h PAM stimulation particularly by Apigenin and Bay613606. Effects of BX795 on MGLL could not be recapitulated in **(J)** TBK1 and **(K)** IKKε knockdown THP1 cell lines suggestive of off target effects. **(L-O)** ABPP gel and densitometry following 24h stimulation demonstrates a reduction in MGLL activity particularly by Apigenin and BX795. qPCR data is mean +/- SEM of 3 (B, C, E, F, H), 4 (A, G) or 5 (D) biological replicates. ANOVA with Bonferroni's correction for selected pairs. *p<0.0332, **p<0.0021, ***p<0.0002, ****p<0.0001. Immunoblots are representative of 2 biological replicates (I) or one technical replicate (J, K) using control and targeting shRNA knockdown. ABPP gel is representative of 2 biological replicates.

Apigenin, an inhibitor of MAPK, resulted in a dose-dependent inhibition of MGLL and TNFα transcription (Figure 3.21A-C). Similar findings were seen with the TBK1 inhibitor, BX795 (Figure 3.21D-F) and the syk inhibitor, Bay613606 (Figure 3.21G/H). These inhibitors also resulted in a reduction in MGLL protein assessed by immunoblotting (Figure 3.21I) although this was less marked with TBK1 inhibition. Gel-based ABPP corroborated transcriptional findings only for apigenin and (partially) for BX795 (Figure 3.21L-O). Furthermore, the THP-1 knockdown cell lines for TBK1 and IKKε showed no difference in MGLL protein following PAM stimulation (Figure 3.21J/K). Whilst this may reflect different responses in different cell types it is plausible that the effects seen with BX795 are due to off-target effects, possibly on NF-κB. No effects were seen with inhibition of a range of other signalling pathways (Figure 3.22). Wortmannin, a PI3K inhibitor, resulted in an increase in MGLL transcription (Figure 3.23A) and MGLL protein assessed by gel-based ABPP (Figure 3.23B/C).

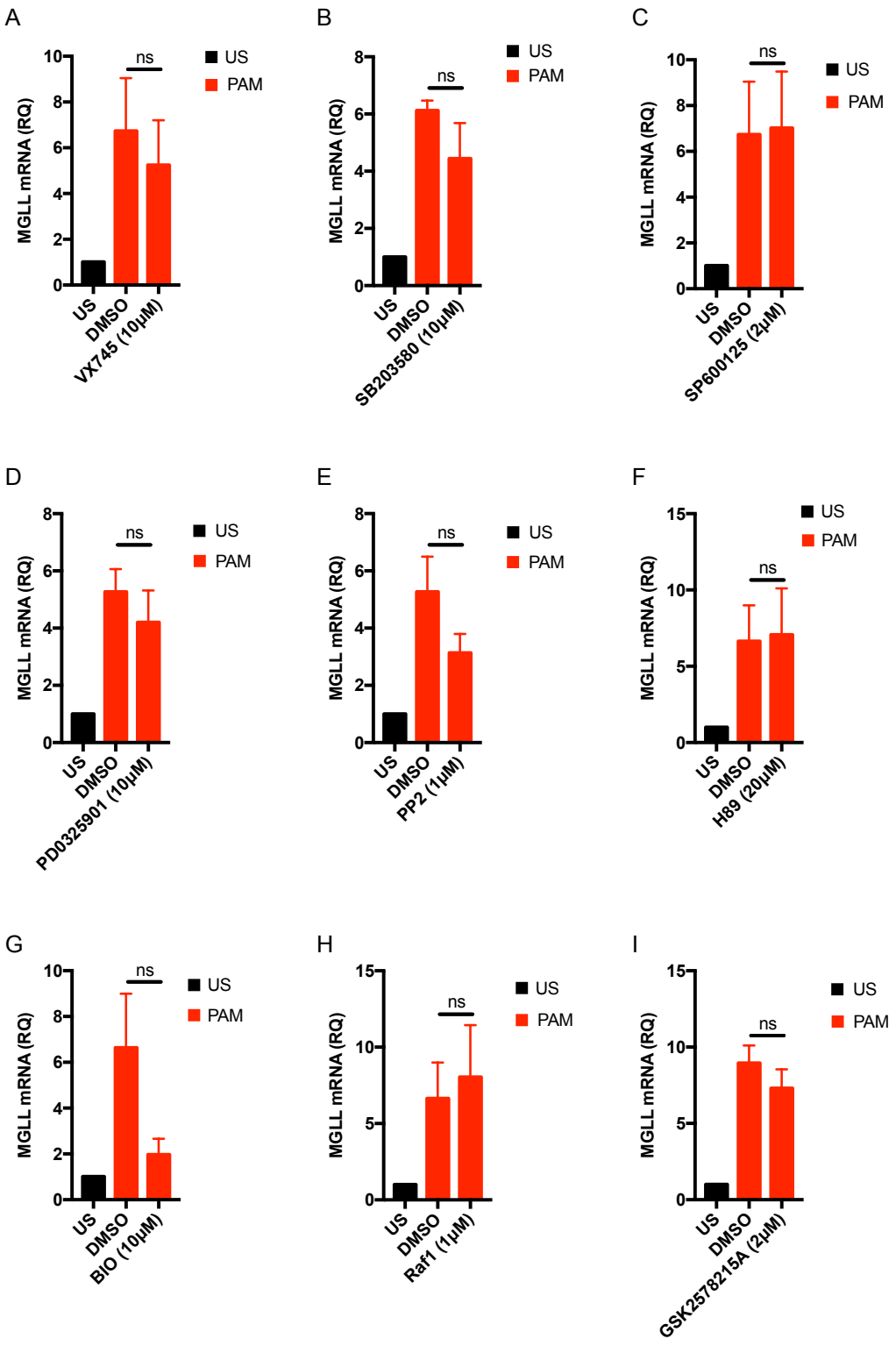

Figure 3.22 Effects of small molecule inhibitors of other signalling pathways on MGLL transcription following stimulation with PAM

moDCs were incubated with small molecule inhibitors for 30 minutes prior to stimulation for 6h with PAM and qPCR for MGLL expression. **(A)** VX745 (p38 inhibitor), **(B)** SB230580 (p38 inhibitor), **(C)** SP600125 (JNK inhibitor), **(D)** PD0325901 (MEK inhibitor), **(E)** PP2 (Src kinase inhibitor), **(F)** H89 (Protein Kinase A inhibitor), **(G)** BIO (GSK3 inhibitor), **(H)** Raf1 (Raf1 kinase inhibitor), **(I)** GSK2578215A (LRRK2 inhibitor). Mean +/- SEM of 4 (A, C-I) or 5 (B) biological replicates. ANOVA with Bonferroni's correction for selected pairs.

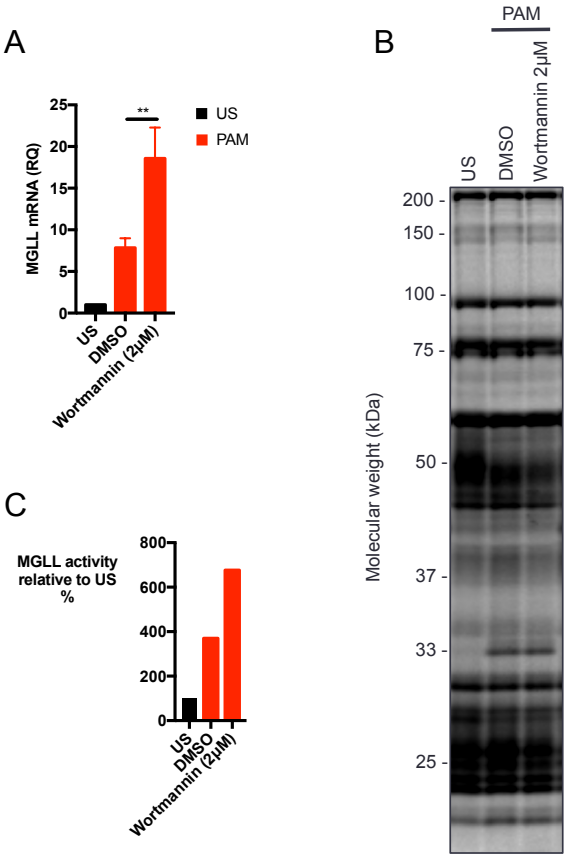

Figure 3.23 Wortmannin (PI3K inhibitor) increases MGLL levels following stimulation with PAM

moDCs were incubated with small molecule inhibitors for 30 minutes prior to stimulation for 6h with PAM and qPCR for MGLL expression, or for 24h for MGLL protein. Wortmannin increase both **(A)** MGLL transcription and protein as assessed by **(B)** gel-based ABPP and **(C)** densitometry of the gel. qPCR data is mean +/- SEM of 8 biological replicates. ABPP gel is representative of 2 biological replicates. ANOVA with Bonferroni's correction for selected pairs. **p<0.0021.

One of the key adaptor proteins for TLR2 signal transduction is MyD88. MGLL expression in MyD88-knockdown THP-1 cells was not different to wild-type or control shRNA transfected cells (Figure 3.24A). This may be because of an incomplete knockdown of MyD88 or because an alternative pathway is implicated in MGLL transcription through TLR2. To attempt to address this, BMDCs were generated from the bone marrow of a wildtype C57BL/6 mouse and a MyD88$^{-/-}$ littermate. Although the production of TNFα and IL6 was impaired in the knockout mouse, there was no difference in MGLL expression (Figure 3.24B-D). Consistent with the results from the THP-1 knockdown cells this may be because MyD88 is not required for MGLL induction. However, MGLL was not induced at 6h following stimulation even in the wildtype cells unlike human moDCs. Indeed with LPS stimulation, MGLL mRNA is reduced in both genetic backgrounds. Therefore, it is plausible that murine BMDCs induce MGLL at different timepoints and to a different extent than human moDCs. If this was the case then this would have implications for extrapolation of results from some murine studies into humans.

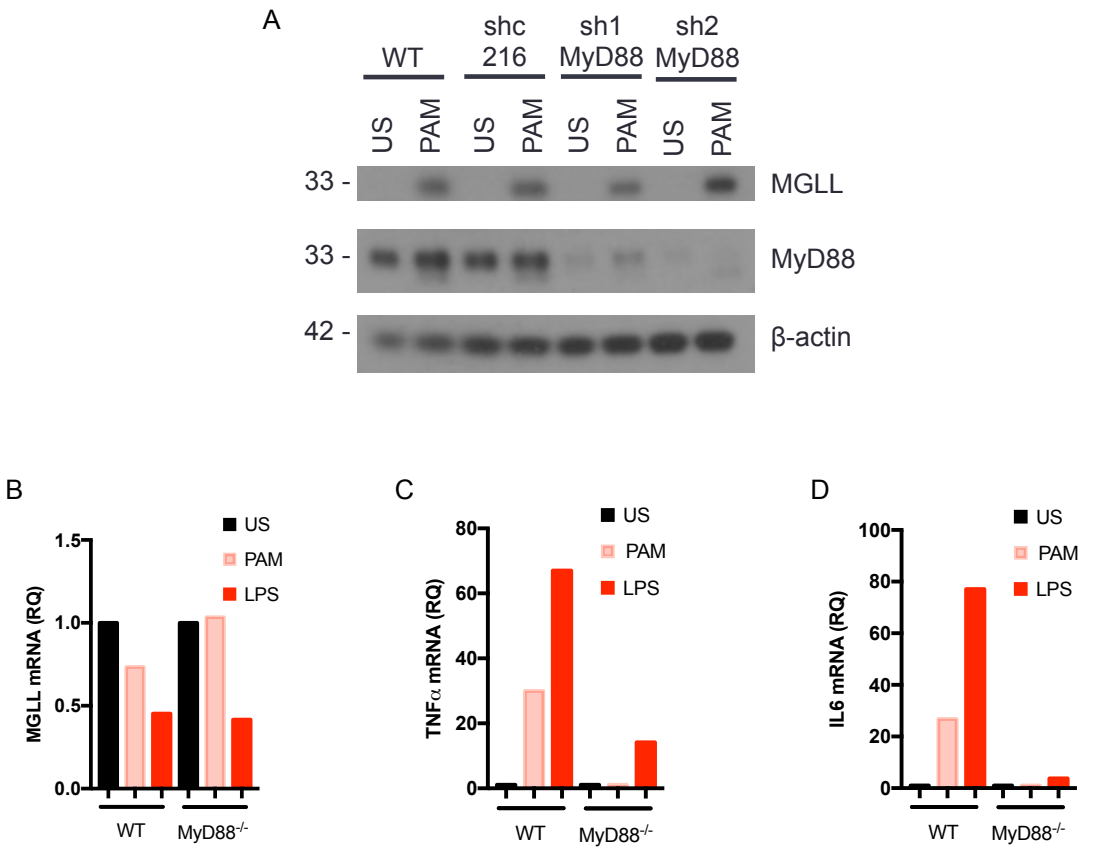

Figure 3.24 MGLL levels are not dependent on MyD88

MyD88 shRNA knockdown THP1 cells were stimulated with PAM for 24h. BMDCs isolated from MyD88$^{-/-}$ or wild-type C57BL/6 mice were stimulated for 6h with PAM or LPS and qPCR performed for MGLL expression. **(A)** MyD88 knockdown does not affect MGLL levels in THP1 cells assessed by immunoblot. Data is from 1 technical replicate. **(B)** MGLL expression is not increased in murine BMDCs at 6h following PAM or LPS stimulation although MyD88$^{-/-}$ ameliorates increases in **(C)** TNFα and **(D)** IL6. Data is from 1 biological replicate for each genetic background.

3.4 Discussion

This is the first account of ABPP profiling of human primary immune cells. moDCs demonstrate a rich repertoire of serine hydrolase enzymes, which are strikingly conserved between donors, with alterations in activity of some enzymes upon NOD2 and/or TLR2 stimulation. Given the functional diversity of the enzymes in this family it would be unlikely that other significant changes in activity were not occurring at different timepoints or with different stimuli. That MGLL was identified to be the enzyme with the most altered activity was serendipitous. Together with PLA2G4A this emphasises a role for arachidonic acid metabolism upon immune cell activation.

Although MGLL is detectable in unstimulated moDCs, MGLL induction has been shown to occur later upon cell activation (from 6-8h) but remains elevated until at least 48h even if the initial stimulus is withdrawn. This suggests that MGLL induction is dependent only on the initial MDP/PAM stimulus rather than requiring ongoing PRR ligation. The timecourse of activation could also suggest roles in immunoregulation to dampen the inflammatory response and restore moDC homeostasis following an initial inflammatory cascade. Furthermore, MGLL induction is a generalised response to PRR ligation and not restricted to NOD2/TLR2. This would suggest it has critical roles in modulating the function of moDCs. It would be fascinating to assay serine hydrolase expression, and MGLL in particular, in moDCs from patients with NOD2 variants to provide further insights into the dysfunction of this pathway in Crohn's disease.

Through pharmacological inhibition studies, JZL184 and MJN110 were shown to be effective at inhibiting MGLL activity and, alongside successful siRNA knock-down of MGLL in moDCs, allows interrogation of enzyme function. Acute pharmacological inhibition of MGLL has been shown to regulate endocannabinoid-related cellular lipids although did not influence arachidonic acid or prostaglandin levels. In murine tissues the degree to which MGLL, rather than PLA2G4A, contributes to prostaglandin production is tissue dependent[154] and this may, therefore, also be true of human cells/tissues. The contributions of each enzyme could be elucidated using indomethacin to inhibit COX enzymes, and inhibitors of PLA2G4A.

The results for LPC and LPE are promising although marked differences in response between donors was seen. In order to further elucidate the effects of MGLL on wider lipids it would be essential to perform lipidomic analysis with a larger number of donors, larger cell pellets and at different timepoints following stimulation. Notably in this analysis only one MAG was identified, 18:0 MAG, with no effects of JZL184. This was likely because of the untargeted, 'high-throughput', experimental approach and small cell numbers.

The finding that MGLL inhibition results in dramatic elevations in secreted 2AG and related lipids is novel and exciting. This suggests that at least some endocannabinoids act in the immune system in a similar way to the central nervous system. Unlike the CNS where signals are retrograde from the post- to pre-synaptic terminal, it may be that in the immune system endocannabinoids act through a different route. One hypothesis is that secreted endocannabinoids act in an auto-

crine manner to modulate ongoing moDC function (retrograde). Alternatively, they may act in a paracrine fashion to influence bystander cells, such as T cells (antegrade).

The results of the inhibitor/knockdown studies of signalling molecules raise more questions than answers. MGLL induction is a generalised response to TLR stimulation and not restricted to TLR2. This being the case, it is difficult to reconcile a single key signalling molecule which orchestrates transcription. Although apigenin resulted in inhibition of MGLL mRNA and protein, no effect was seen using the p38 inhibitors VX745 and SB230580, the JNK inhibitor SP600125, or the MEK inhibitor PD0352901 (Figure 3.22A-D). Apigenin has effects on NF-κB and caspase-1 at doses lower than that used to achieve inhibition of MGLL[386]. It is probable, therefore, that the effects of apigenin seen are due to inhibition of multiple cellular pathways rather than MAPK alone.

The role of syk in MGLL transcription was unexpected. Little is known about the role of syk downstream of TLR2. This kinase is involved with the interaction between Dectin-1 and MyD88 pathways[387] and Dectin-1 is known to synergise with TLR2 to induce IL-12 and TNFα[388]. However, an appropriate positive control cytokine was not identified in this experiment (data not shown) and so it remains possible that the effect seen on MGLL is also off-target. In colorectal cancer cell lines Bay613606, at a similar dose to that used in this experiment, had effects on MAP4K2 to inhibit NF-κB pathways[389]. Given that syk-deficient dendritic cells have a reduced inflammasome response, inflammasome activation was assessed in the presence of MGLL inhibition (Chapter 4). Put together, the effects on MGLL

seen with these two small molecule inhibitors and BX795 are likely due to off-target effects, perhaps on NF-κB, rather than on MAPK, TBK1/IKKε and syk.

Although the effects of wortmannin may be due to off-target actions especially at μM concentrations, it is interesting to speculate as to why PI3K inhibition might increase MGLL levels. PI3K signalling has been demonstrated downstream of TLR2 through recruitment of Rac1 and signals through Akt to induce NF-κB-dependent transcription[382]. However, whether PI3K signalling is pro- or anti-inflammatory is still debated[390] with some evidence that PI3K antagonises TLR signalling by promoting Stat3 and suppressing NF-κB-related gene transcription[391]. Interestingly, MGLL knockdown in HT29 colonic epithelial cells results in increased Akt phosphorylation[171] implying that wildtype MGLL may negatively regulate the PI3K/Akt pathway. The results presented in this chapter might also suggest that the PI3K pathway usually dampens MGLL transcription. So, if TLR2 stimulation wanes, there is reduced signalling to PI3K via BCAP releasing a 'brake' on MGLL transcription. MGLL increases with effects on bystander cells to modulate the ongoing inflammatory response. Given that MyD88 may not be required to induce MGLL upon TLR2 stimulation, signalling through BCAP and PI3K might be an attractive alternative pathway for investigation.

In murine microglia, MGLL transcription has been shown to be Stat6-dependent[225]. MGLL gene expression increases in murine livers in response to fasting and appears to be dependent upon PPARα, the effect being lost in knock-out mice[392]. Both these factors could be interrogated following PRR ligation in

moDCs. Interestingly, diet may also regulate MGLL levels with murine intestinal MGLL increasing following a high fat diet[393].

3.5 Conclusion

MGLL is upregulated in moDCs following PRR ligation, through pathways yet to be adequately annotated, to alter cellular and secreted lipid networks. The ubiquitous expression across innate immune cells, and increase upon cell stimulation, suggests MGLL is likely to have critical roles in immune cell function and response to inflammation.

Chapter 4 – moDCs and other innate immune cells function independently of MGLL activity across a range of assays

4.1 Introduction

The previous chapter has established MGLL to be induced upon PRR ligation and important for the regulation of both endocannabinoid and potentially wider lipid networks. It is not well understood how MGLL functions in innate immune cells and whether the effects of 2AG and MGLL are relevant for cells in isolation or for communication between immune cells. Much of the current literature is dominated by murine studies. These have highlighted roles for cannabinoids (including THC and/or endocannabinoids) in migration of dendritic cells[203], maturation[394], and effects on $T_H1/2$ polarisation favouring T_H2[214,395,396]. Some studies have been performed in human moDCs with one demonstrating that moDCs generated in the presence of THC are functionally impaired with a reduction in IL-12 production and impaired T cell responses[374]. Furthermore, THC and a CB2 agonist have been shown to reduce HIV replication in moDCs[397] and macrophages[398], and the former also suppressed IFNα production from plasmacytoid DCs suggestive of roles in antiviral immunity[399]. However, the effects of endocannabinoids on immune cell function appear to be dose-dependent. 2AG exerts a dose-dependent effect on reducing T cell proliferation[200] but notably this is also dependent on cell density with inhibition of proliferation at low density but increased proliferation at higher cell densities[210]. The effects of 2AG on migration are also dose dependent with optimal effects at 300nM concentration but reduced effects at low nM or high μM concentrations[204]. Similar findings have been

shown for the effects of anandamide on cytokine production[400]. In interpreting the results of studies involving the administration of 2AG exogenously it is important to recognise that 2AG is prone to isomerisation to 1AG in water-based media, unlike anandamide[401]. 1AG is also biologically active, particularly on CB1, with isomerisation occurring rapidly (less than 10 minutes in serum-containing media)[401]. This same study highlighted that as 1AG accumulates so the cannabinoid signalling at CB1 may be maintained. Thus, apparent effects of 2AG at timepoints beyond a few minutes may be partially caused by 1AG. Assessing the functional consequences of modulating endogenous 2AG by MGLL inhibition rather than relying on exogenous lipid administration is therefore attractive.

Although only one paper has examined the effects of 2AG on migration of dendritic cells (murine), another study identified 2AG to have effects on inducing migration of innate HL60, THP-1 and U937 cells and human monocytes[205], again in a dose-dependent manner. Although the authors suggested this was a CB2-dependent mechanism, it has subsequently been demonstrated that CB2 is not required for the effects of CB2 agonists on migration of murine macrophages[402]. 2AG has also been shown to induce migration of myeloid precursors in human leukaemia in a MEK/ERK dependent manner[403]. Interestingly, the CB2 agonists JWH015 and JWH133 reduced, rather than enhanced, migration of human monocytes to CCL2/3[404]. The ability of monocyte migration to be affected by cannabinoids may be reduced in people chronically exposed to THC[405] and it is plausible that this is due to desensitisation of the cannabinoid receptors. If it is indeed the case that 2AG induces migration and that this is not through the CB2 receptor then it is possible that prostaglandin production is important.

As DCs mature, CCR7 is upregulated on the cell surface as a requirement for optimal sensing of CCL19/21 and migration to lymph nodes. PGE2 is required for the generation of migratory DCs and for optimal migration to these chemokines[29,32] but does not alter surface expression of CCR7[30]. Furthermore, PGE2 is required throughout the maturation process to facilitate CCR7 signalling pathways[30]. Therefore it is possible that MGLL inhibition causes prostaglandin flux, although this was not detected at the pre-specified timepoints of the previous lipidomic experiments, and that this influences DC migration.

The data on the impact of cannabinoids on T cell polarisation raises questions about whether MGLL inhibition might modulate cytokine production from moDCs to potentially influence T cell polarisation. Key cytokines of relevance would include the IL-12 family and particularly IL-12p40 ($T_H1/17$), along with IL-10 (T_{reg}), and other common cytokines such as IL-6 and TNFα. Many of these cytokines are released early after PRR ligation. However, later cytokine release might also be relevant given the timescale of MGLL upregulation. In recent years the concept of trained innate immunity has been developed whereby innate cells undergo functional change through epigenetic reprogramming and transcriptional modification following an initial stimulus such that the response to subsequent stimuli is altered[406]. Broadly, innate cells may become tolerant or trained depending on the initial stimulus. Therefore, even if MGLL inhibition were not to affect immediate cytokine release, subsequent responses may be impacted.

4.2 Aims

1. To investigate if pharmacological MGLL inhibition inhibits cytokine release, maturation, migration, or pathogen handling of moDCs.
2. To investigate whether pharmacological MGLL inhibition inhibits cytokine production from trained monocytes.
3. To utilise genetic knockdown of MGLL in moDCs and THP-1 cells to corroborate pharmacological inhibition studies on cytokine production.

4.3 Results

4.3.1 The small molecules JZL184 and MJN110 do not reduce viability of moDCs as measured by an ATP-luminescence assay

Before exploring the potential roles of MGLL on moDC function it was important to confirm that the small molecule inhibitors were not affecting overall cell viability and that MGLL was not crucial for cell survival. A number of methods to assess viability exist including Trypan blue exclusion from intact cells. Although commonly used, this infers viability from cell membrane integrity and is a subjective technique[407]. The luminescence-based assay CellTiter-Glo® (Promega, USA), measures cell viability by quantitating ATP as a marker of metabolically active cells. Straightforward to use, it is suitable for multiplex measurements, with luminescence correlating with viable cell numbers.

moDCs were plated in a 96-well plate (50000 cells/100µl) and exposed to DMSO or MGLL inhibition for 24h. Doses much higher than that needed for target engagement were chosen with no significant effect seen on viability of unstimulated moDCs. moDCs were then stimulated with MDP & PAM for 24h. This similarly did not show an effect on cell viability (Figure 4.1). The use of an ATP-dependent viability measure also suggested that MGLL inhibition was not fundamentally altering ATP levels in moDCs including upon stimulation.

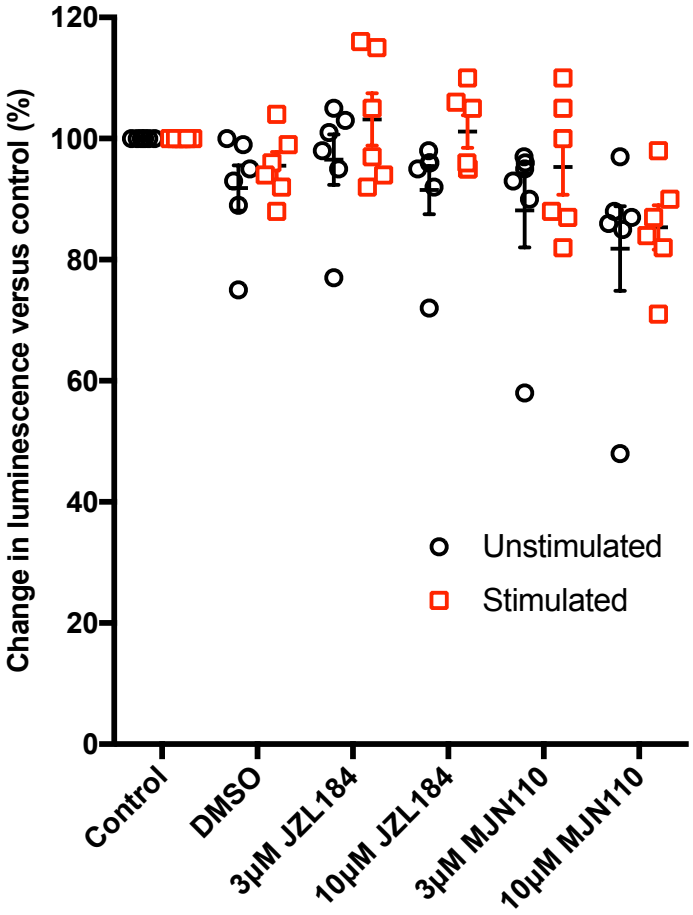

Figure 4.1 JZL184 and MJN110 do not reduce viability of moDCs
moDCs, either unstimulated or stimulated with MDP & PAM were incubated with MGLL inhibitors for 24h and then viability assessed by CellTiter Glo®. Mean +/- SEM of 6 biological replicates.

4.3.2 MGLL inhibition does not impair production of cytokines in moDCs following NOD2/TLR2 stimulation

Having confirmed that 100nM JZL184 was sufficient to achieve target engagement of MGLL in moDCs and that cell viability was not affected, the effect on cytokine production was assessed. After 30 minutes pre-incubation with JZL184 or DMSO, moDCs were stimulated with MDP & PAM and harvested at 2h or 6h for mRNA analysis. Supernatant was harvested at later timepoints (8h, 16h, 24h) for ELISA. The pro-inflammatory cytokines IL-1β, IL-6, and TNFα, the chemokine IL-8, and the anti-inflammatory cytokine IL-10 were chosen for analysis. IL23A was also chosen as the gene coding for IL-23p19 subunit which has been shown to be secreted from dendritic cells[408] and has roles in T_H17 development. IFNβ was included as a negative control as this cytokine is traditionally induced upon TLR3 stimulation and not by TLR2 or NOD2. Although some transcription was detected in this experiment, the cycle thresholds for this were generally over 37 and may therefore not be significant or be caused by non-specific activation of the dendritic cells.

A

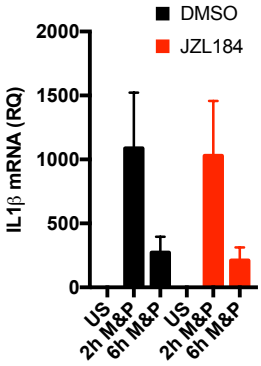
DMSO
JZL184
IL1β mRNA (RQ)
2000
1500
1000
500
0
US
2h M&P
6h M&P
US
2h M&P
6h M&P

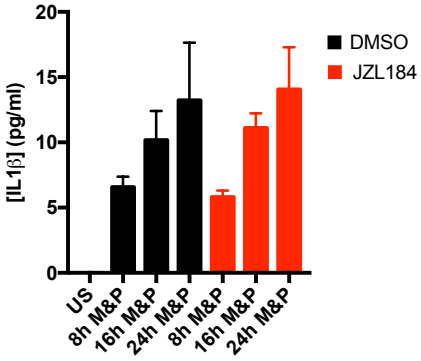
DMSO
JZL184
[IL1β] (pg/ml)
20
15
10
5
0
US
8h M&P
16h M&P
24h M&P
8h M&P
16h M&P
24h M&P

B

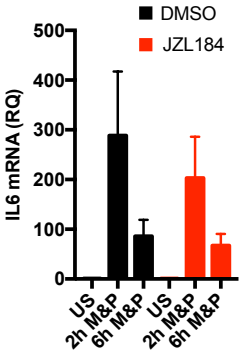
DMSO
JZL184
IL6 mRNA (RQ)
500
400
300
200
100
0
US
2h M&P
6h M&P
US
2h M&P
6h M&P

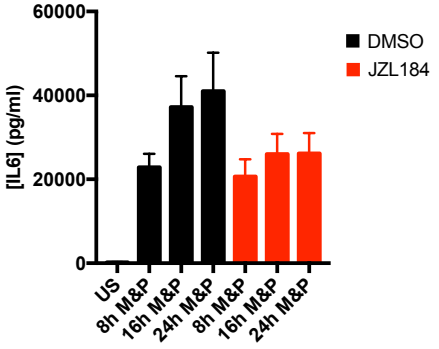
DMSO
JZL184
[IL6] (pg/ml)
60000
40000
20000
0
US
8h M&P
16h M&P
24h M&P
8h M&P
16h M&P
24h M&P

C

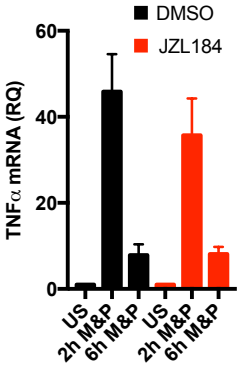
DMSO
JZL184
TNFα mRNA (RQ)
60
40
20
0
US
2h M&P
6h M&P
US
2h M&P
6h M&P

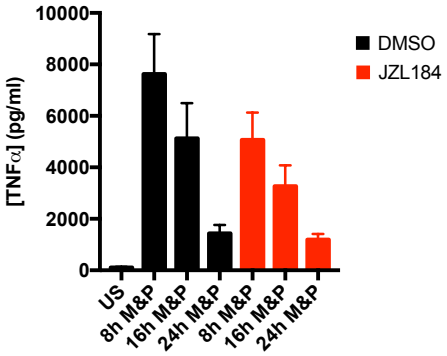
DMSO
JZL184
[TNFα] (pg/ml)
10000
8000
6000
4000
2000
0
US
8h M&P
16h M&P
24h M&P
8h M&P
16h M&P
24h M&P

D

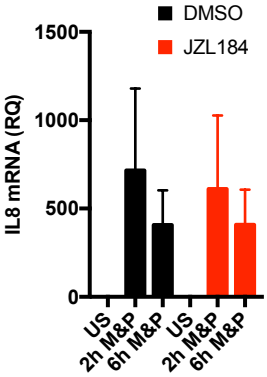
DMSO
JZL184
IL8 mRNA (RQ)
1500
1000
500
0
US
2h M&P
6h M&P
US
2h M&P
6h M&P

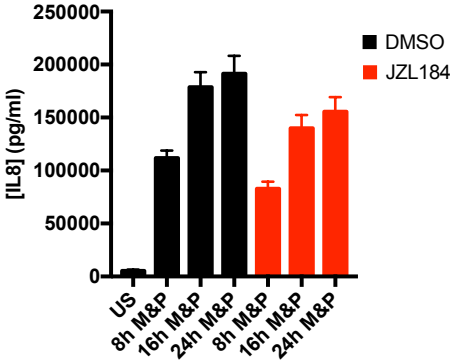
DMSO
JZL184
[IL8] (pg/ml)
250000
200000
150000
100000
50000
0
US
8h M&P
16h M&P
24h M&P
8h M&P
16h M&P
24h M&P

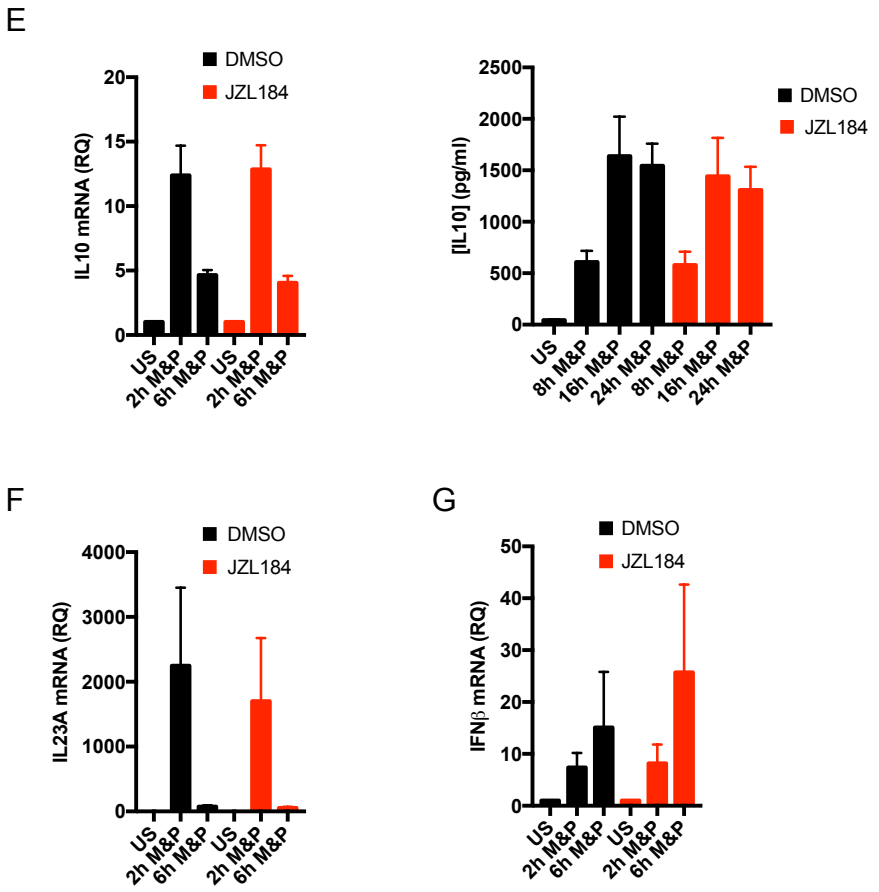

Figure 4.2 Cytokine production by moDCs is not affected by JZL184
moDCs were cultured in media with 10% FCS and stimulated with MDP & PAM in the presence or absence of JZL184. qPCR was performed on the cell pellets, and ELISA on supernatant. No effect of MGLL inhibition was seen on mRNA or protein production of **(A)** IL-1β, **(B)** IL-6, **(C)** TNFα, **(D)** IL-8, **(E)** IL-10 or on mRNA production of **(F)** IL23A and **(G)** IFNβ (ELISA not performed). Mean +/- SEM of 3 biological replicates. ANOVA with Bonferroni correction for selected pairs (DMSO vs JZL184 at each timepoint) were all non-significant. US = Unstimulated; M&P = MDP & PAM.

No significant effect of MGLL inhibition on cytokine production was identified for any of the other measured cytokines either by qPCR or ELISA (Figure 4.2). It is perhaps surprising that a protein so ubiquitously induced upon PRR stimulation does not have any effect on cytokine production. However, it is not altogether unexpected given that MGLL is not induced until 8h after stimulation increasing further to 24h and beyond. This does, however, confirm that MGLL inhibition is not preventing secretion of cytokines into the surrounding media.

An alternative explanation could be that the presence of lipids in serum is in some way affecting the ability of MGLL inhibition to impact upon cytokine production. To assess this, and to measure production of other IL-1 and IL-12 family cytokines, moDCs were resuspended in balanced serum free media (XVivo-15, Lonza). For this experiment, single stimulation with PAM was used rather than dual stimulation. Having removed serum from the media, and not knowing that effect this might have on moDC function, the intention was to remove the potential of crosstalk between pathways. If differences were seen between groups then further experiments could be performed with NOD2 alone and combined NOD2/TLR2 stimulation. Cells were harvested at 2h and 6h for qPCR as before, and for some cytokines supernatant was harvested at 16h (based on the results of the previous experiment) for ELISA.

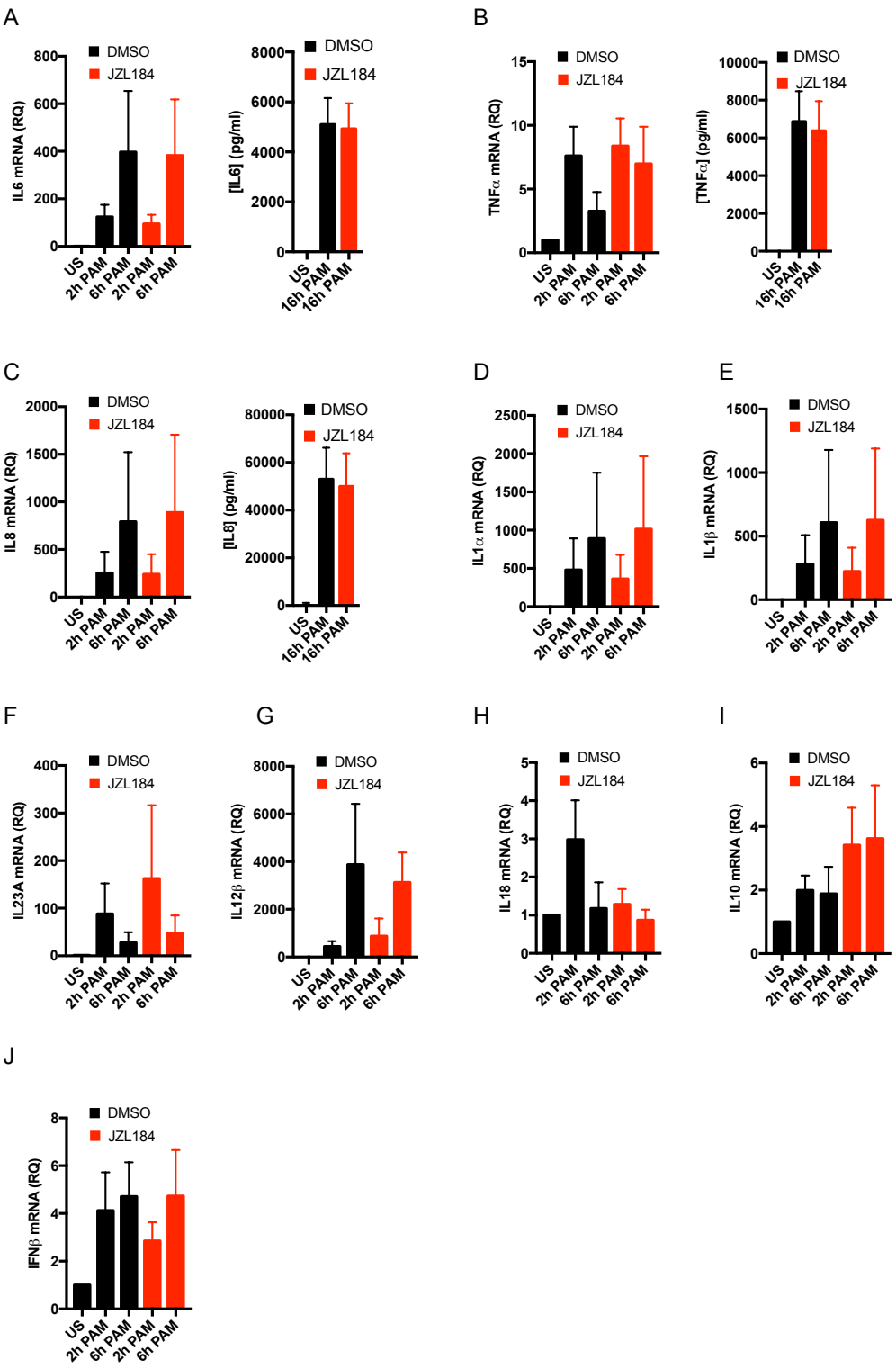

Figure 4.3 The absence of effects of JZL184 on cytokine production in moDCs is not dependent on serum in the media

moDCs were differentiated from monocytes in the presence of serum, washed and resuspended in serum-free media (XVivo-15, Lonza) prior to MGLL inhibition and stimulation with PAM. qPCR was performed on the cell pellets, and ELISA on supernatant from subsequent experiments. No differences were identified at mRNA or protein level for **(A)** IL-6, **(B)** TNFα or **(C)** IL-8, or at mRNA level alone for **(D)** IL1α, **(E)** IL1β, **(F)** IL23A, **(G)** IL12β, **(H)** IL18, **(I)** IL10, or **(J)** IFNβ. Mean +/- SEM of 4 biological replicates. ANOVA with Bonferroni correction for selected pairs (DMSO vs JZL184 at each timepoint) were all non-significant. US = Unstimulated.

Although the pattern of cytokine induction did not differ with MGLL inhibition (Figure 4.3), there was a delay to cytokine transcription in serum-free conditions for IL-6, IL-8, IL-1β and an overall reduction in peak levels. This may be in part due to the effects of loss of serum on cell function but also due to loss of NOD2/TLR2 synergy in boosting cytokine responses. Analysis of IL-1α, IL-12β and IL-18 which were not measured previously, did not show significant differences between groups (Figure 4.3D/G/H). Measurement of IFNβ again showed low levels detectable only at cycle thresholds greater than 37 and so are subject to the same caveats (Figure 4.3J).

The data from ABPP screening confirms target engagement of JZL184 at 100nM in moDCs to inhibit MGLL activity. However, it is possible that this small molecule is insufficient to completely inhibit MGLL activity and this could explain the cytokine findings. To address this, MGLL was knocked down in moDCs using siRNA techniques (Figure 4.4A). The cells were then left unstimulated or stimulated with MDP & PAM and the supernatant harvested for ELISA. No differences in cytokine production were seen for IL-6, TNFα, IL-12p40, or IL-10 between non-targeting and MGLL targeting siRNA (Figure 4.4B-E). Thus, evidence from both pharmacological inhibition and genetic knockdown studies confirm no effect of MGLL on a range of cytokines produced by moDCs, and that the presence or absence of serum is not important for this result.

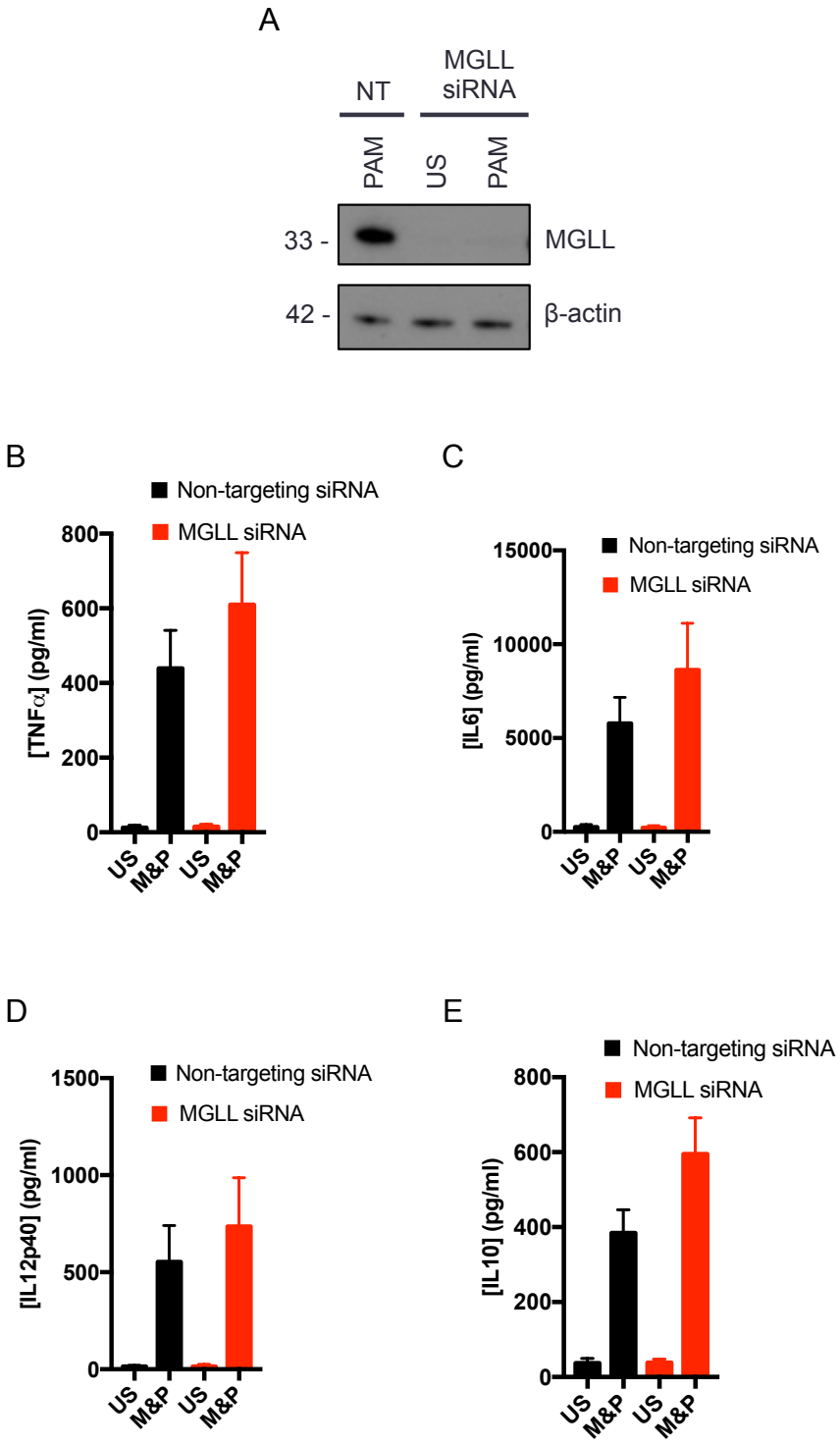

Figure 4.4 Genetic knockdown of MGLL using siRNA in moDCs has no effect on cytokine production

Non-targeting (NT) or MGLL-targeting siRNA was introduced to moDCs using electroporation. Cells were then stimulated with MDP & PAM and ELISA performed on the supernatant. **(A)** Knockdown was confirmed by immunoblot after stimulation of moDCs with PAM for 24h. Representative of 5 biological replicates. **(B-E)** No differences in production of IL-6, TNFα, IL-12p40, or IL-10 were seen. Mean +/- SEM of 5 biological replicates. ANOVA with Bonferroni correction for selected pairs (Non-targeting vs MGLL siRNA in the stimulated condition) were all non-significant. US = Unstimulated; M&P = MDP & PAM.

4.3.3 MGLL inhibition does not impair inflammasome activation in THP-1 cells

Part of the innate immune system, inflammasomes are complexes of proteins which assemble in response to PAMP/DAMP stimulation. One example is the NLRP3 inflammasome which may be associated with development of IBD[409]. This requires two signals for activation. The first signal (priming), for instance TLR ligation, activates NF-κB or AP-1 dependent transcription of genes including NLRP3, IL1β and IL18. This also results in the assembly of the NLRP3 inflammasome comprising NLRP3, the ASC complex (apoptosis-associated speck-like protein containing a CARD), and caspase-1. The second signal (activation) may be provided by PRRs but may also arise from markers of cellular stress or ionic flux[49,410]. This activates caspase-1 (from procaspase-1) which cleaves pro-IL-1β and pro-IL-18 leading to their release from the cell, and also leads to pyroptosis through cleavage of gasdermin-D[410].

Murine peritoneal macrophages have been shown to increase NLRP3 components in response to both LPS and DSS colitis challenge and that preincubation with an agonist of CB2 reduced the inflammasome response[284]. Therefore I hypothesised that MGLL inhibition might affect inflammasome activity in human innate immune cells by increasing 2AG concentrations. Using a model of inflammasome activation in THP-1 cells, which were shown in Chapter 3 to be a cell line expressing MGLL at similar timepoints to dendritic cells, signal 1 was provided by LPS and then signal 2 by nigericin. Nigericin is a potassium ionophore which induces potassium efflux which is known to activate the NLRP3 inflam-

masome[411]. Nigericin alone has been shown to be sufficient to release mature IL-18, but not IL-1β from THP-1 cells in the absence of a signal 1[412].

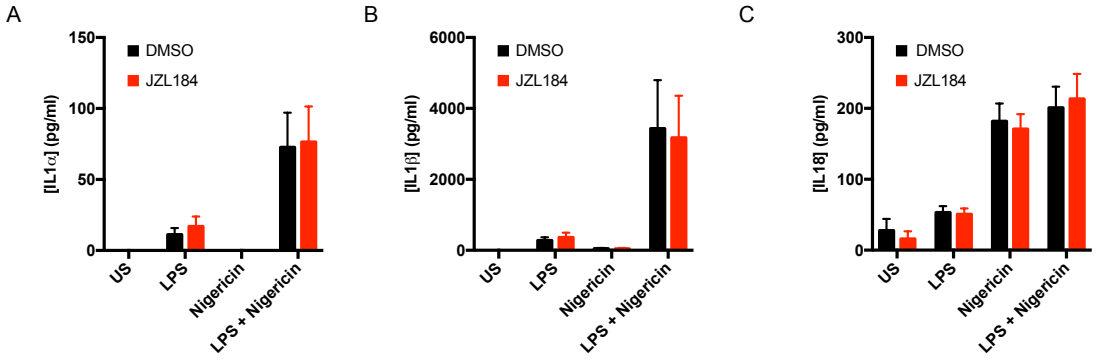

Figure 4.5 Inflammasome activation in THP-1 cells is not impaired by MGLL inhibition
THP-1 cells were stimulated with 1μg/ml LPS for 3h (first signal), or nigericin 5μM for 45 minutes (second signal) or both. ELISA was used to measure production of cytokines **(A-C)**. JZL184 did not affect production of IL-1α, IL-1β, or IL-18. Nigericin alone was able to stimulate IL-18 production. Results are mean +/- SEM for the combined data from 3 separate experiments.

In keeping with current literature, nigericin alone resulted in an increase in IL-18 but not IL-1α/β (Figure 4.5). A modest effect of LPS alone was seen on all three cytokines but marked synergy for IL-1α/β production was seen with both signal 1 and 2. There was no difference in inflammasome activation in the presence or absence of MGLL inhibition.

4.3.4 Gene expression measured by microarray in moDCs shows no significant effect of JZL184

Having identified no effect on cytokine production in moDCs it was questioned whether MGLL inhibition might be affecting expression of other genes in moDCs. To address this hypothesis, moDCs from 4 donors were prepared for microarray analysis. Cells were left unstimulated or stimulated with MDP & PAM for 8h or 16h (for microarray) and for 24h (for ABPP analysis). Experiments on all donors were run simultaneously resulting in a total of 24 samples.

Target engagement of JZL184 was confirmed for each donor using gel-based ABPP (Figure 4.6) alongside incubation of a DMSO stimulated proteome incubated with ABD1970 immediately prior to ABPP analysis to confirm the MGLL band. Quality control analysis of the microarray samples provided to the WTCHG confirmed appropriate clustering of samples both by hierarchical clustering and principal component analysis (Figure 4.7A/B). These data did not identify clear differences between DMSO treated and JZL184 treated samples but did demonstrate an effect of stimulation. There were no outlier samples and high quality data was obtained. A total of 20136 probes were identified in the samples.

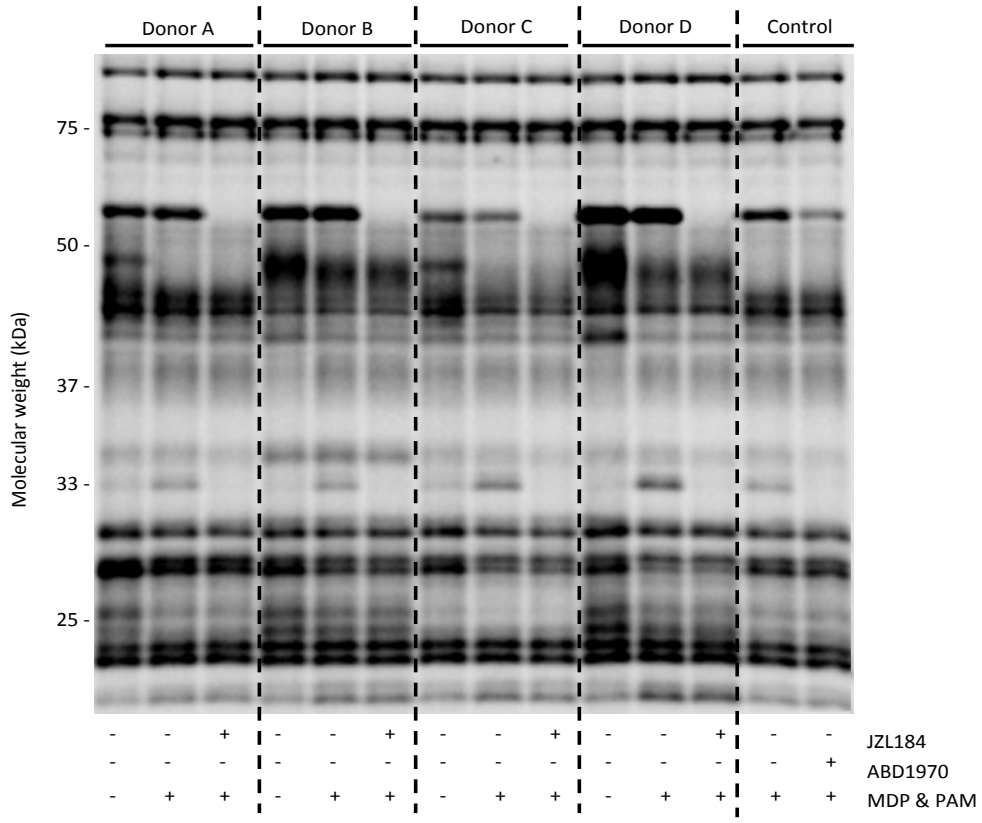

Figure 4.6 Gel-based ABPP confirms target engagement of JZL184 in all 4 replicates
moDCs were stimulated for 24h with MDP & PAM in the presence or absence of JZL184. Proteome from donor A incubated with ABD1970 immediately prior to ABPP to confirm MGLL band.

Comparisons were performed between 16h JZL versus 16h DMSO, and also 8h JZL versus 8h DMSO. No differences were identified at adjusted p<0.05. This included for the detected ECS-related genes encoding MGLL, DAGLα, DAGLβ, and PLA2G4A. CNR1 and CNR2 were not detected.

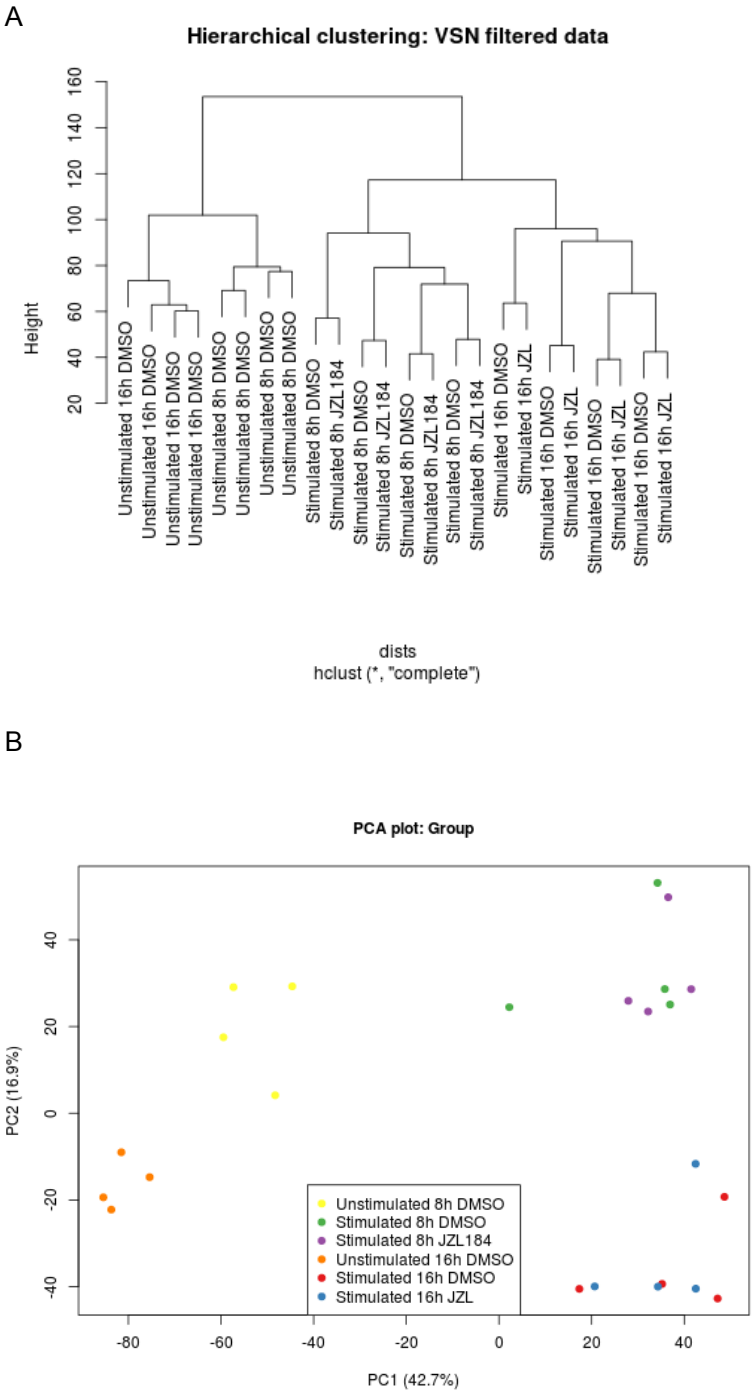

Figure 4.7 Quality control of samples submitted for microarray analysis
(A) Hierarchical clustering and **(B)** Principal Component (PC) Analysis confirms samples cluster by stimulation time but not presence or absence of MGLL inhibition.

In order to confirm this microarray analysis, ten genes with adjusted $p<0.05$ and the greatest fold-change difference with JZL184 treatment were selected to validate by qPCR. For all genes selected, qPCR measurement corroborated the findings of microarray (Figure 4.8) even if the degree of change differed between the two measurement techniques. An earlier 2h timepoint was included for qPCR screening to try and identify earlier changes in gene expression between groups. This timepoint similarly showed no effect of MGLL inhibition.

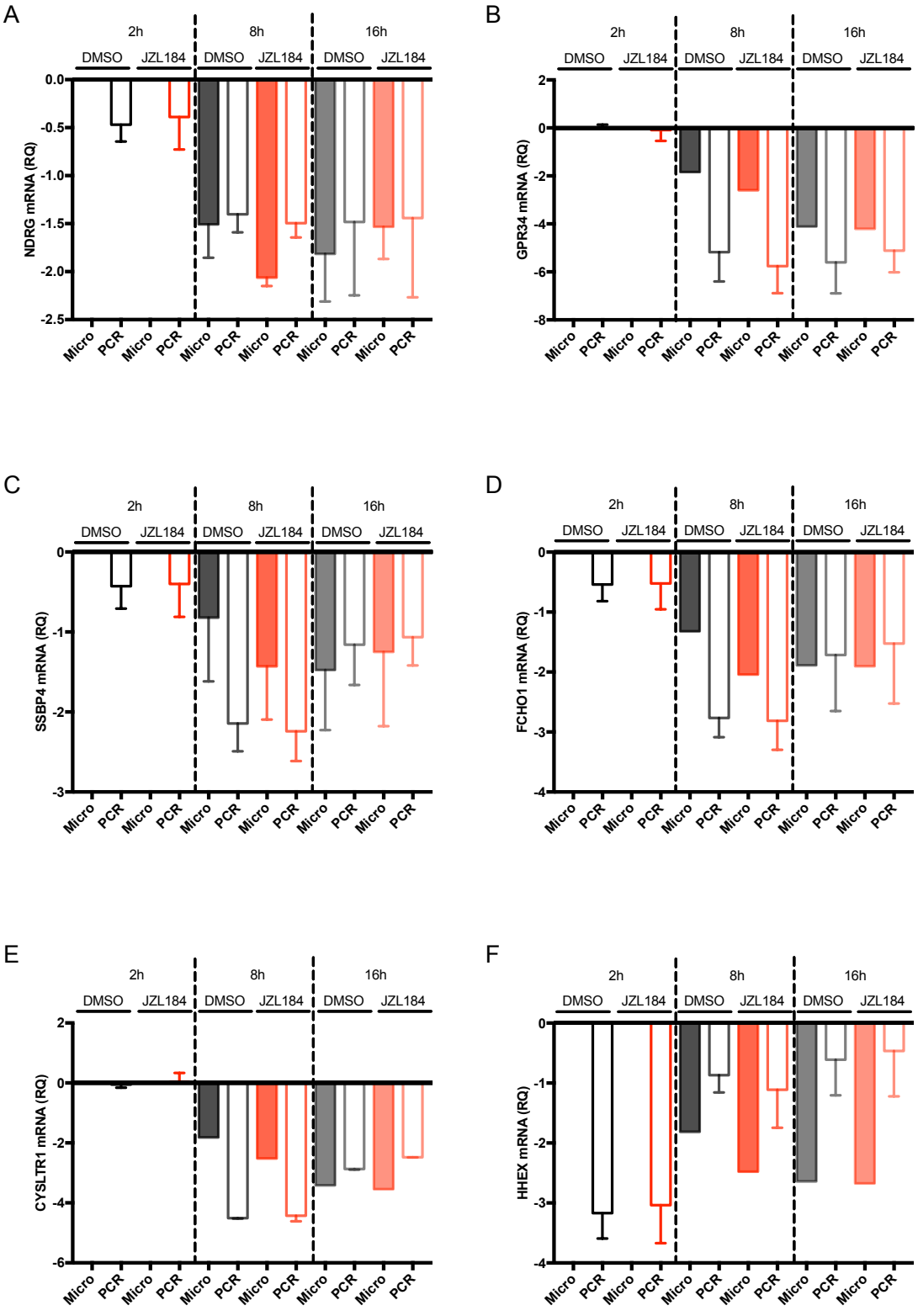
A
2h
8h
16h
DMSO
JZL184
NDRG mRNA (RQ)
0.0
-0.5
-1.0
-1.5
-2.0
-2.5
Micro
PCR
B
GPR34 mRNA (RQ)
2
0
-2
-4
-6
-8
C
SSBP4 mRNA (RQ)
-1
-3
D
FCHO1 mRNA (RQ)
E
CYSLTR1 mRNA (RQ)
F
HHEX mRNA (RQ)

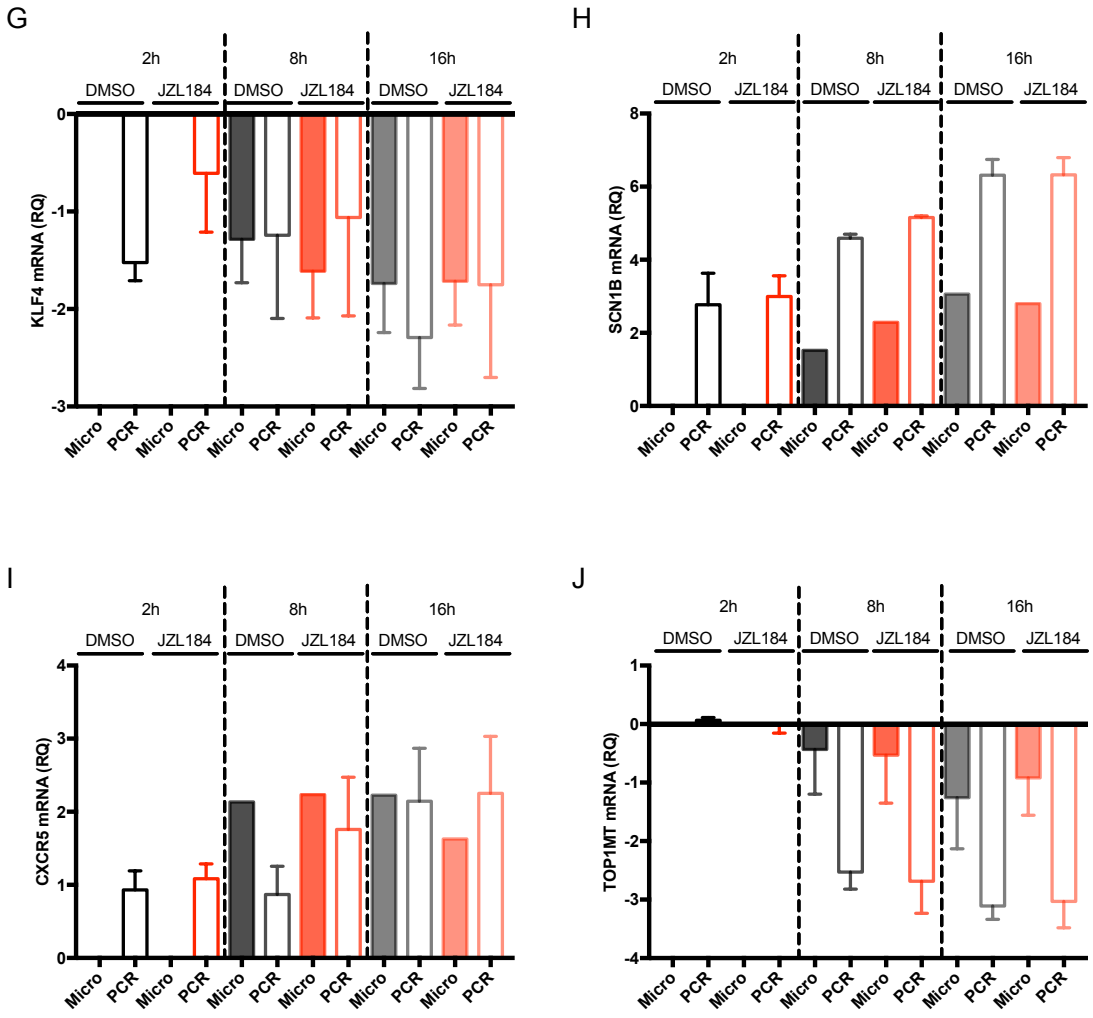

Figure 4.8 Validation of ten genes identified in the microarray by qPCR confirms no effect of MGLL inhibition

moDCs were stimulated for 2, 8 or 16h with MDP & PAM in the presence or absence of JZL184. RNA was extracted and qPCR performed. qPCR data is mean +/- SEM of 2 biological replicates. Microarray data is mean +/- SEM where more than one probe was used for each gene. ANOVA with Bonferroni correction for selected pairs (DMSO vs JZL184 at each timepoint) were all non-significant. Micro = microarray data; PCR = qPCR data.

4.3.5 Expression of cell surface maturation markers and chemotactic migration of moDCs is not impaired by JZL184

In response to PRR stimulation, DCs undergo a maturation programme which results in a functional shift from endocytosis to antigen presentation, migration, and effects on T cell polarisation. Cell surface markers including HLA-DR (MHC-II) and the co-stimulatory molecules CD80/86, CD83, and the chemokine receptor CCR7 are upregulated during maturation. This enables formation of the immunological synapse with T cells and chemotactic migration through CCL19/21 towards lymph nodes.

Using flow cytometry, cell surface markers were quantified and stimulated cells compared to unstimulated (immature) cells. A robust increase in CD80/86, CD83, HLA-DR and CCR7 was demonstrated upon stimulation but this was not affected by MGLL inhibition (Figure 4.9).

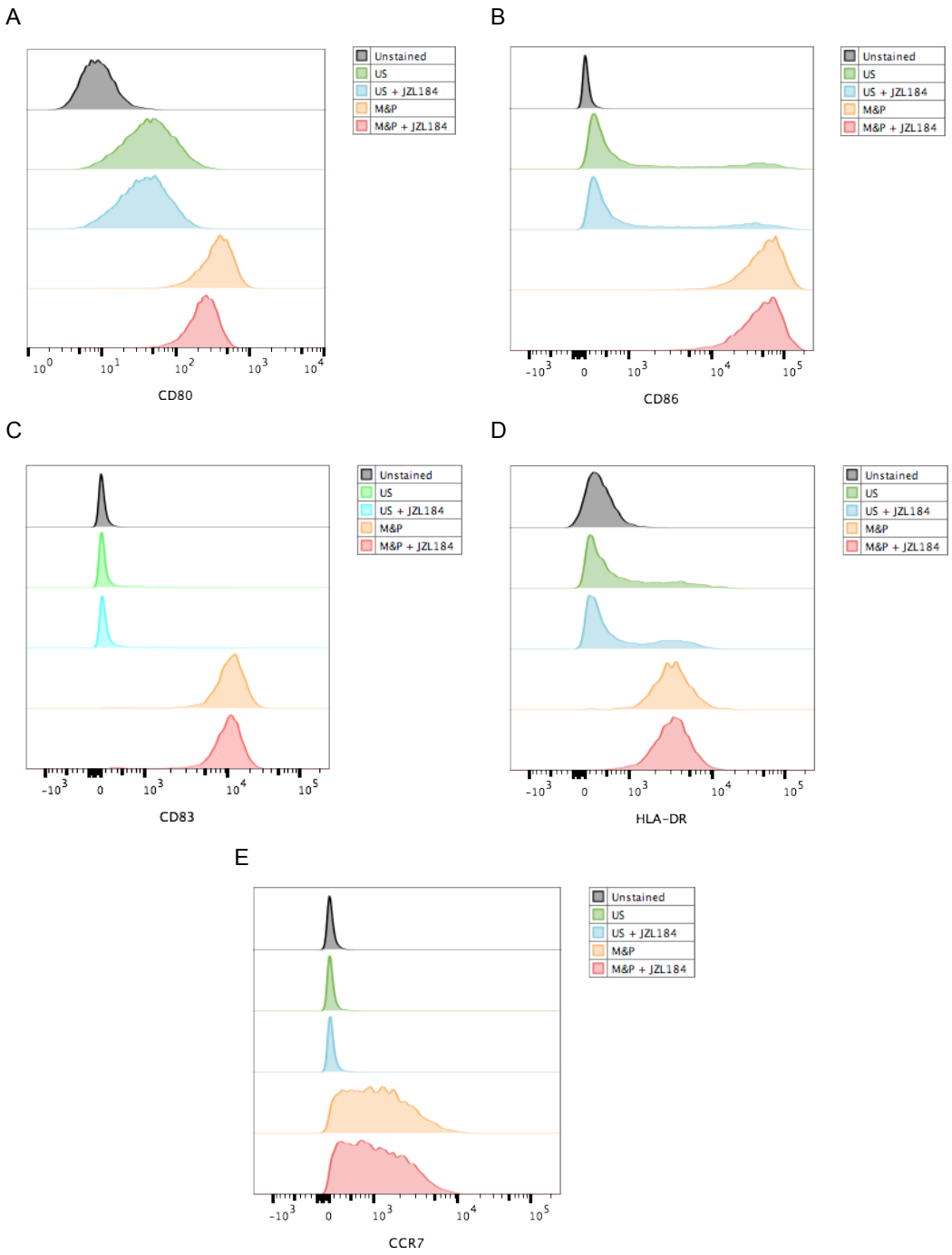

Figure 4.9 Cell surface markers of dendritic cell maturation are increased upon stimulation with MDP & PAM but are not reduced by MGLL inhibition

moDCs were incubated with DMSO or 100nM JZL184 for 30 minutes prior to stimulation with MDP & PAM for 24h. Cells were harvested, stained and analysed by flow cytometry for **(A)** CD80, **(B)** CD86, **(C)** CD83, **(D)** HLA-DR, and **(E)** CCR7. Representative of 3 biological replicates apart from CCR7 (2 biological replicates).

Whilst no differences were identified in CCR7 expression, background literature emphasises the importance of PGE2 to chemotactic migration of dendritic cells and 2AG in migration of monocytic cell lines and murine BMDCs. Although the lipidomic data did not identify an effect of MGLL inhibition on cellular PGE2/D2 at 24h, or secreted PGE2/D2 at 6h or 12h, it is plausible that earlier or more subtle changes in prostaglandin production occur. The lipidomic data did confirm an effect of MGLL inhibition on both cellular and secreted 2AG which could also affect migration.

To investigate migratory capacity in real-time, chemotaxis across a fluorescence-blocking membrane was measured. Migration of moDCs in response to CCL21 was increased upon maturation but there were no significant differences with MGLL inhibition (Figure 4.10). Some migration through the membrane occurred with the unstimulated cells which may not be chemotaxis, rather diffusion-related. It is possible that the dose of CCL21 used is too high to reveal subtle difference in migratory capacity although this dose had previously been optimised for human moDCs (Louise Johnson, University of Oxford, personal communication and [413]). However, given the absence of effect of MGLL inhibition on prostaglandin production by lipidomic analysis and on CCR7 expression by flow cytometry it is likely that there is indeed no effect on chemotactic migratory capacity.

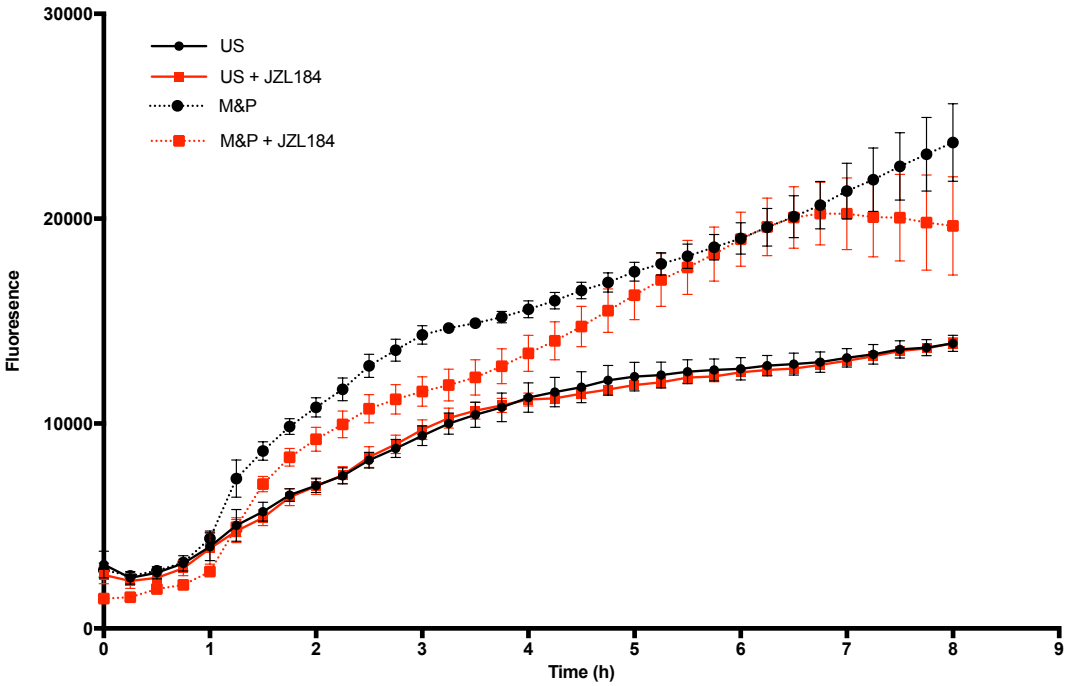

Figure 4.10 Migration of moDCs to CCL21 is increased upon stimulation but no effect of MGLL inhibition is seen

moDCs were labelled with CellTracker Green® and then stimulated with MDP & PAM in the presence or absence of JZL184. Measurement of migration to CCL21 across a fluorescence-blocking membrane was measured every 15 minutes for 8 hours using an inferior reading plate reader. moDCs were seen to migrate to a greater extent after maturation but JZL184 did not reduce migration potential. Representative of 3 biological replicates. Mean +/- SEM of 3 technical replicates per timepoint and per condition. US = Unstimulated; M&P = MDP & PAM.

4.3.6 Optimisation of a direct antigen presentation assay with MGLL inhibition

Endocytosed antigens may be presented as peptides on MHC-II molecules to $CD4^+$ T cells, whereas endogenously synthesised antigens in the cytoplasm are classically presented on MHC-I molecules[22]. However, dendritic cells may also cross-present exogenous antigens on MHC-I molecules to $CD8^+$ T cells[414]. In order to establish a T cell response, both an MHC-peptide complex and co-stimulatory molecules must be present on the surface of the APC. Furthermore, a T cell with a corresponding T-cell receptor must be present to bind to the MHC-peptide complex. The melanA protein is expressed by normal melanocytes and

many types of melanoma and is recognised by HLA-A2 restricted T lymphocytes[347]. The prevalence of melanA-specific cytotoxic T lymphocytes, measured using melanA tetramers, in the healthy population was 60% in one study[415]. Pulsing of moDCs, matured with LPS, with melanA peptide has previously been shown to expand tetramer$^+$CD8$^+$ T cells[347] even at low doses of peptide.

Having established that key cell surface maturation markers associated with class 2 antigen presentation, namely HLA-DR, CD80 and CD86, were not affected by JZL184 we questioned whether antigen presentation to CD8$^+$ lymphocytes might be affected. PBMCs were isolated from leucocyte cones and screened by flow cytometry for cell surface HLA-A2 (Figure 4.11A). The experiment was repeated with 5 independent HLA-A2 positive donors, including two different batches of melanA peptide. Furthermore, advice on optimisation was sought from Mariolina Salio and Isabel Panse (University of Oxford) both of whom have significant expertise in this area. Despite these efforts, it was not possible to demonstrate the presence of significant numbers of tetramer$^+$CD8$^+$ T lymphocytes even in the absence of MGLL inhibition. A representative flow cytometry plot is shown (Figure 4.11B). Therefore it is not possible to comment on a potential role of MGLL inhibition on the presentation of melanA to T lymphocytes. There was also no difference between conditions on expression of CD69, CCR7, and CD45RO (data not shown).

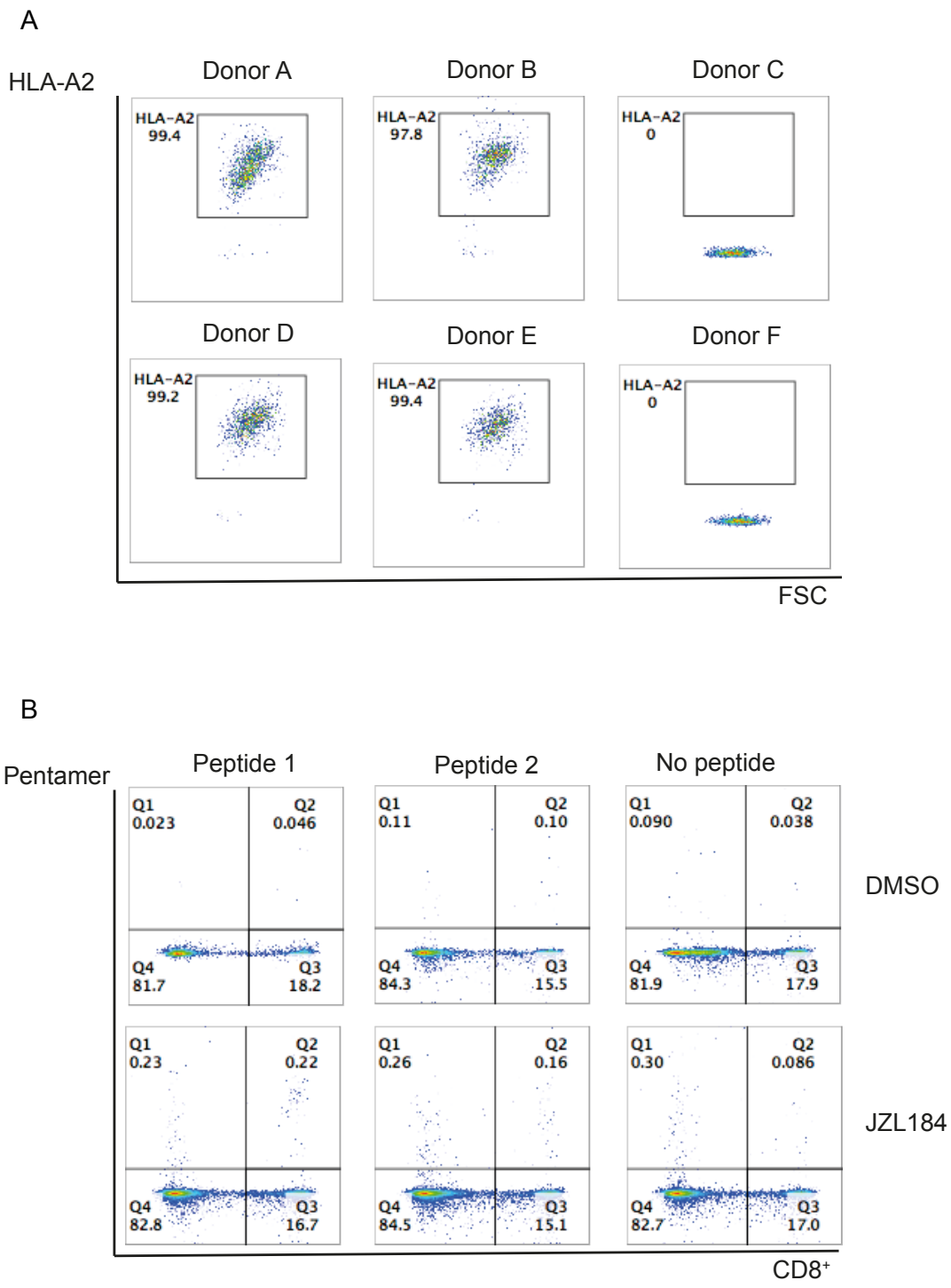

Figure 4.11 MelanA direct antigen presentation assay

HLA-A2 positive moDCs were matured with LPS for 36h and then pulsed with MART-1 peptide. Autologous CD14- PBMCs were added at a ratio of 1:20 and then co-cultured with IL-2 and IL-7 for 14 days. Cells were analysed by flow cytometry for CD8 and pentamer staining. **(A)** HLA-A2 status was assessed by flow cytometry. **(B)** No upregulation of CD8/pentamer double positive cells was seen in the presence of 2 different MART-1 peptides (Peptide 1 and 2) compared to the negative control. No effect of JZL184 could be identified. Representative of 5 biological replicates.

4.3.7 MGLL inhibition does not affect handling of *Salmonella enterica* serovar Typhimurium, replication of human immunodeficiency virus, or cytokine production by T cell subsets in response to *E coli* or influenza infection of PBMCs

With the difficulties encountered in measuring T cell responses to melanA, effects on whole pathogen handling by immune cells was assessed to ascertain an effect of MGLL inhibition. The data from Chapter 3 confirms that MGLL is expressed in THP-1 cells and in PBMCs, along with moDCs and this forms the basis for the three experiments discussed here.

Salmonella Typhimurium is a Gram-negative intracellular bacteria which is adapted to survive and replicate within innate immune cells[416]. Using a gentamicin protection protocol we infected THP-1 derived macrophages with the LT2 strain of *Salmonella* Typhimurium in the presence or absence of JZL184. MGLL inhibition did not affect the ability of the cells to control infection (Figure 4.12A).

Human immunodeficiency virus (HIV) is known to infect dendritic cells and evade detection by innate immune responses to result in effects on $CD4^+$ T cells[417]. The effect of MGLL inhibition on HIV replication was assessed by infecting moDCs, in the presence or absence of JZL184, and measuring p24 levels by ELISA at day 7. There was a clear effect of $CD4^+$-DC co-culture on increased p24 levels, as would be expected given HIV avidly infects CD4 cells, but no effect of MGLL inhibition was seen (Figure 4.12B/C).

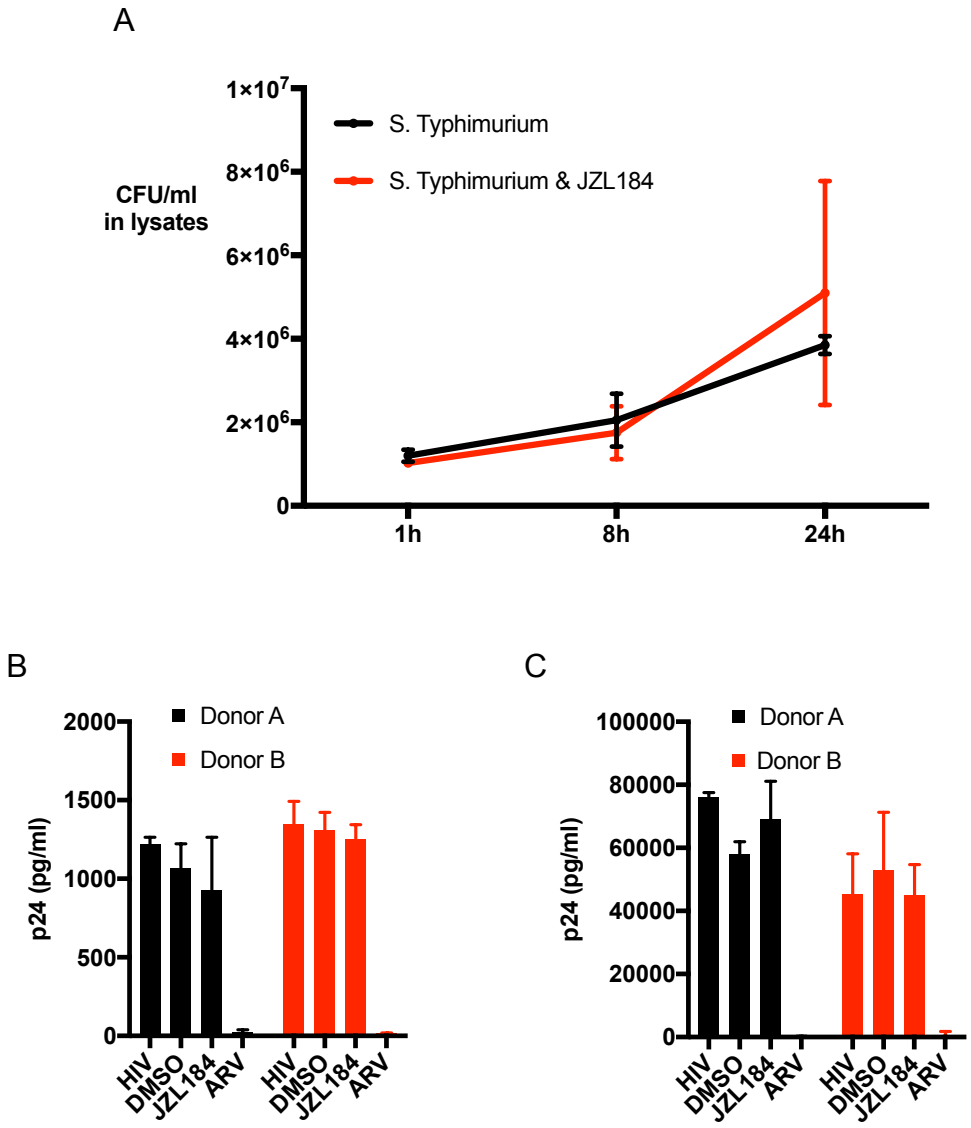

Figure 4.12 MGLL inhibition does not impair handling of a range of pathogens

(A) THP-1 derived macrophages were infected with *Salmonella* Typhimurium in a gentamicin protection assay in the presence/absence of JZL184. No difference in the number of intracellular CFU was identified with MGLL inhibition at the pre-specified timepoints. Mean +/- SEM for each timepoint and representative of 2 separate experiments. moDCs were infected with HIV and then cultured in the absence **(B)** or presence **(C)** of autologous $CD4^+$ T cells. No effect of JZL184 was seen. Results are mean +/- SEM of 3 technical replicates for each of 2 biological replicates. **(D, overleaf)** PBMCs were incubated with JZL184 prior to infection with *Escherichia coli*, influenza or PMA/ionomycin as a positive control. Cytokine production by different T cell subsets was measured by flow cytometry. Results are shown for TNFα and are representative of 2 biological replicates. Similar results were found for IL-17, IFNγ, and IL-2. CFU = Colony forming units; HIV = human immunodeficiency virus; ARV = anti-retroviral (nevirapine); MAIT = mucosal associated invariant T cell; CD40L = CD40 ligand (a marker of T cell cognate activation).

D

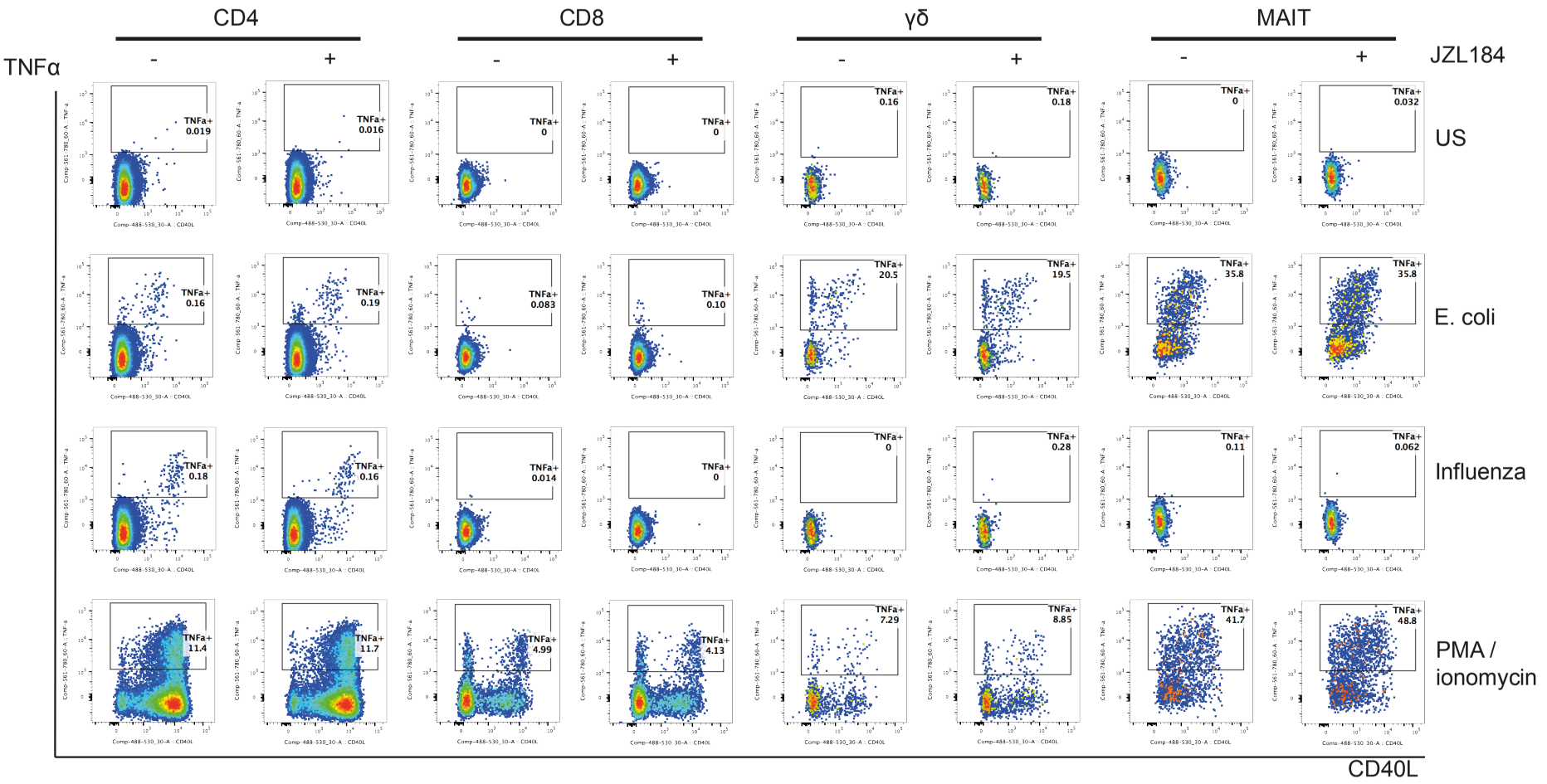
CD4
CD8
γδ
MAIT
TNFα
-
+
-
+
-
+
-
+
JZL184
TNFa+ 0.019
TNFa+ 0.016
TNFa+ 0
TNFa+ 0
TNFa+ 0.16
TNFa+ 0.18
TNFa+ 0
TNFa+ 0.032
US
TNFa+ 0.16
TNFa+ 0.19
TNFa+ 0.083
TNFa+ 0.10
TNFa+ 20.5
TNFa+ 19.5
TNFa+ 35.8
TNFa+ 35.8
E. coli
TNFa+ 0.18
TNFa+ 0.16
TNFa+ 0.014
TNFa+ 0
TNFa+ 0
TNFa+ 0.28
TNFa+ 0.11
TNFa+ 0.062
Influenza
TNFa+ 11.4
TNFa+ 11.7
TNFa+ 4.99
TNFa+ 4.13
TNFa+ 7.29
TNFa+ 8.85
TNFa+ 41.7
TNFa+ 48.8
PMA / ionomycin
CD40L

Having established that MGLL is detectable by immunoblot in PBMCs (Figure 3.10) we tested the hypothesis that MGLL inhibition might impair cytokine production by T cell subsets to *Escherichia coli* or influenza virus. PBMCs were incubated with DMSO or JZL184 prior to infection with live *E. coli*, influenza or PMA/ionomycin as a positive control for T cell activation. After overnight incubation, flow cytometry was used to measure cytokine production (TNFα, IFNγ, IL-17, IL-2) from four $CD3^+$ T cell subsets – $CD4^+$, $CD8^+$, γδ, and MAIT. CD40L was used as a marker of T cell activation, indicative of cognate antigen presentation. No adverse effect of MGLL inhibition was seen on viability of PBMCs (data not shown). Similarly, there was no observable effect of MGLL inhibition on production of any of the four measured cytokines across any of the four T cell subsets. PMA/ionomycin robustly induced T cell responses compared to the unstimulated condition with greater T cell responses to *E coli* than influenza. A representative flow cytometry plot of the results is shown for TNFα production (Figure 4.12D). Although no effect was seen in this assay, it is important to recognise that this is an experiment performed on PBMCs and assesses T cell responses to antigen presentation largely by non-dendritic cells (e.g. monocytes and B cells) and does not look in detail at DC-T cell interactions and the immunological synapse for instance. Furthermore, the CD4 subsets were not examined and subtle effects on $T_H1/2$ polarisation may have been missed. However, across three experiments assessing pathogen handling, no effect of MGLL inhibition could be identified.

4.3.8 Trained immunity in monocytes is not affected by MGLL inhibition

Data from Chapter 3 demonstrates that MGLL is induced not only in moDCs upon stimulation with a range of PRR ligands, but also in monocyte-derived macro-

phages but not in $CD14^+$ monocytes. The effect of M-CSF differentiation was more marked than GM-CSF differentiation (Figure 3.10). Furthermore, MGLL induction occurs from 8h post-stimulation and is particularly marked at 24h and beyond. No effects of pharmacological MGLL inhibition or genetic knockdown have been seen on early cytokine production. We hypothesised that MGLL inhibition, whilst not modulating early cytokine release, might impact upon an innate immune cells ability to respond to subsequent immune challenge.

A schematic of the workflow is shown in Figure 4.13A and explained in detail in Chapter 2. In initial experiments, $CD14^+$ monocytes were isolated from leucocyte cones and cultured in media with 10% FCS. However, generally poor responses were seen possibly due to poor quality monocytes in the cones or the effects of FCS (data not shown). This being the case, experiments were repeated with $CD14^+$ cells isolated from fresh whole blood from healthy donors along with pooled human serum. Furthermore, improved cytokine production was seen when M-CSF was incorporated into the media between the two stimuli (Figure 4.13B/C). This enabled visualisation of the effects of training on subsequent responses in a way which was not possible without M-CSF.

In monocytes which were treated with RPMI as the initial stimulus, a significant cytokine response to the second stimulus was only detected for those cells exposed to LPS (the RPMI/LPS groups in Figure 4.13) with no or minimal response to β-glucan. Cells exposed to LPS for both stimuli became tolerised and mounted less of a cytokine response than those trained with β-glucan where the response was similar to single LPS stimulation. No effect of JZL184 on production of TNFα,

IL-6 or IL-10 was seen. Therefore, MGLL inhibition does not affect training of monocytes by β-glucan or LPS.

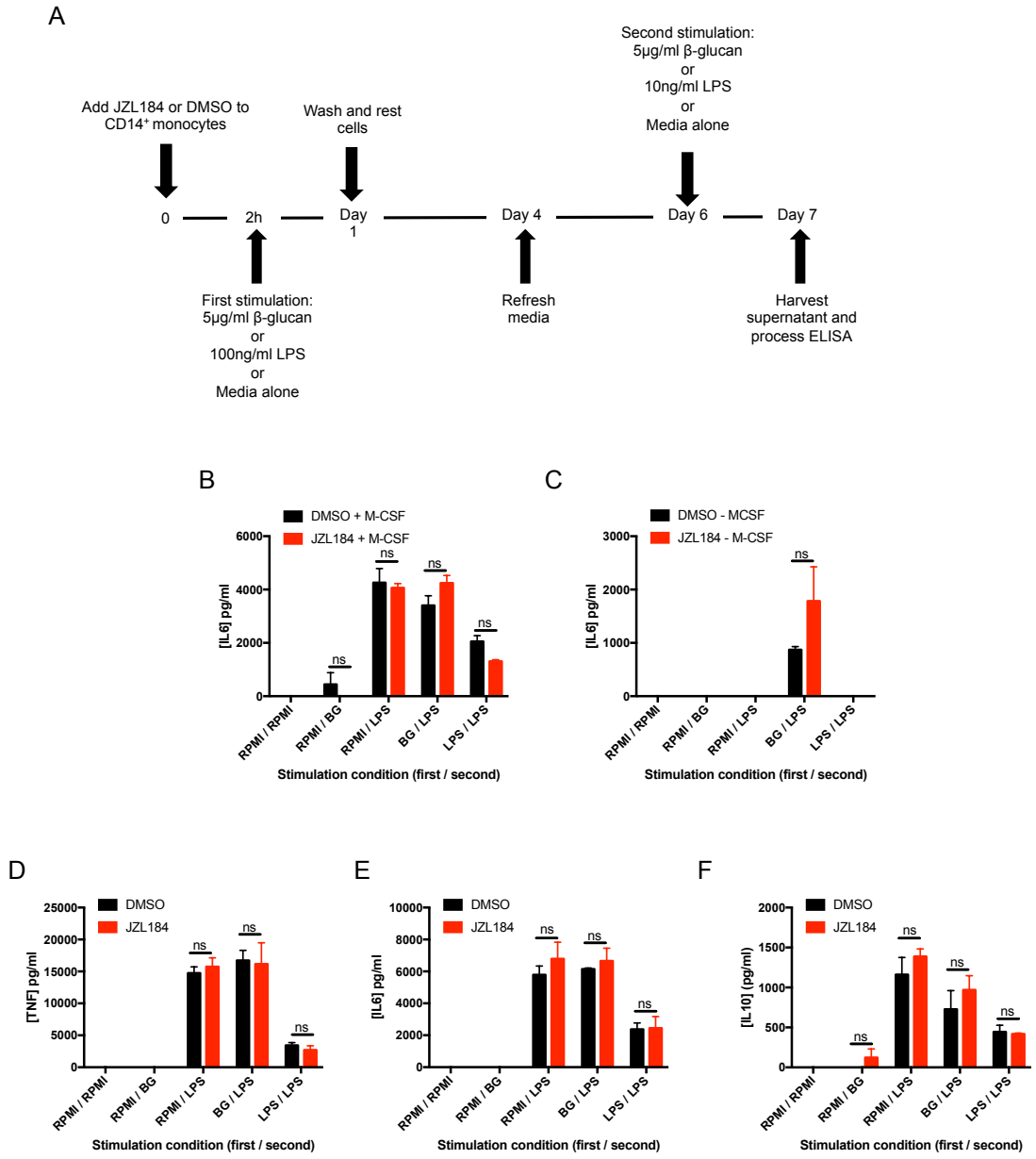

Figure 4.13 Trained immunity in monocytes is not dependent on MGLL

Monocytes isolated from fresh peripheral blood were trained with either LPS or β-glucan, rested, and then exposed to a second stimulus after 6 days. Cytokine production was measured by ELISA. An overview of the experimental workflow is shown **(A)**. M-CSF was identified to be a critical addition to the media in order to elicit training of monocytes **(B)** with poor responses in the absence of M-CSF **(C)**. Although appropriate responses to training were manifest, no effect of JZL184 was identified on production of TNFα, IL-6 or IL-10 **(D-F)**. Data is mean +/- SEM of 3 technical replicates and representative of 3 biological replicates. ANOVA with Bonferroni correction for selected pairs. RPMI = RPMI media alone; LPS = lipopolysaccharide; BG = β-glucan; M-CSF = macrophage colony stimulating factor.

4.3.9 MGLL can be stably knocked down in THP-1 cells using shRNA interference

As discussed in Chapter 1, cannabinoid signalling is altered upon acute versus chronic pharmacological MGLL inhibition or by genetic knockout/down of MGLL. Earlier it was shown that siRNA knockdown of MGLL in moDCs did not result in differences in cytokine production. siRNA knockdown only results in transient knockdown and viability of moDCs declines after a few days and so are unsuitable for longer term experiments. Stable gene knockdown can be achieved with other RNA interference methods. Short hairpin RNA (shRNA) is incorporated into the cellular DNA. Upon transcription, the sequence is recognised by the enzyme Dicer which derives endogenously-synthesised siRNA from the shRNA[418]. These sequences bind the target mRNA and results in degradation via RISC. With the similarities between THP-1 cells and moDCs, a stable MGLL knockdown THP-1 cell line was created to be used in subsequent *in vitro* studies.

Although the shRNA plasmids used contained a puromycin-resistance cassette and so only transduced cells would be expected to survive in puromycin-containing media, the GFP-control transduced cells were used as an alternative marker of transduction efficacy (Figure 4.14A) demonstrating increased GFP-positive cells in the GFP-transduced cells.

Multiple methods were used to confirm MGLL knockdown. At transcriptional level, MGLL mRNA following 6h PAM stimulation was non-significantly reduced with the MGLL-targeting shRNA clones compared to control (Figure 4.14B). More marked differences between the clones were observed with gel-based ABPP pro-

filing (Figure 4.14C/D). Suppression of MGLL activity following 24h PAM was more pronounced for sh2, sh4, and sh5. These clones were further validated by immunoblot with MGLL knockdown observed maximally for sh4 (Figure 4.14E). Therefore this clone was chosen as the most appropriate to use for further *in vitro* experiments.

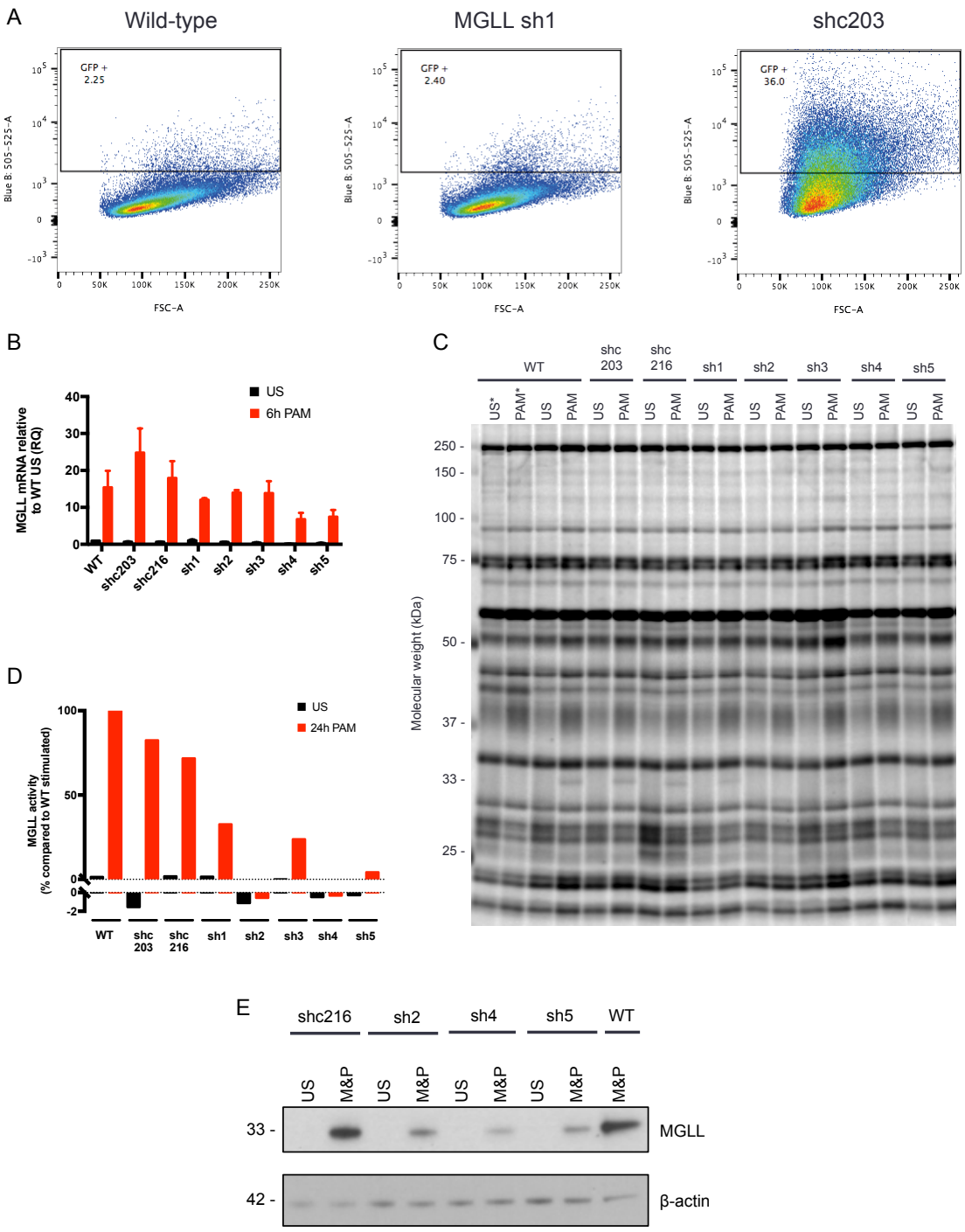

Figure 4.14 Synthesis of a stable shRNA MGLL knockdown THP-1 cell line

THP-1 cells were transfected with shRNA using lentiviral techniques. Five targeting MGLL shRNA were transfected (sh1-5) along with a non-targeting (shc216) and non-targeting GFP-labelled (shc203) shRNA. MGLL was induced by stimulation with PAM alone. **(A)** Transfection efficacy was determined by performing flow cytometry for GFP on wild-type, MGLL sh1, and shc203 cells. Knockdown at mRNA level was assessed by **(B)** qPCR and **(C)** at protein level by gel-based ABPP. **(D)** Densitometry of the MGLL band suggested optimal knockdown using sh2, sh4, or sh5. **(E)** Immunoblotting was performed to corroborate this and confirmed sh4 to yield the greatest protein knockdown. qPCR data is mean +/- SEM of 3 separate experiments. ABPP-gel and immunoblot are from a single experiment. US = Unstimulated; WT = Wild-type. *incubated with MJN110.

4.3.10 MGLL targeting shRNA affects production of TNFα, IL12p40 and IL23 from THP-1 cells

Having established a stable MGLL knockdown THP-1 cell line, the cells were maintained in puromycin-containing media and passaged to maintain cell density at 0.5-1x10^6cells/ml. Cytokine production in supernatant was measured following stimulation alongside wild-type THP-1 cells treated with JZL184.

A small but significant reduction in some cytokines was seen in the shRNA cell line. IL-6 was reduced at 8h, IL-23 and IL-12p40 at 24h, and TNFα at both timepoints (Figure 4.15A-C, E). Minimal effects of JZL184 were identified although a slight increase in IL-6 and IL-12p40 was noted at 24h (Figure 4.15A/C). No effect of MGLL knockdown was observed for IL-1β.

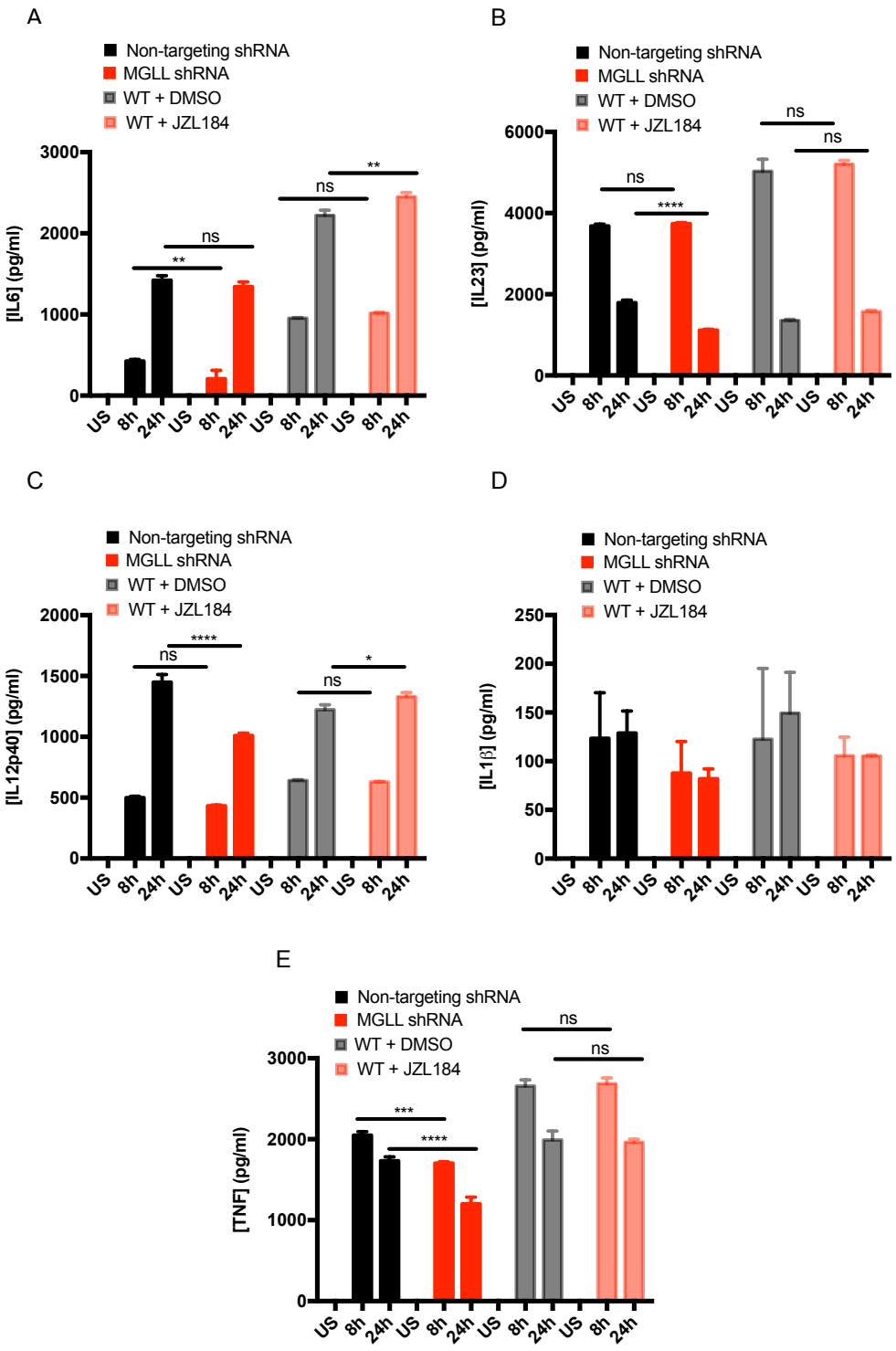

Figure 4.15 Production of IL-6, IL-12p40, IL-23 and TNFα is impaired in MGLL knockdown THP-1 cells

THP-1 cells (wild-type or MGLL shRNA) were stimulated with MDP & PAM for the times specified. Simultaneously, wild-type THP-1 cells were stimulated in the presence/absence of JZL184. Supernatant was harvested and cytokines measured by ELISA. Small but significant effects of shRNA knockdown were seen for IL-6 at 8h **(A)**, IL-23 **(B)** and IL-12p40 **(C)** at 24h, and TNFα **(E)** at both timepoints. There was no effect on IL-1β **(D)**. Results are mean +/- SEM of 3 technical replicates from a single experiment. ANOVA with Bonferroni correction for selected pairs. *p<0.0332, **p<0.0021, ***p<0.0002, ****p<0.0001. US = Unstimulated; WT = Wild-type.

4.4 Discussion

The data presented in this chapter represents the first use of JZL184 and in depth exploration of the role of MGLL in human moDCs, monocytes, and the related cell line THP-1. There is a dearth of published experimental data on function of the endocannabinoid system in human immune cells. It is curious that MGLL inhibition does not have effects on a range of functional assays of dendritic cell and other innate cell biology. Regarding cytokine production there was no effect seen with acute pharmacological MGLL inhibition or transient MGLL siRNA knockdown in moDCs. However, it may be that the effects of MGLL inhibition on cytokine production occur over a longer time period than that studied here. Subtle differences in cytokine production from shRNA THP-1 cells were seen. However, no differences were seen with pharmacological inhibition of MGLL in this cell line. Arguably this could be due to desensitisation of cannabinoid receptors due to prolonged 2AG elevation, as has been shown in other, non-immune, models. However, the lipid profile of THP-1 cells has not been examined in the presence of MGLL inhibition and it is therefore unknown whether these cells behave similarly to moDCs. Furthermore, prolonged pharmacological inhibition of primary monocytes/macrophages in the trained immunity experiment would suggest that even with prolonged elevation of 2AG, cytokine production is not affected. Although JZL184 was present in the media throughout this experiment and binds covalently to MGLL, it was not refreshed daily and therefore it is possible that some MGLL activity remained that might have been sufficient to mask an effect.

shRNA knockdown in THP-1 cells was chosen above other methods due to ease and speed to achieve knockdown. However, it is known that this method can re-

sult in off-target effects[419] and, as shown here, incomplete knockdown. The cytokine effects therefore could be due to off target effects of the MGLL shRNA construct. With the development of CRISPR-Cas9 technology to silence genes this would provide an attractive alternative method to selectively target and knock down MGLL without the array of off-target effects[420]. It is important to bear in mind, however, that any genetic knockdown model is likely to behave differently to acute pharmacological inhibition of MGLL due to desensitisation of the cannabinoid receptors. The degree to which findings from this type of model are therefore clinically relevant is debatable.

It was surprising, although entirely plausible, that no effect was seen on migration of moDCs to a chemokine given the background literature in this area. There are several possible explanations for this. The dose of CCL19 used was determined from previously optimised studies using moDCs. However, these studies migrated moDCs across HUVEC endothelial cells. Therefore the dose of CCL19 might have been too high to reveal subtle differences and so a concentration titration would be a useful extension to this experiment. The migration system used, whilst controlling for temperature over 8h did not control for CO_2 which may have resulted in progressive acidification of the media. It is not known whether pH affects response of moDCs to 2AG and cannabinoids. Other methods exist which control CO_2 along with temperature and can provide a more in depth assessment of migration. These include Incucyte® (imaging based; Essen BioScience) and xCELLigence® (using electrical impedance; ACEA Biosciences) both of which provide automated assessment of migration in a standard incubator. However, it was decided not to pursue further migration studies for two reasons.

Firstly, the evidence that CB2 agonists do not require CB2 to influence migration of murine macrophages[402]. Secondly that the lipidomic data did not reveal an effect of MGLL inhibition on prostaglandin production which might have provided an alternative explanation for previously seen migratory effects.

It is disappointing that the melanA antigen presentation assay could not be optimised. In murine macrophages, THC has been demonstrated to affect antigen processing rather than antigen presentation per se[421,422] and in murine BMDCs a reduction in LPS-induced maturation has been shown[394]. In a murine model of autoimmune uveoretinitis a CB2 agonist, JWH133, modestly affects antigen presentation in an allogeneic mixed leucocyte reaction, but not expression of co-stimulatory molecules by BMDCs[423]. The overall effect however, is a reduction in T cell responses. An alternative method to assess the effects on antigen presentation could be to use the murine OT/ovalbumin model. However, this assumes that the function of MGLL and 2AG is the same between mice and humans. One study has demonstrated that a COX-2 metabolite of 2AG inhibits IL-2 secretion by T cells and that levels of COX-2 differ between murine splenocytes and the human Jurkat cell line[207]. Therefore extrapolating between species may not necessarily yield similar results.

This set of experiments has not identified a role for MGLL inhibition in moDCs in isolation. Given the marked effects of JZL184 on increasing secreted 2AG levels it is probable that the effect is on bystander cells. T cells are known to express CB2[97,105,424] and GPR55[425] albeit at lower levels than monocytes, NK cells or B cells. They have also been shown to upregulate CB1 mRNA following CD3/28

stimulation[426]. In addition to expressing various receptors, activated T cells produce 2AG and this limits T cell proliferation and ongoing activation and this may signal through CB1 rather than CB2[200]. Furthermore a number of studies, discussed in Chapter 1, have shown evidence of an effect of cannabinoids on T cell polarisation.

4.5 Conclusion

In this chapter, it has been demonstrated that acute MGLL inhibition with JZL184 does not affect cytokine production, gene expression, maturation or migration of moDCs. Genetic knockdown in moDCs does not influence cytokine production whereas modest reductions in TNFα, IL-12p40 and IL-23 were seen in the stable shRNA THP-1 cell line. Trained immunity of monocytes and inflammasome activation in THP-1 cells were equally unaffected by MGLL inhibition. Further understanding of the role of MGLL inhibition should focus on DC-T cell interactions at the immunological synapse and T cell polarisation.

Chapter 5 – Prophylactic MGLL inhibition worsens *Citrobacter*-induced murine colitis and profiling of human UC by ABPP highlights novel changes in serine hydrolases

5.1 Introduction

It has been established in Chapter 3 that MGLL is induced upon PRR ligation and, through Chapter 4, that MGLL inhibition does not affect function of dendritic cells *in vitro*. However, given the complexities of the ECS and the limited literature on MGLL *in vivo*, further studies in animal models are necessary. Moreover it is not known to what extent ABPP might reveal novel findings in human IBD.

Modulation of 2AG levels in murine colitis has been investigated twice, the first using MGLL inhibition[273] and the second with rectal 2AG[281]. Both used the TNBS model of chemical colitis which, as discussed in Chapter 1, has similarities with Crohn's disease but has significant limitations. It is particularly limited in that it does not assess the interactions between microbiota and immune responses which is so classical of human IBD. In elucidating the function of MGLL in innate immune cells, a model which requires innate immune sensing, if possible through NOD2/TLR2 to supplement *in vitro* work, is attractive.

Citrobacter rodentium is a Gram-negative, murine restricted pathogen which has similarities with human enteropathogenic and enterohaemorrhagic *E coli*[427]. Notably, human IBD has associations with another subtype, adherent invasive *E coli* (AIEC)[428], emphasising the relevance of *Citrobacter* as a model to understand in-

testinal inflammation. Colonisation is through the formation of attaching/effacing lesions on the intestinal epithelium initially in the caecum with subsequent spread to the distal colon 3-4 days later and spontaneous clearance in most cases by 21 days[429]. Colonic hyperplasia, a typical feature of colitis induced by *Citrobacter*[430] is detectable from day 5-14[431]. Other histological features include goblet cell depletion and leucocyte infiltration of the lamina propria – all features of human colitis[338]. Infection results in dysbiosis with overgrowth of *Citrobacter* and decrease in microbial diversity[427], also seen in human IBD[72]. Infected intestinal epithelial cells are eventually shed into the lumen to aid bacterial clearance but this promotes bacterial spread to co-housed animals through coprophagy[427].

Citrobacter is sensed by TLR2 and 4 to trigger NF-κB-dependent cytokine production through MyD88[427]. $TLR2^{-/-}$ mice develop a severe colitis with increased mortality due to effects on epithelial barrier function[432]. NOD1 and 2 are also involved in sensing this pathogen. Knockout mice for either receptor develop more severe histological disease and are unable to effectively clear the bacteria resulting in increased translocation to the spleen[433]. Similarly, the NLRP3 inflammasome is triggered by *Citrobacter* infection with Caspase-1 mediated responses important for host defence[427]. The adaptive immune response is characterised by T_H1 (IFNγ and TNFα) and T_H17 (IL-17)[427]. Knockout studies of components of the adaptive immune system including B cells, T cells, and $CD4^+$ (but not $CD8^+$) results in more severe colitis and reduced survival[434].

Therefore, although a self-limiting disease process in wild-type mice, *Citrobacter*-induced colitis exhibits similarities with human IBD particularly host-pathogen interactions and the crucial role of innate sensing in disease pathogenesis. JZL184 is the only MGLL inhibitor to have been used in a colitis model. Given the known off target effects on a carboxylesterase and partial, although minimal, impact on FAAH activity, we used our collaboration with Abide Therapeutics to obtain a more selective MGLL inhibitor. ABD1970 (also known as ABD101970) is orally available in rodents and results in elevation of brain 2AG in rodents[435] and human[436] tissue. At doses higher than that needed to achieve MGLL inhibition, off targets are seen on ABHD6 and Ces1c[435]. ABD1970 has been used in rats to doses of 1000mg/kg without significant cannabimimetic side effects (Abide Therapeutics, personal communication).

There is disagreement on the tone of the ECS between studies of human IBD (summarised in Figure 5.1). CB1 has been identified in the colonic epithelium (particularly crypts[437]), some plasma cells of the lamina propria, smooth muscle and the submucosal myenteric plexus[438]. Conversely, CB2 localises in the absorptive and goblet cells of the epithelium, Paneth cells, and some subepithelial macrophages and plasma cells[437,438]. CB2 was expressed at slightly higher levels than CB1 in one study[439]. The effect of inflammation on expression of CB1 and CB2 is less clear. One study showed an increase in both CB1 and 2 in both Crohn's disease and 'IBD', presumed to be UC[438]. However, two further studies have suggested the increase is only in CB1 and not in CB2[440,441] only to be contradicted by a third which demonstrated an increase in CB2 but not CB1[437]. A recent study of CB1 and CB2 gene expression in Crohn's disease, the largest to date, demonstrat-

ed consistent detection of expression albeit at low levels in inflamed, non-inflamed, and healthy samples. A difference in expression patterns was seen between disease affecting the ileum, where both CB1 and 2 were reduced in inflamed/non-inflamed samples, and colon where an increase was seen in CB1 and 2 in the non-inflamed but not inflamed samples[442].

Similar controversy exists for levels of endocannabinoids. AEA has been shown to be increased in inflamed samples from UC patients[302,443], yet reduced in another study[440]. It is more plausible that AEA levels are indeed decreased in inflammation as it has been shown that there is reduced expression of the synthetic enzyme NAPE-PLD and increased expression of the hydrolytic enzyme FAAH in colonic inflammation[334,437,440,444]. PEA is increased in inflammation in one study[443] but does not change in another[440], although the two studies assessing 2AG levels both demonstrate no change in inflammation[302,440].

To date, only one study has attempted to define levels of MGLL and the DAGL enzymes in human IBD[437]. MGLL was localised to the central portion of epithelial cells, polymorphonuclear cells of the lamina propria, and the myenteric plexus and was shown to be increased in inflammation. Previously MGLL has been shown to be widely distributed in the rat intestine, increasing in expression from duodenum to distal colon[445]. DAGLα was similarly increased in inflammation but no difference was seen in DAGLβ.

There are a multitude of potential explanations for the differences between these studies. In particular, the patients studied were not always well phenotyped for

disease severity and extent, and were frequently grouped together. Furthermore, the potential role of medications such as systemic immunosuppression in altering expression levels was not explored. In many studies, comparisons were made between inflamed mucosa in an IBD patient and healthy mucosa from a different person. ECS tone has been shown to be affected by diurnal variation[446] and ethnicity[447], not to mention the likely confounder of any comorbidities such as irritable bowel syndrome in which the involvement of the ECS is well documented[448]. Lastly, a number of different techniques were used to profile the ECS. With the well-documented problems with antibody selectiveness in this system, some results could be called into question. Although applied to cancer cells, ABPP has not previously been applied to study the serine hydrolome in human IBD and offers many advantages in assessing protein activity over conventional immunoblotting for the ECS enzymes.

5.2 Aims

1. To assess the effect of prophylactic MGLL inhibition on *Citrobacter rodentium*-induced murine colitis.
2. To profile serine hydrolases in human primary colonic tissue by ABPP-MuDPIT.
3. To profile ECS components by ABPP-MuDPIT and qPCR.

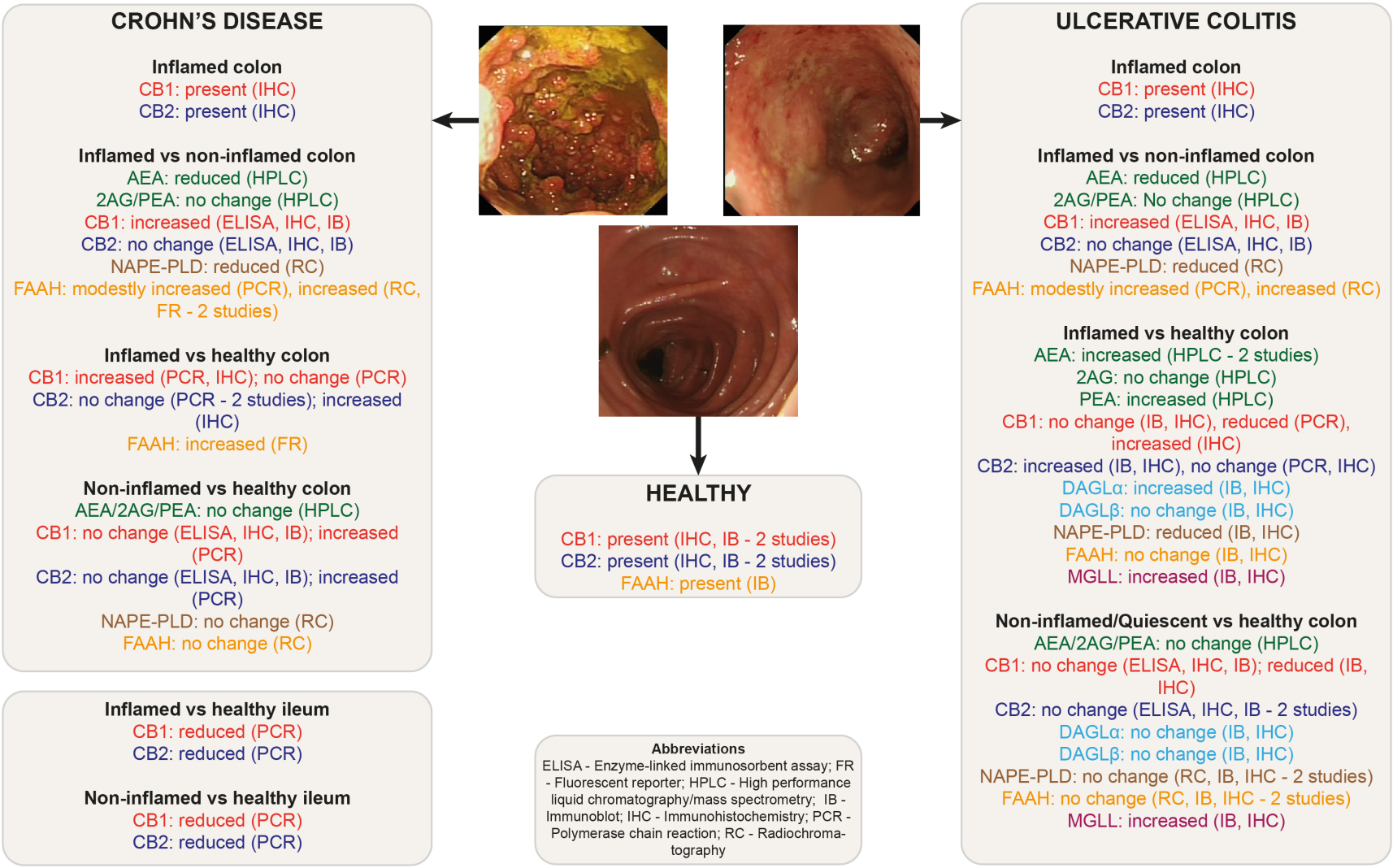

Figure 5.1 A summary of existing studies of the endocannabinoid tone in human ileum and colon in health and IBD

Studies of the ECS in human IBD have yielded conflicting results dependent on the technique used, the site of sampling (ileum vs colon) and the comparison used (inflamed vs non-inflamed vs healthy). Only one study has assessed the synthetic (DAGL) and key hydrolytic (MGLL) enzyme involved in 2AG metabolism. No studies have examined the presence of ABHD6 or 12.

5.3 Results

5.3.1 ABD1970 inhibits MGLL in C57BL/6 mice and does not result in an adverse phenotype

In order to confirm that, in our hands, ABD1970 could be successfully reconstituted and administered *in vivo* to inhibit MGLL a pilot study was performed. Six female, wild-type C57BL/6 mice received intraperitoneal ABD1970 daily for 8 doses and were then culled on day 7 (Figure 5.2A). Two doses were chosen for the pilot study, 2mg/kg and 6mg/kg, based on discussions with the scientists at Abide Therapeutics in order to achieve partial and near-complete MGLL inhibition. This was deemed necessary due to known pharmacological effects of partial versus complete MGLL inhibition on CB receptor desensitisation (discussed in Chapter 1). There was no difference in weight between the groups (Figure 5.2B) and no cannabimimetic behavioural differences identified (the 'tetrad' test of hypolocomotion, hypothermia, catalepsy and antinociception). Gel-based ABPP was performed on the colon and spleen of each mouse in order to detect MGLL activity. *In vitro* ABD1970 1μM was added to the proteome of mouse 1 to positively identify the MGLL band (Figure 5.2C). Analysis of the gel including by densitometry (Figure 5.2D) confirmed differential MGLL inhibition depending on the dose administered. This also provided confidence that MGLL was both present and effectively inhibited in the murine colon.

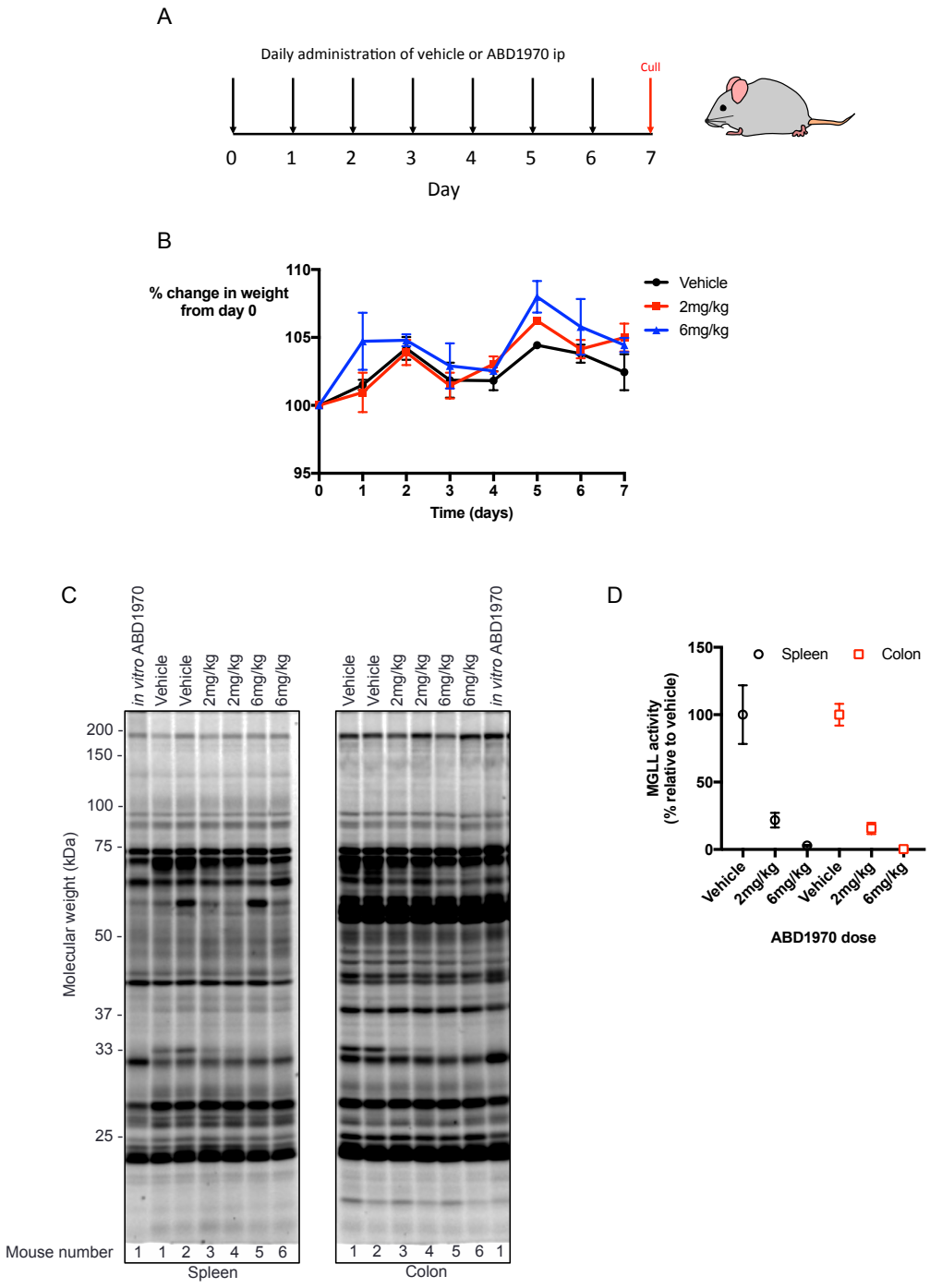

Figure 5.2 ABD1970 effectively inhibits MGLL in C57BL/6 mice and has no adverse effect on weight

ABD1970 (2mg/kg or 6mg/kg) or vehicle was administered to C57BL/6 mice via the intraperitoneal route daily for 7 days with colon and spleen harvested for gel-based ABPP. **(A)** Schematic of dosing schedule of vehicle or MGLL inhibition. **(B)** ABD1970 did not affect murine weight across the duration of the study. Mean +/- SEM. **(C)** Gel-based ABPP demonstrates effective inhibition of MGLL with ABD1970 but not vehicle in both colon and spleen. Band position was confirmed by *in vitro* incubation of proteome with 1μM ABD1970. **(D)** Densitometry of the gel confirms differing degrees of MGLL inhibition dependent on dose administered. Mean +/- SEM.

5.3.2 Induction of colitis with *Citrobacter rodentium* and confirmation of target engagement by ABD1970

Having identified two doses to use through the pilot study the effect of prophylactic ABD1970 on *Citrobacter rodentium* colitis was assessed. Female C57BL/6 mice were divided into groups (Table 5.1). Those mice not receiving *Citrobacter* were housed in a single cage. Two mice from each group receiving *Citrobacter* were housed in single cages of six mice in order to control any environmental and microbial factors affecting induction of colitis.

Group	*Citrobacter*	ABD1970	Number of mice
1	No	Untreated	3
2	No	Vehicle	3
3	Yes	Vehicle	6
4	Yes	2mg/kg	6
5	Yes	6mg/kg	6

Table 5.1 Treatment arms for mice for *Citrobacter* experiment

ABD1970 or vehicle was administered intraperitoneally 4h prior to *Citrobacter* gavage and then at the same time each day for 11 doses before the mice were culled on day 11 (Figure 5.3A). One mouse from group 5 was culled on day 3 due to loss of more than 20% baseline weight. Post-mortem did not reveal an obvious cause for the weight loss (such as florid colitis) and it was not felt that ABD1970 was causative.

Gel-based ABPP was performed on colonic samples from each mouse and confirmed inhibition of MGLL in those receiving ABD1970 (Figure 5.3B). Although the degree of MGLL inhibition assessed by densitometry (Figure 5.3C) varied slightly between low and high dose ABD1970 this effect was not as pronounced

as seen in the pilot study. Although this may be due to the effects of colitis on MGLL inhibition it may also represent the relatively subjective nature of densitometry. Certainly visual analysis of the gel would suggest a greater difference in degrees of MGLL inhibition than the densitometry. Notably a MGLL doublet is seen on the ABPP gel with a second band at 35kDa, a feature occasionally seen when profiling murine MGLL due to alternative splicing[449].

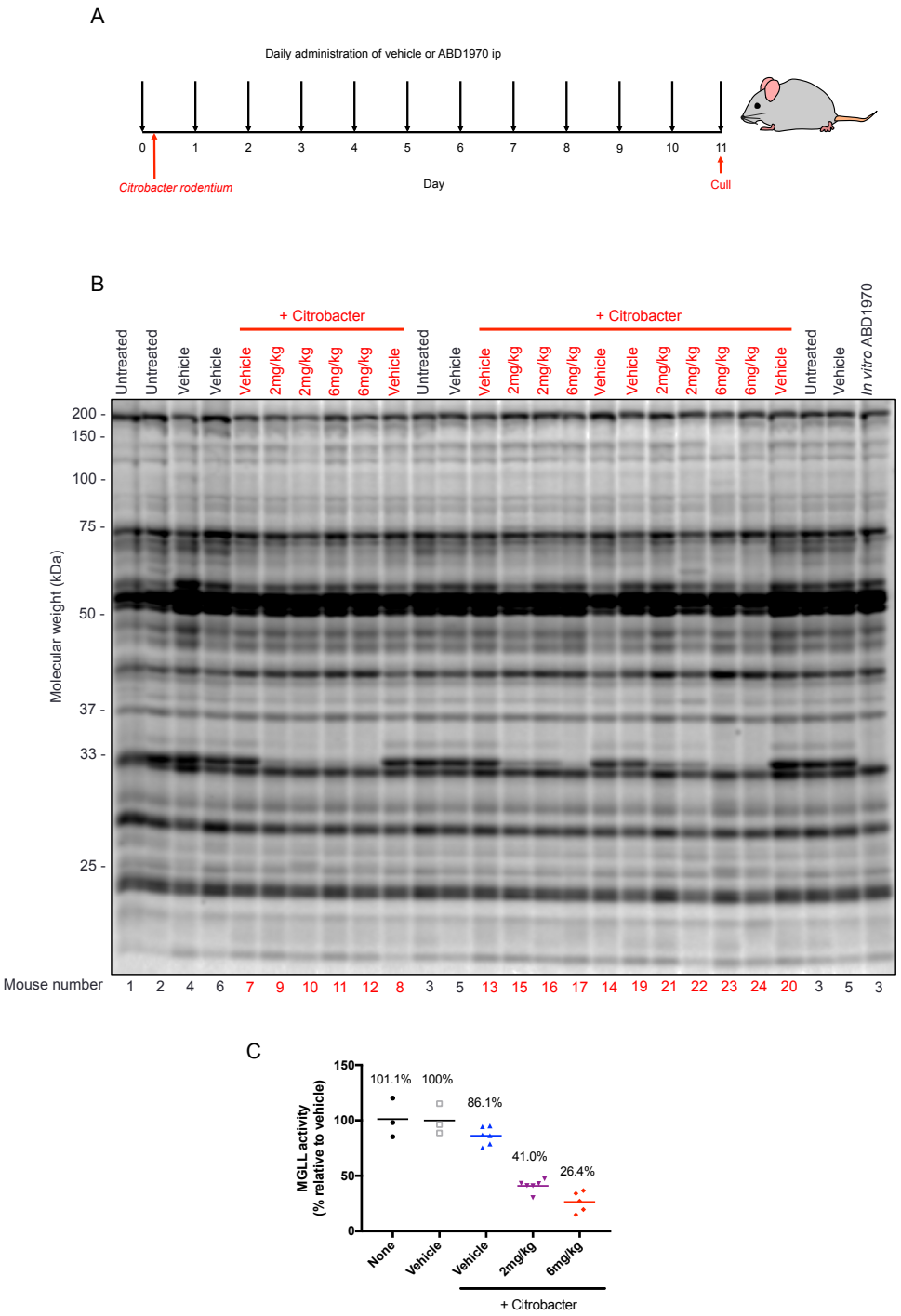

Figure 5.3 In the presence of *Citrobacter rodentium* infection, MGLL activity decreases and this reduction is enhanced by ABD1970

ABD1970 (2mg/kg or 6mg/kg) or vehicle was administered to C57BL/6 mice via the intraperitoneal route 4 hours prior to oral gavage of 5x10^9 CFU *Citrobacter rodentium*. Mice then received daily vehicle or ABD1970 and were culled at day 11. One mouse from the high dose ABD1970 group was culled on d5 due to loss of greater than 20% baseline weight. **(A)** Schematic of dosing schedule of vehicle or MGLL inhibition and timing of *Citrobacter* gavage. **(B)** Gel-based ABPP of serine hydrolase activity in colon demonstrates a MGLL doublet at 33 and 35kDa. **(C)** Densitometry of band at 33kDa confirms no effect of vehicle alone (n=3) on MGLL activity compared to untreated mice (n=3). In the presence of *Citrobacter* a reduction in MGLL activity was seen with vehicle alone (n=6). The ABD1970 dosing schedule achieved a modest differential in MGLL inhibition between 2mg/kg (n=6) and 6mg/kg (n=5) with both doses inhibiting MGLL to a greater extent than vehicle alone. Line represents mean MGLL activity for each condition.

5.3.3 ABD1970 worsens histological colitis induced by *Citrobacter rodentium* and this is not due to differences in bacterial colonisation and translocation

Samples of caecum and distal colon were processed for histological assessment using a validated scoring system (Table 5.2) and blindly scored by two independent, experienced assessors from the Powrie group, Kennedy Institute of Rheumatology, University of Oxford (Figure 5.4A/B).

Score	1a) Epithelial hyperplasia	1b) Goblet cell depletion	2) Lamina propria inflammation	3) Area affected (% of section)	4) Markers of severe inflammation
0	None	None	None (few leucocytes)	None	None
1	Mild (1.5x)	Mild (25%)	Mild (some increase in leucocytes at tips of crypts OR many lymphoid follicles)	Up to 25%	Submucosal inflammation OR <5 crypt abscesses
2	Moderate (2-3x)	Marked (25-50%)	Moderate (marked infiltrate with broadening of crypt)	25-50%	Submucosal inflammation AND <5 crypt abscesses OR >5 crypt abscesses OR Extensive submucosal inflammation OR Crypt branching
3	Severe (>3x)	Substantial (>50%)	Severe (dense infiltrate throughout)	Over 50%	>5 crypt abscesses AND extensive submucosal inflammation/crypt branching OR Ulceration OR Extensive fibrosis

Table 5.2 Histological scoring system for *Citrobacter* colitis
Total score = 1a (or 1b) + 2 + 3 + 4; Max score = 12. Score worst affected area. Adapted from [354].

In the absence of *Citrobacter* there was no effect of vehicle alone. *Citrobacter* robustly induced colitis particularly in the colon, in keeping with the pattern of in-

fection at this timepoint, and less so in the caecum. However, in both areas a significant effect of ABD1970 2mg/kg was seen on worsening colitis including epithelial hyperplasia and infiltration of the lamina propria by lymphocytes. A numerical, but non-significant, effect of higher dose ABD1970 was seen.

Despite the differences in degrees of colitis induction, there were no differences in body weight between groups (Figure 5.4C). Nor was a difference seen in splenic weight (Figure 5.4D) as a surrogate for systemic inflammation. One hypothesis behind the worsened colitis in the MGLL inhibited groups was that there were effects on bacterial colonisation and translocation. However, counting of CFUs from both local colonic and systemic tissues (liver, spleen) did not reveal differences in counts between groups (Figure 5.4E-H).

A

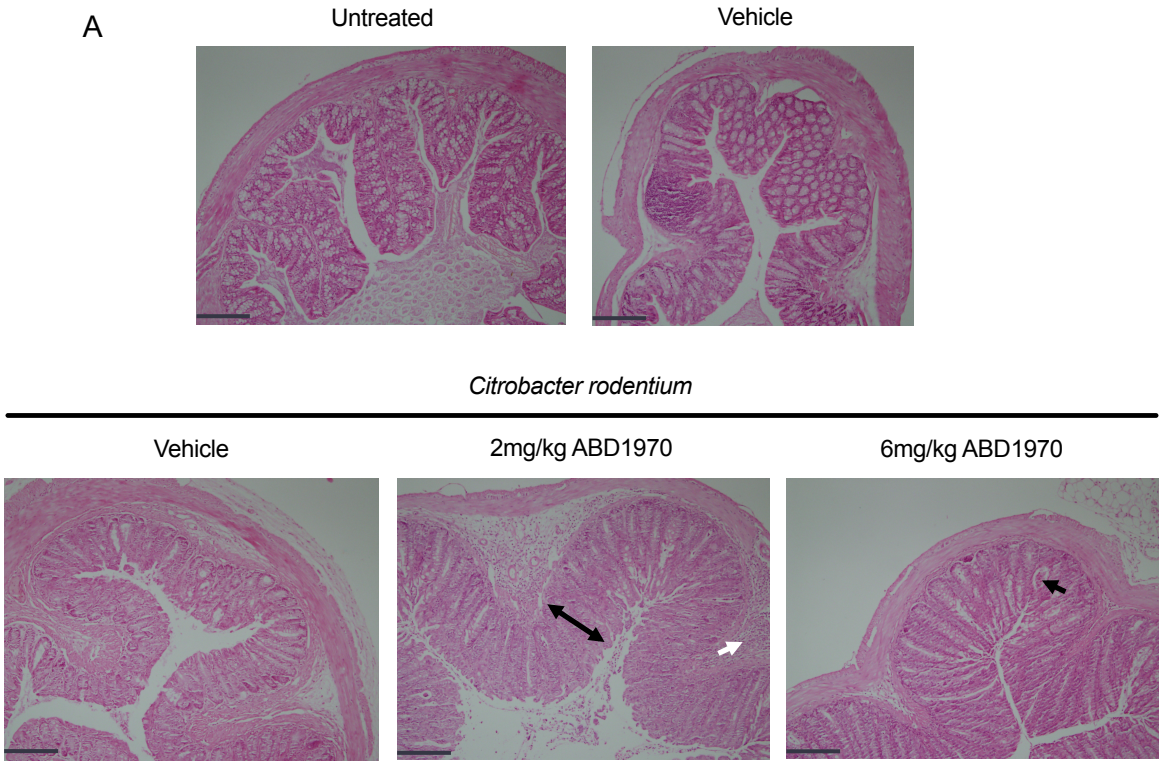
Untreated
Vehicle
Citrobacter rodentium
Vehicle
2mg/kg ABD1970
6mg/kg ABD1970

B

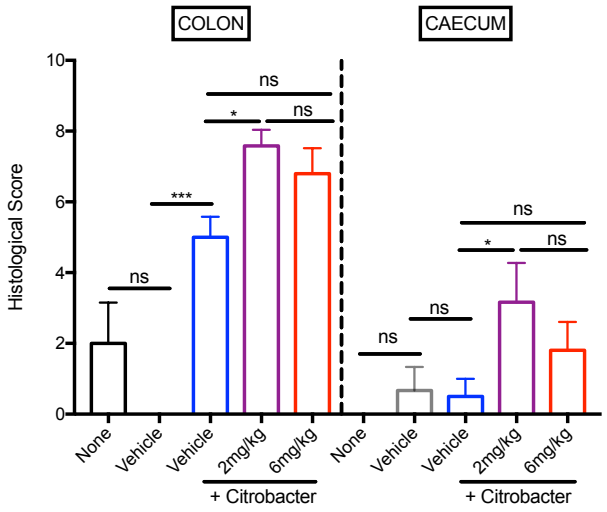
COLON
CAECUM
Histological Score
10
8
6
4
2
0
ns
***
*
ns
ns
ns
*
ns
None
Vehicle
Vehicle
2mg/kg
6mg/kg
None
Vehicle
Vehicle
2mg/kg
6mg/kg
+ Citrobacter
+ Citrobacter

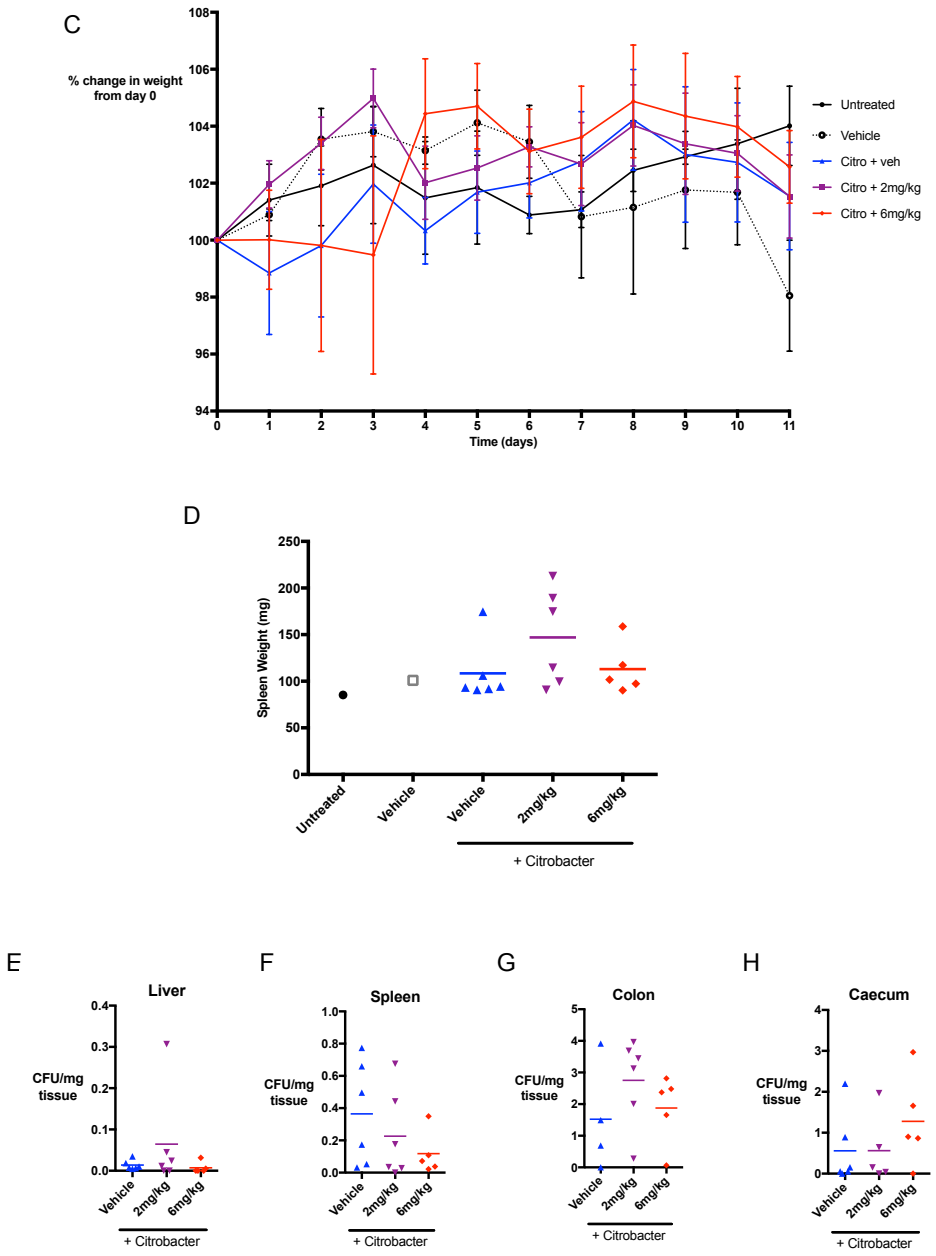

Figure 5.4 Prophylactic administration of ABD1970 results in more severe *Citrobacter*-induced murine colitis but does not affect bacterial colonisation or translocation

Samples of colon and caecum were placed in formalin, embedded in paraffin and stained with haematoxylin and eosin. Histological scoring was blinded to the treatment groups. Separately, samples of liver, spleen, colon and caecum were weighed, homogenised and cultured in nalidixic acid-containing agar overnight prior to manual counting of CFU. **(A)** Representative slices of colonic histology from each group demonstrating colitis in the *Citrobacter*-group with epithelial hyperplasia (double-headed black arrow), lamina propria infiltration (white arrow), and crypt abscess formation (single-headed black arrow). Caecal histology not shown. X100 magnification. Scale bars = 200µm. **(B)** Histological scoring of colonic and caecal histology confirming induction of colitis with *Citrobacter* and more severe histological disease in the colon than caecum, and with MGLL inhibition. Mean +/- SEM of scores for all mice in that group, results of scoring by one experienced assessor. ANOVA with Bonferroni correction for selected pairs as shown. *p<0.0332, ***p<0.0002, ns = not significant. **(C)** There was no difference in weight between the groups and no effect of *Citrobacter* on weight gain. Mean +/- SEM of all mice in each group. One mouse from the 6mg/kg group was culled on day 3 due to significant weight loss. **(D)** Mean splenic weight did not differ significantly between groups. **(E-H)** Mean mucosal and systemic bacterial CFUs did not differ between groups. Citro = *Citrobacter*

5.3.4 The histopathological differences in colitis are mirrored by effects on mucosal cytokine production

RNA was extracted from colonic and caecal samples and processed by qPCR. In the previous study of MGLL inhibition in TNBS colitis[273], JZL184 improved levels of IL12, TNFα, IL6 and MCP1 (also known as CCL2). In this *Citrobacter* model, there were no differences in IL12A, IL23A or TNFα (Figure 5.5G, K, L). Expression of IL6 and CCL2 were increased with MGLL inhibition at the lower dose but not the higher dose (Figure 5.5C, H). Furthermore, MGLL inhibition resulted in increases of T_H1 (IFNγ low and high dose) and T_H17 (IL17 low dose), but not T_H2 (IL4) or T_{reg} (IL10) cytokines (Figure 5.5A, B, E, F). IL1β mRNA was also increased with low dose MGLL inhibition (Figure 5.5D) but there were no effects on IL1α or IL18 (Figure 5.5I/J). Although *Citrobacter* infection resulted in an increase in cytokine production from MLNs this did not meet statistical significance for any group (Figure 5.6).

A

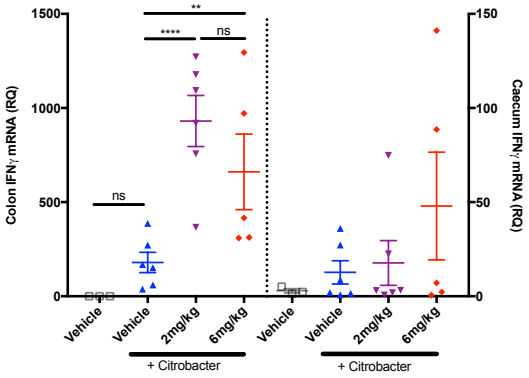
Colon IFNγ mRNA (RQ)
Caecum IFNγ mRNA (RQ)
1500
1000
500
0
150
100
50
0
**
****
ns
ns
Vehicle
Vehicle
2mg/kg
6mg/kg
+ Citrobacter
Vehicle
Vehicle
2mg/kg
6mg/kg
+ Citrobacter

B

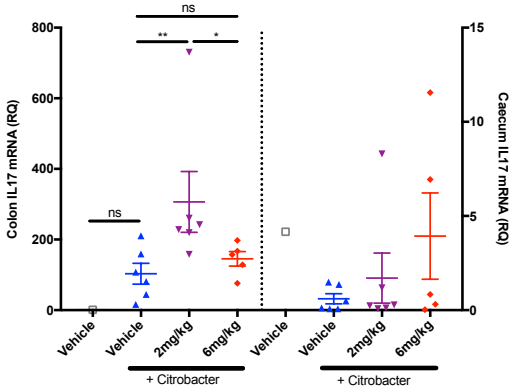
Colon IL17 mRNA (RQ)
Caecum IL17 mRNA (RQ)
800
600
400
200
0
15
10
5
0
ns
**
*
ns
Vehicle
Vehicle
2mg/kg
6mg/kg
+ Citrobacter
Vehicle
Vehicle
2mg/kg
6mg/kg
+ Citrobacter

C

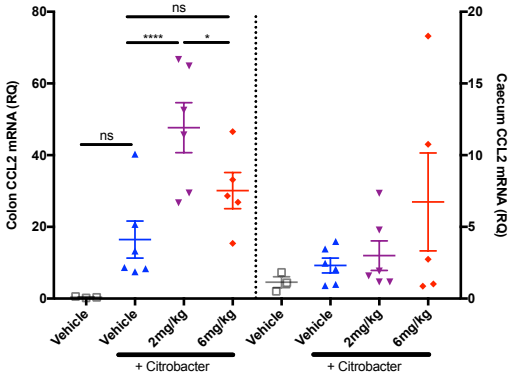
Colon CCL2 mRNA (RQ)
Caecum CCL2 mRNA (RQ)
80
60
40
20
0
20
15
10
5
0
ns
****
*
ns
Vehicle
Vehicle
2mg/kg
6mg/kg
+ Citrobacter
Vehicle
Vehicle
2mg/kg
6mg/kg
+ Citrobacter

D

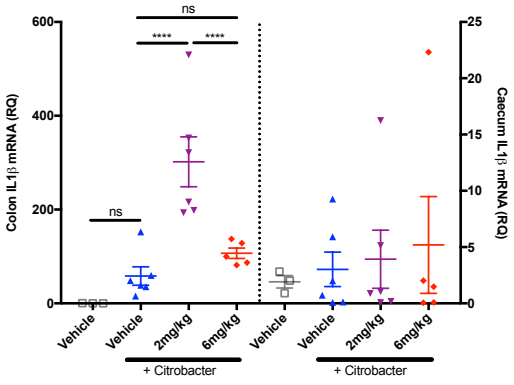
Colon IL1β mRNA (RQ)
Caecum IL1β mRNA (RQ)
600
400
200
0
25
20
15
10
5
0
ns
****
****
ns
Vehicle
Vehicle
2mg/kg
6mg/kg
+ Citrobacter
Vehicle
Vehicle
2mg/kg
6mg/kg
+ Citrobacter

E

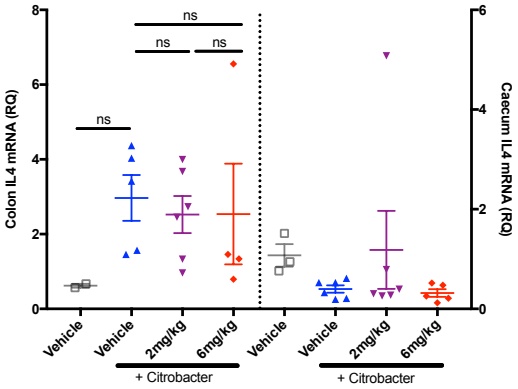
Colon IL4 mRNA (RQ)
Caecum IL4 mRNA (RQ)
8
6
4
2
0
6
4
2
0
ns
ns
ns
ns
Vehicle
Vehicle
2mg/kg
6mg/kg
+ Citrobacter
Vehicle
Vehicle
2mg/kg
6mg/kg
+ Citrobacter

F

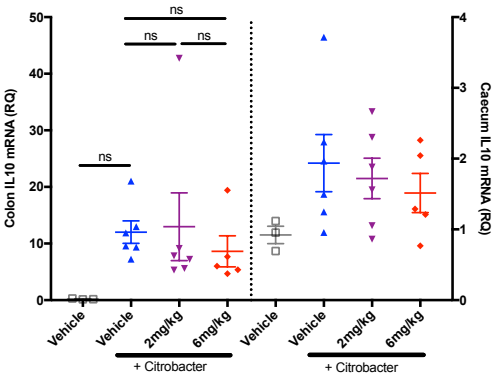
Colon IL10 mRNA (RQ)
Caecum IL10 mRNA (RQ)
50
40
30
20
10
0
4
3
2
1
0
ns
ns
ns
ns
Vehicle
Vehicle
2mg/kg
6mg/kg
+ Citrobacter
Vehicle
Vehicle
2mg/kg
6mg/kg
+ Citrobacter

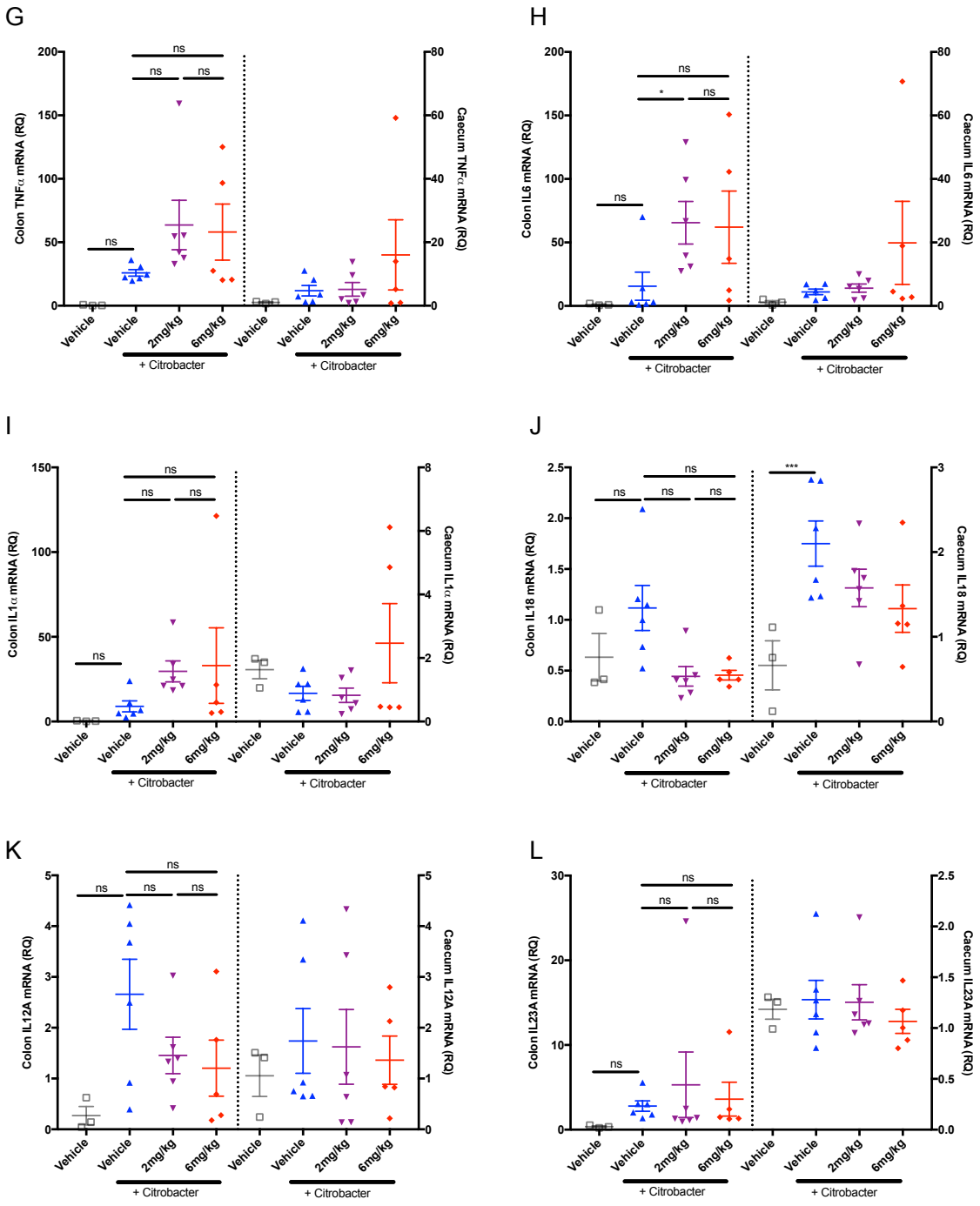

Figure 5.5 Mucosal cytokine production mirrors histological changes for T_H1 and T_H17 cytokines

RNA was extracted from samples of colon and caecum and analysed by qPCR for mucosal cytokine production normalised to β-actin. Significant differences in colonic IFNγ **(A)**, IL-17 **(B)**, CCL2 **(C)**, IL-1β **(D)** and IL-6 **(H)** were seen with ABD1970 2mg/kg, and with 6mg/kg for IFNγ only. No effect of ABD1970 was seen for all other cytokines assayed **(E, F, G, I, J, K, L)**. Caecal cytokine production was generally lower than colonic in keeping with the natural history of *Citrobacter* colitis. Mean +/- SEM. ANOVA with Bonferroni correction for selected pairs as shown.

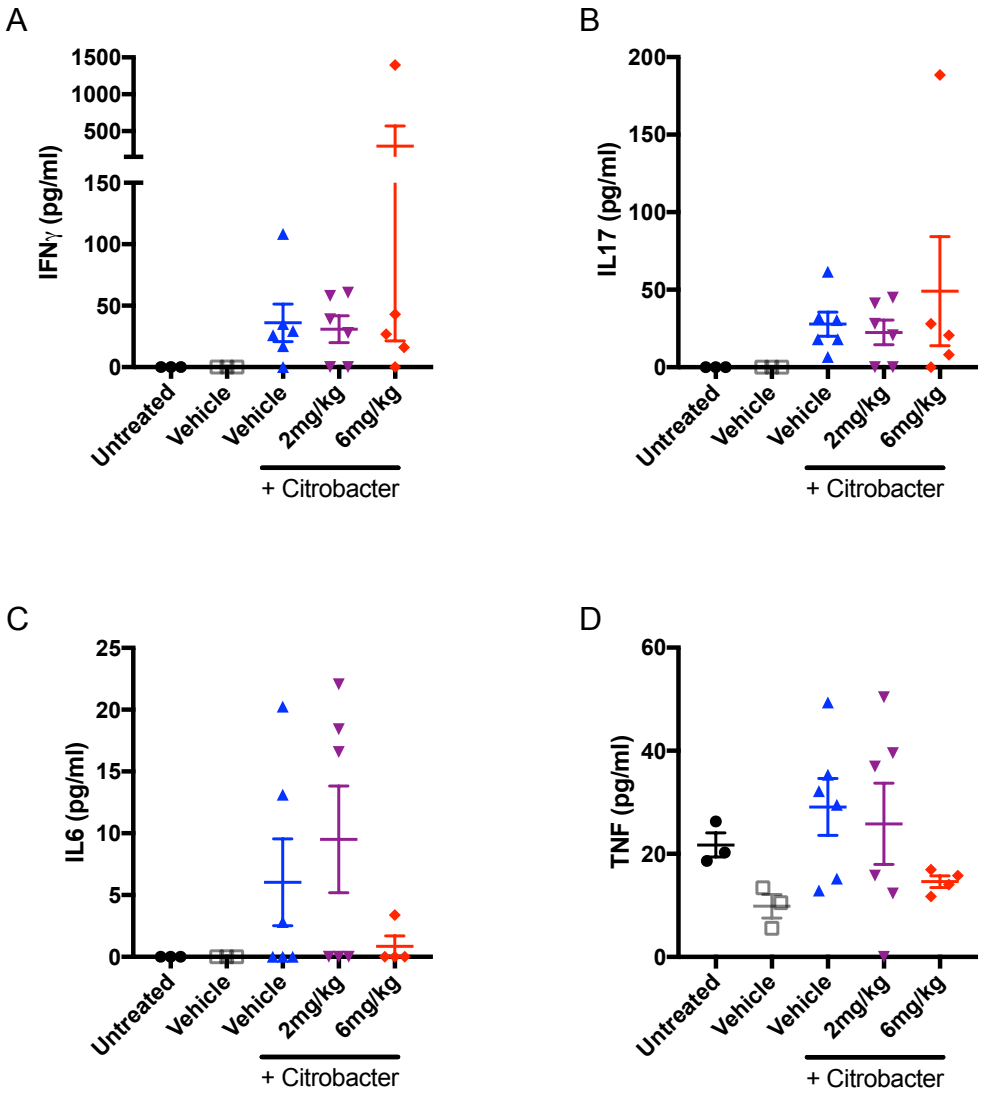

Figure 5.6 Measurement of cytokines from cells isolated from mesenteric lymph nodes did not differ with *Citrobacter* infection or with MGLL inhibition

Mesenteric lymph nodes (MLNs) were passed through a cell strainer and the cells placed in wells of a 96-well plate coated with anti-CD3e and anti-CD28. The supernatant was harvested at 72h and processed for cytokines by ELISA. No significant differences were observed for any of the measured cytokines. Mean +/- SEM.

Due to delays encountered in obtaining a Project Licence through the United Kingdom Home Office, further *in vivo* experiments with ABD1970 were not possible as part of this thesis.

5.3.5 Serine hydrolases can be detected by gel-based ABPP profiling of primary human colonic tissue

A pilot study to determine the amount of colonic tissue required to perform ABPP was performed. Three patients were identified – two healthy controls and one with endoscopically and histologically confirmed UC. Four endoscopic biopsies were taken from each of the healthy controls, and four biopsies taken from both inflamed and non-inflamed colon in the patient with IBD. Demographics of the patient are shown in Table 5.3. Patients on no medications were selected to try and obviate any influence of medical therapy (particularly systemic immunosuppressants, steroids and NSAIDs) on serine hydrolase expression including MGLL. Endoscopic severity was assessed according to the Ulcerative Colitis Endoscopic Index of Severity (UCEIS), a validated scoring system[338].

Patient	Gender	Age	Endoscopy	UCEIS (/8)	Histology	Medications
Healthy (a)	M	61	Normal	na	na	Nil
Healthy (b)	F	56	Normal	na	na	Nil
Colitis	F	60	Proctitis	5	UC	Nil

Table 5.3 Demographics of patients for pilot gel-based ABPP profiling of colonic biopsies

The proteome from each sample was divided into soluble and particulate (membrane) fractions and probed with both FP-Rh and HT-01 to maximise coverage of the serine hydrolome (Figure 5.7A/B) with different serine hydrolases detectable with each probe. A larger number of serine hydrolases were identified with the former probe. Unlike profiling of moDCs, there were greater differences between the healthy controls although some similarities were apparent – including bands at 23, 27, and 60kDa in the FP-Rh soluble fraction for instance. Marked differences were seen between non-inflamed and inflamed colon in the patient with

UC. A relative drop out of higher molecular weight proteins was balanced with an increase in activity of lower molecular weight proteins. This may partly reflect an increase in protease activity at lower molecular weights leading to digestion of others.

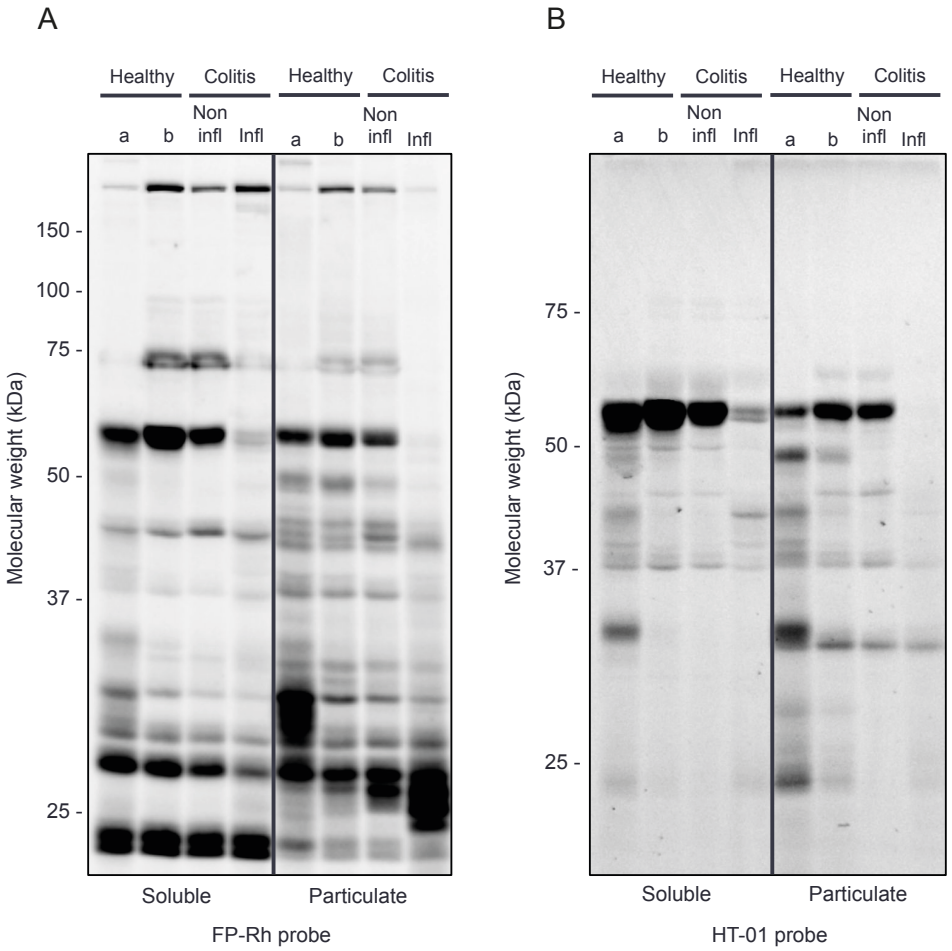

Figure 5.7 Pilot gel-based ABPP of human colonic biopsies demonstrates a rich serine hydrolase repertoire with differences seen in inflammation

The soluble and particulate (membrane) proteome was extracted from colonic biopsies obtained endoscopically. Samples were incubated with either FP-Rh **(A)** or HT-01 **(B)** prior to gel-based ABPP. Multiple serine hydrolases were identified with differences between donors and an effect of inflammation particularly at lower molecular weight. Non infl = non-inflamed; Infl = inflamed.

5.3.6 ABPP-MuDPIT of colonic biopsies from IBD patients reveals a dynamic serine hydrolome but with differences between patients

Having identified that the serine hydrolome could be resolved by gel-based ABPP further patients were profiled. In order to have sufficient material to proceed to ABPP-MuDPIT, 6 biopsies were taken from each site rather than 4. A total of 8 additional healthy controls with endoscopically normal colons and on no medications were recruited. 10 additional patients with IBD were recruited. Demographics are shown in Table 5.4. Although the intention was to only include those on no medications this resulted in difficulties in meeting our recruitment target. Therefore we extended eligible patients to include those on oral and/or rectal 5-aminosalicylic acid derivatives (5ASA; mesalazine, sulphasalazine, balsalazide) but no systemic immunosuppression or NSAIDs. As 5ASA acts locally on the colonocytes this could arguably influence the serine hydrolome. However, there was not another viable option to meet recruitment. Inclusion of patients with more extensive colitis was considered but this would negate the benefits of the internal control of non-inflamed and inflamed colon in the same patient.

Patient	Gender	Age	Endoscopy	UCEIS (/8)	Histology	Medications
1	M	61	Normal	na	na	Nil
2	F	56	Normal	na	na	Nil
3	F	60	Normal	na	na	Nil
4	F	71	Normal	na	na	Nil
5	F	62	Normal	na	na	Nil
6	M	50	Normal	na	na	Nil
7	F	71	Normal	na	na	Nil
8	F	46	Normal	na	na	Nil
9	M	41	Patchy inflam-mation	3	UC	Nil
10	M	44	Left sided colitis	na	CD	Nil
11	M	50	Proctitis	3	UC	Sulphasalazine
12	F	29	Left sided colitis	nr	UC	Mesalazine rectal
13	F	41	Left sided loss of vascular pattern	1	Normal	Mesalazine oral
14	M	36	Left sided colitis	5	UC	Mesalazine oral and rectal
15	F	46	Proctitis	4	UC	Mesalazine oral
16	M	46	Proctitis	3	UC	Mesalazine rectal
17	F	56	Proctitis	4	UC	Mesalazine oral and rectal
18	M	72	Left sided colitis	2	UC	Balsalazide

Table 5.4 Demographics of patients for wider gel-based ABPP and ABPP-MuDPIT analysis of colonic tissue in health and IBD
na = not applicable; nr = not recorded

Gel-based ABPP was performed on the 8 additional healthy patients and on 6 of the additional IBD patients (Figure 5.8) but not the final four due to delays obtaining samples and need to have sufficient material for MuDPIT. Gel-based ABPP was performed on these samples before the results of histology were known. However, it is important to note that patient 10 and 13, although having endoscopic features of UC had histological evidence of CD or no evidence of inflammation.

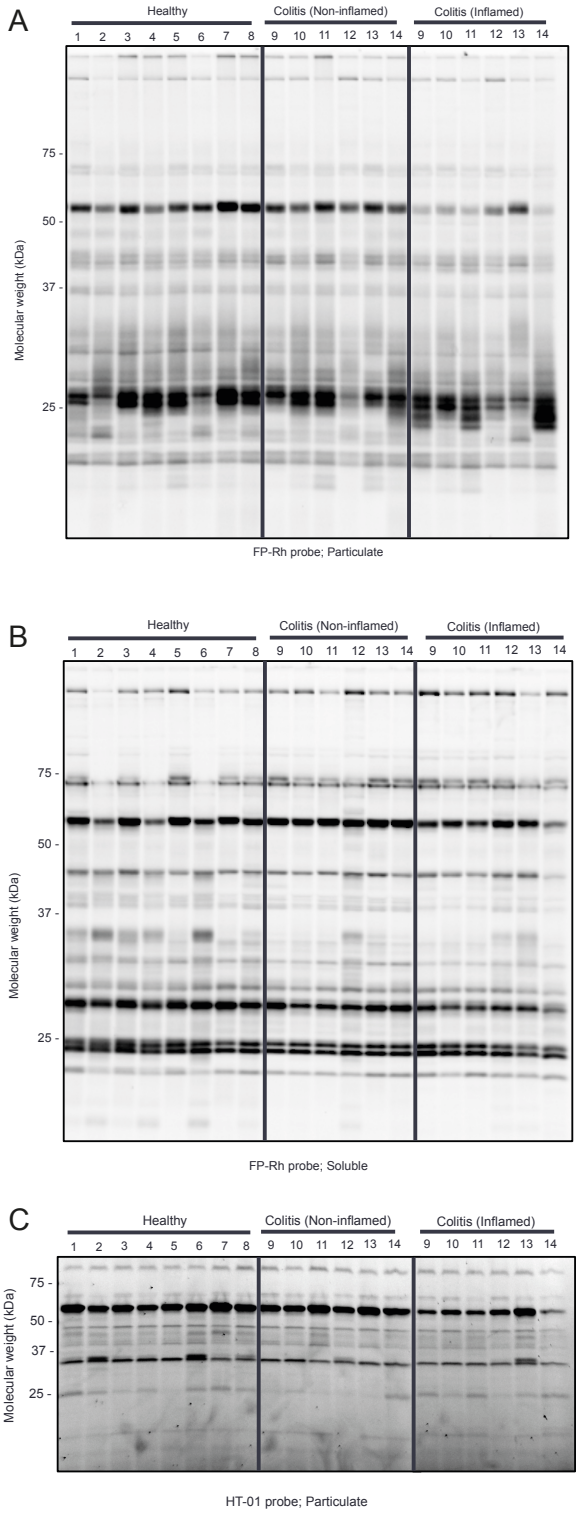

Figure 5.8 Gel-based ABPP of a larger number of colonic samples demonstrates variability between patients both in health and ulcerative colitis

Gel-based ABPP was performed with either FP-Rh **(A, B)** or HT-01 **(C)** probes on both particulate and soluble proteomes of healthy controls (n=8) and patients with endoscopic colitis (n=6). Appreciable differences in the serine hydrolome is seen between healthy controls and in colitis most marked in the FP-Rh particulate fraction. Insufficient material remained for ABPP of the HT-01 soluble fraction.

The differences in serine hydrolome activity in healthy colon is more apparent in this experiment than the pilot experiment. Marked changes in activity of proteins of approximately 25kDa are seen in the FP-Rh particulate fraction (Figure 5.8). The effects of inflammation on serine hydrolases identified in this fraction is similar to the pilot study but again there are marked differences between patients. There was no obvious effect of 5ASA on serine hydrolase activity but the numbers are too small for this to be necessarily significant.

Having established a rich serine hydrolome in human IBD by gel-based techniques, where sufficient proteome remained, samples were processed by ABPP-MuDPIT for relative differences between inflamed and non-inflamed samples. For all patients, both the soluble and particulate fractions were processed to maximise coverage of the enzyme family. The particulate fraction for patient 17 was lost at Abide Therapeutics and therefore does not appear on the figure. A total of 88 SHs were identified across all samples although not every enzyme was detected in each sample (Figure 5.9). However, some reproducible changes in enzyme activity were seen between samples, albeit with substantial variation between donors for some enzymes (Table 5.5). Many of these have not previously been annotated with respect to IBD. A greater number of SHs were identified in those samples from patients on 5ASA therapy (14-18) versus the patient on no medications (9). Whilst this may represent effects of 5ASA on SH activity, it may simply reflect more active inflammation in these patients – these were patients who had active colitis despite oral and/or rectal 5ASA and likely would need escalation of therapy to systemic agents.

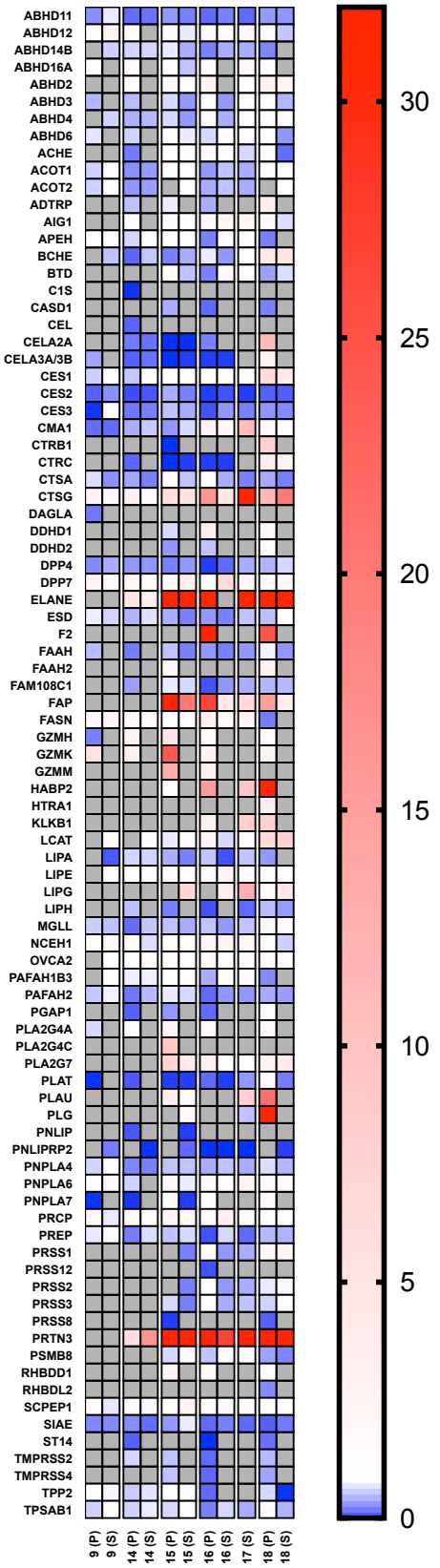

Figure 5.9 ABPP-MuDPIT of ulcerative colitis samples confirms a diversity of serine hydrolase enzymes some of which are altered in the inflamed colon

The particulate and soluble proteomes from colonic samples from 6 donors were processed for ABPP-MuDPIT (inflamed vs non-inflamed) and the results displayed on a heatmap. A grey box implies the protein was not identified. Significant differences correspond with a fold change >2 (increased activity, red) or <0.5 (decreased activity, blue) with a fold change of 1 (white colour) implying no difference between samples. The particulate sample for donor 17 was lost and is not displayed. (P) = particulate; (S) = soluble.

Abbreviation	Enzyme	Number of samples (/11)	Median fold change (SD)	Previously linked to IBD?	Previously linked to inflammation?
Reduced in inflamed colon					
ABHD11	αβ-hydrolase domain containing 11	11	0.4 (0.16)	No	No
CELA2A	Chymotrypsin-like elastase family member 2A	6	0.36 (4.13)	No	No
CELA3A/3B	Chymotrypsin-like elastase family member 3A/3B	8	0.18 (0.84)	No	No
CES2	Carboxylesterase-2	11	0.25 (0.15)	No	Yes
CES3	Carboxylesterase-3	11	0.44 (0.29)	No	Yes
CTRC	Chymotrypsin C	7	0.1 (1.49)	No	Yes
DPP4	Dipeptidyl peptidase 4	11	0.49 (0.18)	Yes	Yes
LIPH	Lipase H	6	0.46 (0.18)	No	No
PAFAH2	Platelet activating factor acetylhydrolase-2			No	Yes
PLAT	Tissue-type plasminogen activator	9	0.23 (0.51)	No	Yes
PNLIPRP2	Pancreatic lipase related protein-2	7	0.03 (0.15)	No	No
SIAE	Sialate O-acetylesterase	11	0.4 (0.17)	No	Yes
Increased in inflamed colon					
ABHD2	αβ-hydrolase domain containing 2	7	2 (0.81)	No	No
CTSG	Cathepsin G	11	5.3 (9.23)	Yes	Yes
ELANE	Neutrophil elastase	8	32 (12.29)	No	Yes
FAP	Fibroblast-activation protein	7	14.9 (10.45)	No	Yes
PLA2G7	Lipoprotein-associated phospholipase A2 (group 7)	7	3.5 (2.03)	No	Yes
PRTN3	Proteinase-3	9	32 (8.96)	No	Yes

Table 5.5 Significant changes in serine hydrolase activity between inflamed and non-inflamed colon
Enzymes identified in at least 6 of 11 samples with a median fold change ≥2 or ≤0.5.

5.3.7 Profiling of the ECS by ABPP and qPCR in human IBD show promising but discordant results

Data on the relative activity of synthetic and hydrolytic enzymes for 2AG were extracted from the ABPP-MuDPIT results and plotted alongside PLA2G4A (Figure 5.10). This experiment represents the first profiling of activity of ECS enzymes in human IBD. The data demonstrate a general increase in activity of ABHD12 although this does not reach the significance threshold of a fold change of 2 in most cases. A reduction in MGLL and FAAH activity across samples is reproducible, with variable responses for ABHD6 and DAGLB. PLA2G4A was only identified in the membrane fraction commensurate with its mode of action on membrane phospholipids. Changes in activity are variable between patients but do not quite reach the significance threshold.

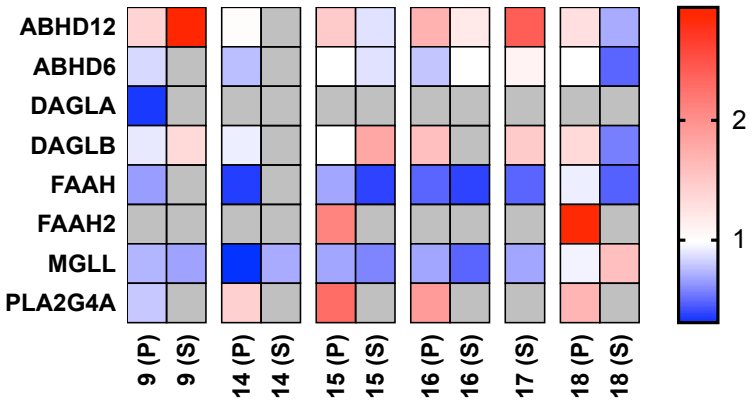

Figure 5.10 ABPP-MuDPIT of ECS enzymes in ulcerative colitis
Data were extracted from Figure 5.9 to display ABPP-MuDPIT results for ECS enzymes and PLA2G4A. Marked differences were seen between donors with a broad trend to an increase in ABHD12 and DAGLB in inflammation, and a reduction in MGLL and FAAH activity.

qPCR was performed on colonic samples from a separate cohort of healthy patients and those with endoscopically and histologically confirmed UC. Similar to the ABPP samples, where possible patients on no medications were recruited but

due to low numbers eligibility was extended to those on 5ASA therapy. Demographics of the colitis patients are shown in Table 5.6. Patients 1, 2, 4 and 21 were subsequently excluded due to histology which was not clearly consistent with UC, and patient 16 who was subsequently found to have been taking azathioprine at the time of biopsy. A total of 17 healthy patients were recruited as controls (12 female, mean age 47, none on medications).

Patient	Gender	Age	Endoscopy	UCEIS (/8)	Histology	Medications
1	F	28	Patchy erythema	2	Normal	Mesalazine oral and rectal
2	M	33	Loss of vascular pattern	nr	Normal	Nil
3	F	34	Proctitis	4	UC	Nil
4	F	56	Proctitis	nr	Focal active colitis	Nil
5	M	25	Proctitis	nr	UC	Nil
6	F	49	Proctitis	4	UC	Mesalazine oral and rectal
7	M	43	Left sided colitis	3	UC	Nil
8	F	34	Proctitis	nr	UC	Nil
9	F	42	Proctitis	2	UC	Mesalazine oral
10	F	51	Proctitis	3	UC	Mesalazine oral and rectal
11	M	31	Proctitis	nr	UC	Nil
12	F	41	Proctitis	4	UC	Mesalazine oral
13	F	64	Proctitis	3	UC	Mesalazine oral
14	M	45	Left sided colitis	6	UC	Mesalazine rectal
15	F	29	Proctitis	4	UC	Mesalazine oral
16	M	34	Proctitis	5	UC	Mesalazine oral and rectal, and azathioprine
17	F	52	Proctitis	4	UC	Mesalazine oral
18	F	39	Proctitis	3	UC	Mesalazine oral
19	M	41	Left sided colitis	4	nr	Mesalazine oral
20	F	60	Left sided colitis	2	UC	Sulphasalazine oral and mesalazine rectal
21	F	31	Proctitis	4	UC and focal active colitis	Mesalazine oral and rectal

Table 5.6 Demographics of patients for qPCR analysis of ECS components
nr = not recorded

A number of methods were trialled for homogenisation and RNA extraction (data not shown) including manual homogenisation and extraction using Tri-

zol/chloroform. However, the greatest RNA yield was obtained using the technique described in Chapter 2. A clear increase in CNR2 was demonstrated in inflamed tissue compared to both non-inflamed and healthy colon (Figure 5.11B). A small but significant reduction in MGLL mRNA was seen in inflamed colon (Figure 5.11E). More exciting were the changes in ABHD12, DAGLα and DAGLβ (Figure 5.11D, G, H). Expression of these three genes was reduced not only in inflamed IBD samples but also in non-inflamed IBD samples. No significant differences were seen in CNR1, ABHD6, FAAH or PLA2G4A (Figure 5.11A, C, F, I). Stratification of the patients based on whether or not they were receiving 5ASA therapy or not did not result in differences in the findings (data not shown).

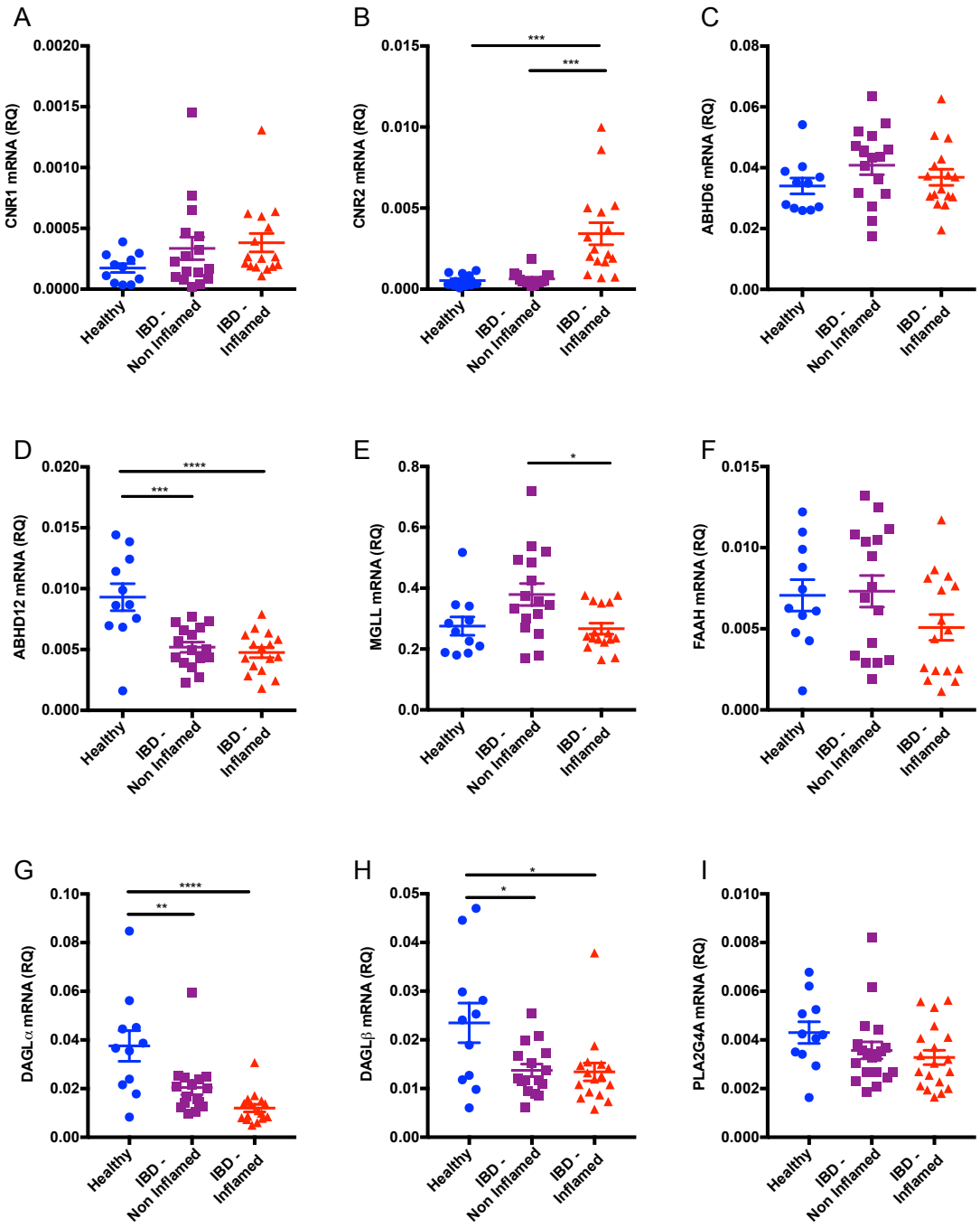

Figure 5.11 Gene expression of cannabinoid receptors and ECS enzymes in health and ulcerative colitis

Colonic biopsies were obtained endoscopically from healthy patients (n=17) and those with distal ulcerative colitis where both inflamed and non-inflamed colon could be sampled in the same patient (n=16). RNA was extracted and qPCR performed for cannabinoid receptors CNR1 and CNR2, together with ECS enzymes. An increase in CNR2 expression was seen in active inflammation **(B)**, and an increase in MGLL in non-inflamed colon versus inflamed **(E)**. A reduction in both non-inflamed and inflamed samples versus healthy was seen for ABHD12 **(D)**, DAGLα **(G)** and DAGLβ **(H)**. No differences were seen in the other genes profiled. Mean +/- SEM. *p<0.0332, **p<0.0021, ***p<0.0002, ****p<0.0001.

5.4 Discussion

Of all experiments within the 40 published papers assessing modulation of ECS components on experimental ileitis/colitis, only 4 have used non-chemical models – $IL10^{-/-}$ colitis (2 studies), $TNF^{\Delta ARE}$ ileitis, and LPS colitis. None of the models used thus far recapitulate the complexities of host-pathogen interaction in the gut. Although *Citrobacter* is a self-limiting disease in wildtype mice and does not therefore capture the more chronic/fibrotic phase of human IBD, there is not currently an experimental model which reproduces all aspects of human disease. That said, the findings presented in this chapter add to and challenge the existing literature.

Firstly, this data is the first use of gel-based ABPP in experimental colitis. MGLL is clearly present in murine colon and can be inhibited effectively *in vivo* using ABD1970. In those mice receiving *Citrobacter* and vehicle alone there is a reduction in mean MGLL activity, measured by densitometry, of almost 15%. There was not, however, an effect of vehicle on MGLL activity in the absence of *Citrobacter*. The reduction might be explained by generalised proteolysis in inflammation although there are few other serine hydrolase whose activity changes with *Citrobacter* by gel-based techniques. An alternative explanation could be that *Citrobacter* exerts some effect on innate immune cells to impair upregulation of MGLL in response to PRR stimulation although the nature of such an effect is not clear. It would be intriguing to measure MGLL activity at earlier timepoints in infection as it is possible that MGLL activity increases early after infection (in a similar manner to human moDCs) and subsequently reduces as the inflammatory process begins to settle.

Secondly, the data shows a clear negative effect of MGLL inhibition on severity of colitis with correlation between colonic histology and mucosal cytokine production. Only one other study has shown a negative impact of increasing ECS ligands on colitis production – PF3845, a FAAH inhibitor, in 4% DSS but not TNBS colitis[308]. This may simply highlight the differences between different models of intestinal inflammation and then need to perform extensive pre-clinical studies across multiple models to understand the mode of action of an enzyme inhibitor. Furthermore, in *Citrobacter* colitis the negative effects of MGLL inhibition do not follow a linear dose-response trajectory with lower dose inhibition worsening disease more than higher dose. This is difficult to reconcile.

It is possible the results are a statistical anomaly given the numerical, but non-significant, increase in histology score at 6mg/kg compared to vehicle, and relatively small number of mice per group. Certainly for IFNγ there is a significant increase at 6mg/kg compared to vehicle but this is not true of a number of other cytokines which are significant at the lower dose. It is also notable that the degree of MGLL inhibition between the two doses (41% vs 26.4%) is more similar than intended from the pilot experiment. It seems unlikely that such a small degree of difference should result in such profound differences in colitis severity. However, if the higher dose was sufficient to alter cannabinoid receptor signalling through desensitisation then this might provide an explanation for a difference between the groups. Certainly there is no difference in bacterial counts between the groups which might suggest the effect is mediated through immune cells. It is also possible that differential signalling through CB1 or CB2 results in

pro- or anti-inflammatory effects and this differs between models. One way to test the hypothesis of cannabinoid receptor desensitisation modulating colitis severity would be to use a $MGLL^{-/-}$ mouse. Whilst these mice exhibit enhanced learning[450] and impaired diet-induced insulin resistance[451], no studies have challenged the knockout with an inflammatory stimulus. These mice exhibit chronically elevated 2AG and reduced arachidonic acid together with desensitisation of CB1[181,182,452,453].

It is possible that the timing of administration of MGLL inhibitor relative to inflammatory stimulus is also relevant. If MGLL has anti-inflammatory roles, potentially to switch off inflammation and restore homeostasis by altering signalling between immune cells, then MGLL-inhibited mice may be relatively immunosuppressed when exposed to *Citrobacter*. Therefore it would be essential not only to repeat the prophylactic experiment but also to administer MGLL inhibition after colitis is established. This should ideally be repeated across a number of different models including chemical and spontaneous colitis. In any case, a therapeutic approach has more translational potential than a prophylactic one.

The profiling by ABPP-MuDPIT of inflamed versus non-inflamed human colon has mapped serine hydrolase expression for the first time. Activity of a number of enzymes are shown to be altered and it would be interesting to know whether the same enzymes are altered between inflamed and healthy (rather than non-inflamed) and whether ileum behaves differently to colon as might be expected. Only DPP4 and CTSG have previously been linked with IBD in the literature. DPP4 protein is reduced in plasma and tissue from patients with CD[454] whereas

data from gene expression profiling is less clear cut[455]. Antibodies against CTSG have been demonstrated in patients with IBD[456,457] and CTSG expression is higher in colonic biopsies from patients with UC[458]. A number of novel enzymes not previously linked to inflammation in the literature are highlighted including ABHD11, ABHD2, LIPH and PNLIPRP2. Given only 6 patients were profiled by ABPP-MuDPIT and the variation between donors it would be essential to validate these findings by alternative methods. If suitable antibodies were obtained, immunohistochemistry could be used for example. With the advent of single cell RNA technologies to interrogate the potential roles of different cell types in inflammation it would be interesting to combine this with ABPP-MuDPIT to assess activity of serine hydrolase enzymes within individual cells. However, due to the large amount of material currently needed for MuDPIT this is not something that can be performed at present.

Extraction of the data for ECS components from the MuDPIT results and comparison with qPCR shows notable differences with poor correlation between the techniques. However, this is the first data to assess expression of ABHD6 and 12 in human colitis, and the second to profile MGLL and DAGL enzymes. CB2 expression by qPCR was increased, and CB1 unchanged, in inflammation in this study but neither were validated at protein level. These findings are in keeping with some but not all previous studies (Figure 5.1).

More interesting are the results for ABHD12 and DAGL enzymes. The concept of field change is well established for colitis-associated carcinogenesis[459,460] and a non-invasive biomarker is needed for IBD. Furthermore, 20-50% of patients with

left-sided UC or proctitis are known to extend colonic inflammation proximally over time[461]. If confirmed, it is possible that changes in expression of these components of the ECS might represent field change in IBD and pre-empt parts of the colon which may become inflamed in the future. This might enable early modification of the inflammatory pathway to prevent disease extension. Whilst promising, the differences between gene expression and ABPP data indicate the need for further study at protein level to confirm whether ABHD12 and DAGLα/β are indeed altered in non-inflamed colon.

5.5 Conclusion

In this chapter, prophylactic MGLL inhibition has been demonstrated to worsen *Citrobacter rodentium* colitis particularly at lower dose (achieving a 60% reduction in MGLL activity). The mechanism remains unclear and requires further study. ABPP profiling has been used in colonic samples from patients with ulcerative colitis and demonstrates some novel enzymes not previously associated with inflammation or IBD. ABHD12 and DAGL enzymes may have roles not only in colitis but also in adjacent non-inflamed bowel potentially as a biomarker of future inflammation.

Chapter 6 - Discussion

Understanding of the ECS and the action of exocannabinoids including THC and CBD has advanced rapidly since the identification of CB1. The system is now known to contain at least two key receptors with different tissue distributions and downstream cascades which are subject to desensitisation and biased signalling; lipid ligands which act as full or partial agonists on one or both receptors and other related bioactive lipids which also exert actions to modify receptor signalling through an entourage effect; and an increasing number of degradative enzymes for these ligands with modes of action that differ depending on the cellular or tissue context. Moreover the products of endocannabinoid metabolism, namely arachidonic acid, prostaglandins and leukotrienes, exert their own biological effects.

From the clinical observation of the analgesic potential of cannabis to the experimental modulation of the ECS to achieve antinociceptive results, there is also an increasingly appreciated role in inflammation. Much of these findings arise from *in vitro* or *in vivo* experimental models of inflammation often of rodent origin. This may not necessarily be directly translatable to human disease. In order to better understand roles of the ECS in human disease, an exploration of effects on human immune cells is crucial. A critical player in the immune response is the dendritic cell. Displaying a raft of PRRs to detect evolutionarily conserved components of pathogens, these cells orchestrate the immune response including T cell differentiation and activation. Therefore a better understanding of dendritic

cell biology should lead to novel therapies to modulate the immune response with benefit for autoimmune disease and cancer.

With regard to IBD, it is well documented through the results of GWAS and experimental studies that the innate immune response is critical. Particularly relevant are mutations in NOD2 which predispose to Crohn's disease and alter dendritic cell biology (discussed in Chapter 1). Further evidence for the role of the innate immune system in IBD pathogenesis arises from the numerous experimental and clinical trials of PRR modulation[462]. Several models of chemical colitis have shown benefit of increasing endocannabinoid levels, either by exogenous application or inhibition of hydrolytic enzymes, or activating the CB1 and/or CB2 signalling pathways. However, the clinical studies of cannabinoids in IBD, whilst highlighting increased usage of these substances in patients to control symptoms, have so far failed to demonstrate significant positive effects on disease activity. A significant problem of cannabinoid therapy is the unwanted neuropsychiatric side effects mediated by CB1 in the central nervous system. Therefore, modulation of endocannabinoids in cells and tissues where they are already present, by inhibition or activation of the synthetic/degradative enzymes should mitigate at least some of these effects.

MGLL, a serine hydrolase, has been demonstrated to be the main hydrolytic enzyme for the endocannabinoid, 2AG, in the murine brain[151]. Benefits of MGLL inhibition have been shown in models of neuroinflammation[154], gastritis[184], fever[267,268], lung injury[270] and a single report of chemical colitis[273]. Furthermore, *in vitro* data has shown an active ECS in moDCs[201] and roles for THC in moDCs on

modulating T cell polarisation[463]. Inhibition of other enzymes from the serine hydrolase family have already shown potential therapeutically. Therefore, the work described in this thesis sought to explore serine hydrolase activity, and MGLL in particular, in human moDCs; to understand what role MGLL might play in dendritic cell biology and whether this might underscore the anti-inflammatory roles seen in the literature; to describe the use of MGLL inhibition in a host-pathogen model of intestinal inflammation relevant for human IBD; and to profile serine hydrolases in human IBD to identify potential targets for future study which might be therapeutically tangible.

6.1 Serine hydrolase profiling of dendritic cells confirms increased MGLL activity following PRR ligation which modulates lipid levels

Utilising the technique of ABPP for the first time in primary human moDCs, MGLL was demonstrated to be the most upregulated serine hydrolase upon stimulation of TLR2/NOD2. This correlated with an increase by immunoblot and was not restricted to these PRRs with similar increases on stimulation of TLR3, 4, 5, and 7/8. Unlike many pro-inflammatory cytokines, MGLL upregulation occurs later after stimulation, from 6-8h. This might suggest roles in immunoregulation rather than perpetuating a pro-inflammatory response. Using a mass spectrometry approach to lipidomics, MGLL inhibition with the small molecule inhibitor JZL184 increases cellular and secreted 2AG with off-target effects through FAAH on AEA levels. Cellular 2AG was shown to reproducibly reduce upon stimulation across 6 donors, contrary to the previous literature where 2AG was shown to increase after LPS stimulation in humans[201] and mice[198]. There are several explanations for this: the lipidomic technique used may be subtly different although this

should not explain such a divergence of results. Alternatively, the effects of NOD2/TLR2 stimulation may be different to TLR4 which was used in the other human study, there may be inter-species differences, or there could have been contamination of the cellular specimen with media in the human study which could have potentially increased 2AG levels.

Interestingly, there was no detectable effect of MGLL inhibition on the composite level of PGE2/D2 or arachidonic acid in moDCs. This is striking because the two most altered serine hydrolases upon stimulation were MGLL and PLA2G4A both of which feed into production of arachidonic acid. This may be a feature of the timepoints used in the assays with prostaglandin production occurring earlier (or later) for instance. However, it is possible that the role of MGLL in moDCs is to alter 2AG levels and not to regulate eicosanoid production. It has been shown in murine tissues that the ability of MGLL to affect eicosanoid levels is tissue dependent[154]. It would be interesting to investigate this further by measuring lipid levels in the presence of inhibition of PLA2G4A and/or COX enzymes alongside MGLL inhibition.

An untargeted screen of wider lipidomics did not identify clear effects on other lipids such as LPC and LPE unlike previous studies of human cancer cell lines[167,169]. This is not entirely surprising as there is no biological variation in cell lines whereas the responses from the 3 donors profiled here varied appreciably. However, in order to yield meaningful results from primary human immune cells it would be essential to profile a large number of donors, with sufficient cell numbers, and to explore earlier timepoints for lipid flux. It would also be inter-

esting to explore acute versus chronic MGLL inhibition on lipid profiles as the effects on LPC in a prostate cancer cell line varied depending on the condition[167]. Were effects on LPC and LPE to be confirmed this may also have exciting implications for innate immune biology. LPCs have, for instance, been shown to be ligands for CD1d-restricted T cells in patients with multiple myeloma[464].

6.2 MGLL transcription following NOD2 ligation is RIPK2-dependent but the pathways following TLR2 ligation are less clear

Using a number of pharmacological inhibitors of signalling molecules downstream of PRRs, MGLL transcription following MDP stimulation of NOD2 has been shown to be RIPK2-dependent. TLR2 is known to signal through the adaptor molecules MyD88, MAL, and BCAP to activate MAPK and NF-κB dependent cytokine transcription. Whilst small molecule inhibition of MAPK (apigenin), TBK1 (BX795) and syk (Bay613606) resulted in inhibition of MGLL transcription this did not always correlate with ABPP assessment of activity. Moreover, MGLL levels were not affected by TBK1 knockdown in THP1 cells. Whilst this may be due to differences in MGLL between cell types, it is possible that the effects seen with the small molecule inhibitors are off target. MyD88 knockdown in THP1 cells also had no effect on MGLL levels suggesting that the increase in MGLL levels following TLR2 ligation may be MyD88-independent. Of potential greater concern was the lack of MGLL induction in murine BMDCs at the timepoint assayed. Whilst this may simply represent an experiment with a single mouse or that the timescale for MGLL induction differs between species, if MGLL was confirmed not to be significantly upregulated upon PRR ligation in mice this would

have implications for translation of animal studies of MGLL inhibition into human disease.

The TLR-BCAP-PI3K/mTOR pathway has only recently been described and is not yet well understood[465]. Although there exists controversy as to pro- and anti-inflammatory roles, PI3K is felt to reduce the ensuing inflammatory response and PI3K inhibitors have effects on increasing pro-inflammatory cytokines and T cell priming[391]. The observation of increased MGLL transcription following PI3K inhibition with wortmannin is interesting and may lend further credence to a potential anti-inflammatory role of MGLL to dampen the effects of PI3K inhibition. It would be important to explore this in future work.

6.3 The role of MGLL in dendritic cell biology may involve communication with other cells

Although both cellular and secreted 2AG/AEA were significantly altered by JZL184 this did not translate to quantifiable differences in dendritic cell, and other innate immune cell, biology across a range of experiments. This included immediate and delayed cytokine production, maturation, migration, and pathogen handling. In the central nervous system, 2AG is released from the post-synaptic terminal into the synaptic cleft upon receipt of a stimulus, whereupon it acts retrogradely on CB1 receptors in the pre-synaptic terminal[145]. Here it is rapidly degraded by MGLL. The immune synapse between antigen presenting cells and T cells is increasingly understood[466]. It is possible and likely that 2AG and MGLL have paracrine effects on bystander cells perhaps on T cell polarisation as has been shown for THC (Figure 6.1).

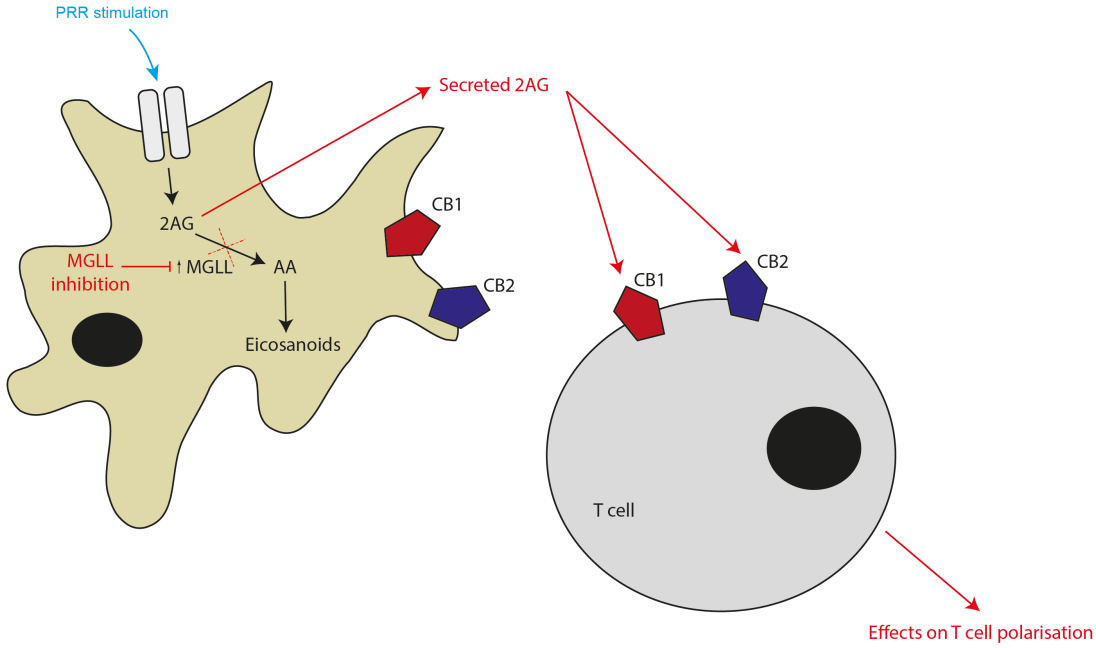

Figure 6.1 Proposed model for action of MGLL and 2AG on bystander T-cells
PRR ligation results in 2AG metabolism through MGLL induction. It is likely that some 2AG is secreted from the cell. Inhibition of MGLL increases secreted 2AG with no effect on moDC function. An effect on bystander T cells is probable through CB1, CB2 and/or other, as yet uncharacterised, cannabinoid receptors, to alter polarisation.

6.4 MGLL inhibition in intestinal inflammation *in vivo* is not always beneficial

A key finding of the work presented in this thesis is that MGLL inhibition may not universally have anti-inflammatory effects on intestinal inflammation *in vivo*. The literature is biased towards chemical models of colitis which, although displaying some features of human IBD, do not reproduce the host-pathogen interaction which is thought to be so relevant to human disease pathogenesis. To explore this for the first time, the *Citrobacter rodentium* model of intestinal inflammation was used. This pathogen has similarities with human *E coli*, is sensed by cells of the innate immune system especially NOD2 and TLR2, and recruits an adaptive response which is $T_H1/17$ biased, similar to Crohn's disease. This model therefore complements the *in vitro* MGLL inhibition work with innate immune cells presented in this thesis. Administration of a novel MGLL inhibitor, ABD1970, prior to

administration of *Citrobacter* resulted in worsened colitis measured both by histology and by mucosal cytokine production. There was no effect on bacterial counts locally or systemically nor on systemic cytokine production from MLNs and is therefore likely due to effects on immune cells in the colon. This reinforces the importance of studying different experimental models of disease and that there is no single model of IBD which recapitulates all aspects of human disease. This merits further study both to confirm and extend the findings. Use of ABD1970 after the onset of colitis and with different models (chemical or genetic for instance) would be essential.

6.5 The ECS and wider serine hydrolases are altered in inflamed colonic IBD tissue

Profiling of serine hydrolase activity by ABPP-MuDPIT in colonic tissue from healthy and IBD patients had not been performed prior to the work presented in this thesis. A rich array of serine hydrolases were identified in colonic tissue and clear effects of inflammation described. Variation between patients was greater than that seen with moDCs. This is likely to represent an environment which is more complicated in the gut than the circulation with the presence of a complex microbiota and dietary antigens. Despite this, reproducible changes were seen in several enzymes some of which have not been annotated with respect to inflammation and many of which have not been annotated with respect to IBD. These include ABHD2, PLA2G7 and ABHD11. Validation of these results and exploration of effects *in vitro/in vivo* should be expected to identify novel pathways in inflammation.

The current literature on ECS tone is confused and is limited by small numbers, poor reagents (particularly antibodies), potential effects of drug therapy, and poor phenotyping of patients. The data in Chapter 5 profiles gene expression of ABHD6 and 12 for the first time in human IBD and is the second study to profile MGLL and DAGL enzymes. ABHD12 and DAGL enzyme gene expression is reduced in IBD tissue regardless of the presence or absence of active inflammation. This holds potential therefore as a marker of field effect in IBD but requires further study including validation at protein level, analysis of the effect of medications, and correlation with severity of disease. This is particularly important given the ABPP-MuDPIT results are discordant with the qPCR data. This may, however, be due to general proteolysis in an area of inflammation. Alongside an increased understanding of the ECS tone in human tissues it would be possible to profile gene expression at a single cell level to better understand how modulation of endocannabinoids might exert effects on human disease. For instance, MGLL gene expression is higher in goblet cells from CD ileum than in healthy controls (Ana-Maria Catuneanu, personal communication), and is expressed in endothelial cells and myofibroblasts in healthy and DSS-treated mice with lower expression in the epithelial compartment (James Kinchen, personal communication).

6.6 Future directions for this research

6.6.1 *In vitro* experiments

1) Effects of MGLL inhibition in moDCs on bystander cells including T cell polarization
    a. An initial approach to addressing this question would be to use conditioned media from stimulated moDCs with/without MGLL inhibition and effects on naïve T cell polarization.
2) Regulatory pathways for MGLL transcription
    a. To confirm the timing of MGLL transcription in murine cells and the role of MyD88 knockout
    b. To further explore the potential role of the PI3K pathway, and also of Stat6 and PPARα.
3) Effect of MGLL on cellular and secreted lipids beyond the ECS
    a. I have instigated a collaboration with the Kessler group, (Target Discovery Institute, University of Oxford) to investigate lipid flux in moDCs using incorporation of ^{13}C-labelled glucose – known as fluxomics[467]. A promising technique, it is not yet known to what extent isotopically labelled carbon will be taken up by moDCs which are non-proliferative.
4) Subcellular localisation of MGLL upon PRR ligation
    a. I have obtained an RFP-tagged human MGLL plasmid (a generous gift from Professor Ying Huang, State University of New York, USA). Sanger sequencing confirms it to be full length human MGLL and preliminary experiments using confocal microscopy following transfection in HeLa cells show it to be a promising resource to interrogate localisation.

5) Effects of MGLL inhibition on antigen presentation assays
    a. Use of the OT1/2 mouse to interrogate antigen presentation pathways and the role of MGLL inhibition would be useful.
6) Immunoprecipitation to identify binding partners of MGLL
    a. Although preliminary work with the antibody used for MGLL immunoblotting in this thesis has not been successful for immunoprecipitation this has not been optimised. Furthermore the RFP-tagged MGLL construct could be used for this purpose.
7) Explore the function of the other significantly altered serine hydrolases in moDCs (PLA2G4A, PLA2G15, LIPA, LPL, ABHD2) and measure activity by ABPP-MuDPIT of serine hydrolases at earlier timepoints.

6.6.2 *In vivo* experiments

1) Repeat prophylactic ABD1970 in *Citrobacter* colitis and extend to a therapeutic experiment.
2) Use of ABD1970 in other model systems e.g. DSS/TNBS colitis, *Helicobacter hepaticus*, SAMP1/YitFc ileitis.

6.6.3 *Ex vivo* experiments

1) Validate ABPP-MuDPIT findings from human IBD and consider effects of disease severity and treatment effects (e.g. ABHD2, ABHD11, DPP4, SIAE).
2) Single cell experiments to identify expression of ECS components in different cell types and under different conditions.

3) Validate RNA data with protein expression particularly for ABHD12 and DAG-Lα/β as potential markers of field effect. This would need validation of antibody specificity.

6.7 Conclusion

The work which forms this thesis identifies MGLL, a serine hydrolase and key component of the ECS, to be upregulated upon stimulation of PRRs in human moDCs. MGLL inhibition results in alterations in lipid profiles, especially upon secreted 2AG. This does not have effects on dendritic cell biology in isolation but may act across synapses to influence bystander cells. MGLL inhibition has been shown to be detrimental in *Citrobacter rodentium* colitis when administered prophylactically, challenging the current literature. The ECS is altered in human IBD but there are wider changes in the serine hydrolome identified by ABPP-MuDPIT which may yet yield novel understanding of inflammatory disease in humans.

References

1 Johansson, M. E. *et al.* Composition and functional role of the mucus layers in the intestine. *Cell Mol Life Sci* **68**, 3635-3641, doi:10.1007/s00018-011-0822-3 (2011).

2 Cope, G. F., Heatley, R. V., Kelleher, J. & Axon, A. T. In vitro mucus glycoprotein production by colonic tissue from patients with ulcerative colitis. *Gut* **29**, 229-234 (1988).

3 Johansson, M. E. *et al.* Bacteria penetrate the normally impenetrable inner colon mucus layer in both murine colitis models and patients with ulcerative colitis. *Gut* **63**, 281-291, doi:10.1136/gutjnl-2012-303207 (2014).

4 Gibson, P. R. & Muir, J. G. Reinforcing the mucus: a new therapeutic approach for ulcerative colitis? *Gut* **54**, 900-903, doi:10.1136/gut.2004.058453 (2005).

5 Wenzel, U. A. *et al.* Spontaneous colitis in Muc2-deficient mice reflects clinical and cellular features of active ulcerative colitis. *PloS one* **9**, e100217, doi:10.1371/journal.pone.0100217 (2014).

6 Visschedijk, M. C. *et al.* Pooled Resequencing of 122 Ulcerative Colitis Genes in a Large Dutch Cohort Suggests Population-Specific Associations of Rare Variants in MUC2. *PloS one* **11**, e0159609, doi:10.1371/journal.pone.0159609 (2016).

7 Bevins, C. L. & Salzman, N. H. Paneth cells, antimicrobial peptides and maintenance of intestinal homeostasis. *Nat Rev Microbiol* **9**, 356-368, doi:10.1038/nrmicro2546 (2011).

8 Antoni, L., Nuding, S., Wehkamp, J. & Stange, E. F. Intestinal barrier in inflammatory bowel disease. *World J Gastroenterol* **20**, 1165-1179, doi:10.3748/wjg.v20.i5.1165 (2014).

9 Mantis, N. J., Rol, N. & Corthesy, B. Secretory IgA's complex roles in immunity and mucosal homeostasis in the gut. *Mucosal immunology* **4**, 603-611, doi:10.1038/mi.2011.41 (2011).

10 Spits, H. & Cupedo, T. Innate lymphoid cells: emerging insights in development, lineage relationships, and function. *Annu Rev Immunol* **30**, 647-675, doi:10.1146/annurev-immunol-020711-075053 (2012).

11 Spits, H. *et al.* Innate lymphoid cells--a proposal for uniform nomenclature. *Nat Rev Immunol* **13**, 145-149, doi:10.1038/nri3365 (2013).

12 Wang, S. *et al.* Regulatory Innate Lymphoid Cells Control Innate Intestinal Inflammation. *Cell* **171**, 201-216 e218, doi:10.1016/j.cell.2017.07.027 (2017).

13 Saeed, S. *et al.* Epigenetic programming of monocyte-to-macrophage differentiation and trained innate immunity. *Science* **345**, 1251086, doi:10.1126/science.1251086 (2014).

14 Guilliams, M. *et al.* Dendritic cells, monocytes and macrophages: a unified nomenclature based on ontogeny. *Nat Rev Immunol* **14**, 571-578, doi:10.1038/nri3712 (2014).

15 Swiecki, M. & Colonna, M. The multifaceted biology of plasmacytoid dendritic cells. *Nat Rev Immunol* **15**, 471-485, doi:10.1038/nri3865 (2015).

16 Shortman, K. & Liu, Y. J. Mouse and human dendritic cell subtypes. *Nat Rev Immunol* **2**, 151-161, doi:10.1038/nri746 (2002).
17 Mogensen, T. H. Pathogen recognition and inflammatory signaling in innate immune defenses. *Clin Microbiol Rev* **22**, 240-273, Table of Contents, doi:10.1128/CMR.00046-08 (2009).
18 Janeway, C. A., Jr. Approaching the asymptote? Evolution and revolution in immunology. *Cold Spring Harb Symp Quant Biol* **54 Pt 1**, 1-13 (1989).
19 Matzinger, P. Tolerance, danger, and the extended family. *Annu Rev Immunol* **12**, 991-1045, doi:10.1146/annurev.iy.12.040194.005015 (1994).
20 Yu, L., Wang, L. & Chen, S. Endogenous toll-like receptor ligands and their biological significance. *J Cell Mol Med* **14**, 2592-2603, doi:10.1111/j.1582-4934.2010.01127.x (2010).
21 Tang, D., Kang, R., Coyne, C. B., Zeh, H. J. & Lotze, M. T. PAMPs and DAMPs: signal 0s that spur autophagy and immunity. *Immunol Rev* **249**, 158-175, doi:10.1111/j.1600-065X.2012.01146.x (2012).
22 Rock, K. L., Reits, E. & Neefjes, J. Present Yourself! By MHC Class I and MHC Class II Molecules. *Trends Immunol* **37**, 724-737, doi:10.1016/j.it.2016.08.010 (2016).
23 Mellman, I. & Steinman, R. M. Dendritic cells: specialized and regulated antigen processing machines. *Cell* **106**, 255-258 (2001).
24 Worbs, T., Hammerschmidt, S. I. & Forster, R. Dendritic cell migration in health and disease. *Nat Rev Immunol* **17**, 30-48, doi:10.1038/nri.2016.116 (2017).
25 Fogel-Petrovic, M., Long, J. A., Knight, D. A., Thompson, P. J. & Upham, J. W. Activated human dendritic cells express inducible cyclo-oxygenase and synthesize prostaglandin E2 but not prostaglandin D2. *Immunol Cell Biol* **82**, 47-54, doi:10.1111/j.1440-1711.2004.01213.x (2004).
26 Kalinski, P., Hilkens, C. M., Snijders, A., Snijdewint, F. G. & Kapsenberg, M. L. Dendritic cells, obtained from peripheral blood precursors in the presence of PGE2, promote Th2 responses. *Adv Exp Med Biol* **417**, 363-367 (1997).
27 Agard, M., Asakrah, S. & Morici, L. A. PGE(2) suppression of innate immunity during mucosal bacterial infection. *Front Cell Infect Microbiol* **3**, 45, doi:10.3389/fcimb.2013.00045 (2013).
28 Kalinski, P., Vieira, P. L., Schuitemaker, J. H., de Jong, E. C. & Kapsenberg, M. L. Prostaglandin E(2) is a selective inducer of interleukin-12 p40 (IL-12p40) production and an inhibitor of bioactive IL-12p70 heterodimer. *Blood* **97**, 3466-3469 (2001).
29 Scandella, E., Men, Y., Gillessen, S., Forster, R. & Groettrup, M. Prostaglandin E2 is a key factor for CCR7 surface expression and migration of monocyte-derived dendritic cells. *Blood* **100**, 1354-1361, doi:10.1182/blood-2001-11-0017 (2002).
30 Scandella, E. *et al.* CCL19/CCL21-triggered signal transduction and migration of dendritic cells requires prostaglandin E2. *Blood* **103**, 1595-1601, doi:10.1182/blood-2003-05-1643 (2004).
31 Muthuswamy, R. *et al.* PGE(2) transiently enhances DC expression of CCR7 but inhibits the ability of DCs to produce CCL19 and attract naive T cells. *Blood* **116**, 1454-1459, doi:10.1182/blood-2009-12-258038 (2010).

32 Luft, T. *et al.* Functionally distinct dendritic cell (DC) populations induced by physiologic stimuli: prostaglandin E(2) regulates the migratory capacity of specific DC subsets. *Blood* **100**, 1362-1372, doi:10.1182/blood-2001-12-0360 (2002).
33 Kalinski, P. Regulation of immune responses by prostaglandin E2. *Journal of immunology* **188**, 21-28, doi:10.4049/jimmunol.1101029 (2012).
34 Yao, C. *et al.* Prostaglandin E2-EP4 signaling promotes immune inflammation through Th1 cell differentiation and Th17 cell expansion. *Nature medicine* **15**, 633-640, doi:10.1038/nm.1968 (2009).
35 Gay, N. J. & Gangloff, M. Structure and function of Toll receptors and their ligands. *Annu Rev Biochem* **76**, 141-165, doi:10.1146/annurev.biochem.76.060305.151318 (2007).
36 Lemaitre, B., Nicolas, E., Michaut, L., Reichhart, J. M. & Hoffmann, J. A. The dorsoventral regulatory gene cassette spatzle/Toll/cactus controls the potent antifungal response in Drosophila adults. *Cell* **86**, 973-983 (1996).
37 Gay, N. J. & Keith, F. J. Drosophila Toll and IL-1 receptor. *Nature* **351**, 355-356, doi:10.1038/351355b0 (1991).
38 Balenga, N. A. & Balenga, N. A. Human TLR11 gene is repressed due to its probable interaction with profilin expressed in human. *Med Hypotheses* **68**, 456, doi:10.1016/j.mehy.2006.07.015 (2007).
39 Akira, S., Uematsu, S. & Takeuchi, O. Pathogen recognition and innate immunity. *Cell* **124**, 783-801, doi:10.1016/j.cell.2006.02.015 (2006).
40 Abreu, M. T. Toll-like receptor signalling in the intestinal epithelium: how bacterial recognition shapes intestinal function. *Nat Rev Immunol* **10**, 131-144, doi:10.1038/nri2707 (2010).
41 O'Neill, L. A., Golenbock, D. & Bowie, A. G. The history of Toll-like receptors - redefining innate immunity. *Nat Rev Immunol* **13**, 453-460, doi:10.1038/nri3446 (2013).
42 Carty, M. *et al.* The human adaptor SARM negatively regulates adaptor protein TRIF-dependent Toll-like receptor signaling. *Nat Immunol* **7**, 1074-1081, doi:10.1038/ni1382 (2006).
43 Ni, M. *et al.* B-cell adaptor for PI3K (BCAP) negatively regulates Toll-like receptor signaling through activation of PI3K. *Proceedings of the National Academy of Sciences of the United States of America* **109**, 267-272, doi:10.1073/pnas.1111957108 (2012).
44 Halabi, S., Sekine, E., Verstak, B., Gay, N. J. & Moncrieffe, M. C. Structure of the Toll/Interleukin-1 Receptor (TIR) Domain of the B-cell Adaptor That Links Phosphoinositide Metabolism with the Negative Regulation of the Toll-like Receptor (TLR) Signalosome. *The Journal of biological chemistry* **292**, 652-660, doi:10.1074/jbc.M116.761528 (2017).
45 Chamaillard, M. *et al.* An essential role for NOD1 in host recognition of bacterial peptidoglycan containing diaminopimelic acid. *Nat Immunol* **4**, 702-707, doi:10.1038/ni945 (2003).
46 Caruso, R., Warner, N., Inohara, N. & Nunez, G. NOD1 and NOD2: signaling, host defense, and inflammatory disease. *Immunity* **41**, 898-908, doi:10.1016/j.immuni.2014.12.010 (2014).
47 Keestra-Gounder, A. M. & Tsolis, R. M. NOD1 and NOD2: Beyond Peptidoglycan Sensing. *Trends Immunol*, doi:10.1016/j.it.2017.07.004 (2017).

48 Zhong, Y., Kinio, A. & Saleh, M. Functions of NOD-Like Receptors in Human Diseases. *Front Immunol* **4**, 333, doi:10.3389/fimmu.2013.00333 (2013).
49 Evavold, C. & Kagan, J. C. How inflammasomes inform adaptive immunity. *Journal of molecular biology*, doi:10.1016/j.jmb.2017.09.019 (2017).
50 Reikine, S., Nguyen, J. B. & Modis, Y. Pattern Recognition and Signaling Mechanisms of RIG-I and MDA5. *Front Immunol* **5**, 342, doi:10.3389/fimmu.2014.00342 (2014).
51 Geijtenbeek, T. B. & Gringhuis, S. I. Signalling through C-type lectin receptors: shaping immune responses. *Nat Rev Immunol* **9**, 465-479, doi:10.1038/nri2569 (2009).
52 Tukhvatulin, A. I. *et al.* Combined stimulation of Toll-like receptor 5 and NOD1 strongly potentiates activity of NF-kappaB, resulting in enhanced innate immune reactions and resistance to Salmonella enterica serovar Typhimurium infection. *Infect Immun* **81**, 3855-3864, doi:10.1128/IAI.00525-13 (2013).
53 Kim, Y. G. *et al.* The cytosolic sensors Nod1 and Nod2 are critical for bacterial recognition and host defense after exposure to Toll-like receptor ligands. *Immunity* **28**, 246-257, doi:10.1016/j.immuni.2007.12.012 (2008).
54 van Heel, D. A. *et al.* Synergy between TLR9 and NOD2 innate immune responses is lost in genetic Crohn's disease. *Gut* **54**, 1553-1557, doi:10.1136/gut.2005.065888 (2005).
55 Netea, M. G. *et al.* Nucleotide-binding oligomerization domain-2 modulates specific TLR pathways for the induction of cytokine release. *Journal of immunology* **174**, 6518-6523 (2005).
56 Borm, M. E., van Bodegraven, A. A., Mulder, C. J., Kraal, G. & Bouma, G. The effect of NOD2 activation on TLR2-mediated cytokine responses is dependent on activation dose and NOD2 genotype. *Genes Immun* **9**, 274-278, doi:10.1038/gene.2008.9 (2008).
57 van Heel, D. A. *et al.* Muramyl dipeptide and toll-like receptor sensitivity in NOD2-associated Crohn's disease. *Lancet* **365**, 1794-1796, doi:10.1016/S0140-6736(05)66582-8 (2005).
58 van Heel, D. A. *et al.* Synergistic enhancement of Toll-like receptor responses by NOD1 activation. *Eur J Immunol* **35**, 2471-2476, doi:10.1002/eji.200526296 (2005).
59 Honda, K. *et al.* Role of a transductional-transcriptional processor complex involving MyD88 and IRF-7 in Toll-like receptor signaling. *Proceedings of the National Academy of Sciences of the United States of America* **101**, 15416-15421, doi:10.1073/pnas.0406933101 (2004).
60 Cusson-Hermance, N., Khurana, S., Lee, T. H., Fitzgerald, K. A. & Kelliher, M. A. Rip1 mediates the Trif-dependent toll-like receptor 3- and 4-induced NF-{kappa}B activation but does not contribute to interferon regulatory factor 3 activation. *The Journal of biological chemistry* **280**, 36560-36566, doi:10.1074/jbc.M506831200 (2005).
61 Molodecky, N. A. *et al.* Increasing incidence and prevalence of the inflammatory bowel diseases with time, based on systematic review. *Gastroenterology* **142**, 46-54 e42; quiz e30, doi:10.1053/j.gastro.2011.10.001 (2012).

62 Jess, T. *et al.* Changes in clinical characteristics, course, and prognosis of inflammatory bowel disease during the last 5 decades: a population-based study from Copenhagen, Denmark. *Inflammatory bowel diseases* **13**, 481-489, doi:10.1002/ibd.20036 (2007).
63 Loftus, C. G. *et al.* Update on the incidence and prevalence of Crohn's disease and ulcerative colitis in Olmsted County, Minnesota, 1940-2000. *Inflammatory bowel diseases* **13**, 254-261, doi:10.1002/ibd.20029 (2007).
64 Ahuja, V. & Tandon, R. K. Inflammatory bowel disease in the Asia-Pacific area: a comparison with developed countries and regional differences. *J Dig Dis* **11**, 134-147, doi:10.1111/j.1751-2980.2010.00429.x (2010).
65 Ananthakrishnan, A. N. Epidemiology and risk factors for IBD. *Nat Rev Gastroenterol Hepatol* **12**, 205-217, doi:10.1038/nrgastro.2015.34 (2015).
66 Jostins, L. *et al.* Host-microbe interactions have shaped the genetic architecture of inflammatory bowel disease. *Nature* **491**, 119-124, doi:10.1038/nature11582 (2012).
67 Liu, J. Z. *et al.* Association analyses identify 38 susceptibility loci for inflammatory bowel disease and highlight shared genetic risk across populations. *Nat Genet* **47**, 979-986, doi:10.1038/ng.3359 (2015).
68 Huang, H. *et al.* Fine-mapping inflammatory bowel disease loci to single-variant resolution. *Nature* **547**, 173-178, doi:10.1038/nature22969 (2017).
69 Khor, B., Gardet, A. & Xavier, R. J. Genetics and pathogenesis of inflammatory bowel disease. *Nature* **474**, 307-317, doi:10.1038/nature10209 (2011).
70 Van Limbergen, J., Radford-Smith, G. & Satsangi, J. Advances in IBD genetics. *Nat Rev Gastroenterol Hepatol* **11**, 372-385, doi:10.1038/nrgastro.2014.27 (2014).
71 Abraham, C. & Cho, J. H. Inflammatory bowel disease. *N Engl J Med* **361**, 2066-2078, doi:10.1056/NEJMra0804647 (2009).
72 de Souza, H. S. & Fiocchi, C. Immunopathogenesis of IBD: current state of the art. *Nat Rev Gastroenterol Hepatol* **13**, 13-27, doi:10.1038/nrgastro.2015.186 (2016).
73 Lee, J. C. *et al.* Genome-wide association study identifies distinct genetic contributions to prognosis and susceptibility in Crohn's disease. *Nat Genet* **49**, 262-268, doi:10.1038/ng.3755 (2017).
74 Hugot, J. P. *et al.* Association of NOD2 leucine-rich repeat variants with susceptibility to Crohn's disease. *Nature* **411**, 599-603, doi:10.1038/35079107 (2001).
75 Ogura, Y. *et al.* A frameshift mutation in NOD2 associated with susceptibility to Crohn's disease. *Nature* **411**, 603-606, doi:10.1038/35079114 (2001).
76 Lesage, S. *et al.* CARD15/NOD2 mutational analysis and genotype-phenotype correlation in 612 patients with inflammatory bowel disease. *Am J Hum Genet* **70**, 845-857, doi:10.1086/339432 (2002).
77 Linde, K. *et al.* Card15 and Crohn's disease: healthy homozygous carriers of the 3020insC frameshift mutation. *The American journal of gastroenterology* **98**, 613-617 (2003).

78 Hampe, J. *et al.* Association between insertion mutation in NOD2 gene and Crohn's disease in German and British populations. *Lancet* **357**, 1925-1928, doi:10.1016/S0140-6736(00)05063-7 (2001).
79 Gutierrez, O. *et al.* Induction of Nod2 in myelomonocytic and intestinal epithelial cells via nuclear factor-kappa B activation. *J Biol Chem* **277**, 41701-41705, doi:10.1074/jbc.M206473200 (2002).
80 Hisamatsu, T. *et al.* CARD15/NOD2 functions as an antibacterial factor in human intestinal epithelial cells. *Gastroenterology* **124**, 993-1000, doi:10.1053/gast.2003.50153 (2003).
81 Maeda, S. *et al.* Nod2 mutation in Crohn's disease potentiates NF-kappaB activity and IL-1beta processing. *Science* **307**, 734-738, doi:10.1126/science.1103685 (2005).
82 Yamamoto, S. & Ma, X. Role of Nod2 in the development of Crohn's disease. *Microbes Infect* **11**, 912-918, doi:10.1016/j.micinf.2009.06.005 (2009).
83 Cooney, R. *et al.* NOD2 stimulation induces autophagy in dendritic cells influencing bacterial handling and antigen presentation. *Nature medicine* **16**, 90-97, doi:10.1038/nm.2069 (2010).
84 Brain, O. *et al.* The intracellular sensor NOD2 induces microRNA-29 expression in human dendritic cells to limit IL-23 release. *Immunity* **39**, 521-536, doi:10.1016/j.immuni.2013.08.035 (2013).
85 Kramer, M., Netea, M. G., de Jong, D. J., Kullberg, B. J. & Adema, G. J. Impaired dendritic cell function in Crohn's disease patients with NOD2 3020insC mutation. *Journal of leukocyte biology* **79**, 860-866, doi:10.1189/jlb.0805484 (2006).
86 Trinchieri, G. & Sher, A. Cooperation of Toll-like receptor signals in innate immune defence. *Nat Rev Immunol* **7**, 179-190, doi:10.1038/nri2038 (2007).
87 Netea, M. G. *et al.* NOD2 mediates anti-inflammatory signals induced by TLR2 ligands: implications for Crohn's disease. *Eur J Immunol* **34**, 2052-2059, doi:10.1002/eji.200425229 (2004).
88 Butler, M., Chaudhary, R., van Heel, D. A., Playford, R. J. & Ghosh, S. NOD2 activity modulates the phenotype of LPS-stimulated dendritic cells to promote the development of T-helper type 2-like lymphocytes - Possible implications for NOD2-associated Crohn's disease. *J Crohns Colitis* **1**, 106-115, doi:10.1016/j.crohns.2007.08.006 (2007).
89 Watanabe, T. *et al.* Muramyl dipeptide activation of nucleotide-binding oligomerization domain 2 protects mice from experimental colitis. *J Clin Invest* **118**, 545-559, doi:10.1172/JCI33145 (2008).
90 Clendinning, J. Observations on the medicinal properties of the Cannabis Sativa of India. *Med Chir Trans* **26**, 188-210 (1843).
91 Gaoni, Y. & Mechoulam, R. Isolation, Structure, and Partial Synthesis of an Active Constituent of Hashish. *Journal of the American Chemical Society* **86**, 1646-+, doi:DOI 10.1021/ja01062a046 (1964).
92 Mechoulam, R., Hanus, L. O., Pertwee, R. & Howlett, A. C. Early phytocannabinoid chemistry to endocannabinoids and beyond. *Nature reviews. Neuroscience* **15**, 757-764, doi:10.1038/nrn3811 (2014).
93 Gerard, C., Mollereau, C., Vassart, G. & Parmentier, M. Nucleotide sequence of a human cannabinoid receptor cDNA. *Nucleic Acids Res* **18**, 7142 (1990).

94 Matsuda, L. A., Lolait, S. J., Brownstein, M. J., Young, A. C. & Bonner, T. I. Structure of a cannabinoid receptor and functional expression of the cloned cDNA. *Nature* **346**, 561-564, doi:10.1038/346561a0 (1990).
95 Herkenham, M. *et al.* Cannabinoid receptor localization in brain. *Proceedings of the National Academy of Sciences of the United States of America* **87**, 1932-1936 (1990).
96 Bouaboula, M. *et al.* Cannabinoid-receptor expression in human leukocytes. *Eur J Biochem* **214**, 173-180 (1993).
97 Galiegue, S. *et al.* Expression of central and peripheral cannabinoid receptors in human immune tissues and leukocyte subpopulations. *Eur J Biochem* **232**, 54-61 (1995).
98 Daaka, Y., Friedman, H. & Klein, T. W. Cannabinoid receptor proteins are increased in Jurkat, human T-cell line after mitogen activation. *The Journal of pharmacology and experimental therapeutics* **276**, 776-783 (1996).
99 Sugamura, K. *et al.* Activated endocannabinoid system in coronary artery disease and antiinflammatory effects of cannabinoid 1 receptor blockade on macrophages. *Circulation* **119**, 28-36, doi:10.1161/CIRCULATIONAHA.108.811992 (2009).
100 Krishnan, G. & Chatterjee, N. Endocannabinoids alleviate proinflammatory conditions by modulating innate immune response in muller glia during inflammation. *Glia* **60**, 1629-1645, doi:10.1002/glia.22380 (2012).
101 de Campos-Carli, S. M. *et al.* Cannabinoid receptors on peripheral leukocytes from patients with schizophrenia: Evidence for defective immunomodulatory mechanisms. *J Psychiatr Res* **87**, 44-52, doi:10.1016/j.jpsychires.2016.12.001 (2017).
102 Buchholz, H. G. *et al.* Whole-body biodistribution of the cannabinoid type 1 receptor ligand [18F]MK-9470 in the rat. *Nucl Med Biol* **52**, 63-69, doi:10.1016/j.nucmedbio.2017.06.003 (2017).
103 Martin-Fontecha, M. *et al.* A fluorescent probe to unravel functional features of cannabinoid receptor CB1 in human blood and tonsil immune system cells. *Bioconjug Chem*, doi:10.1021/acs.bioconjchem.7b00680 (2018).
104 Munro, S., Thomas, K. L. & Abu-Shaar, M. Molecular characterization of a peripheral receptor for cannabinoids. *Nature* **365**, 61-65, doi:10.1038/365061a0 (1993).
105 Graham, E. S., Angel, C. E., Schwarcz, L. E., Dunbar, P. R. & Glass, M. Detailed characterisation of CB2 receptor protein expression in peripheral blood immune cells from healthy human volunteers using flow cytometry. *Int J Immunopathol Pharmacol* **23**, 25-34, doi:10.1177/039463201002300103 (2010).
106 Castaneda, J. T., Harui, A., Kiertscher, S. M., Roth, J. D. & Roth, M. D. Differential expression of intracellular and extracellular CB(2) cannabinoid receptor protein by human peripheral blood leukocytes. *Journal of neuroimmune pharmacology : the official journal of the Society on NeuroImmune Pharmacology* **8**, 323-332, doi:10.1007/s11481-012-9430-8 (2013).
107 Castaneda, J. T., Harui, A. & Roth, M. D. Regulation of Cell Surface CB2 Receptor during Human B Cell Activation and Differentiation. *Journal of neuroimmune pharmacology : the official journal of the Society on*

NeuroImmune Pharmacology **12**, 544-554, doi:10.1007/s11481-017-9744-7 (2017).
108 Carlisle, S. J., Marciano-Cabral, F., Staab, A., Ludwick, C. & Cabral, G. A. Differential expression of the CB2 cannabinoid receptor by rodent macrophages and macrophage-like cells in relation to cell activation. *Int Immunopharmacol* **2**, 69-82 (2002).
109 Onaivi, E. S. *et al.* Expression of cannabinoid receptors and their gene transcripts in human blood cells. *Prog Neuropsychopharmacol Biol Psychiatry* **23**, 1063-1077 (1999).
110 Hua, T. *et al.* Crystal Structure of the Human Cannabinoid Receptor CB1. *Cell* **167**, 750-762 e714, doi:10.1016/j.cell.2016.10.004 (2016).
111 Shao, Z. *et al.* High-resolution crystal structure of the human CB1 cannabinoid receptor. *Nature*, doi:10.1038/nature20613 (2016).
112 Hua, T. *et al.* Crystal structures of agonist-bound human cannabinoid receptor CB1. *Nature* **547**, 468-471, doi:10.1038/nature23272 (2017).
113 Rosenbaum, D. M., Rasmussen, S. G. & Kobilka, B. K. The structure and function of G-protein-coupled receptors. *Nature* **459**, 356-363, doi:10.1038/nature08144 (2009).
114 Thomsen, A. R. *et al.* GPCR-G Protein-beta-Arrestin Super-Complex Mediates Sustained G Protein Signaling. *Cell* **166**, 907-919, doi:10.1016/j.cell.2016.07.004 (2016).
115 Mascia, F. *et al.* CRIP1a inhibits endocytosis of G-protein coupled receptors activated by endocannabinoids and glutamate by a common molecular mechanism. *J Neurochem*, doi:10.1111/jnc.14021 (2017).
116 Pierce, K. L., Premont, R. T. & Lefkowitz, R. J. Seven-transmembrane receptors. *Nat Rev Mol Cell Biol* **3**, 639-650, doi:10.1038/nrm908 (2002).
117 Luttrell, L. M. & Lefkowitz, R. J. The role of beta-arrestins in the termination and transduction of G-protein-coupled receptor signals. *J Cell Sci* **115**, 455-465 (2002).
118 Violin, J. D., Crombie, A. L., Soergel, D. G. & Lark, M. W. Biased ligands at G-protein-coupled receptors: promise and progress. *Trends in pharmacological sciences* **35**, 308-316, doi:10.1016/j.tips.2014.04.007 (2014).
119 Soethoudt, M., van Gils, N., van der Stelt, M. & Heitman, L. H. Protocol to Study beta-Arrestin Recruitment by CB1 and CB2 Cannabinoid Receptors. *Methods Mol Biol* **1412**, 103-111, doi:10.1007/978-1-4939-3539-0_11 (2016).
120 Delgado-Peraza, F. *et al.* Mechanisms of Biased beta-Arrestin-Mediated Signaling Downstream from the Cannabinoid 1 Receptor. *Molecular pharmacology* **89**, 618-629, doi:10.1124/mol.115.103176 (2016).
121 Soethoudt, M. *et al.* Cannabinoid CB2 receptor ligand profiling reveals biased signalling and off-target activity. *Nat Commun* **8**, 13958, doi:10.1038/ncomms13958 (2017).
122 Console-Bram, L., Brailoiu, E., Brailoiu, G. C., Sharir, H. & Abood, M. E. Activation of GPR18 by cannabinoid compounds: a tale of biased agonism. *British journal of pharmacology* **171**, 3908-3917, doi:10.1111/bph.12746 (2014).

123 Ryberg, E. *et al.* The orphan receptor GPR55 is a novel cannabinoid receptor. *British journal of pharmacology* **152**, 1092-1101, doi:10.1038/sj.bjp.0707460 (2007).
124 Hansen, K. B. *et al.* 2-Oleoyl glycerol is a GPR119 agonist and signals GLP-1 release in humans. *J Clin Endocrinol Metab* **96**, E1409-1417, doi:10.1210/jc.2011-0647 (2011).
125 De Petrocellis, L. *et al.* Effects of cannabinoids and cannabinoid-enriched Cannabis extracts on TRP channels and endocannabinoid metabolic enzymes. *British journal of pharmacology* **163**, 1479-1494, doi:10.1111/j.1476-5381.2010.01166.x (2011).
126 Pertwee, R. G. *et al.* International Union of Basic and Clinical Pharmacology. LXXIX. Cannabinoid receptors and their ligands: beyond CB(1) and CB(2). *Pharmacological reviews* **62**, 588-631, doi:10.1124/pr.110.003004 (2010).
127 Howlett, A. C. *et al.* International Union of Pharmacology. XXVII. Classification of cannabinoid receptors. *Pharmacological reviews* **54**, 161-202 (2002).
128 Borner, C., Smida, M., Hollt, V., Schraven, B. & Kraus, J. Cannabinoid receptor type 1- and 2-mediated increase in cyclic AMP inhibits T cell receptor-triggered signaling. *The Journal of biological chemistry* **284**, 35450-35460, doi:10.1074/jbc.M109.006338 (2009).
129 Turcotte, C., Blanchet, M. R., Laviolette, M. & Flamand, N. The CB2 receptor and its role as a regulator of inflammation. *Cell Mol Life Sci* **73**, 4449-4470, doi:10.1007/s00018-016-2300-4 (2016).
130 Sugiura, T. *et al.* 2-Arachidonoylglycerol, a putative endogenous cannabinoid receptor ligand, induces rapid, transient elevation of intracellular free Ca2+ in neuroblastoma x glioma hybrid NG108-15 cells. *Biochem Biophys Res Commun* **229**, 58-64, doi:10.1006/bbrc.1996.1757 (1996).
131 Turu, G. & Hunyady, L. Signal transduction of the CB1 cannabinoid receptor. *J Mol Endocrinol* **44**, 75-85, doi:10.1677/JME-08-0190 (2010).
132 Malfitano, A. M., Basu, S., Maresz, K., Bifulco, M. & Dittel, B. N. What we know and do not know about the cannabinoid receptor 2 (CB2). *Semin Immunol* **26**, 369-379, doi:10.1016/j.smim.2014.04.002 (2014).
133 Basu, S. & Dittel, B. N. Unraveling the complexities of cannabinoid receptor 2 (CB2) immune regulation in health and disease. *Immunol Res* **51**, 26-38, doi:10.1007/s12026-011-8210-5 (2011).
134 Herrera, B., Carracedo, A., Diez-Zaera, M., Guzman, M. & Velasco, G. p38 MAPK is involved in CB2 receptor-induced apoptosis of human leukaemia cells. *FEBS Lett* **579**, 5084-5088, doi:10.1016/j.febslet.2005.08.021 (2005).
135 Prather, P. L. in *Cannabinoids and the Brain* (ed Attila Köfalvi) 75-90 (Springer US, 2008).
136 Nithipatikom, K. *et al.* Cannabinoid receptor type 1 (CB1) activation inhibits small GTPase RhoA activity and regulates motility of prostate carcinoma cells. *Endocrinology* **153**, 29-41, doi:10.1210/en.2011-1144 (2012).
137 Devane, W. A. *et al.* Isolation and structure of a brain constituent that binds to the cannabinoid receptor. *Science* **258**, 1946-1949 (1992).

138 Mechoulam, R. *et al.* Identification of an endogenous 2-monoglyceride, present in canine gut, that binds to cannabinoid receptors. *Biochem Pharmacol* **50**, 83-90 (1995).
139 Sugiura, T. *et al.* 2-Arachidonoylglycerol: a possible endogenous cannabinoid receptor ligand in brain. *Biochem Biophys Res Commun* **215**, 89-97 (1995).
140 Rodriguez de Fonseca, F. *et al.* The endocannabinoid system: physiology and pharmacology. *Alcohol Alcohol* **40**, 2-14, doi:10.1093/alcalc/agh110 (2005).
141 Ben-Shabat, S. *et al.* An entourage effect: inactive endogenous fatty acid glycerol esters enhance 2-arachidonoyl-glycerol cannabinoid activity. *Eur J Pharmacol* **353**, 23-31 (1998).
142 Murataeva, N. *et al.* Where's my entourage? The curious case of 2-oleoylglycerol, 2-linolenoylglycerol, and 2-palmitoylglycerol. *Pharmacol Res* **110**, 173-180, doi:10.1016/j.phrs.2016.04.015 (2016).
143 Lambert, D. M. & Di Marzo, V. The palmitoylethanolamide and oleamide enigmas : are these two fatty acid amides cannabimimetic? *Curr Med Chem* **6**, 757-773 (1999).
144 Cohen, L. J. *et al.* Commensal bacteria make GPCR ligands that mimic human signalling molecules. *Nature* **549**, 48-53, doi:10.1038/nature23874 (2017).
145 Di Marzo, V., Stella, N. & Zimmer, A. Endocannabinoid signalling and the deteriorating brain. *Nature reviews. Neuroscience* **16**, 30-42, doi:10.1038/nrn3876 (2015).
146 Yates, M. L. & Barker, E. L. Inactivation and biotransformation of the endogenous cannabinoids anandamide and 2-arachidonoylglycerol. *Molecular pharmacology* **76**, 11-17, doi:10.1124/mol.109.055251 (2009).
147 Rouzer, C. A. & Marnett, L. J. Endocannabinoid oxygenation by cyclooxygenases, lipoxygenases, and cytochromes P450: cross-talk between the eicosanoid and endocannabinoid signaling pathways. *Chemical reviews* **111**, 5899-5921, doi:10.1021/cr2002799 (2011).
148 Zelasko, S., Arnold, W. R. & Das, A. Endocannabinoid metabolism by cytochrome P450 monooxygenases. *Prostaglandins Other Lipid Mediat* **116-117**, 112-123, doi:10.1016/j.prostaglandins.2014.11.002 (2015).
149 Tornqvist, H. & Belfrage, P. Purification and some properties of a monoacylglycerol-hydrolyzing enzyme of rat adipose tissue. *The Journal of biological chemistry* **251**, 813-819 (1976).
150 Dinh, T. P. *et al.* Brain monoglyceride lipase participating in endocannabinoid inactivation. *Proceedings of the National Academy of Sciences of the United States of America* **99**, 10819-10824, doi:10.1073/pnas.152334899 (2002).
151 Blankman, J. L., Simon, G. M. & Cravatt, B. F. A comprehensive profile of brain enzymes that hydrolyze the endocannabinoid 2-arachidonoylglycerol. *Chem Biol* **14**, 1347-1356, doi:10.1016/j.chembiol.2007.11.006 (2007).
152 Cravatt, B. F. *et al.* Molecular characterization of an enzyme that degrades neuromodulatory fatty-acid amides. *Nature* **384**, 83-87, doi:10.1038/384083a0 (1996).

153 Wang, R. *et al.* Identification of palmitoyl protein thioesterase 1 in human THP1 monocytes and macrophages and characterization of unique biochemical activities for this enzyme. *Biochemistry* **52**, 7559-7574, doi:10.1021/bi401138s (2013).
154 Nomura, D. K. *et al.* Endocannabinoid hydrolysis generates brain prostaglandins that promote neuroinflammation. *Science* **334**, 809-813, doi:10.1126/science.1209200 (2011).
155 Savinainen, J. R. *et al.* Robust hydrolysis of prostaglandin glycerol esters by human monoacylglycerol lipase (MAGL). *Molecular pharmacology* **86**, 522-535, doi:10.1124/mol.114.094284 (2014).
156 Kupiecki, F. P. Partial purification of monoglyceride lipase from adipose tissue. *J Lipid Res* **7**, 230-235 (1966).
157 Karlsson, M., Contreras, J. A., Hellman, U., Tornqvist, H. & Holm, C. cDNA cloning, tissue distribution, and identification of the catalytic triad of monoglyceride lipase. Evolutionary relationship to esterases, lysophospholipases, and haloperoxidases. *The Journal of biological chemistry* **272**, 27218-27223 (1997).
158 Labar, G., Wouters, J. & Lambert, D. M. A review on the monoacylglycerol lipase: at the interface between fat and endocannabinoid signalling. *Curr Med Chem* **17**, 2588-2607 (2010).
159 Zvonok, N. *et al.* Full mass spectrometric characterization of human monoacylglycerol lipase generated by large-scale expression and single-step purification. *J Proteome Res* **7**, 2158-2164, doi:10.1021/pr700839z (2008).
160 Labar, G. *et al.* Crystal structure of the human monoacylglycerol lipase, a key actor in endocannabinoid signaling. *Chembiochem* **11**, 218-227, doi:10.1002/cbic.200900621 (2010).
161 Zvonok, N. *et al.* Covalent inhibitors of human monoacylglycerol lipase: ligand-assisted characterization of the catalytic site by mass spectrometry and mutational analysis. *Chem Biol* **15**, 854-862, doi:10.1016/j.chembiol.2008.06.008 (2008).
162 Schalk-Hihi, C. *et al.* Crystal structure of a soluble form of human monoglyceride lipase in complex with an inhibitor at 1.35 A resolution. *Protein Sci* **20**, 670-683, doi:10.1002/pro.596 (2011).
163 Karageorgos, I. *et al.* The role of human monoacylglycerol lipase (hMAGL) binding pocket in breakup of unsaturated phospholipid membranes. *Anal Biochem* **536**, 90-95, doi:10.1016/j.ab.2017.08.009 (2017).
164 Ghafouri, N. *et al.* Inhibition of monoacylglycerol lipase and fatty acid amide hydrolase by analogues of 2-arachidonoylglycerol. *British journal of pharmacology* **143**, 774-784, doi:10.1038/sj.bjp.0705948 (2004).
165 Vandevoorde, S. *et al.* Influence of the degree of unsaturation of the acyl side chain upon the interaction of analogues of 1-arachidonoylglycerol with monoacylglycerol lipase and fatty acid amide hydrolase. *Biochem Biophys Res Commun* **337**, 104-109, doi:10.1016/j.bbrc.2005.09.015 (2005).
166 Dinh, T. P., Freund, T. F. & Piomelli, D. A role for monoglyceride lipase in 2-arachidonoylglycerol inactivation. *Chem Phys Lipids* **121**, 149-158 (2002).

167 Nomura, D. K. *et al.* Monoacylglycerol lipase exerts dual control over endocannabinoid and fatty acid pathways to support prostate cancer. *Chem Biol* **18**, 846-856, doi:10.1016/j.chembiol.2011.05.009 (2011).
168 Baba, Y. *et al.* Expression of monoacylglycerol lipase as a marker of tumour invasion and progression in malignant melanoma. *J Eur Acad Dermatol Venereol*, doi:10.1111/jdv.14455 (2017).
169 Nomura, D. K. *et al.* Monoacylglycerol lipase regulates a fatty acid network that promotes cancer pathogenesis. *Cell* **140**, 49-61, doi:10.1016/j.cell.2009.11.027 (2010).
170 Zhang, J. *et al.* Monoacylglycerol Lipase: A Novel Potential Therapeutic Target and Prognostic Indicator for Hepatocellular Carcinoma. *Sci Rep* **6**, 35784, doi:10.1038/srep35784 (2016).
171 Sun, H. *et al.* Potential tumor-suppressive role of monoglyceride lipase in human colorectal cancer. *Oncogene* **32**, 234-241, doi:10.1038/onc.2012.34 (2013).
172 Ye, L. *et al.* Monoacylglycerol lipase (MAGL) knockdown inhibits tumor cells growth in colorectal cancer. *Cancer Lett* **307**, 6-17, doi:10.1016/j.canlet.2011.03.007 (2011).
173 Ahamed, M. *et al.* Synthesis and preclinical evaluation of [11C]MA-PB-1 for in vivo imaging of brain monoacylglycerol lipase (MAGL). *Eur J Med Chem* **136**, 104-113, doi:10.1016/j.ejmech.2017.04.066 (2017).
174 Hauser, A. S. *et al.* Pharmacogenomics of GPCR Drug Targets. *Cell*, doi:10.1016/j.cell.2017.11.033 (2017).
175 Scalvini, L., Piomelli, D. & Mor, M. Monoglyceride lipase: Structure and inhibitors. *Chem Phys Lipids* **197**, 13-24, doi:10.1016/j.chemphyslip.2015.07.011 (2016).
176 Hohmann, A. G. *et al.* An endocannabinoid mechanism for stress-induced analgesia. *Nature* **435**, 1108-1112, doi:10.1038/nature03658 (2005).
177 Long, J. Z. *et al.* Selective blockade of 2-arachidonoylglycerol hydrolysis produces cannabinoid behavioral effects. *Nat Chem Biol* **5**, 37-44, doi:10.1038/nchembio.129 (2009).
178 Laitinen, T. *et al.* Mutation of Cys242 of human monoacylglycerol lipase disrupts balanced hydrolysis of 1- and 2-monoacylglycerols and selectively impairs inhibitor potency. *Molecular pharmacology* **85**, 510-519, doi:10.1124/mol.113.090795 (2014).
179 Long, J. Z., Nomura, D. K. & Cravatt, B. F. Characterization of monoacylglycerol lipase inhibition reveals differences in central and peripheral endocannabinoid metabolism. *Chem Biol* **16**, 744-753, doi:10.1016/j.chembiol.2009.05.009 (2009).
180 Niphakis, M. J. *et al.* Evaluation of NHS carbamates as a potent and selective class of endocannabinoid hydrolase inhibitors. *ACS Chem Neurosci* **4**, 1322-1332, doi:10.1021/cn400116z (2013).
181 Schlosburg, J. E. *et al.* Chronic monoacylglycerol lipase blockade causes functional antagonism of the endocannabinoid system. *Nature neuroscience* **13**, 1113-1119, doi:10.1038/nn.2616 (2010).
182 Chanda, P. K. *et al.* Monoacylglycerol lipase activity is a critical modulator of the tone and integrity of the endocannabinoid system. *Molecular pharmacology* **78**, 996-1003, doi:10.1124/mol.110.068304 (2010).

183 Kinsey, S. G. *et al.* Inhibition of monoacylglycerol lipase attenuates nonsteroidal anti-inflammatory drug-induced gastric hemorrhages in mice. *The Journal of pharmacology and experimental therapeutics* **338**, 795-802, doi:10.1124/jpet.110.175778 (2011).
184 Kinsey, S. G. *et al.* Repeated low-dose administration of the monoacylglycerol lipase inhibitor JZL184 retains cannabinoid receptor type 1-mediated antinociceptive and gastroprotective effects. *The Journal of pharmacology and experimental therapeutics* **345**, 492-501, doi:10.1124/jpet.112.201426 (2013).
185 Ghosh, S. *et al.* The monoacylglycerol lipase inhibitor JZL184 suppresses inflammatory pain in the mouse carrageenan model. *Life Sci* **92**, 498-505, doi:10.1016/j.lfs.2012.06.020 (2013).
186 Ignatowska-Jankowska, B. M. *et al.* In vivo characterization of the highly selective monoacylglycerol lipase inhibitor KML29: antinociceptive activity without cannabimimetic side effects. *British journal of pharmacology* **171**, 1392-1407, doi:10.1111/bph.12298 (2014).
187 Schlosburg, J. E. *et al.* Prolonged monoacylglycerol lipase blockade causes equivalent cannabinoid receptor type 1 receptor-mediated adaptations in fatty acid amide hydrolase wild-type and knockout mice. *The Journal of pharmacology and experimental therapeutics* **350**, 196-204, doi:10.1124/jpet.114.212753 (2014).
188 Vujic, N. *et al.* Monoglyceride lipase deficiency modulates endocannabinoid signaling and improves plaque stability in ApoE-knockout mice. *Atherosclerosis* **244**, 9-21, doi:10.1016/j.atherosclerosis.2015.10.109 (2015).
189 Ahn, K., Johnson, D. S. & Cravatt, B. F. Fatty acid amide hydrolase as a potential therapeutic target for the treatment of pain and CNS disorders. *Expert Opin Drug Discov* **4**, 763-784, doi:10.1517/17460440903018857 (2009).
190 Ghosh, S. *et al.* Full FAAH inhibition combined with partial monoacylglycerol lipase inhibition: Augmented and sustained antinociceptive effects with negligible cannabimimetic side effects in mice. *The Journal of pharmacology and experimental therapeutics*, doi:10.1124/jpet.115.222851 (2015).
191 Adamson Barnes, N. S., Mitchell, V. A., Kazantzis, N. P. & Vaughan, C. W. Actions of the dual FAAH/MAGL inhibitor JZL195 in a murine neuropathic pain model. *British journal of pharmacology* **173**, 77-87, doi:10.1111/bph.13337 (2016).
192 Viader, A. *et al.* Metabolic Interplay between Astrocytes and Neurons Regulates Endocannabinoid Action. *Cell reports* **12**, 798-808, doi:10.1016/j.celrep.2015.06.075 (2015).
193 Chen, Y. *et al.* Neuronal and Astrocytic Monoacylglycerol Lipase Limit the Spread of Endocannabinoid Signaling in the Cerebellum. *eNeuro* **3**, doi:10.1523/ENEURO.0048-16.2016 (2016).
194 Grabner, G. F. *et al.* Deletion of Monoglyceride Lipase in Astrocytes Attenuates Lipopolysaccharide-induced Neuroinflammation. *The Journal of biological chemistry* **291**, 913-923, doi:10.1074/jbc.M115.683615 (2016).

195 Chiurchiu, V. *et al.* Detailed characterization of the endocannabinoid system in human macrophages and foam cells, and anti-inflammatory role of type-2 cannabinoid receptor. *Atherosclerosis* **233**, 55-63, doi:10.1016/j.atherosclerosis.2013.12.042 (2014).
196 Borner, C., Hollt, V., Sebald, W. & Kraus, J. Transcriptional regulation of the cannabinoid receptor type 1 gene in T cells by cannabinoids. *Journal of leukocyte biology* **81**, 336-343, doi:10.1189/jlb.0306224 (2007).
197 Matthews, A. T. *et al.* Oxyradical stress increases the biosynthesis of 2-arachidonoylglycerol: involvement of NADPH oxidase. *Am J Physiol Cell Physiol* **311**, C960-C974, doi:10.1152/ajpcell.00251.2015 (2016).
198 Dotsey, E. *et al.* Transient Cannabinoid Receptor 2 Blockade during Immunization Heightens Intensity and Breadth of Antigen-specific Antibody Responses in Young and Aged mice. *Sci Rep* **7**, 42584, doi:10.1038/srep42584 (2017).
199 Staiano, R. I. *et al.* Human lung-resident macrophages express CB1 and CB2 receptors whose activation inhibits the release of angiogenic and lymphangiogenic factors. *Journal of leukocyte biology* **99**, 531-540, doi:10.1189/jlb.3HI1214-584R (2016).
200 Sido, J. M., Nagarkatti, P. S. & Nagarkatti, M. Production of endocannabinoids by activated T cells and B cells modulates inflammation associated with delayed-type hypersensitivity. *Eur J Immunol* **46**, 1472-1479, doi:10.1002/eji.201546181 (2016).
201 Matias, I. *et al.* Presence and regulation of the endocannabinoid system in human dendritic cells. *European Journal of Biochemistry* **269**, 3771-3778, doi:10.1046/j.1432-1033.2002.03078.x (2002).
202 Liu, J. *et al.* Lipopolysaccharide induces anandamide synthesis in macrophages via CD14/MAPK/phosphoinositide 3-kinase/NF-kappaB independently of platelet-activating factor. *The Journal of biological chemistry* **278**, 45034-45039, doi:10.1074/jbc.M306062200 (2003).
203 Maestroni, G. J. The endogenous cannabinoid 2-arachidonoyl glycerol as in vivo chemoattractant for dendritic cells and adjuvant for Th1 response to a soluble protein. *FASEB journal : official publication of the Federation of American Societies for Experimental Biology* **18**, 1914-1916, doi:10.1096/fj.04-2190fje (2004).
204 Jorda, M. A. *et al.* Hematopoietic cells expressing the peripheral cannabinoid receptor migrate in response to the endocannabinoid 2-arachidonoylglycerol. *Blood* **99**, 2786-2793 (2002).
205 Kishimoto, S. *et al.* 2-arachidonoylglycerol induces the migration of HL-60 cells differentiated into macrophage-like cells and human peripheral blood monocytes through the cannabinoid CB2 receptor-dependent mechanism. *The Journal of biological chemistry* **278**, 24469-24475, doi:10.1074/jbc.M301359200 (2003).
206 Kurihara, R. *et al.* Effects of peripheral cannabinoid receptor ligands on motility and polarization in neutrophil-like HL60 cells and human neutrophils. *The Journal of biological chemistry* **281**, 12908-12918, doi:10.1074/jbc.M510871200 (2006).
207 Rockwell, C. E., Raman, P., Kaplan, B. L. & Kaminski, N. E. A COX-2 metabolite of the endogenous cannabinoid, 2-arachidonyl glycerol,

mediates suppression of IL-2 secretion in activated Jurkat T cells. *Biochem Pharmacol* **76**, 353-361, doi:10.1016/j.bcp.2008.05.005 (2008).
208 Ouyang, Y., Hwang, S. G., Han, S. H. & Kaminski, N. E. Suppression of interleukin-2 by the putative endogenous cannabinoid 2-arachidonyl-glycerol is mediated through down-regulation of the nuclear factor of activated T cells. *Molecular pharmacology* **53**, 676-683 (1998).
209 Rockwell, C. E., Snider, N. T., Thompson, J. T., Vanden Heuvel, J. P. & Kaminski, N. E. Interleukin-2 suppression by 2-arachidonyl glycerol is mediated through peroxisome proliferator-activated receptor gamma independently of cannabinoid receptors 1 and 2. *Molecular pharmacology* **70**, 101-111, doi:10.1124/mol.105.019117 (2006).
210 Lee, M., Yang, K. H. & Kaminski, N. E. Effects of putative cannabinoid receptor ligands, anandamide and 2-arachidonyl-glycerol, on immune function in B6C3F1 mouse splenocytes. *The Journal of pharmacology and experimental therapeutics* **275**, 529-536 (1995).
211 Gokoh, M., Kishimoto, S., Oka, S. & Sugiura, T. 2-Arachidonoylglycerol enhances the phagocytosis of opsonized zymosan by HL-60 cells differentiated into macrophage-like cells. *Biol Pharm Bull* **30**, 1199-1205 (2007).
212 Shiratsuchi, A., Watanabe, I., Yoshida, H. & Nakanishi, Y. Involvement of cannabinoid receptor CB2 in dectin-1-mediated macrophage phagocytosis. *Immunol Cell Biol* **86**, 179-184, doi:10.1038/sj.icb.7100121 (2008).
213 Gallily, R., Breuer, A. & Mechoulam, R. 2-Arachidonylglycerol, an endogenous cannabinoid, inhibits tumor necrosis factor-alpha production in murine macrophages, and in mice. *Eur J Pharmacol* **406**, R5-7 (2000).
214 Lu, T., Newton, C., Perkins, I., Friedman, H. & Klein, T. W. Role of cannabinoid receptors in Delta-9-tetrahydrocannabinol suppression of IL-12p40 in mouse bone marrow-derived dendritic cells infected with Legionella pneumophila. *Eur J Pharmacol* **532**, 170-177, doi:10.1016/j.ejphar.2005.12.040 (2006).
215 Kaplan, B. L., Ouyang, Y., Rockwell, C. E., Rao, G. K. & Kaminski, N. E. 2-Arachidonoyl-glycerol suppresses interferon-gamma production in phorbol ester/ionomycin-activated mouse splenocytes independent of CB1 or CB2. *Journal of leukocyte biology* **77**, 966-974, doi:10.1189/jlb.1104652 (2005).
216 Carrier, E. J. *et al.* Cultured rat microglial cells synthesize the endocannabinoid 2-arachidonylglycerol, which increases proliferation via a CB2 receptor-dependent mechanism. *Molecular pharmacology* **65**, 999-1007, doi:10.1124/mol.65.4.999 (2004).
217 Kishimoto, S. *et al.* 2-Arachidonoylglycerol, an endogenous cannabinoid receptor ligand, induces accelerated production of chemokines in HL-60 cells. *J Biochem* **135**, 517-524 (2004).
218 Han, K. H. *et al.* CB1 and CB2 cannabinoid receptors differentially regulate the production of reactive oxygen species by macrophages. *Cardiovasc Res* **84**, 378-386, doi:10.1093/cvr/cvp240 (2009).
219 Jourdan, T. *et al.* Activation of the Nlrp3 inflammasome in infiltrating macrophages by endocannabinoids mediates beta cell loss in type 2 diabetes. *Nature medicine* **19**, 1132-1140, doi:10.1038/nm.3265 (2013).

220 Chang, Y. H., Lee, S. T. & Lin, W. W. Effects of cannabinoids on LPS-stimulated inflammatory mediator release from macrophages: involvement of eicosanoids. *J Cell Biochem* **81**, 715-723 (2001).
221 Stefano, G. B., Bilfinger, T. V., Rialas, C. M. & Deutsch, D. G. 2-arachidonyl-glycerol stimulates nitric oxide release from human immune and vascular tissues and invertebrate immunocytes by cannabinoid receptor 1. *Pharmacol Res* **42**, 317-322, doi:10.1006/phrs.2000.0702 (2000).
222 Kreutz, S., Koch, M., Ghadban, C., Korf, H. W. & Dehghani, F. Cannabinoids and neuronal damage: differential effects of THC, AEA and 2-AG on activated microglial cells and degenerating neurons in excitotoxically lesioned rat organotypic hippocampal slice cultures. *Exp Neurol* **203**, 246-257, doi:10.1016/j.expneurol.2006.08.010 (2007).
223 Kerr, D. M. *et al.* The monoacylglycerol lipase inhibitor JZL184 attenuates LPS-induced increases in cytokine expression in the rat frontal cortex and plasma: differential mechanisms of action. *British journal of pharmacology* **169**, 808-819, doi:10.1111/bph.2013.169.issue-4 (2013).
224 Bernal-Chico, A. *et al.* Blockade of monoacylglycerol lipase inhibits oligodendrocyte excitotoxicity and prevents demyelination in vivo. *Glia* **63**, 163-176, doi:10.1002/glia.22742 (2015).
225 Kouchi, Z. Monoacylglycerol lipase promotes Fcgamma receptor-mediated phagocytosis in microglia but does not regulate LPS-induced upregulation of inflammatory cytokines. *Biochem Biophys Res Commun*, doi:10.1016/j.bbrc.2015.07.019 (2015).
226 Flannery, L. E., Henry, R. J., Kerr, D. M., Finn, D. P. & Roche, M. FAAH, but not MAGL, inhibition modulates acute TLR3-induced neuroimmune signaling in the rat, independent of sex. *J Neurosci Res*, doi:10.1002/jnr.24120 (2017).
227 Carloni, S. *et al.* Pretreatment with the monoacylglycerol lipase inhibitor URB602 protects from the long-term consequences of neonatal hypoxic-ischemic brain injury in rats. *Pediatr Res* **72**, 400-406, doi:10.1038/pr.2012.91 (2012).
228 Wang, F. *et al.* 2-Arachidonylglycerol Protects Primary Astrocytes Exposed to Oxygen-Glucose Deprivation Through a Blockade of NDRG2 Signaling and STAT3 Phosphorylation. *Rejuvenation Res* **19**, 215-222, doi:10.1089/rej.2015.1703 (2016).
229 Shearer, J. A., Coker, S. J. & Carswell, H. V. C. Detrimental effects of 2-arachidonoylglycerol on whole blood platelet aggregation and on cerebral blood flow after a focal ischemic insult in rats. *American journal of physiology. Heart and circulatory physiology*, doi:10.1152/ajpheart.00299.2017 (2018).
230 Katz, P. S. *et al.* Endocannabinoid degradation inhibition improves neurobehavioral function, blood-brain barrier integrity, and neuroinflammation following mild traumatic brain injury. *J Neurotrauma* **32**, 297-306, doi:10.1089/neu.2014.3508 (2015).
231 Mayeux, J., Katz, P., Edwards, S., Middleton, J. W. & Molina, P. E. Inhibition of Endocannabinoid Degradation Improves Outcomes from Mild Traumatic Brain Injury: A Mechanistic Role for Synaptic Hyperexcitability. *J Neurotrauma* **34**, 436-443, doi:10.1089/neu.2016.4452 (2017).

232 Zhang, X. & Thayer, S. A. Monoacylglycerol lipase inhibitor JZL184 prevents HIV-1 gp120-induced synapse loss by altering endocannabinoid signaling. *Neuropharmacology* **128**, 269-281, doi:10.1016/j.neuropharm.2017.10.023 (2018).
233 Li, B. *et al.* Endocannabinoid 2-arachidonoylglycerol protects inflammatory insults from sulfur dioxide inhalation via cannabinoid receptors in the brain. *J Environ Sci (China)* **51**, 265-274, doi:10.1016/j.jes.2016.05.031 (2017).
234 Moon, K. H. *et al.* Phospholipase A2, oxidative stress, and neurodegeneration in binge ethanol-treated organotypic slice cultures of developing rat brain. *Alcohol Clin Exp Res* **38**, 161-169, doi:10.1111/acer.12221 (2014).
235 Chen, X., Zhang, J. & Chen, C. Endocannabinoid 2-arachidonoylglycerol protects neurons against beta-amyloid insults. *Neuroscience* **178**, 159-168, doi:10.1016/j.neuroscience.2011.01.024 (2011).
236 Pihlaja, R. *et al.* Monoacylglycerol lipase inhibitor JZL184 reduces neuroinflammatory response in APdE9 mice and in adult mouse glial cells. *J Neuroinflammation* **12**, 81, doi:10.1186/s12974-015-0305-9 (2015).
237 Chen, R. *et al.* Monoacylglycerol lipase is a therapeutic target for Alzheimer's disease. *Cell reports* **2**, 1329-1339, doi:10.1016/j.celrep.2012.09.030 (2012).
238 Zhang, J., Hu, M., Teng, Z., Tang, Y. P. & Chen, C. Synaptic and cognitive improvements by inhibition of 2-AG metabolism are through upregulation of microRNA-188-3p in a mouse model of Alzheimer's disease. *The Journal of neuroscience : the official journal of the Society for Neuroscience* **34**, 14919-14933, doi:10.1523/JNEUROSCI.1165-14.2014 (2014).
239 Zhang, J. & Chen, C. Alleviation of Neuropathology by Inhibition of Monoacylglycerol Lipase in APP Transgenic Mice Lacking CB2 Receptors. *Mol Neurobiol*, doi:10.1007/s12035-017-0689-x (2017).
240 Fernandez-Suarez, D. *et al.* Monoacylglycerol lipase inhibitor JZL184 is neuroprotective and alters glial cell phenotype in the chronic MPTP mouse model. *Neurobiol Aging* **35**, 2603-2616, doi:10.1016/j.neurobiolaging.2014.05.021 (2014).
241 Pasquarelli, N. *et al.* Contrasting effects of selective MAGL and FAAH inhibition on dopamine depletion and GDNF expression in a chronic MPTP mouse model of Parkinson's disease. *Neurochem Int* **110**, 14-24, doi:10.1016/j.neuint.2017.08.003 (2017).
242 Mounsey, R. B. *et al.* Increasing levels of the endocannabinoid 2-AG is neuroprotective in the 1-methyl-4-phenyl-1,2,3,6-tetrahydropyridine mouse model of Parkinson's disease. *Exp Neurol* **273**, 36-44, doi:10.1016/j.expneurol.2015.07.024 (2015).
243 Aymerich, M. S. *et al.* Neuroprotective Effect of JZL184 in MPP-Treated SH-SY5Y Cells Through CB Receptors. *Mol Neurobiol*, doi:10.1007/s12035-015-9213-3 (2015).
244 Lysenko, L. V. *et al.* Monoacylglycerol lipase inhibitor JZL184 improves behavior and neural properties in Ts65Dn mice, a model of down syndrome. *PloS one* **9**, e114521, doi:10.1371/journal.pone.0114521 (2014).

245 Pasquarelli, N. *et al.* Evaluation of monoacylglycerol lipase as a therapeutic target in a transgenic mouse model of ALS. *Neuropharmacology*, doi:10.1016/j.neuropharm.2017.03.037 (2017).
246 Valdeolivas, S. *et al.* The inhibition of 2-arachidonoyl-glycerol (2-AG) biosynthesis, rather than enhancing striatal damage, protects striatal neurons from malonate-induced death: a potential role of cyclooxygenase-2-dependent metabolism of 2-AG. *Cell Death Dis* **4**, e862, doi:10.1038/cddis.2013.387 (2013).
247 Huggins, J. P., Smart, T. S., Langman, S., Taylor, L. & Young, T. An efficient randomised, placebo-controlled clinical trial with the irreversible fatty acid amide hydrolase-1 inhibitor PF-04457845, which modulates endocannabinoids but fails to induce effective analgesia in patients with pain due to osteoarthritis of the knee. *Pain* **153**, 1837-1846, doi:10.1016/j.pain.2012.04.020 (2012).
248 Li, G. L. *et al.* Assessment of the pharmacology and tolerability of PF-04457845, an irreversible inhibitor of fatty acid amide hydrolase-1, in healthy subjects. *Br J Clin Pharmacol* **73**, 706-716, doi:10.1111/j.1365-2125.2011.04137.x (2012).
249 van Esbroeck, A. C. M. *et al.* Activity-based protein profiling reveals off-target proteins of the FAAH inhibitor BIA 10-2474. *Science* **356**, 1084-1087, doi:10.1126/science.aaf7497 (2017).
250 Kinsey, S. G. *et al.* Blockade of endocannabinoid-degrading enzymes attenuates neuropathic pain. *The Journal of pharmacology and experimental therapeutics* **330**, 902-910, doi:10.1124/jpet.109.155465 (2009).
251 Khasabova, I. A. *et al.* JZL184 is anti-hyperalgesic in a murine model of cisplatin-induced peripheral neuropathy. *Pharmacol Res* **90**, 67-75, doi:10.1016/j.phrs.2014.09.008 (2014).
252 Burston, J. J. *et al.* Robust anti-nociceptive effects of MAG lipase inhibition in a model of osteoarthritis pain. *British journal of pharmacology*, doi:10.1111/bph.13574 (2016).
253 Greco, R. *et al.* P007. Inhibition of monoacylglycerol lipase activity modulates the activation of brain structures relevant for migraine pathogenesis. *J Headache Pain* **16**, A165, doi:10.1186/1129-2377-16-S1-A165 (2015).
254 Guindon, J., Guijarro, A., Piomelli, D. & Hohmann, A. G. Peripheral antinociceptive effects of inhibitors of monoacylglycerol lipase in a rat model of inflammatory pain. *British journal of pharmacology* **163**, 1464-1478, doi:10.1111/j.1476-5381.2010.01192.x (2011).
255 Woodhams, S. G. *et al.* Spinal administration of the monoacylglycerol lipase inhibitor JZL184 produces robust inhibitory effects on nociceptive processing and the development of central sensitization in the rat. *British journal of pharmacology* **167**, 1609-1619, doi:10.1111/j.1476-5381.2012.02179.x (2012).
256 Zygmunt, P. M. *et al.* Monoacylglycerols activate TRPV1--a link between phospholipase C and TRPV1. *PloS one* **8**, e81618, doi:10.1371/journal.pone.0081618 (2013).

257 Gao, F. *et al.* Electroacupuncture Inhibits NLRP3 Inflammasome Activation through CB2 Receptors in Inflammatory Pain. *Brain Behav Immun*, doi:10.1016/j.bbi.2017.08.004 (2017).
258 Petrenko, A. B., Yamazaki, M., Sakimura, K., Kano, M. & Baba, H. Augmented tonic pain-related behavior in knockout mice lacking monoacylglycerol lipase, a major degrading enzyme for the endocannabinoid 2-arachidonoylglycerol. *Behav Brain Res* **271**, 51-58, doi:10.1016/j.bbr.2014.05.063 (2014).
259 Anderson, W. B., Gould, M. J., Torres, R. D., Mitchell, V. A. & Vaughan, C. W. Actions of the dual FAAH/MAGL inhibitor JZL195 in a murine inflammatory pain model. *Neuropharmacology* **81**, 224-230, doi:10.1016/j.neuropharm.2013.12.018 (2014).
260 Sakin, Y. S. *et al.* The effect of FAAH, MAGL, and Dual FAAH/MAGL inhibition on inflammatory and colorectal distension-induced visceral pain models in Rodents. *Neurogastroenterology and motility : the official journal of the European Gastrointestinal Motility Society* **27**, 936-944, doi:10.1111/nmo.12563 (2015).
261 Oliveira, C. D. *et al.* Peltatoside Isolated from Annona crassiflora Induces Peripheral Antinociception by Activation of the Cannabinoid System. *Planta Med* **83**, 261-267, doi:10.1055/s-0042-113386 (2017).
262 Crowe, M. S. *et al.* The monoacylglycerol lipase inhibitor KML29 with gabapentin synergistically produces analgesia in mice. *British journal of pharmacology*, doi:10.1111/bph.14055 (2017).
263 Crowe, M. S. *et al.* Combined inhibition of monoacylglycerol lipase and cyclooxygenases synergistically reduces neuropathic pain in mice. *British journal of pharmacology* **172**, 1700-1712, doi:10.1111/bph.13012 (2015).
264 Wilkerson, J. L. *et al.* The selective monoacylglycerol lipase inhibitor MJN110 produces opioid sparing effects in a mouse neuropathic pain model. *The Journal of pharmacology and experimental therapeutics*, doi:10.1124/jpet.115.229971 (2016).
265 Borner, C., Hollt, V. & Kraus, J. Cannabinoid receptor type 2 agonists induce transcription of the mu-opioid receptor gene in Jurkat T cells. *Molecular pharmacology* **69**, 1486-1491, doi:10.1124/mol.105.018325 (2006).
266 Taschler, U. *et al.* Monoglyceride lipase-deficiency causes desensitization of intestinal cannabinoid receptor type 1 and increased colonic mu-opioid receptor sensitivity. *British journal of pharmacology*, doi:10.1111/bph.13224 (2015).
267 Kita, Y. *et al.* Fever Is Mediated by Conversion of Endocannabinoid 2-Arachidonoylglycerol to Prostaglandin E2. *PloS one* **10**, e0133663, doi:10.1371/journal.pone.0133663 (2015).
268 Sanchez-Alavez, M. *et al.* Monoacylglycerol Lipase Regulates Fever Response. *PloS one* **10**, e0134437, doi:10.1371/journal.pone.0134437 (2015).
269 Nass, S. R. *et al.* Endocannabinoid Catabolic Enzymes Play Differential Roles in Thermal Homeostasis in Response to Environmental or Immune Challenge. *Journal of neuroimmune pharmacology : the official journal of the Society on NeuroImmune Pharmacology* **10**, 364-370, doi:10.1007/s11481-015-9593-1 (2015).

270 Costola-de-Souza, C. *et al.* Monoacylglycerol lipase (MAGL) inhibition attenuates acute lung injury in mice. *PloS one* **8**, e77706, doi:10.1371/journal.pone.0077706 (2013).
271 Cao, Z. *et al.* Monoacylglycerol lipase controls endocannabinoid and eicosanoid signaling and hepatic injury in mice. *Gastroenterology* **144**, 808-817 e815, doi:10.1053/j.gastro.2012.12.028 (2013).
272 Vujic, N. *et al.* Monoglyceride lipase deficiency modulates endocannabinoid signaling and improves plaque stability in ApoE-knockout mice. *Atherosclerosis* **244**, 9-21, doi:10.1016/j.atherosclerosis.2015.10.109 (2016).
273 Alhouayek, M., Lambert, D. M., Delzenne, N. M., Cani, P. D. & Muccioli, G. G. Increasing endogenous 2-arachidonoylglycerol levels counteracts colitis and related systemic inflammation. *FASEB journal : official publication of the Federation of American Societies for Experimental Biology* **25**, 2711-2721, doi:10.1096/fj.10-176602 (2011).
274 Alhamoruni, A., Lee, A. C., Wright, K. L., Larvin, M. & O'Sullivan, S. E. Pharmacological effects of cannabinoids on the Caco-2 cell culture model of intestinal permeability. *The Journal of pharmacology and experimental therapeutics* **335**, 92-102, doi:10.1124/jpet.110.168237 (2010).
275 Karwad, M. A. *et al.* The role of CB1 in intestinal permeability and inflammation. *FASEB journal : official publication of the Federation of American Societies for Experimental Biology* **31**, 3267-3277, doi:10.1096/fj.201601346R (2017).
276 Alhamoruni, A., Wright, K. L., Larvin, M. & O'Sullivan, S. E. Cannabinoids mediate opposing effects on inflammation-induced intestinal permeability. *British journal of pharmacology* **165**, 2598-2610, doi:10.1111/bph.2012.165.issue-8 (2012).
277 Wirtz, S., Neufert, C., Weigmann, B. & Neurath, M. F. Chemically induced mouse models of intestinal inflammation. *Nat Protoc* **2**, 541-546, doi:10.1038/nprot.2007.41 (2007).
278 Antoniou, E. *et al.* The TNBS-induced colitis animal model: An overview. *Ann Med Surg (Lond)* **11**, 9-15, doi:10.1016/j.amsu.2016.07.019 (2016).
279 Chassaing, B., Aitken, J. D., Malleshappa, M. & Vijay-Kumar, M. Dextran sulfate sodium (DSS)-induced colitis in mice. *Curr Protoc Immunol* **104**, Unit 15 25, doi:10.1002/0471142735.im1525s104 (2014).
280 Tao, L. & Reese, T. A. Making Mouse Models That Reflect Human Immune Responses. *Trends Immunol*, doi:10.1016/j.it.2016.12.007 (2017).
281 Hassanzadeh, P., Arbabi, E., Atyabi, F. & Dinarvand, R. Application of carbon nanotubes as the carriers of the cannabinoid, 2-arachidonoylglycerol: Towards a novel treatment strategy in colitis. *Life Sci* **179**, 66-72, doi:10.1016/j.lfs.2016.11.015 (2017).
282 Massa, F. *et al.* The endogenous cannabinoid system protects against colonic inflammation. *J Clin Invest* **113**, 1202-1209, doi:10.1172/JCI19465 (2004).
283 Engel, M. A. *et al.* Mice lacking cannabinoid CB1-, CB2-receptors or both receptors show increased susceptibility to trinitrobenzene sulfonic acid (TNBS)-induced colitis. *J Physiol Pharmacol* **61**, 89-97 (2010).

284 Ke, P. *et al.* Activation of Cannabinoid Receptor 2 Ameliorates DSS-Induced Colitis through Inhibiting NLRP3 Inflammasome in Macrophages. *PloS one* **11**, e0155076, doi:10.1371/journal.pone.0155076 (2016).
285 Kimball, E. S., Schneider, C. R., Wallace, N. H. & Hornby, P. J. Agonists of cannabinoid receptor 1 and 2 inhibit experimental colitis induced by oil of mustard and by dextran sulfate sodium. *American journal of physiology. Gastrointestinal and liver physiology* **291**, G364-371, doi:10.1152/ajpgi.00407.2005 (2006).
286 El Bakali, J. *et al.* Conformational Restriction Leading to a Selective CB2 Cannabinoid Receptor Agonist Orally Active Against Colitis. *ACS Med Chem Lett* **6**, 198-203, doi:10.1021/ml500439x (2015).
287 Storr, M. A. *et al.* Activation of the cannabinoid 2 receptor (CB2) protects against experimental colitis. *Inflammatory bowel diseases* **15**, 1678-1685, doi:10.1002/ibd.20960 (2009).
288 Singh, U. P. *et al.* Cannabinoid receptor-2 (CB2) agonist ameliorates colitis in IL-10(-/-) mice by attenuating the activation of T cells and promoting their apoptosis. *Toxicol Appl Pharmacol* **258**, 256-267, doi:10.1016/j.taap.2011.11.005 (2012).
289 Tourteau, A. *et al.* 3-Carboxamido-5-aryl-isoxazoles as new CB2 agonists for the treatment of colitis. *Bioorganic & medicinal chemistry* **21**, 5383-5394, doi:10.1016/j.bmc.2013.06.010 (2013).
290 Cluny, N. L. *et al.* Naphthalen-1-yl-(4-pentyloxynaphthalen-1-yl)methanone (SAB378), a peripherally restricted cannabinoid CB1/CB2 receptor agonist, inhibits gastrointestinal motility but has no effect on experimental colitis in mice. *The Journal of pharmacology and experimental therapeutics* **334**, 973-980, doi:10.1124/jpet.110.169946 (2010).
291 Li, Y. Y. *et al.* Inhibition of p38/Mk2 signaling pathway improves the anti-inflammatory effect of WIN55 on mouse experimental colitis. *Lab Invest* **93**, 322-333, doi:10.1038/labinvest.2012.177 (2013).
292 Feng, Y. J., Li, Y. Y., Lin, X. H., Li, K. & Cao, M. H. Anti-inflammatory effect of cannabinoid agonist WIN55, 212 on mouse experimental colitis is related to inhibition of p38MAPK. *World J Gastroenterol* **22**, 9515-9524, doi:10.3748/wjg.v22.i43.9515 (2016).
293 Fichna, J. *et al.* Cannabinoids alleviate experimentally induced intestinal inflammation by acting at central and peripheral receptors. *PloS one* **9**, e109115, doi:10.1371/journal.pone.0109115 (2014).
294 Lin, S. *et al.* The Anti-Inflammatory Effect and Intestinal Barrier Protection of HU210 Differentially Depend on TLR4 Signaling in Dextran Sulfate Sodium-Induced Murine Colitis. *Dig Dis Sci* **62**, 372-386, doi:10.1007/s10620-016-4404-y (2017).
295 Dziadulewicz, E. K. *et al.* Naphthalen-1-yl-(4-pentyloxynaphthalen-1-yl)methanone: a potent, orally bioavailable human CB1/CB2 dual agonist with antihyperalgesic properties and restricted central nervous system penetration. *Journal of medicinal chemistry* **50**, 3851-3856, doi:10.1021/jm070317a (2007).
296 Engel, M. A. *et al.* Ulcerative colitis in AKR mice is attenuated by intraperitoneally administered anandamide. *J Physiol Pharmacol* **59**, 673-689 (2008).

297 Alhouayek, M. *et al.* N-Acylethanolamine-hydrolyzing acid amidase inhibition increases colon N-palmitoylethanolamine levels and counteracts murine colitis. *FASEB journal : official publication of the Federation of American Societies for Experimental Biology* **29**, 650-661, doi:10.1096/fj.14-255208 (2015).
298 Esposito, G. *et al.* Palmitoylethanolamide improves colon inflammation through an enteric glia/toll like receptor 4-dependent PPAR-alpha activation. *Gut* **63**, 1300-1312, doi:10.1136/gutjnl-2013-305005 (2014).
299 Borrelli, F. *et al.* Palmitoylethanolamide, a naturally occurring lipid, is an orally effective intestinal anti-inflammatory agent. *British journal of pharmacology* **172**, 142-158, doi:10.1111/bph.12907 (2015).
300 Cordaro, M. *et al.* Adelmidrol, a Palmitoylethanolamide Analogue, as a New Pharmacological Treatment for the Management of Inflammatory Bowel Disease. *Molecular pharmacology* **90**, 549-561, doi:10.1124/mol.116.105668 (2016).
301 Andrzejak, V. *et al.* New FAAH inhibitors based on 3-carboxamido-5-aryl-isoxazole scaffold that protect against experimental colitis. *Bioorganic & medicinal chemistry* **19**, 3777-3786, doi:10.1016/j.bmc.2011.04.057 (2011).
302 D'Argenio, G. *et al.* Up-regulation of anandamide levels as an endogenous mechanism and a pharmacological strategy to limit colon inflammation. *FASEB journal : official publication of the Federation of American Societies for Experimental Biology* **20**, 568-570, doi:10.1096/fj.05-4943fje (2006).
303 Storr, M. A. *et al.* Targeting endocannabinoid degradation protects against experimental colitis in mice: involvement of CB1 and CB2 receptors. *J Mol Med (Berl)* **86**, 925-936, doi:10.1007/s00109-008-0359-6 (2008).
304 Tourteau, A. *et al.* Switching cannabinoid response from CB(2) agonists to FAAH inhibitors. *Bioorg Med Chem Lett* **24**, 1322-1326, doi:10.1016/j.bmcl.2014.01.056 (2014).
305 Sasso, O. *et al.* Multitarget fatty acid amide hydrolase/cyclooxygenase blockade suppresses intestinal inflammation and protects against nonsteroidal anti-inflammatory drug-dependent gastrointestinal damage. *FASEB journal : official publication of the Federation of American Societies for Experimental Biology*, doi:10.1096/fj.15-270637 (2015).
306 Shamran, H. *et al.* Fatty acid amide hydrolase (FAAH) blockade ameliorates experimental colitis by altering microRNA expression and suppressing inflammation. *Brain Behav Immun*, doi:10.1016/j.bbi.2016.06.008 (2016).
307 Zhao, X. *et al.* Elevation of arachidonoylethanolamide levels by activation of the endocannabinoid system protects against colitis and ameliorates remote organ lesions in mice. *Exp Ther Med* **14**, 5664-5670, doi:10.3892/etm.2017.5222 (2017).
308 Salaga, M. *et al.* Experimental colitis in mice is attenuated by changes in the levels of endocannabinoid metabolites induced by selective inhibition of fatty acid amide hydrolase (FAAH). *J Crohns Colitis* **8**, 998-1009, doi:10.1016/j.crohns.2014.01.025 (2014).
309 Schicho, R. *et al.* The atypical cannabinoid O-1602 protects against experimental colitis and inhibits neutrophil recruitment. *Inflammatory bowel diseases* **17**, 1651-1664, doi:10.1002/ibd.21538 (2011).

310 Stancic, A. *et al.* The GPR55 antagonist CID16020046 protects against intestinal inflammation. *Neurogastroenterology and motility : the official journal of the European Gastrointestinal Motility Society* **27**, 1432-1445, doi:10.1111/nmo.12639 (2015).
311 Bento, A. F. *et al.* beta-Caryophyllene inhibits dextran sulfate sodium-induced colitis in mice through CB2 receptor activation and PPARgamma pathway. *Am J Pathol* **178**, 1153-1166, doi:10.1016/j.ajpath.2010.11.052 (2011).
312 De Filippis, D. *et al.* Cannabidiol reduces intestinal inflammation through the control of neuroimmune axis. *PloS one* **6**, e28159, doi:10.1371/journal.pone.0028159 (2011).
313 Borrelli, F. *et al.* Cannabidiol, a safe and non-psychotropic ingredient of the marijuana plant Cannabis sativa, is protective in a murine model of colitis. *J Mol Med (Berl)* **87**, 1111-1121, doi:10.1007/s00109-009-0512-x (2009).
314 Schicho, R. & Storr, M. Topical and systemic cannabidiol improves trinitrobenzene sulfonic acid colitis in mice. *Pharmacology* **89**, 149-155, doi:10.1159/000336871 (2012).
315 Jamontt, J. M., Molleman, A., Pertwee, R. G. & Parsons, M. E. The effects of Delta-tetrahydrocannabinol and cannabidiol alone and in combination on damage, inflammation and in vitro motility disturbances in rat colitis. *British journal of pharmacology* **160**, 712-723, doi:10.1111/j.1476-5381.2010.00791.x (2010).
316 Krohn, R. M. *et al.* Abnormal cannabidiol attenuates experimental colitis in mice, promotes wound healing and inhibits neutrophil recruitment. *Journal of inflammation* **13**, 21, doi:10.1186/s12950-016-0129-0 (2016).
317 Pagano, E. *et al.* An Orally Active Cannabis Extract with High Content in Cannabidiol attenuates Chemically-induced Intestinal Inflammation and Hypermotility in the Mouse. *Frontiers in pharmacology* **7**, 341, doi:10.3389/fphar.2016.00341 (2016).
318 Malfait, A. M. *et al.* The nonpsychoactive cannabis constituent cannabidiol is an oral anti-arthritic therapeutic in murine collagen-induced arthritis. *Proceedings of the National Academy of Sciences of the United States of America* **97**, 9561-9566, doi:10.1073/pnas.160105897 (2000).
319 Karmaus, P. W., Wagner, J. G., Harkema, J. R., Kaminski, N. E. & Kaplan, B. L. Cannabidiol (CBD) enhances lipopolysaccharide (LPS)-induced pulmonary inflammation in C57BL/6 mice. *J Immunotoxicol* **10**, 321-328, doi:10.3109/1547691X.2012.741628 (2013).
320 Wallace, J. L. *et al.* Pro-resolution, protective and anti-nociceptive effects of a cannabis extract in the rat gastrointestinal tract. *J Physiol Pharmacol* **64**, 167-175 (2013).
321 Borrelli, F. *et al.* Beneficial effect of the non-psychotropic plant cannabinoid cannabigerol on experimental inflammatory bowel disease. *Biochem Pharmacol* **85**, 1306-1316, doi:10.1016/j.bcp.2013.01.017 (2013).
322 Romano, B. *et al.* The cannabinoid TRPA1 agonist cannabichromene inhibits nitric oxide production in macrophages and ameliorates murine colitis. *British journal of pharmacology* **169**, 213-229, doi:10.1111/bph.12120 (2013).

323 Sipe, J. C., Arbour, N., Gerber, A. & Beutler, E. Reduced endocannabinoid immune modulation by a common cannabinoid 2 (CB2) receptor gene polymorphism: possible risk for autoimmune disorders. *Journal of leukocyte biology* **78**, 231-238, doi:10.1189/jlb.0205111 (2005).
324 Strisciuglio, C. *et al.* Cannabinoid Receptor 2 Functional Variant Contributes to the Risk for Pediatric Inflammatory Bowel Disease. *J Clin Gastroenterol*, doi:10.1097/MCG.0000000000000755 (2016).
325 Yonal, O., Eren, F., Yilmaz, Y., Atug, O. & Over, H. H. No association between the functional cannabinoid receptor type 2 Q63R variants and inflammatory bowel disease in Turkish subjects. *Turk J Gastroenterol* **25**, 639-643, doi:10.5152/tjg.2014.6568 (2014).
326 Storr, M. *et al.* The cannabinoid 1 receptor (CNR1) 1359 G/A polymorphism modulates susceptibility to ulcerative colitis and the phenotype in Crohn's disease. *PloS one* **5**, e9453, doi:10.1371/journal.pone.0009453 (2010).
327 Storr, M. *et al.* The role of fatty acid hydrolase gene variants in inflammatory bowel disease. *Aliment Pharmacol Ther* **29**, 542-551, doi:10.1111/j.1365-2036.2008.03910.x (2009).
328 Camilleri, M. *et al.* Genetic variation in endocannabinoid metabolism, gastrointestinal motility, and sensation. *American journal of physiology. Gastrointestinal and liver physiology* **294**, G13-19, doi:10.1152/ajpgi.00371.2007 (2008).
329 Nallathambi, R. *et al.* Anti-Inflammatory Activity in Colon Models Is Derived from Delta9-Tetrahydrocannabinolic Acid That Interacts with Additional Compounds in Cannabis Extracts. *Cannabis Cannabinoid Res* **2**, 167-182, doi:10.1089/can.2017.0027 (2017).
330 Garcia-Planella, E. *et al.* [Use of complementary and alternative medicine and drug abuse in patients with inflammatory bowel disease]. *Med Clin (Barc)* **128**, 45-48 (2007).
331 Lal, S. *et al.* Cannabis use amongst patients with inflammatory bowel disease. *Eur J Gastroenterol Hepatol* **23**, 891-896, doi:10.1097/MEG.0b013e328349bb4c (2011).
332 Ravikoff Allegretti, J., Courtwright, A., Lucci, M., Korzenik, J. R. & Levine, J. Marijuana use patterns among patients with inflammatory bowel disease. *Inflammatory bowel diseases* **19**, 2809-2814, doi:10.1097/01.MIB.0000435851.94391.37 (2013).
333 Weiss, A. & Friedenberg, F. Patterns of cannabis use in patients with Inflammatory Bowel Disease: A population based analysis. *Drug Alcohol Depend* **156**, 84-89, doi:10.1016/j.drugalcdep.2015.08.035 (2015).
334 Storr, M., Devlin, S., Kaplan, G. G., Panaccione, R. & Andrews, C. N. Cannabis use provides symptom relief in patients with inflammatory bowel disease but is associated with worse disease prognosis in patients with Crohn's disease. *Inflammatory bowel diseases* **20**, 472-480, doi:10.1097/01.MIB.0000440982.79036.d6 (2014).
335 Naftali, T., Lev, L. B., Yablecovitch, D., Half, E. & Konikoff, F. M. Treatment of Crohn's disease with cannabis: an observational study. *Isr Med Assoc J* **13**, 455-458 (2011).
336 Lahat, A., Lang, A. & Ben-Horin, S. Impact of cannabis treatment on the quality of life, weight and clinical disease activity in inflammatory bowel

disease patients: a pilot prospective study. *Digestion* **85**, 1-8, doi:10.1159/000332079 (2012).
337 Naftali, T. *et al.* Cannabis induces a clinical response in patients with Crohn's disease: a prospective placebo-controlled study. *Clin Gastroenterol Hepatol* **11**, 1276-1280 e1271, doi:10.1016/j.cgh.2013.04.034 (2013).
338 Walsh, A. J., Bryant, R. V. & Travis, S. P. Current best practice for disease activity assessment in IBD. *Nat Rev Gastroenterol Hepatol* **13**, 567-579, doi:10.1038/nrgastro.2016.128 (2016).
339 Naftali, T. *et al.* Low-Dose Cannabidiol Is Safe but Not Effective in the Treatment for Crohn's Disease, a Randomized Controlled Trial. *Dig Dis Sci* **62**, 1615-1620, doi:10.1007/s10620-017-4540-z (2017).
340 Irving, P. *et al.* Trial to Assess Cannabidiol in the Symptomatic Treatment of Ulcerative Colitis. *Gut* **64**, A430-A430, doi:10.1136/gutjnl-2015-309861.944 (2015).
341 Irving, P. *et al.* Cannabidiol for symptomatic treatment of ulcerative colitis: Results from a randomised, double-blind, placebo-controlled, parallel group, multi-centred pilot study. *Journal of Crohns & Colitis* **9**, S287-S287 (2015).
342 Irving, P. M. *et al.* A Randomised, Double-Blind, Placebo-Controlled, Parallel Group, Multi-Centred Pilot Study to Assess the Symptomatic Treatment of Ulcerative Colitis With Cannabidiol. *Gastroenterology* **148**, S275-S275 (2015).
343 Kalenderoglou, N., Macpherson, T. & Wright, K. L. Cannabidiol Reduces Leukemic Cell Size - But Is It Important? *Frontiers in pharmacology* **8**, 144, doi:10.3389/fphar.2017.00144 (2017).
344 Colgan, S. P. & Taylor, C. T. Hypoxia: an alarm signal during intestinal inflammation. *Nat Rev Gastroenterol Hepatol* **7**, 281-287, doi:10.1038/nrgastro.2010.39 (2010).
345 Ohradanova-Repic, A., Machacek, C., Fischer, M. B. & Stockinger, H. Differentiation of human monocytes and derived subsets of macrophages and dendritic cells by the HLDA10 monoclonal antibody panel. *Clin Transl Immunology* **5**, e55, doi:10.1038/cti.2015.39 (2016).
346 Jessani, N. *et al.* A streamlined platform for high-content functional proteomics of primary human specimens. *Nat Methods* **2**, 691-697, doi:10.1038/nmeth778 (2005).
347 Salio, M. *et al.* Mature dendritic cells prime functionally superior melan-A-specific CD8+ lymphocytes as compared with nonprofessional APC. *Journal of immunology* **167**, 1188-1197 (2001).
348 R Development Core Team. *R: A language and environment for statistical computing*, <http://www.R-project.org> (2007).
349 Gentleman, R. C. *et al.* Bioconductor: open software development for computational biology and bioinformatics. *Genome Biol* **5**, R80, doi:10.1186/gb-2004-5-10-r80 (2004).
350 Huber, W., von Heydebreck, A., Sultmann, H., Poustka, A. & Vingron, M. Variance stabilization applied to microarray data calibration and to the quantification of differential expression. *Bioinformatics* **18 Suppl 1**, S96-104 (2002).
351 Smyth, G. K. in *Bioinformatics and Computational Biology Solutions using R and Bioconductor* (ed R. Gentleman) 397-420 (Springer-Verlag, 2005).

352 Benjamini, Y. & Hochberg, Y. Controlling the false discovery rate: a practical and powerful approach to multiple testing. *J R Stat Soc Series B Stat Methodol* **57**, 289-300 (1995).
353 Bekkering, S. *et al.* In Vitro Experimental Model of Trained Innate Immunity in Human Primary Monocytes. *Clin Vaccine Immunol* **23**, 926-933, doi:10.1128/CVI.00349-16 (2016).
354 Izcue, A. *et al.* Interleukin-23 restrains regulatory T cell activity to drive T cell-dependent colitis. *Immunity* **28**, 559-570, doi:10.1016/j.immuni.2008.02.019 (2008).
355 Long, J. Z. & Cravatt, B. F. The metabolic serine hydrolases and their functions in mammalian physiology and disease. *Chemical reviews* **111**, 6022-6063, doi:10.1021/cr200075y (2011).
356 Bachovchin, D. A. & Cravatt, B. F. The pharmacological landscape and therapeutic potential of serine hydrolases. *Nat Rev Drug Discov* **11**, 52-68, doi:10.1038/nrd3620 (2012).
357 Kim, D. *et al.* (2R)-4-oxo-4-[3-(trifluoromethyl)-5,6-dihydro[1,2,4]triazolo[4,3-a]pyrazin-7(8H)- yl]-1-(2,4,5-trifluorophenyl)butan-2-amine: a potent, orally active dipeptidyl peptidase IV inhibitor for the treatment of type 2 diabetes. *Journal of medicinal chemistry* **48**, 141-151, doi:10.1021/jm0493156 (2005).
358 Polinsky, R. J. Clinical pharmacology of rivastigmine: a new-generation acetylcholinesterase inhibitor for the treatment of Alzheimer's disease. *Clin Ther* **20**, 634-647 (1998).
359 Hauel, N. H. *et al.* Structure-based design of novel potent nonpeptide thrombin inhibitors. *Journal of medicinal chemistry* **45**, 1757-1766 (2002).
360 Roehrig, S. *et al.* Discovery of the novel antithrombotic agent 5-chloro-N-({(5S)-2-oxo-3- [4-(3-oxomorpholin-4-yl)phenyl]-1,3-oxazolidin-5-yl}methyl)thiophene- 2-carboxamide (BAY 59-7939): an oral, direct factor Xa inhibitor. *Journal of medicinal chemistry* **48**, 5900-5908, doi:10.1021/jm050101d (2005).
361 Liu, Y., Patricelli, M. P. & Cravatt, B. F. Activity-based protein profiling: The serine hydrolases. *Proceedings of the National Academy of Sciences* **96**, 14694-14699, doi:10.1073/pnas.96.26.14694 (1999).
362 Simon, G. M. & Cravatt, B. F. Activity-based proteomics of enzyme superfamilies: serine hydrolases as a case study. *The Journal of biological chemistry* **285**, 11051-11055, doi:10.1074/jbc.R109.097600 (2010).
363 Hsu, K. L. *et al.* DAGLbeta inhibition perturbs a lipid network involved in macrophage inflammatory responses. *Nat Chem Biol* **8**, 999-1007, doi:10.1038/nchembio.1105 (2012).
364 Washburn, M. P., Wolters, D. & Yates, J. R., 3rd. Large-scale analysis of the yeast proteome by multidimensional protein identification technology. *Nat Biotechnol* **19**, 242-247, doi:10.1038/85686 (2001).
365 Liu, H., Sadygov, R. G. & Yates, J. R., 3rd. A model for random sampling and estimation of relative protein abundance in shotgun proteomics. *Anal Chem* **76**, 4193-4201, doi:10.1021/ac0498563 (2004).
366 Boersema, P. J., Raijmakers, R., Lemeer, S., Mohammed, S. & Heck, A. J. Multiplex peptide stable isotope dimethyl labeling for quantitative proteomics. *Nat Protoc* **4**, 484-494, doi:10.1038/nprot.2009.21 (2009).

367 Yang, P. & Liu, K. Activity-based protein profiling: recent advances in probe development and applications. *Chembiochem* **16**, 712-724, doi:10.1002/cbic.201402582 (2015).
368 Sadler, N. C. & Wright, A. T. Activity-based protein profiling of microbes. *Curr Opin Chem Biol* **24**, 139-144, doi:10.1016/j.cbpa.2014.10.022 (2015).
369 Lehmann, J. *et al.* An antibacterial beta-lactone kills Mycobacterium tuberculosis by infiltrating mycolic acid biosynthesis. *Angew Chem Int Ed Engl*, doi:10.1002/anie.201709365 (2017).
370 Baillie, T. A. Targeted Covalent Inhibitors for Drug Design. *Angew Chem Int Ed Engl* **55**, 13408-13421, doi:10.1002/anie.201601091 (2016).
371 Singh, J., Petter, R. C., Baillie, T. A. & Whitty, A. The resurgence of covalent drugs. *Nat Rev Drug Discov* **10**, 307-317, doi:10.1038/nrd3410 (2011).
372 Kerbrat, A. *et al.* Acute Neurologic Disorder from an Inhibitor of Fatty Acid Amide Hydrolase. *N Engl J Med* **375**, 1717-1725, doi:10.1056/NEJMoa1604221 (2016).
373 Nomura, D. K., Dix, M. M. & Cravatt, B. F. Activity-based protein profiling for biochemical pathway discovery in cancer. *Nat Rev Cancer* **10**, 630-638, doi:10.1038/nrc2901 (2010).
374 Roth, M. D., Castaneda, J. T. & Kiertscher, S. M. Exposure to Delta9-Tetrahydrocannabinol Impairs the Differentiation of Human Monocyte-derived Dendritic Cells and their Capacity for T cell Activation. *Journal of neuroimmune pharmacology : the official journal of the Society on NeuroImmune Pharmacology*, doi:10.1007/s11481-015-9587-z (2015).
375 Grimsey, N. L. *et al.* Specific detection of CB1 receptors; cannabinoid CB1 receptor antibodies are not all created equal! *J Neurosci Methods* **171**, 78-86, doi:10.1016/j.jneumeth.2008.02.014 (2008).
376 Marchalant, Y., Brownjohn, P. W., Bonnet, A., Kleffmann, T. & Ashton, J. C. Validating Antibodies to the Cannabinoid CB2 Receptor: Antibody Sensitivity Is Not Evidence of Antibody Specificity. *J Histochem Cytochem* **62**, 395-404, doi:10.1369/0022155414530995 (2014).
377 Marrs, W. R. *et al.* The serine hydrolase ABHD6 controls the accumulation and efficacy of 2-AG at cannabinoid receptors. *Nature neuroscience* **13**, 951-957, doi:10.1038/nn.2601 (2010).
378 Klein, T. W., Newton, C. A., Widen, R. & Friedman, H. The effect of delta-9-tetrahydrocannabinol and 11-hydroxy-delta-9-tetrahydrocannabinol on T-lymphocyte and B-lymphocyte mitogen responses. *J Immunopharmacol* **7**, 451-466 (1985).
379 Marazzi, J., Kleyer, J., Paredes, J. M. & Gertsch, J. Endocannabinoid content in fetal bovine sera - unexpected effects on mononuclear cells and osteoclastogenesis. *J Immunol Methods* **373**, 219-228, doi:10.1016/j.jim.2011.08.021 (2011).
380 Peng, J. C., Thomas, R. & Nielsen, L. K. Generation and maturation of dendritic cells for clinical application under serum-free conditions. *J Immunother* **28**, 599-609 (2005).
381 Canning, P. *et al.* Inflammatory Signaling by NOD-RIPK2 Is Inhibited by Clinically Relevant Type II Kinase Inhibitors. *Chemistry & Biology* **22**, 1174-1184, doi:10.1016/j.chembiol.2015.07.017 (2015).

382 Arbibe, L. *et al.* Toll-like receptor 2-mediated NF-kappa B activation requires a Rac1-dependent pathway. *Nat Immunol* **1**, 533-540, doi:10.1038/82797 (2000).
383 Clark, K., Takeuchi, O., Akira, S. & Cohen, P. The TRAF-associated protein TANK facilitates cross-talk within the IkappaB kinase family during Toll-like receptor signaling. *Proceedings of the National Academy of Sciences of the United States of America* **108**, 17093-17098, doi:10.1073/pnas.1114194108 (2011).
384 Falker, K., Klarstrom-Engstrom, K., Bengtsson, T., Lindahl, T. L. & Grenegard, M. The toll-like receptor 2/1 (TLR2/1) complex initiates human platelet activation via the src/Syk/LAT/PLCgamma2 signalling cascade. *Cell Signal* **26**, 279-286, doi:10.1016/j.cellsig.2013.11.011 (2014).
385 Lowell, C. A. Src-family and Syk kinases in activating and inhibitory pathways in innate immune cells: signaling cross talk. *Cold Spring Harb Perspect Biol* **3**, doi:10.1101/cshperspect.a002352 (2011).
386 Zhang, X., Wang, G., Gurley, E. C. & Zhou, H. Flavonoid apigenin inhibits lipopolysaccharide-induced inflammatory response through multiple mechanisms in macrophages. *PloS one* **9**, e107072, doi:10.1371/journal.pone.0107072 (2014).
387 Dennehy, K. M. *et al.* Syk kinase is required for collaborative cytokine production induced through Dectin-1 and Toll-like receptors. *Eur J Immunol* **38**, 500-506, doi:10.1002/eji.200737741 (2008).
388 Rogers, N. C. *et al.* Syk-dependent cytokine induction by Dectin-1 reveals a novel pattern recognition pathway for C type lectins. *Immunity* **22**, 507-517, doi:10.1016/j.immuni.2005.03.004 (2005).
389 Lau, K. S. *et al.* BAY61-3606 affects the viability of colon cancer cells in a genotype-directed manner. *PloS one* **7**, e41343, doi:10.1371/journal.pone.0041343 (2012).
390 Gunzl, P. & Schabbauer, G. Recent advances in the genetic analysis of PTEN and PI3K innate immune properties. *Immunobiology* **213**, 759-765, doi:10.1016/j.imbio.2008.07.028 (2008).
391 Fruman, D. A. *et al.* The PI3K Pathway in Human Disease. *Cell* **170**, 605-635, doi:10.1016/j.cell.2017.07.029 (2017).
392 Rakhshandehroo, M. *et al.* Comprehensive analysis of PPARalpha-dependent regulation of hepatic lipid metabolism by expression profiling. *PPAR Res* **2007**, 26839, doi:10.1155/2007/26839 (2007).
393 Chon, S. H., Zhou, Y. X., Dixon, J. L. & Storch, J. Intestinal monoacylglycerol metabolism: developmental and nutritional regulation of monoacylglycerol lipase and monoacylglycerol acyltransferase. *The Journal of biological chemistry* **282**, 33346-33357, doi:10.1074/jbc.M706994200 (2007).
394 Karmaus, P. W., Chen, W., Crawford, R., Kaplan, B. L. & Kaminski, N. E. Delta9-tetrahydrocannabinol impairs the inflammatory response to influenza infection: role of antigen-presenting cells and the cannabinoid receptors 1 and 2. *Toxicol Sci* **131**, 419-433, doi:10.1093/toxsci/kfs315 (2013).
395 Newton, C. A., Chou, P. J., Perkins, I. & Klein, T. W. CB(1) and CB(2) cannabinoid receptors mediate different aspects of delta-9-

tetrahydrocannabinol (THC)-induced T helper cell shift following immune activation by Legionella pneumophila infection. *Journal of neuroimmune pharmacology : the official journal of the Society on NeuroImmune Pharmacology* **4**, 92-102, doi:10.1007/s11481-008-9126-2 (2009).

396 Lu, T., Newton, C., Perkins, I., Friedman, H. & Klein, T. W. Cannabinoid treatment suppresses the T-helper cell-polarizing function of mouse dendritic cells stimulated with Legionella pneumophila infection. *The Journal of pharmacology and experimental therapeutics* **319**, 269-276, doi:10.1124/jpet.106.108381 (2006).

397 Agudelo, M. *et al.* Alcohol and Cannabinoids Differentially Affect HIV Infection and Function of Human Monocyte-Derived Dendritic Cells (MDDC). *Front Microbiol* **6**, 1452, doi:10.3389/fmicb.2015.01452 (2015).

398 Ramirez, S. H. *et al.* Attenuation of HIV-1 replication in macrophages by cannabinoid receptor 2 agonists. *Journal of leukocyte biology* **93**, 801-810, doi:10.1189/jlb.1012523 (2013).

399 Henriquez, J. E. *et al.* Delta9-Tetrahydrocannabinol Suppresses Secretion of IFNalpha by Plasmacytoid Dendritic Cells From Healthy and HIV-Infected Individuals. *J Acquir Immune Defic Syndr* **75**, 588-596, doi:10.1097/QAI.0000000000001449 (2017).

400 Ribeiro, A. *et al.* Anandamide prior to sensitization increases cell-mediated immunity in mice. *Int Immunopharmacol* **10**, 431-439, doi:10.1016/j.intimp.2009.12.017 (2010).

401 Docs, K. *et al.* The Ratio of 2-AG to Its Isomer 1-AG as an Intrinsic Fine Tuning Mechanism of CB1 Receptor Activation. *Front Cell Neurosci* **11**, 39, doi:10.3389/fncel.2017.00039 (2017).

402 Taylor, L. *et al.* Primary Macrophage Chemotaxis Induced by Cannabinoid Receptor 2 Agonists Occurs Independently of the CB2 Receptor. *Sci Rep* **5**, 10682, doi:10.1038/srep10682 (2015).

403 Alberich Jorda, M. *et al.* The peripheral cannabinoid receptor Cb2, frequently expressed on AML blasts, either induces a neutrophilic differentiation block or confers abnormal migration properties in a ligand-dependent manner. *Blood* **104**, 526-534, doi:10.1182/blood-2003-12-4357 (2004).

404 Montecucco, F., Burger, F., Mach, F. & Steffens, S. CB2 cannabinoid receptor agonist JWH-015 modulates human monocyte migration through defined intracellular signaling pathways. *American journal of physiology. Heart and circulatory physiology* **294**, H1145-1155, doi:10.1152/ajpheart.01328.2007 (2008).

405 Sexton, M., Silvestroni, A., Moller, T. & Stella, N. Differential migratory properties of monocytes isolated from human subjects naive and non-naive to Cannabis. *Inflammopharmacology* **21**, 253-259, doi:10.1007/s10787-012-0133-9 (2013).

406 Netea, M. G. *et al.* Trained immunity: A program of innate immune memory in health and disease. *Science* **352**, aaf1098, doi:10.1126/science.aaf1098 (2016).

407 Strober, W. Trypan blue exclusion test of cell viability. *Curr Protoc Immunol* **Appendix 3**, Appendix 3B, doi:10.1002/0471142735.ima03bs21 (2001).

408 Smits, H. H. *et al.* Commensal Gram-negative bacteria prime human dendritic cells for enhanced IL-23 and IL-27 expression and enhanced Th1 development. *Eur J Immunol* **34**, 1371-1380, doi:10.1002/eji.200324815 (2004).
409 Zaki, M. H., Lamkanfi, M. & Kanneganti, T. D. The Nlrp3 inflammasome: contributions to intestinal homeostasis. *Trends Immunol* **32**, 171-179, doi:10.1016/j.it.2011.02.002 (2011).
410 Malik, A. & Kanneganti, T. D. Inflammasome activation and assembly at a glance. *J Cell Sci* **130**, 3955-3963, doi:10.1242/jcs.207365 (2017).
411 Katsnelson, M. A., Rucker, L. G., Russo, H. M. & Dubyak, G. R. K+ efflux agonists induce NLRP3 inflammasome activation independently of Ca2+ signaling. *Journal of immunology* **194**, 3937-3952, doi:10.4049/jimmunol.1402658 (2015).
412 Hentze, H., Lin, X. Y., Choi, M. S. & Porter, A. G. Critical role for cathepsin B in mediating caspase-1-dependent interleukin-18 maturation and caspase-1-independent necrosis triggered by the microbial toxin nigericin. *Cell Death Differ* **10**, 956-968, doi:10.1038/sj.cdd.4401264 (2003).
413 Johnson, L. A. & Jackson, D. G. Inflammation-induced secretion of CCL21 in lymphatic endothelium is a key regulator of integrin-mediated dendritic cell transmigration. *Int Immunol* **22**, 839-849, doi:10.1093/intimm/dxq435 (2010).
414 Corridoni, D. & Simmons, A. Innate immune receptors for cross-presentation: The expanding role of NLRs. *Mol Immunol*, doi:10.1016/j.molimm.2017.11.028 (2017).
415 Pittet, M. J. *et al.* High frequencies of naive Melan-A/MART-1-specific CD8(+) T cells in a large proportion of human histocompatibility leukocyte antigen (HLA)-A2 individuals. *J Exp Med* **190**, 705-715 (1999).
416 Broz, P., Ohlson, M. B. & Monack, D. M. Innate immune response to Salmonella typhimurium, a model enteric pathogen. *Gut Microbes* **3**, 62-70, doi:10.4161/gmic.19141 (2012).
417 Khatamzas, E. *et al.* Snapin promotes HIV-1 transmission from dendritic cells by dampening TLR8 signaling. *EMBO J* **36**, 2998-3011, doi:10.15252/embj.201695364 (2017).
418 Moore, C. B., Guthrie, E. H., Huang, M. T. & Taxman, D. J. Short hairpin RNA (shRNA): design, delivery, and assessment of gene knockdown. *Methods Mol Biol* **629**, 141-158, doi:10.1007/978-1-60761-657-3_10 (2010).
419 Fellmann, C. & Lowe, S. W. Stable RNA interference rules for silencing. *Nat Cell Biol* **16**, 10-18, doi:10.1038/ncb2895 (2014).
420 Xiao-Jie, L., Hui-Ying, X., Zun-Ping, K., Jin-Lian, C. & Li-Juan, J. CRISPR-Cas9: a new and promising player in gene therapy. *J Med Genet* **52**, 289-296, doi:10.1136/jmedgenet-2014-102968 (2015).
421 McCoy, K. L., Gainey, D. & Cabral, G. A. delta 9-Tetrahydrocannabinol modulates antigen processing by macrophages. *The Journal of pharmacology and experimental therapeutics* **273**, 1216-1223 (1995).
422 McCoy, K. L., Matveyeva, M., Carlisle, S. J. & Cabral, G. A. Cannabinoid inhibition of the processing of intact lysozyme by macrophages: evidence for CB2 receptor participation. *The Journal of pharmacology and experimental therapeutics* **289**, 1620-1625 (1999).

423 Xu, H. *et al.* Anti-inflammatory property of the cannabinoid receptor-2-selective agonist JWH-133 in a rodent model of autoimmune uveoretinitis. *Journal of leukocyte biology* **82**, 532-541, doi:10.1189/jlb.0307159 (2007).
424 Ghosh, S., Preet, A., Groopman, J. E. & Ganju, R. K. Cannabinoid receptor CB2 modulates the CXCL12/CXCR4-mediated chemotaxis of T lymphocytes. *Mol Immunol* **43**, 2169-2179, doi:10.1016/j.molimm.2006.01.005 (2006).
425 Chiurchiu, V., Lanuti, M., De Bardi, M., Battistini, L. & Maccarrone, M. The differential characterization of GPR55 receptor in human peripheral blood reveals a distinctive expression in monocytes and NK cells and a proinflammatory role in these innate cells. *Int Immunol* **27**, 153-160, doi:10.1093/intimm/dxu097 (2015).
426 Borner, C., Hollt, V. & Kraus, J. Activation of human T cells induces upregulation of cannabinoid receptor type 1 transcription. *Neuroimmunomodulation* **14**, 281-286, doi:10.1159/000117809 (2007).
427 Collins, J. W. *et al.* Citrobacter rodentium: infection, inflammation and the microbiota. *Nat Rev Microbiol* **12**, 612-623, doi:10.1038/nrmicro3315 (2014).
428 Palmela, C. *et al.* Adherent-invasive Escherichia coli in inflammatory bowel disease. *Gut*, doi:10.1136/gutjnl-2017-314903 (2017).
429 Wiles, S. *et al.* Organ specificity, colonization and clearance dynamics in vivo following oral challenges with the murine pathogen Citrobacter rodentium. *Cell Microbiol* **6**, 963-972, doi:10.1111/j.1462-5822.2004.00414.x (2004).
430 Luperchio, S. A. & Schauer, D. B. Molecular pathogenesis of Citrobacter rodentium and transmissible murine colonic hyperplasia. *Microbes Infect* **3**, 333-340 (2001).
431 Mundy, R., MacDonald, T. T., Dougan, G., Frankel, G. & Wiles, S. Citrobacter rodentium of mice and man. *Cell Microbiol* **7**, 1697-1706, doi:10.1111/j.1462-5822.2005.00625.x (2005).
432 Gibson, D. L. *et al.* Toll-like receptor 2 plays a critical role in maintaining mucosal integrity during Citrobacter rodentium-induced colitis. *Cell Microbiol* **10**, 388-403, doi:10.1111/j.1462-5822.2007.01052.x (2008).
433 Geddes, K. *et al.* Identification of an innate T helper type 17 response to intestinal bacterial pathogens. *Nature medicine* **17**, 837-844, doi:10.1038/nm.2391 (2011).
434 Koroleva, E. P. *et al.* Citrobacter rodentium-induced colitis: A robust model to study mucosal immune responses in the gut. *J Immunol Methods* **421**, 61-72, doi:10.1016/j.jim.2015.02.003 (2015).
435 Clapper, J. R. *et al.* in *Society for Neuroscience* Vol. 2016 Neuroscience Meeting Planner OO4 (Online, San Diego, CA, USA, 2016).
436 Blankman, J. L. *et al.* in *Society for Neuroscience* Vol. 2016 Neuroscience Meeting Planner OO5 (Online, San Diego, CA, USA, 2016).
437 Marquez, L. *et al.* Ulcerative colitis induces changes on the expression of the endocannabinoid system in the human colonic tissue. *PloS one* **4**, e6893, doi:10.1371/journal.pone.0006893 (2009).

438 Wright, K. *et al.* Differential expression of cannabinoid receptors in the human colon: cannabinoids promote epithelial wound healing. *Gastroenterology* **129**, 437-453, doi:10.1016/j.gastro.2005.05.026 (2005).
439 Harvey, B. S., Nicotra, L. L., Vu, M. & Smid, S. D. Cannabinoid CB2 receptor activation attenuates cytokine-evoked mucosal damage in a human colonic explant model without changing epithelial permeability. *Cytokine* **63**, 209-217, doi:10.1016/j.cyto.2013.04.032 (2013).
440 Di Sabatino, A. *et al.* The endogenous cannabinoid system in the gut of patients with inflammatory bowel disease. *Mucosal immunology* **4**, 574-583, doi:10.1038/mi.2011.18 (2011).
441 Stintzing, S. *et al.* Role of cannabinoid receptors and RAGE in inflammatory bowel disease. *Histol Histopathol* **26**, 735-745 (2011).
442 Leinwand, K. L. *et al.* Cannabinoid Receptor-2 Ameliorates Inflammation in Murine Model of Crohn's Disease. *J Crohns Colitis*, doi:10.1093/ecco-jcc/jjx096 (2017).
443 Darmani, N. A. *et al.* Involvement of the cannabimimetic compound, N-palmitoyl-ethanolamine, in inflammatory and neuropathic conditions: review of the available pre-clinical data, and first human studies. *Neuropharmacology* **48**, 1154-1163, doi:10.1016/j.neuropharm.2005.01.001 (2005).
444 Nicotra, L. L., Vu, M., Harvey, B. S. & Smid, S. D. Prostaglandin ethanolamides attenuate damage in a human explant colitis model. *Prostaglandins Other Lipid Mediat* **100-101**, 22-29, doi:10.1016/j.prostaglandins.2013.01.003 (2013).
445 Duncan, M. *et al.* Distribution and function of monoacylglycerol lipase in the gastrointestinal tract. *American journal of physiology. Gastrointestinal and liver physiology* **295**, G1255-1265, doi:10.1152/ajpgi.90500.2008 (2008).
446 Hanlon, E. C. *et al.* Circadian rhythm of circulating levels of the endocannabinoid 2-arachidonoylglycerol. *J Clin Endocrinol Metab* **100**, 220-226, doi:10.1210/jc.2014-3455 (2015).
447 Kantae, V. *et al.* Endocannabinoid tone is higher in healthy lean South Asian than white Caucasian men. *Sci Rep* **7**, 7558, doi:10.1038/s41598-017-07980-5 (2017).
448 Storr, M. A., Yuce, B., Andrews, C. N. & Sharkey, K. A. The role of the endocannabinoid system in the pathophysiology and treatment of irritable bowel syndrome. *Neurogastroenterology and motility : the official journal of the European Gastrointestinal Motility Society* **20**, 857-868, doi:10.1111/j.1365-2982.2008.01175.x (2008).
449 Karlsson, M. *et al.* Exon-intron organization and chromosomal localization of the mouse monoglyceride lipase gene. *Gene* **272**, 11-18 (2001).
450 Pan, B. *et al.* Alterations of endocannabinoid signaling, synaptic plasticity, learning, and memory in monoacylglycerol lipase knock-out mice. *The Journal of neuroscience : the official journal of the Society for Neuroscience* **31**, 13420-13430, doi:10.1523/JNEUROSCI.2075-11.2011 (2011).
451 Taschler, U. *et al.* Monoglyceride lipase deficiency in mice impairs lipolysis and attenuates diet-induced insulin resistance. *The Journal of biological chemistry* **286**, 17467-17477, doi:10.1074/jbc.M110.215434 (2011).

452 Zhong, P. *et al.* Genetic deletion of monoacylglycerol lipase alters endocannabinoid-mediated retrograde synaptic depression in the cerebellum. *J Physiol* **589**, 4847-4855, doi:10.1113/jphysiol.2011.215509 (2011).
453 Navia-Paldanius, D. *et al.* Increased tonic cannabinoid CB1R activity and brain region-specific desensitization of CB1R Gi/o signaling axis in mice with global genetic knockout of monoacylglycerol lipase. *European journal of pharmaceutical sciences : official journal of the European Federation for Pharmaceutical Sciences* **77**, 180-188, doi:10.1016/j.ejps.2015.06.005 (2015).
454 Moran, G. W., O'Neill, C., Padfield, P. & McLaughlin, J. T. Dipeptidyl peptidase-4 expression is reduced in Crohn's disease. *Regul Pept* **177**, 40-45, doi:10.1016/j.regpep.2012.04.006 (2012).
455 Rybaczyk, L. *et al.* New bioinformatics approach to analyze gene expressions and signaling pathways reveals unique purine gene dysregulation profiles that distinguish between CD and UC. *Inflammatory bowel diseases* **15**, 971-984, doi:10.1002/ibd.20893 (2009).
456 Mayet, W. J. *et al.* Antibodies to cathepsin G in Crohn's disease. *Eur J Clin Invest* **22**, 427-433 (1992).
457 Halbwachs-Mecarelli, L. *et al.* Antineutrophil cytoplasmic antibodies (ANCA) directed against cathepsin G in ulcerative colitis, Crohn's disease and primary sclerosing cholangitis. *Clin Exp Immunol* **90**, 79-84 (1992).
458 Dabek, M. *et al.* Luminal cathepsin g and protease-activated receptor 4: a duet involved in alterations of the colonic epithelial barrier in ulcerative colitis. *Am J Pathol* **175**, 207-214, doi:10.2353/ajpath.2009.080986 (2009).
459 Leedham, S. J. *et al.* Clonality, founder mutations, and field cancerization in human ulcerative colitis-associated neoplasia. *Gastroenterology* **136**, 542-550 e546, doi:10.1053/j.gastro.2008.10.086 (2009).
460 Galandiuk, S. *et al.* Field cancerization in the intestinal epithelium of patients with Crohn's ileocolitis. *Gastroenterology* **142**, 855-864 e858, doi:10.1053/j.gastro.2011.12.004 (2012).
461 Magro, F. *et al.* Third European Evidence-based Consensus on Diagnosis and Management of Ulcerative Colitis. Part 1: Definitions, Diagnosis, Extra-intestinal Manifestations, Pregnancy, Cancer Surveillance, Surgery, and Ileo-anal Pouch Disorders. *J Crohns Colitis* **11**, 649-670, doi:10.1093/ecco-jcc/jjx008 (2017).
462 Corridoni, D., Chapman, T., Ambrose, T. & Simmons, A. Emerging mechanisms of innate immunity and their translational potential in inflammatory bowel disease. *Front Med*, doi:10.3389/fmed.2018.00032 (2018).
463 Roth, M. D., Castaneda, J. T. & Kiertscher, S. M. Exposure to Delta9-Tetrahydrocannabinol Impairs the Differentiation of Human Monocyte-derived Dendritic Cells and their Capacity for T cell Activation. *Journal of neuroimmune pharmacology : the official journal of the Society on NeuroImmune Pharmacology* **10**, 333-343, doi:10.1007/s11481-015-9587-z (2015).

464 Chang, D. H. *et al.* Inflammation-associated lysophospholipids as ligands for CD1d-restricted T cells in human cancer. *Blood* **112**, 1308-1316, doi:10.1182/blood-2008-04-149831 (2008).
465 Troutman, T. D., Bazan, J. F. & Pasare, C. Toll-like receptors, signaling adapters and regulation of the pro-inflammatory response by PI3K. *Cell Cycle* **11**, 3559-3567, doi:10.4161/cc.21572 (2012).
466 Dustin, M. L. The immunological synapse. *Cancer Immunol Res* **2**, 1023-1033, doi:10.1158/2326-6066.CIR-14-0161 (2014).
467 Heux, S., Berges, C., Millard, P., Portais, J. C. & Letisse, F. Recent advances in high-throughput 13C-fluxomics. *Curr Opin Biotechnol* **43**, 104-109, doi:10.1016/j.copbio.2016.10.010 (2017).

Supplementary Figure

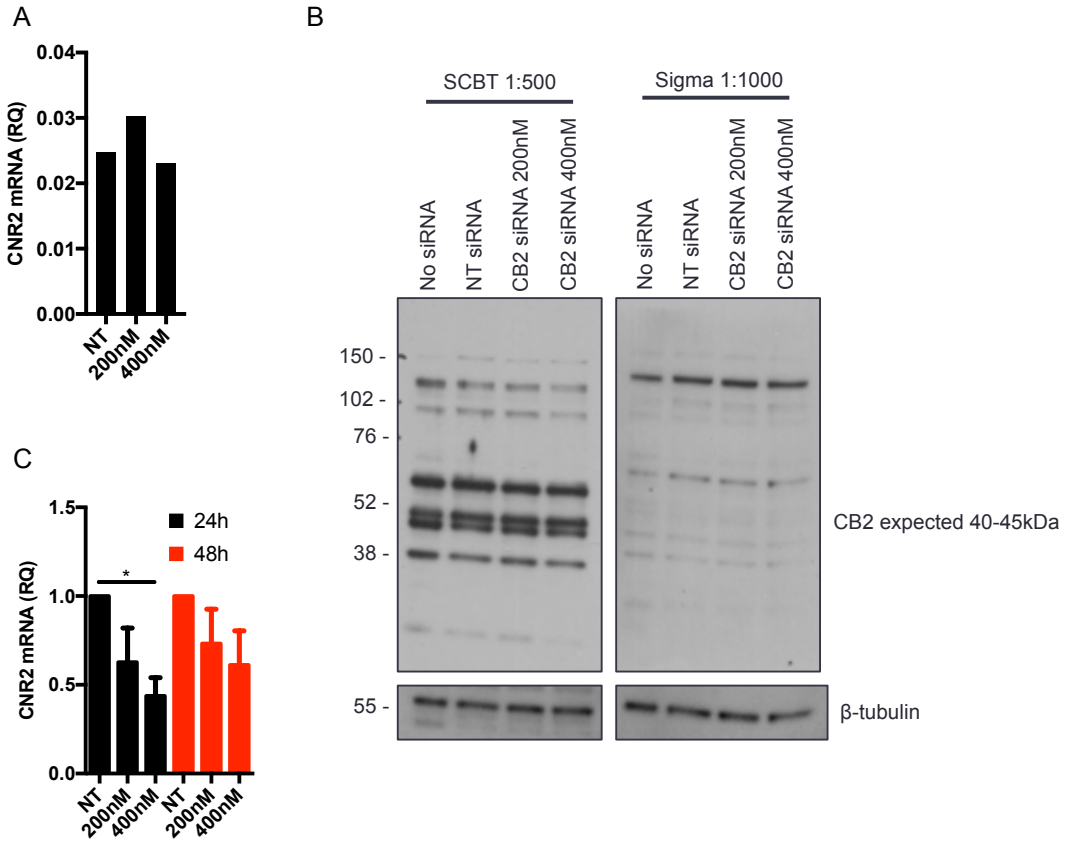

Supplementary Figure CB2 cannot be knocked down at mRNA level by siRNA electroporation in Jurkat cells, but can in moDCs, and two commercially available CB2 antibodies could not be validated in this cell line

siRNA was introduced to Jurkat cells or unstimulated moDCs by electroporation. **(A)** siRNA knockdown of CB2 in Jurkat cells, a positive control for CB2, was unsuccessful by qPCR. Results are from 1 technical replicate. **(B)** Immunoblot for CB2 using two commercially available antibodies at the concentrations shown resulted in widespread non-specific binding and no effects of CB2 knockdown. Results are from 1 technical replicate. **(C)** siRNA knockdown of CB2 in moDCs results in reduced CB2 mRNA at 24h. Mean +/- SEM of 4 biological replicates. ANOVA with Bonferroni's correction for selected pairs. *p<0.0332. NT = Non-targeting; SCBT = Santa Cruz Biotechnology.

Appendix 1 – List of serine hydrolases identified in moDCs by ABPP-MuDPIT

Symbol	Description	Molecular Weight (kDa)
MGLL	Monoacylglycerol lipase	33.3
PLA2G4A	Cytosolic phospholipase A2	82.4
ABHD13	αβ-hydrolase domain containing protein 13	37.1
RBBP9	Putative hydrolase RBBP9	20.5
ABHD16A	αβ-hydrolase domain containing protein 16A	61.4
GLS	Glutaminase kidney isoform, mitochondrial	73.6
SEC23IP	SEC23-interacting protein	110
TPP2	Tripeptidyl-peptidase 2	137.4
DAGLB	Sn1-specific diacylglycerol lipase beta	73.9
LONP1	Lon protease homolog, mitochondrial	105.5
FAM108B1	Abhydrolase domain-containing protein FAM108B1	31.7
OVCA2	Ovarian cancer-associated gene 2 protein	25
PAFAH1B2	Platelet-activating factor acetylhydrolase IB subunit beta	25.2
PPME1	Protein phosphatase methylesterase 1	42.5
FASN	Fatty acid synthase	276.2
PNPLA8	Calcium-independent phospholipase A2-gamma	86
ABHD14B	αβ-hydrolase domain containing protein 14B	23.1
DPP9	Dipeptidyl peptidase 9	94.9
IAH1	Isoamyl acetate-hydrolyzing esterase 1 homolog	27.3
ESD	S-formylglutathione hydrolase	31
LACTB	Serine beta-lactamase-like protein LACTB, mitochondrial	60.2
PNPLA7	Patatin-like phospholipase domain-containing protein 7	144.9
LYPLA2	Acyl-protein thioesterase 2	25.4
AFMID	Kynurenine formamidase	33.3
CES1	Liver carboxylesterase 1	62.4
FAAH	Fatty-acid amide hydrolase 1	63.7
PAFAH1B3	Platelet-activating factor acetylhydrolase IB subunit gamma	25.4
PAFAH2	Platelet-activating factor acetylhydrolase 2, cytoplasmic	43.1
PREP	Prolyl endopeptidase	78.1
PNPLA4	Patatin-like phospholipase domain-containing protein 4	27.8
ABHD12	αβ-hydrolase domain containing protein 12	43.8
DPP8	Dipeptidyl peptidase 8	98.8
PLA2G7	Platelet-activating factor acetylhydrolase	48.5
AOAH	Acyloxyacyl hydrolase	63.2
FAM108A1	αβ-hydrolase domain containing protein	34.1

	FAM108A1	
APEH	Acylamino-acid-releasing enzyme	80.5
LYPLA1	Acyl-protein thioesterase 1	25.3
LYPLAL1	Lysophospholipase-like protein 1	26.1
CES2	Cocaine esterase	61.5
PARL	Presenilins-associated rhomboid-like protein, mitochondrial	41.7
ABHD3	αβ-hydrolase domain containing protein 3	45
ACOT2	Acyl-coenzyme A thioesterase 2, mitochondrial	53.1
NCEH1	Neutral cholesterol ester hydrolase 1	44.9
ABHD6	αβ-hydrolase domain containing protein 6	37.1
ABHD10	αβ-hydrolase domain containing protein 10, mitochondrial	33.7
PNPLA6	Neuropathy target esterase	150.3
SCPEP1	Retinoid-inducible serine carboxypeptidase	49.7
ABHD11	αβ-hydrolase domain containing protein 11	34.6
PRCP	Lysosomal Pro-X carboxypeptidase	54.6
TPP1	Tripeptidyl-peptidase 1	61.9
ELANE	Neutrophil elastase	29.4
DPP7	Dipeptidyl peptidase 7	54.1
SIAE	Sialate O-acetylesterase	57.5
CTSG	Cathepsin G	28.1
PNPLA2	Patatin-like phospholipase domain-containing protein 2	55.4
CTSA	Lysosomal protective protein	52.8
CPVL	Probable serine carboxypeptidase CPVL	52.4
PREPL	Prolyl endopeptidase-like	80
PRTN3	Myeloblastin	28.2
ABHD2	αβ-hydrolase domain containing protein 2	46.8
PLA2G15	Group XV phospholipase A2	45.3
LPL	Lipoprotein lipase	52.2
LIPA	Lysosomal acid lipase/cholesteryl ester hydrolase	43.9
ACOT1	Acyl-coenzyme A thioesterase 1	46.3

Appendix 2 - List of lipids identified by high throughput screening of moDCs

Number	Lipid class	Abbreviation	Number of lipids
1	Alkyl diacylglycerol	aDAG	11
2	Alkyl lysophosphatidylcholine	aLPC	8
3	Alkyl lysophosphatidylethanolamine	aLPE	6
4	Alkyl phosphatidylcholine	aPC	20
5	Alkyl phosphatidylethanolamine	aPE	34
6	Alkyl triacylglycerol	aTAG	22
7	Cardiolipin	CL	21
8	Ceramide	Cer	21
9	Cholesterol ester	CE	6
10	Diacylglycerol	DAG	19
11	Fatty acid	FA	25
12	Fatty acyl carnitine	FACN	4
13	Fatty acyl CoA	FACoA	8
14	Lysophosphatidylcholine	LPC	15
15	Lysophosphatidylethanolamine	LPE	17
16	Lysophosphatidylglycerol	LPG	4
17	Lysophosphatidylinositol	LPI	12
18	Lysophosphatidylserine	LPS	9
19	Monoacylglycerol	MAG	1
20	Phosphatidic acid	PA	17
21	Phosphatidylcholine	PC	39
22	Phosphatidylethanolamine	PE	38
23	Phosphatidylglycerol	PG	20
24	Phosphatidylinositol	PI	28
25	Phosphatidylserine	PS	27
26	Sphingomyelin	SM	21
27	Sphingosine	SG	1
28	Sphingosine-1-phosphate	S1P	1
29	Triacylglycerol	TAG	45
	Total lipids identified		500